LEABHARLANN CHOLÁISTE NA TRÍONÓIDE, BAILE ÁTHA CLIATH | TRINITY COLLEGE LIBRARY DUBLIN
Ollscoil Átha Cliath | The University of Dublin

Terms and Conditions of Use of Digitised Theses from Trinity College Library Dublin

Copyright statement

All material supplied by Trinity College Library is protected by copyright (under the Copyright and Related Rights Act, 2000 as amended) and other relevant Intellectual Property Rights. By accessing and using a Digitised Thesis from Trinity College Library you acknowledge that all Intellectual Property Rights in any Works supplied are the sole and exclusive property of the copyright and/or other IPR holder. Specific copyright holders may not be explicitly identified. Use of materials from other sources within a thesis should not be construed as a claim over them.

A non-exclusive, non-transferable licence is hereby granted to those using or reproducing, in whole or in part, the material for valid purposes, providing the copyright owners are acknowledged using the normal conventions. Where specific permission to use material is required, this is identified and such permission must be sought from the copyright holder or agency cited.

Liability statement

By using a Digitised Thesis, I accept that Trinity College Dublin bears no legal responsibility for the accuracy, legality or comprehensiveness of materials contained within the thesis, and that Trinity College Dublin accepts no liability for indirect, consequential, or incidental, damages or losses arising from use of the thesis for whatever reason. Information located in a thesis may be subject to specific use constraints, details of which may not be explicitly described. It is the responsibility of potential and actual users to be aware of such constraints and to abide by them. By making use of material from a digitised thesis, you accept these copyright and disclaimer provisions. Where it is brought to the attention of Trinity College Library that there may be a breach of copyright or other restraint, it is the policy to withdraw or take down access to a thesis while the issue is being resolved.

Access Agreement

By using a Digitised Thesis from Trinity College Library you are bound by the following Terms & Conditions. Please read them carefully.

I have read and I understand the following statement: All material supplied via a Digitised Thesis from Trinity College Library is protected by copyright and other intellectual property rights, and duplication or sale of all or part of any of a thesis is not permitted, except that material may be duplicated by you for your research use or for educational purposes in electronic or print form providing the copyright owners are acknowledged using the normal conventions. You must obtain permission for any other use. Electronic or print copies may not be offered, whether for sale or otherwise to anyone. This copy has been supplied on the understanding that it is copyright material and that no quotation from the thesis may be published without proper acknowledgement.

INVESTIGATING THE ROLE OF DNA HYPERMETHYLATION AS A KEY CONTROLLER OF ABERRANT CELL DEATH IN PROSTATE CANCER.

A thesis submitted for the degree of Doctor of Philosophy

Therese Murphy BA (Genetics) Hons.

Trinity College, University of Dublin

April 2010

Declaration

I hereby certify that this thesis, submitted for the degree of Doctor of Philosophy to the University of Dublin, has not been previously submitted for a degree or diploma to this or any other university. The work presented here is entirely my own, except where stated.

This thesis may be available for consultation within the University library and may be photocopied or lent to other libraries for the purpose of consultation.

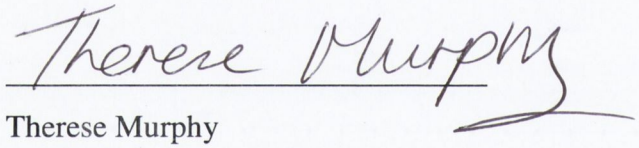

Therese Murphy

April 2010

TRINITY COLLEGE
27 AUG 2010
LIBRARY DUBLIN
THESIS
8903

ABSTRACT

Prostate cancer remains a global public health problem. Worldwide, it is the most common noncutaneous cancer in men and is a leading cause of cancer-related deaths among men in North America and Western\Northern Europe. Currently, PSA is the screening tool of choice and has been estimated to reduce the rate of death from prostate cancer by 20% but fails to adequately distinguish between clinically indolent versus aggressive forms of prostate cancers. Development, therefore, of novel diagnostic and prognostic markers is imperative to enhance the predictive value of current screening tools.

Uncharacteristic DNA methylation has been implicated as a key survival mechanism in cancer, whereby promoter hypermethylation silences genes essential for many important cellular processes, such as apoptosis. Disruption of apoptosis, via both genetic and epigenetic mechanisms is one of the principal factors contributing to the evolution of the carcinogenic phenotype. To date, studies on the methylation profile of apoptotic genes have largely focused on cancers of the breast, colon and stomach, with only limited data available on prostate cancer.

The objective of this study was to profile the methylation status of apoptotic-related genes in prostate cancer using a novel Denaturing High Performance Liquid Chromatography (DHPLC) platform. Based on an *in silico* selection process, thirteen genes were screened for CpG methylation in a panel of prostate cancer cell lines (LNCaP, DU145, PC3, 22RV1, RC58) and normal prostate cell lines (RWPE1 and PWR1E) using DHPLC. Our results demonstrate that the CpG promoter regions of *BIK, BNIP3, cFLIP, TMS1*, *DCR1*, *DCR2* and *CDKN2A* appear fully or partially methylated in a high number of the malignant cell lines examined. We next studied the expression of these genes in the relevant prostate cancer cell lines and in DNA methyltransferase inhibitor (5aza2'deoxycytidine) treated PC3 cells. Consistent with our methylation data, expression of *cFLIP*, *BIK, BNIP3, TMS1, CDKN2A* and *DCR1/2* are significantly reduced in multiple cell lines. Furthermore, treatment of PC3 cells with 5aza2'deoxycytidine causes a moderate to strong increase in expression in *BIK, TMS1, CDKN2A* and *DCR1/2*. Thus, this work

demonstrates the utility of a combined *in silico* and DHPLC screening platform for identification of novel gene-targets of promoter hypermethylation in cancer.

This is the first report of aberrant methylation of *BIK*, *BNIP3*, and *cFLIP* in prostate cancer. Three genes *TMS1*, *DCR1* and *DCR2* identified in our study have previously shown utility as potential new biomarkers of risk prediction in prostate cancer (Suzuki et al., 2006), while *CDKN2A*, is known to be aberrantly methylated in prostate but its potential as a tumour biomarker is unknown. Further examination of the methylation profile of these 7 apoptotic-related genes in samples representing prostate cancer (n=50), HGPIN (n=17), normal adjacent prostate (n=43) and BPH (n=35) using QMSP identified 5 genes (*BNIP3, CDKN2A, DCR1, DCR2* and *TMS1*) which had a significantly higher frequency of methylation in their promoter CpG islands in prostate cancer than normal prostate. Approximately 69% of tumour samples and 0% of normal tissues were methylated in at least one of our 5- apoptotic gene panel. Furthermore, this 5 gene "apoptotic methylation signature" is more frequently methylated in prostate cancer with a Gleason score ≥ 7, which is associated with a poorer prognosis. In addition, combination of this panel of genes with *GSTP1* increased the frequency of methylation detection in prostate cancer from 80% to 89% than if *GSTP1* were used alone. Thus, future examination of this "apoptotic methylation signature" in a larger cohort of patients is justified to further evaluate its value in a diagnostic and prognostic setting and its potential to stratify patients into chemo-resistant/chemo-sensitive group.

"For most of human history we have searched for our place in the cosmos. Who are we? What are we? We find that we inhabit an insignificant planet of a hum-drum star lost in a galaxy tucked away in some forgotten corner of a universe in which there are far more galaxies than people. We make our world significant by the courage of our questions and by the depth of our answers". -
Carl Sagan

For my parents Michael and Bernadette

ACKNOWLEDGEMENTS

There are so many people I wish to thank I hardly know where to begin. Firstly, I'd like to thank my supervisor Professor Mark Lawler for all his advice and encouragement over the past four years and for allowing me the opportunity to become a member of a wonderful and broad spectrum laboratory that is the Durkan lab! Finally I would sincerely like to thank him for introducing me to the wonderful world of epigenetics! A big heartfelt thank you to my co-supervisor Dr. Antoinette Perry, who has not only been a wonderful supervisor but also a great friend. Antoinette, without your kind encouragement, exceptional knowledge, time and dedication this PhD would not have been possible, you are a truly inspiring individual and I am so incredibly lucky to have had you as a supervisor and a friend.

Acknowledgement must be made to my funding body the HRB and the four year PhD in molecular medicine. A thank you to organisers, Dr. Ross McManus and Dr. Michael Freeley and all IMM staff past and present for their help throughout the last 4 years. I am very grateful to my mentor for my PhD programme, Professor John O'Leary, for his kind words of encouragement, knowledge and advice. A sincere thank you for all your help and guidance!

I have had the great pleasure of working with a wonderful team (Antoinette, Linda, Lisa, Alice, Ruth, Omar, James, Laure, Tony, Prerna, Jackie, Elaina, Danni, Lynn, Frances) for the last 3 years. You have all in one form or another helped and guided me and for that I am sincerely grateful and it has been an absolute pleasure working with you all. There are so many people I would like to acknowledge specifically and I truly hope I do not forget anyone. Lisa, thank you for all you advise and help with the dreaded DHPLC! Linda, your hard work and long hours slaving over those prostate tissue samples will not be forgotten, thank you!! I must also thank Prerna for giving up her precious time to help me with the hydra and 7900. To the prostate cancer group (Ruth, Linda, Antoinette, Lynn, Laure, Alice, James), whose discussion and advice are much appreciated. To Derek and Andreia for help with the 7900 and the Hydra. I would like to acknowledge my collaborators Dr. Daniel Longley (Queen's University, Belfast), Dr. David Waugh (Queen's University, Belfast), Professor Bill Watson (UCD, Dublin) and Professor John O'Leary (TCD, Dublin).

Finally, I would like to acknowledge the prostate cancer research consortium, funded by the Irish cancer society. Thank you to all involved from pathologist to research nurses and all those who come in between. A special thank you to all the men whose prostates were used on this research, without whom none of this research would be possible.

A special shout out to the Orla Sheil's laboratory (Sinead, Karen, Paul, Darragh, Richie and Jing Yuan and not forgetting Orla)!! Thank you so much for 4 years of bizarre lunch time conversation (Many of which I probably initiated ;)! I must also mention other fellow companions in the windowless basement, Alice and Darragh (not forgetting honorary member Ruth) for putting up with myself and Sinead's constant moaning! It's been a pleasure! And not forgetting the IMM lab rat team members, it's been great playing with you guys.

To my PhD girls (Sinead, Cathy, Christine), where do I begin, you have all in your individual ways been my rock for the last four years! I am truly lucky to not only have you as great classmates but as lifelong friends also! And not forgetting Karen, you like the girls have been a great friend and hopefully will be for a very long time- I miss our tea time scones, bizarre conversations, laughs (would ya just come home from oz, it's not the same here without ya ☺). Thank you all so very much! I must make a special mention to Sinead Aherne, who I have sat beside everyday for four years now! You have made the dreary basement a pleasure to walk into everyday! For all the chats, for all the laughs, for all the tears, for having the same brain!!! Thank you a million times over!!!

You don't get many chances in life to thank your friends and family and I would like to use this opportunity to do so. To my wonderful, wonderful friends of which there are too many to name but you have all in your individual ways helped and supported me! Thank you all for putting up with a pauper friend and listening to and not judging me for (well maybe a little bit?) my many (yet highly informative ;)) genetic rants over the years. A special thank you to Lorna who knows the woes of a PhD and has been a constant support to me and a truly great friend for many years now. Last but not least to my

donnybrook girls, Erin and Carly, Thank you for a wonderful 3 years in donnybrook, I miss you both very much and I am blessed to have made lifelong great friends- you will never know how much I appreciate your friendship, support and endless encouragement of my career!!

Thanks also to Paul, who only met me in the final year of my PhD and put up with me none the less ;), for your never-ending patience and understanding! For listening to my incessant moaning and ranting (scientific or not), you're a saint and I am so very lucky that I have you in my life! Last but not least I would like to thank my family. My siblings (Karren, Mark, Damien), my brother and sister in law (John and Rachael), and my wonderful nephews (Sean and Sartori) for their endless support and encouragement and for listening to rambling lectures on various scientific topics and putting up with my never ending studies and financial woes! You've all been great and your belief and support has always been felt! Finally to my parents, Michael and Bernadette, to whom I dedicate this thesis; you have been a constant support financially and more importantly emotionally and I can say without a single doubt in my mind that I would not have been able to finish this PhD without your never-ending love and support. Your genuine interest in my work has never ceased to amaze me. You have both been (in your own unique ways) and will always remain a constant source of inspiration for me and have made me the person I am today. I'm finished now so no need to worry anymore☺.

LIST OF FIGURES

CHAPTER 1: INTRODUCTION

Fig 1.1 Prostate and seminal vesicles
Fig 1.2 Different zones of the prostate.
Fig 1.3 Prostatic tissue specimen
Fig 1.4 Prostate cancer development.
Fig 1.5 Worldwide view of prostate cancer
Fig 1.6 Age-adjusted incidence of prostate cancer
Fig 1.7 Incidence and mortality rates
Fig 1.8 Trends in European age-standardised incidence rates for prostate cancer by country:1994-200
Fig 1.9 Trends in European age-standardised mortality rates for prostate cancer by country:1994-2004
Fig 1.10 nternational comparison of world age-standardised incidence rate for prostate cancer: 1998-20
Fig 1.11 Prostate cancer incidence and mortality rates Ireland
Fig 1.12 Schematic representation of the workflow utilised in the PCRC
Fig 1.13 The appearance of cancer cells according to the Gleason system
Fig 1.14 Development of androgen independence
Fig 1.15 Methylation of cytosine
Fig 1.16 Chromatin structure of active and inactive promoters
Fig 1.17 DNA methylation in normal and cancer cells
Fig 1.18 Pathways affected by hypermethylation in prostate cancer.
Fig 1.19 Apoptosis Pathways.

CHAPTER 2: MATERIALS AND METHODS

Fig 2.1 Navigation of iHOP.
Fig 2.2 Bisulfite conversion reaction of DNA.
Fig 2.3 Genetic map of vector pCR4-TOPO.
Fig 2.4 Chemistry of Taqman Real-time PCR.
Fig 2.5 Real-time TaqMan PCR
Fig 2.6 Layout of 96-well tissue sample plate.

CHAPTER 3: *IN SILICO* IDENTIFICATION OF POTENTIAL APOPTOSIS-RELATED GENE TARGETS OF PROMOTER HYPERMETHYLATION IN PROSTATE CANCER.

Fig 3.1 In silico selection
Fig 3.2 UCSC Human genome Browser graphical representation of *FAS*

CHAPTER 4: DISCOVERY OF APOPTOTIC-RELATED GENE TARGETS OF ABERRANT METHYLATION IN PROSTATE CANCER UTILIZING A DHPLC METHYLATION SCREENING STRATEGY

Fig 4.1 Methylation profiling by DHPLC
Fig 4.2 DHPLC chromatograms of unmethylated genes in prostate cancer cell lines.
Fig 4.3 DHPLC chromatograms of methylated genes in prostate cancer cell lines.
Fig 4.4 Agarose gel results for *APAF1* and *BNIP3* amplification of fresh frozen tissue
Fig 4.5 Validation of DHPLC methylation results for *CDKN2A*
Fig 4.6 Validation of DHPLC methylation results for *cFLIP*
Fig 4.7 Validation of DHPLC methylation results for *DCR1*
Fig 4.8 Gel electrophoresis of DNA treated with restriction enzyme BsiEI
Fig 4.9 DHPLC chromatogram of the promoter CpG Islands 1 and 2 of cFLIP in colon cancer c
Fig 4.10 Investigating the methylation status of *BIK* in docetaxel resistant Cells

CHAPTER 5: QUANTIFYING METHYLATION AND GENE EXPRESSION LEVELS OF APOPTOTIC-GENE TARGETS OF METHYLATION IN PROSTATE CANCER CELL LINES

Fig 5.1 Promoter CpG island characterisation
Fig 5.2 Standard curve of QMSP assays
Fig 5.3 Amplification plot of *ACTB*

Fig 5.4 Methylation levels of the 7-gene panel determined by QMSP
Fig 5.5 Comparison of promoter methylation and gene expression

CHAPTER 6: INVESTIGATING THE METHYLATION STATUS OF A PANEL OF SEVEN APOPTOTIC-RELATED GENES IN PROSTATE CANCER TISSUE SAMPLES.

Fig 6.1 Prostate tissue samples.
Fig 6.2 Methylation frequencies for 7-gene panel in prostate cancer, HGPIN, Normal prostate
Fig 6.3 Methylation Heat map of 5-gene apoptotic panel in Tumour, HGPIN, Benign prostate
Fig 6.4 Methylation Heat Map of 5-gene apoptotic panel and *GSTP1* in prostate cancer
Fig 6.5 Correlation of promoter hypermethylation with clinicopathological features of prostat
Fig 6.6 Correlation of hypermethylation of all 5 apoptotic gene and clinicopathological featu

CHAPTER 7: DISCUSSION & FUTURE DIRECTIONS

Fig 7.1 Hypothetical sub grouping of prostate cancer
Fig 7.2 p53/miR-34 pathway regulation of apoptosis

APPENDICES

Fig A1.1 Gel analysis of APAF1 PCR products
Fig A212 Gel analysis of BIK PCR products
Fig A1.3 Gel analysis of BNIP3 PCR products
Fig A1.4 Gel analysis of CDK2NA PCR products
Fig A1.5 Gel analysis of CFLAR PCR products
Fig A1.6 Gel analysis of CASP8 PCR products
Fig A1.7 Gel analysis of CASP3 PCR products
Fig A1.8 Gel analysis of DCR1 PCR products
Fig A1.9 Gel analysis of DCR2 PCR products
Fig A1.10 Gel analysis of DR5 PCR products
Fig A1.11 Gel analysis of FADD PCR products
Fig A1.12 Gel analysis of PIGPC1 PCR products
Fig A1.13 Gel analysis of TMS1 PCR products
Fig A2.1 DHPLC chromatograms
Fig A4.1 *BIK* QMSP primer/probe optimisation
Fig A4.2 *BNIP3* QMSP primer/probe optimisation
Fig A4.3 *CDKN2A* QMSP primer/probe optimisation
Fig A4.4 *CpG1 cFLIP* QMSP primer/probe optimisation
Fig A4.5 *CpG2 cFLIP* QMSP primer/probe optimisation
Fig A4.6 *DCR1* QMSP primer/probe optimisation
Fig A4.7 *DCR2* QMSP primer/probe optimisation
Fig A4.8 *TMS1* QMSP primer/probe optimisation
Fig A4.9 *TMS1* QRT-PCR primer/probe optimisation
Fig A4.10 *CDKN2A* QRT-PCR primer/probe optimisation
Fig A4.11 DDCT validation for TMS1
Fig A4.12 DDCT validation for CDKN2A
Fig A4.13 Efficiency of TMS1 reactions
Fig A4.14 Efficiency of CDKN2A
Fig A5.1 Normal probability plot of age of tumour samples
Fig A5.2 Normal probability plot of age of BPH samples
Fig A5.3 Normal probability plot of PSA of tumour samples
Fig A5.4 Normal probability plot of PSA of BPH samples
Fig A8.1 Methylation heat map for GSTP1, IGFBP7 and SFRP2 in prostate cancer samples

LIST OF TABLES

CHAPTER 1: INTRODUCTION

Table 1.1 Tumour, Node, Metastases (TNM) classification of prostate cancer

CHAPTER 2: MATERIALS AND METHODS

Table 2.1 2X Reverse Transcription master mix
Table 2.2 PCR primer sets and assay conditions
Table 2.3 Bisulfite sequencing reaction
Table 2.4 QMSP primers and probes
Table 2.5 TaqMan Gene Expression assays

CHAPTER 3: *IN SILICO* IDENTIFICATION OF POTENTIAL APOPTOSIS-RELATED GENE TARGETS OF PROMOTER HYPERMETHYLATION IN PROSTATE CANCER.

Table 3.1 Apoptotic gene identified from a methylation candidate gene bank.
Table 3.2 List of Key Apoptotic genes
Table 3.3 List of apoptotic genes with a 5' promoter CpG island
Table 3.4 In silico identification of potential apoptotic-related gene targets of promoter hypermethylation in prostate cancer

CHAPTER 4: DISCOVERY OF APOPTOTIC-RELATED GENE TARGETS OF ABERRANT METHYLATION IN PROSTATE CANCER UTILIZING A DHPLC METHYLATION SCREENING STRATEGY

Table 4.1 Summary of prostate cancer cell lines
Table 4.2 Summary of DHPLC Methylation screen in prostate cancer cell lines

CHAPTER 5: QUANTIFYING METHYLATION AND GENE EXPRESSION LEVELS OF APOPTOTIC-GENE TARGETS OF METHYLATION IN PROSTATE CANCER CELL LINES

Table 5.1 Summary of QMSP results

CHAPTER 6: INVESTIGATING THE METHYLATION STATUS OF A PANEL OF SEVEN APOPTOTIC-RELATED GENES IN PROSTATE CANCER TISSUE SAMPLES.

Table 6.1 Characteristics of AMNCH & IMM prostate cancer groups
Table 6.2 Summary data for patient groups
Table 6.3 Slope and correlation co-efficient of standard curves
Table 6.4 Methylation frequency of a 7-gene apoptotic gene panel in prostate cancer, normal prostate, HGPIN and BPH
Table 6.5 Summary of methylation status of 5-gene Panel and relationship to clinicopathologic factors

APPENDICES

Table A3.1 Predicted transcription factor binding sites for BIK that cover CpG sites
Table A3.2 Predicted transcription factor binding sites for BNIP3 that cover CpG sites
Table A3.3 Predicted transcription factor binding sites for CDK2NA that cover CpG sites
Table A3.3 Predicted transcription factor binding sites for CpG1 CFLIP that cover CpG sites
Table A3.5 Predicted transcription factor binding sites for TMS1 that cover CpG sites
Table A3.6 IUB Ambiguity code
Table A4.1 BIK Primer/Probe optimisation
Table A4.2 BNIP3 Primer/Probe optimisation
Table A4.3 CDK2NA Primer/Probe optimisation
Table A4.4 CpG 1 cFLIP Primer/Probe optimisation
Table A4.5 CpG 2 cFLIP Primer/Probe optimisation
Table A4.6 DCR1 Primer/Probe optimisation
Table A4.7 DCR2 Primer/Probe optimisation
Table A4.8 TMS1 Primer/Probe optimisation
Table A4.9 TMS1 QRT-PCR Primer/Probe gene expression optimisation
Table A4.10 CDKN2A QRT-PCR Primer/Probe gene expression optimisation
Table A4.11 Average CT value for PGK1 in various cell lines and after treatment with 5-Aza-CdR
Table A6.1 Characteristics of AMNCH prostate cancer study population
Table A6.2 Characteristics of IMM prostate cancer study population
Table A6.3 HGPIN study population
Table A6.4 Normal study population
Table A6.5 BPH study population
Table A7.1 Summary of QMSP results for prostate cancer tissue samples
Table A7.2 Summary of QMSP results for benign tissue samples
Table A7.3 Summary of QMSP results for HGPIN tissue samples
Table A7.4 Summary of QMSP results for BPH tissue samples

ABBREVIATIONS

5AR	5α-reductase
AIF	Apoptosis inducing factor
AMACR	Alpha-methylacyl-CoA racemase
AMNCH	Adelaide and Meath Hospital incorporating the Children's Hospital
APAF1	Apoptotic peptidase activating factor
AR	Androgen receptor
ATCC	American Type Culture Collection
BAD	BCL2-associated agonist of cell death
BAX	BCL2-associated X protein
BH	Bcl-2 homology
BID	BH3 interacting domain death agonist
BIM	Bcl2-interacting mediator of cell death
BIMS	Bio-resource Information Management System
BIMS	Biobank Information Management System
BPH	Benign prostatic hyperplasia
CAD (DFF40)	Carbamoyl-phosphate synthetase 2
CASP3	Caspase 3
CASP7	Caspase 7
CASP8	Caspase 8
CASP9	Caspase 9
CDKN2A	Cyclin-dependent kinase inhibitor 2A
CFOS	v-fos FBJ murine osteosarcoma viral oncogene homolog
ChIP	Chromatin immunoprecipitation
CIMP	CpG island methylator phenotype
COBRA	Combined Bisulfite Restriction Analysis
CpGs	cytosine-guanine dinucleotides
CYCS	Cytochrome C
DAPk	Death-associated protein kinase 1
DED	death effector domains
DHPLC	Denaturing high performance liquid chromatography
DHT	Dihydrotestosterone
DIABLO	Diablo homolog (Drosophila)
DISC	Death Inducing Signalling Complex
DMSO	dimethyl sulfoxide
DNMT	DNA methyltransferase
DOP-PCR	Degenerate oligonucleotides primered PCR
DRE	Digital Rectal Examination
EAU	European Association of Urology
EGCG	Epigallocatectin 3-gallate
EGF	Bovine pituitary extract
ERSPC	European Randomized Study of Screening for Prostate Cancer
ETAO	Ethidium bromide acridine orange
FADD	Fas (TNFRSF6)-associated via death domain
FAS	Fas (TNF receptor superfamily, member 6)

FASL	FAS ligand
FCS	Foetal calf serum
FFPE	Formalin-fixed and paraffin-embedded
FRET	Fluorescence resonance energy transfer
H&E	Haematoxylin and eosin
HDAC	Histone deacetylase
HGPIN	High-Grade Prostatic Intraepithelial Neoplasia
HIF	Hypoxic inducible factor
HP1	heterochromatin protein 1
HRE	(HIF)-1α responsive element
HRK	Harakiri
Hypo M	hypomethylation
IAP	Integrin-associated protein
IAPs	inhibitor of apoptosis proteins
IAPs	inhibitor of apoptosis proteins
ICAD (DFF45)	Inhibitor of CAD
LDA	Low Density Array
MBD	Methylcytosine DNA-binding domain
MeSH	Medical Subject headings
MGB	Minor-groove binding
miRNAs	MicroRNAs
MOMP	Mitochondrial outer membrane potential
MSI	Microsatellite instability
MSP	Methylation specific PCR
NI	Northern Ireland
NIM	Normalized index of methylation
PAR4 (PAWR)	Prostate apoptosis response 4 protein (PRKC apoptosis WT1 regulator)
PCRC	Prostate Cancer Research Consortium
PGK1	Phosphoglycerate kinase
PIN	Prostatic intraepithelial neoplasia
PMAIP1	Phorbol-12-myristate-13-acetate-induced protein 1
PMC	Partial methylation control
PSA	Prostate Specific Antigen
PUMA	p53 up-regulated modulator of apoptosis
QMSP	Quantitative methylation specific PCR
QRT-PCR	Quantitative real-time PCR
RB	Retinoblastoma
RISC	RNA Induced Silencing complex
RMS	Relative methylation score
ROI	Republic of Ireland
SAM	S-adenosylmethione
SFN	Sulforaphane
SJH	St. James's Hospital
SNPs	Single nucleotide polymorphisms
SOP	Standard Operating Procedures
SPHK2	Sphingosine kinase 2

TFBS	Transcription factor binding sites
TMS1	Target of methylation induced silencing
TMS1	Target of methylation-induced silencing 1
TNF	Tumour necrosis factor
TNFSF10	Tumor necrosis factor (ligand) superfamily, member 10
TNM	Tumour, Node, Metastases
TRADD	TNFRSF1A-associated via death domain
Trail	TNF-related apoptosis-inducing ligand
TRUS	Transrectal ultrasound
TURP	Transurethral resection
UCSC	University of California Santa Cruz
UMA	Universal unmethylated DNA A
UMB	Universal unmethylated DNA B
VDR	Vitamin D receptor
XAF1	XIAP Inhibitor of apoptosis factor 1

PUBLICATIONS

- Review article: "The emergence of DNA methylation as a key modulator of aberrant cell death in prostate cancer". Murphy TM, Perry AS, Lawler M. Endocrine-Related Cancer (2008) **15** 11-25

- Research paper: "DHPLC screening strategy identifies novel apoptotic gene targets of aberrant promoter hypermethylation in prostate cancer". Murphy TM, Lawler M, Sullivan L, Lane C, O'Connor L, Barrett C, Hollywood D, Lynch T, Perry AS . Manuscript submitted to "The Prostate".

PRESENTATIONS (Oral/Poster)

- Irish Association of Cancer research: Galway, Mar (Poster)
- Cancer Genomics Masterclass: IMM, TCD Dec 08 (Oral; First Prize)
- All Ireland Cancer Conference: Four Seasons Dec 08 (Poster)
- IMM Annual meeting, TCD: November 08 (Poster)
- AACR Cancer epigenetics conference: Boston May 08 (Poster).
- Cancer 08: Dublin Castle, May 08 (Poster; First prize).
- 7th World Basic Urological Research Congress, UCD: September 07 (Poster)
- School of Medicine Postgraduate Research day, IMM, TCD: September 07 (Oral)
- IMM Annual meeting, TCD: November 07 (Poster)
- DMMC international workshop: Epigenetics, from Mechanisms to Medicines: UCD June 07 (Poster)
- Gordon Research Conference: Cancer Genetics and Epigenetics (Il Cioco, Italy) May, 2007 (Poster)

AWARDS

- HRB travel grant award to attend the NCI summer curriculum in cancer prevention (Washington, Aug 2009)
- First prize, Oral presentation. Cancer Genomics Masterclass, IMM, TCD (Dec 2008)
- First prize, Poster presentation. Cancer 2008, Dublin Castle (May, 2008)
- Cancer Research Ireland "Oncology Scholars Travel Award" (2007)

TABLE OF CONTENTS

CHAPTER 1 INTRODUCTION

1.1 General introduction **2**

1.2 The prostate gland **2**

1.2.1 Anatomy 3

1.2.2 Function 5

1.2.3 Endocrine control of prostate growth 5

1.3 Diseases of the prostate **6**

1.3.1 Benign prostatic hyperplasia 6

1.3.2 Neoplasia 7

1.3.2.1 High-grade prostatic intraepithelial neoplasia of the prostate 7

1.3.2.2 Pathophysiology and natural history of prostate cancer 9

1.4 Epidemiology **11**

1.4.1 Prostate cancer incidence rate 11

1.4.2 Prostate cancer mortality rates 12

1.4.3 Prostate cancer in Ireland 14

1.4.3.1 Prostate cancer research consortium 18

1.5 Diagnosis and prognostic measures in prostate cancer **21**

1.5.1 Prostate specific antigen (PSA) 21

1.5.2 Limitations of PSA as a prostate cancer biomarker 22

1.5.3 PSA screening: Decreasing mortality rates or over-diagnosis? 22

1.5.4 TRUS biopsy and Gleason grading 24

1.6 Treatment of prostate cancer **25**

1.6.1 Early and locally advanced prostate cancer 25

1.6.1.2 Pathologic staging of prostate cancer 27

1.6.2 Metastatic disease 28

1.7 Risk factors and aetiology **29**

1.7.1 Environmental influences on prostate cancer 29

1.7.2 Genetics of prostate cancer 31

1.7.2.1 Inherited prostate cancer 31

1.7.2.2 Chromosomal alterations in prostate cancer 31

1.7.2.3 Polymorphisms and susceptibly to prostate cancer 32

1.7.2.4 Androgen independent prostate cancer and the role of genetics 33

1.7.2.5 Alterations of gene expression patterns in prostate cancer versus normal prostate 34

1.8 Epigenetics and prostate cancer **35**

1.8.1 The "Prima Donna" of epigenetics: DNA methylation 35

1.8.2 DNA methylation and transcriptional repression 37

1.8.3 Gene methylation in cancer 39

1.8.3.1 DNA hypomethylation in cancer 39

1.8.3.2 DNA hypermethylation and cancer 39
1.9 Apoptosis 43
1.9.1 Death receptor pathway: caspase activation 43
1.9.2 Mitochondrial apoptotic pathway: caspase activation 44
1.9.3 The deregulation of apoptosis in prostate cancer 48
1.10 DNA methylation of apoptotic genes: A key survival mechanism in prostate cancer 49
1.11 Hypothesis 51

CHAPTER 2 MATERIALS AND METHODS

2.1 Identifying potential targets of promoter hypermethylation 53
2.1.1 Searching a methylation candidate gene bank 53
2.1.2 Identifying biological role in apoptosis 53
2.1.3 Screening genes for 5' CpG Islands 55
2.1.4 Identifying genes with susceptibility to hypermethylation and/or reduced expression 56
2.1.4.1 Microarray studies 56
2.1.4.2 Literature review 56
2.1.5 Candidate prioritising 56
2.2 Cell culture 56
2.2.1 Solutions and media 56
2.2.2 Prostate cell lines 57
2.2.3 Colon Cancer cell lines 57
2.2.4 Thawing cells 58
2.2.5 Culturing cells 58
2.2.6 Passaging cells 58
2.2.7 Freezing cells 59
2.2.8 Drug Treatment to induce DNA hypomethylation 59
2.2.9 Preparation of cells for nucleic acid extractions 59
2.3 Prostate tissue samples 60
2.3.1 Ethical approval 60
2.3.2 Retrospective sample collection 60
2.3.2.1 Patient selection 60
2.3.2.2 Specimen retrieval 61
2.4 Nucleic acid isolation 63
2.4.1 Nucleic acid isolation from cultured cell lines 63
2.4.1.1 DNA extraction 63
2.4.1.2 RNA extraction 64
2.4.1.3 cDNA Synthesis 64
2.4.2 From formalin fixed paraffin embedded (FFPE) tissue 65
2.4.2.1 Deparifinization of FFPE tissue 65
2.4.2.2 DNA extraction 66

2.5 Methylation techniques **67**
2.5.1 Methylation Controls 67
2.5.2 Partial Methylation Control 67
2.5.2.1 Restriction digestion of SSsI methylase treated DNA 67
2.5.3 Bisulfite modification 68
2.5.4 Bisulfite Polymerase chain reaction 70
2.5.5 Denaturing High Performance Liquid Chromatography (DHPLC) 74
2.5.5.1 Optimisation of DHPLC assay: Choosing the best partially denaturing temperature. 75
2.5.5.2 Analysis of PCR products using DHPLC 75
2.5.6 Bisulfite sequencing 75
2.5.6.1 Cloning PCR products 76
2.5.6.2 Bisulfite Sequencing 79
2.5.7 Quantitative methylation specific PCR 80
2.5.7.1 Real-Time (TaqMan) PCR 81
2.5.7.2 QMSP primer and probe design 85
2.5.7.3 QMSP reactions 87
2.5.7.4 Quantitation of methylation levels 88
2.6 Expression analysis in prostate cancer cell lines **90**
2.6.1 Relative quantitation using the comparative C_T method 90
2.6.2 Quantitative RT-PCR assay design 90
2.6.3 Quantitative RT-PCR reactions 91
2.7 Statistical analysis **92**

CHAPTER 3 IN SILICO IDENTIFICATION OF POTENTIAL APOPTOSIS-RELATED GENE TARGETS OF PROMOTER HYPERMETHYLATION IN PROSTATE CANCER.

3.1 Introduction **95**
3.2 Experimental strategy **95**
3.3 Identifying apoptotic gene targets of hypermethylation in prostate cancer. **97**
3.3.1 Searching a methylation candidate gene bank 97
3.3.2 Identifying key apoptotic genes 97
3.3.3 Screening for 5'CpG islands 98
3.3.4 Identifying genes with susceptibility to hypermethylation and/or reduced expression in prostate cancer. 100
3.3.4.1 Microarray studies 100
3.3.4.2 Literature review 100
3.3.5 Candidate prioritising 101
3.4 Discussion **104**

CHAPTER 4 DISCOVERY OF APOPTOTIC-RELATED GENE TARGETS OF ABERRANT METHYLATION IN PROSTATE CANCER UTILIZING A DHPLC METHYLATION SCREENING STRATEGY

4.1 Introduction **109**

4.2 Methylation unbiased PCR **112**

4.3 Methylation screen using a DHPLC platform **112**

4.3.1 Screening genes for methylation in prostate cell lines using DHPLC 113

4.4 Validation of DHPLC methylation profiles using bisulfite sequencing **118**

4.5 Generating a partial methylation control **121**

4.6 Investigating the methylation status of cFLIP in colon cancer samples **123**

4.7 Investigating the methylation status of docetaxel resistant PC3 prostate cancer cell line (D12-PC3) and age-matched PC3 control **124**

4.6 Discussion. **125**

CHAPTER 5 QUANTIFYING METHYLATION AND GENE EXPRESSION LEVELS OF APOPTOTIC-GENE TARGETS OF METHYLATION IN PROSTATE CANCER CELL LINES

5.1 Introduction **134**

5.2 In silico promoter CpG characterization **134**

5.3 QMSP assay validation **139**

5.4 Quantitative methylation analysis of a 7-gene apoptotic panel **142**

5.4.1 Methylation frequency of the 7- gene apoptotic panel 143

5.5 Gene expression analysis of 7-gene panel **146**

5.5.1 Validation of TMS1 and CDKN2A gene expression assays. 147

5.5.2 Gene expression analysis in prostate cancer cells 147

5.6 Discussion **153**

CHAPTER 6 INVESTIGATING THE METHYLATION STATUS OF A PANEL OF SEVEN APOPTOTIC-RELATED GENES IN PROSTATE CANCER TISSUE SAMPLES.

6.1 Introduction **158**

6.2 Clinical and pathological features of study population **160**

6.3 Methylation status in prostate tissue samples **163**

6.3.1 Methylation frequency of a 7-gene apoptotic panel. 164

6.3.2 Methylation levels in prostate cancer 167

6.3.3 Correlation between methylation of genes 168

6.3.4 Associations with clinicopathologic features 172

6.4 Discussion **175**

6.4.1 Cell lines versus prostate cancer: Similar methylation patterns? 177

6.4.2 5-gene panel in a diagnostic and prognostic setting 178

CHAPTER 7 DISCUSSION & FUTURE DIRECTIONS

7.1 General discussion **182**

7.1.1 In Silico analysis and DHPLC screening strategy identifies novel apoptotic gene targets of aberrant promoter hypermethylation in prostate cancer 172
7.1.2 Quantification of methylation levels using quantitative methylation specific PCR 185
7.1.3 Identification of a 5 gene "apoptotic methylation signature" 187
7.1.3.1 Methylation of 5-gene apoptotic panel in metastatic prostate cancer 189
7.1.4 Methylation and therapeutic targeting 189
7.2 Future directions 193
7.2.1 Future investigation of possible apoptotic-related gene targets of methylation in prostate cancer 193
7.2.2 CpG island methylator phenotype in prostate cancer 193
7.2.3 5-gene "apoptotic methylation signature": putative cancer biomarker? 195
7.2.3.1 DNA methylation: a promising new cancer biomarker 195
7.2.3.2 Detection of hypermethylation in biopsies 196
7.2.3.3 Detection of hypermethylation in bodily fluids 196
7.2.4 The cFLIP paradox: Examining the role of differential expression of cFLIP splice variants 198
7.2.5 Investigating the methylation status of Docetaxel resistant PC3 prostate cancer cell line (D12-PC3) and an age-matched PC3 control using a nimblegen array 199
7.2.6 Investigating racial differences among men with prostate cancer 200
7.2.7 DNA methylation, miRNAs and histone modifications: Linking it all together. 200
7.2.7.1 Methylation of miRNA 201
7.2.7.2 Histone modifications 202
7.3 Conclusion 203

APPENDIX

A1 PCR products generated and analysed by gel electrophoresis for each of the target genes in the prostate cell lines 205
A1.1 PCR agarose gel analysis for the 7 prostate cell lines 205
A2 DHPLC chromatograms 214
A3 Transcriptional elements associated with promoter regions 217
A4 Taqman real-time PCR primer and probe optimisation and validation 222
A4.1 QMSP primer/probe optimisation 222
A4.1.1 BIK QMSP primer and probe optimisation 222
A4.1.2 BNIP3 QMSP primer and probe optimisation 223
A4.1.3 CDKN2A QMSP primer and probe optimisation 224
A4.1.4 CpG1 cFLIP QMSP primer and probe optimisation 225
A4.1.5 CpG2 cFLIP QMSP primer and probe optimisation 226
A4.1.6 DCR1 QMSP primer and probe optimisation 227
A4.1.7 DCR2 QMSP primer and probe optimisation 228
A4.1.8 TMS1 QMSP primer and probe optimisation 229
A4.1.9 TMS1 QRT-PCR primer and probe optimisation 230
A4.10 CDKN2A QRT-PCR primer and probe optimisation 231
A4.2 Validation of ΔΔCt and efficiency test for non-inventoried primers and probes 232

A4.2.1 Validation of ΔΔCt of gene targets 232
A4.2.2 Individual efficiency test for non-inventoried primers and probes 234
A5 Statistics 236
A5.1 Paired T test. 236
A5.2 Unpaired T- Test 238
A5.3 Fisher's Exact test. 241
A5.4 Krustal-Wallis test and one-way ANOVA Tukey pairwise. 257
A6 Patient clinicopathological features 268
A7 Relative methylation scores of patient samples 273
A8 Methylation heat map for GSTP1, IGFBP7 and SFRP2. 305

REFERENCES 307

CHAPTER 1
INTRODUCTION

1.1 GENERAL INTRODUCTION

Prostate cancer represents an important global public health problem. Worldwide, it is the most common noncutaneous cancer in men (Jemal et al., 2008). In Ireland alone, over 700 deaths per year are attributable to the disease (Donnelly, 2009). In recent years, prostate cancer five year survival rates have been ranked third highest of all cancers (Toms, 2004). Much of this improvement is due to an increase in the number of men being diagnosed with early stage prostate cancer as a result of widespread use of prostate specific antigen (PSA) testing. However, PSA has a number of limitations as a cancer biomarker. Firstly, it lacks both specificity and sensitivity and its role in decreasing mortality rates is highly controversial. PSA-based screening has been shown to reduce the rate of death from prostate cancer by 20% but was also associated with a high risk of over diagnosis in the screening population (Schroder et al., 2009). Currently, the European Association of Urology does not advocate the adoption of population screening for prostate cancer as a public health policy due to the large overtreatment effect. The difficulty, therefore, remains in distinguishing between clinically indolent prostate cancers and aggressive prostate cancers with the potential to kill the patient.

The identification of novel diagnostic and prognostic markers is urgently required to enhance the predictive value of current screening tools. Understanding the natural history and aetiology of prostate cancer is essential. Dissecting disease initiation and progression at the molecular scale, specifically focussing on fundamental pathways (such as cellular death) which are deregulated in cancer, is likely to be a significant source of information to aid in target identification for novel disease biomarkers and therapeutic targets. Recently, analysis of gene methylation has emerged as a putative source of prostate specific cancer biomarkers (Ellinger et al., 2008; Soengas et al., 2001).

1.2 THE PROSTATE GLAND

The prostate is a small exocrine gland found only in the male reproductive system. Prostate is derived from the Greek word "prostates" literally meaning "the one who stands before" and was termed so by the anatomist Herophilus, as it stood before the testes (http://www.medterms.com). A complete description

of the gland's internal structure, physiology and pathology is relatively recent (Kirby et al., 2001).

1.2.1 Anatomy

A healthy prostate gland is a walnut-sized organ, which lies in the pelvic cavity immediately in front of the rectum (Figure 1.1) and weighs ~ 18 g, measures 3 cm in length, 4 cm in width and 2 cm in depth. In unhealthy prostates, the gland can weigh as much as 100g, resembling the size of an orange (Bostwick, 1999). The entire prostate gland is enclosed by an outer capsule of fibrous tissue (Ross J.S., 1971).

The prostatic epithelium is composed of two major cell types, epithelial cells and stromal cells. Epithelial cells can be further characterised into columnar secretory, neuroendocrine, transient proliferating and basal cells (Veltri, 2007). Columnar secretary cells are terminally differentiated and have a low proliferation rate. These cells are morphologically distinct due to the large number of secretary granules present. Neuroendocrine cells reside among the more abundant columnar cells in the normal prostate. There are two types of neuroendocrine cells, one type which possesses specialised microvilli that protrude into the lumen and the second contain long dendrite-like structures, which extend to nearby epithelial and basal cells. Transit-amplifying cells are a class of intermediate epithelial cells and are similar to undifferentiated stem cells and non-proliferating basal cells. Basal cells reside on the basement membrane in between that of the columnar epithelial cells. Basal cells have a low mitotic index and are less abundant, accounting for less than 10% of the total cell number. Moreover, basal cells express keratin subtypes that are specific to basal cells (Veltri, 2007).

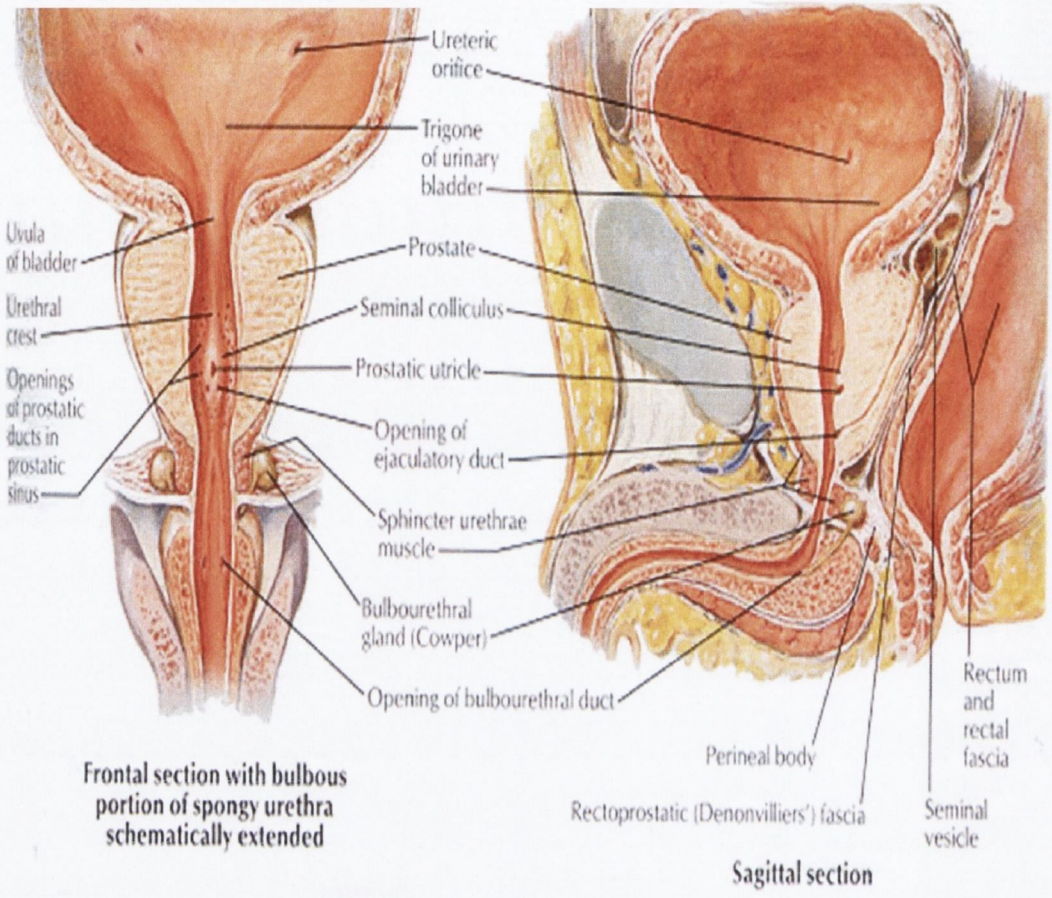

Figure 1.1

Prostate and seminal vesicles. a) Frontal section, b) sagittal section. From Netter FH: Atlas of human anatomy, 2nd ed. New Jersey, ICON Learning Systems, 2001, p358.

The stroma is continuous with the capsule and composed of collagen, elastin and abundant smooth and striated muscle. It surrounds and supplies the glands of the prostate and contracts during ejaculation to express prostate secretions into the urethra (Veltri, 2007).

Figure 1.2 illustrates the different zones of the prostate. The transition zone surrounds the urethra proximal to the entry of the ejaculatory ducts and consists of 5-10% of the glandular prostate mass (Crawford, 2009). The central zone is located below the proximal urethral segment and consists of ~20-25% of the mass of the prostate. The ejaculatory ducts pass through this zone prior to entering the urethra (Scardino, 2000). The peripheral zone covers the majority

(70-75%) of the adult structure of the prostate gland (Crawford, 2009).

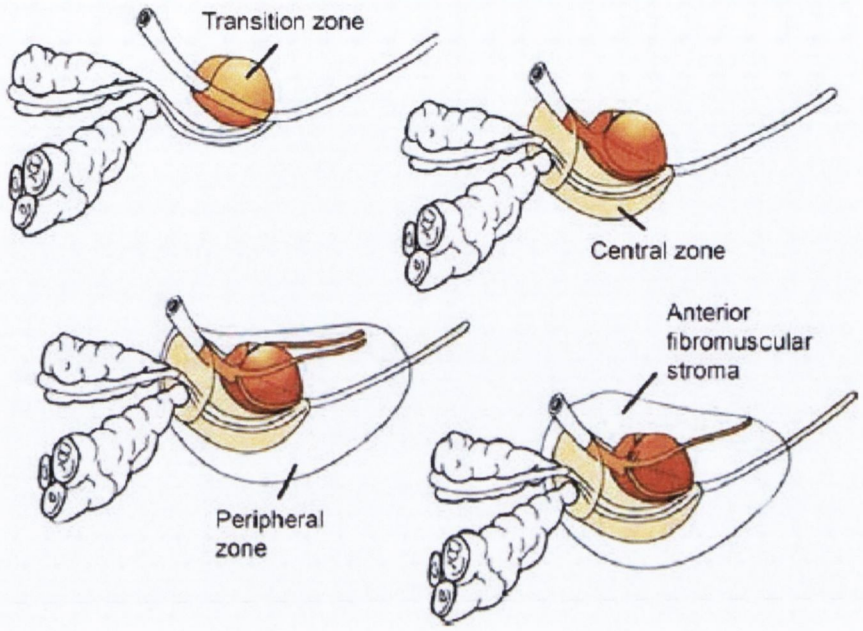

Figure 1.2

Different zones of the prostate. Image obtained from (Crawford, 2009).

1.2.2 Function

The primary function of the prostate is to store and secrete an alkaline fluid that constitutes 25-30% of semen volume. The prostate contains smooth muscles which contract to expel prostatic fluid through tiny ducts into the urethra, where it mixes with spermatozoa and other fluid.

1.2.3 Endocrine control of prostate growth

Prostate growth, maintenance and secretary function are stimulated by the presence of particular hormones and growth factors. Testosterone is the key circulating androgen in men (Chodak et al., 1994). Testosterone functions as a pro-hormone, whereby it is converted to dihydrotestosterone (DHT) in the prostatic stromal and basal cells by an enzyme known as 5α-reductase(5AR) (Crawford, 2009). The process of testosterone conversion by 5AR into DHT or estrogens by aromatase is irreversible (Veltri, 2007). Androgens, estrogens and adrenal steroids have an important effect on different cells and tissue that can vary dependent on development stage and age (Veltri, 2007).

Signalling for prostate growth begins in the hypothalamus, whereby it releases a small peptide referred to as luteinizing hormone-release hormone. Upon stimulation of this hormone, the pituitary releases luteinizing hormone which is transported to the testes, whereby it stimulates the leydig cells to produce *de novo* steroid synthesis and the release of testosterone, the major serum androgen. The peripheral conversion of testosterone by aromatization forms estrogens in the male. In addition, the adrenal gland is under stimulation by adrenocortocotrophic hormone and releases the minor androgens (Veltri, 2007), contributing to control of prostate growth.

Inside the cell, both testosterone and DHT bind to the same high-affinity androgen receptor (AR) protein. The AR binds to specific DNA binding sites in the nucleus, whereby it acts as a potent transcription factor and increases transcription of androgen dependent genes (including both 5α-reductase and PSA). Androgen withdrawal results in both inactivation of key androgen-dependent genes and activation of specific genes involved in programmed cell death (Isaacs, 1984).

1.3 DISEASES OF THE PROSTATE

1.3.1 Benign prostatic hyperplasia

Benign prostatic hyperplasia (BPH) can be defined as the non-malignant enlargement of the prostate. BPH is the most common benign tumour in men ages >60 years (Ziada et al., 1999). BPH primarily affects the transition and periurethral zones. The two most important contributory factors in BPH in man are aging and the presence of functional testes. (Ziada et al., 1999). BPH is characterised by proliferation of stromal and epithelial cells of the prostate, resulting in an enlarged prostate. However these proliferating cells do not habitually progress to malignancy. Hence, BPH serves as a useful model for comparison with prostate cancer cells.

The clinical systems of BPH include urinary retention, poor bladder emptying and lower urinary tract symptoms (Roehrborn and McConnell, 2002). Men

who exhibit mild- moderate symptoms of BPH are the best candidates for watchful waiting. However patients who present with severe symptoms will require surgery. Transurethral resection of the prostate (TURP) is considered the gold standard for the surgical management of BPH (McEleny et al., 2002). Many of the symptoms of prostate cancer and BPH are similar, however there is no evidence to suggest that BPH is a precursor for prostate cancer (McEleny et al., 2002).

1.3.2 Neoplasia

1.3.2.1 High-grade prostatic intraepithelial neoplasia of the prostate: the precursor lesion of prostate cancer

In 1969, prostatic intraepithelial neoplasia (PIN) was first described as a neoplastic proliferation of prostatic epithelial cells confined to prostatic ducts of acini (McNeal, 1969). In 1987, the widely used terminology "prostatic intraepithelial neoplasia" was introduced by Bostwick and Brawler (Bostwick and Brawer, 1987).

A number of morphologic changes define PIN, whereby prostatic epithelia cells are present in large and branched glands. Epithelial proliferation typical of PIN produced crowded layer of cells with cytologic atypia, such as hyperchromasia, nuclear irregularity and prominent nucleoli (Zynger and Yang, 2009). Such cytological characteristics are similar to those identified in invasive prostate cancer. The architecture of PIN however appears normal, whereby basal cells can be observed around the periphery of the gland (Figure 1.3), which can be readily visualised using haematoxylin and eosin (H&E) staining. Often the presence of basal cells helps distinguish high grade prostatic intraepithelial neoplasia (HGPIN) from prostate cancer (Bostwick and Brawer, 1987; Brawer et al., 1985).

PIN can be subdivided into two groups, low-grade and high-grade (Drago J.R., 1992). HGPIN is a major precursor of prostate cancer and hence is more clinically significant than low-grade (Zynger and Yang, 2009). Diagnosis of HGPIN can only be determined by microscopic examination of prostatic tissue

taken from needle core biopsy, transurethral resection (TURP) or radical prostatectomy (Zynger and Yang, 2009).

In 1986, an association between PIN and invasive cancer was first described (McNeal and Bostwick, 1986). Similar to prostate cancer, HGPIN is multifocal, occurs in the peripheral zone of the prostate and was found more often in men with a diagnosis of prostate cancer than persons without (Zynger and Yang, 2009). Indeed, 80-90% of radical prostectomy specimens with a diagnosis of prostate cancer also contained adjacent HGPIN (Qian et al., 1997).

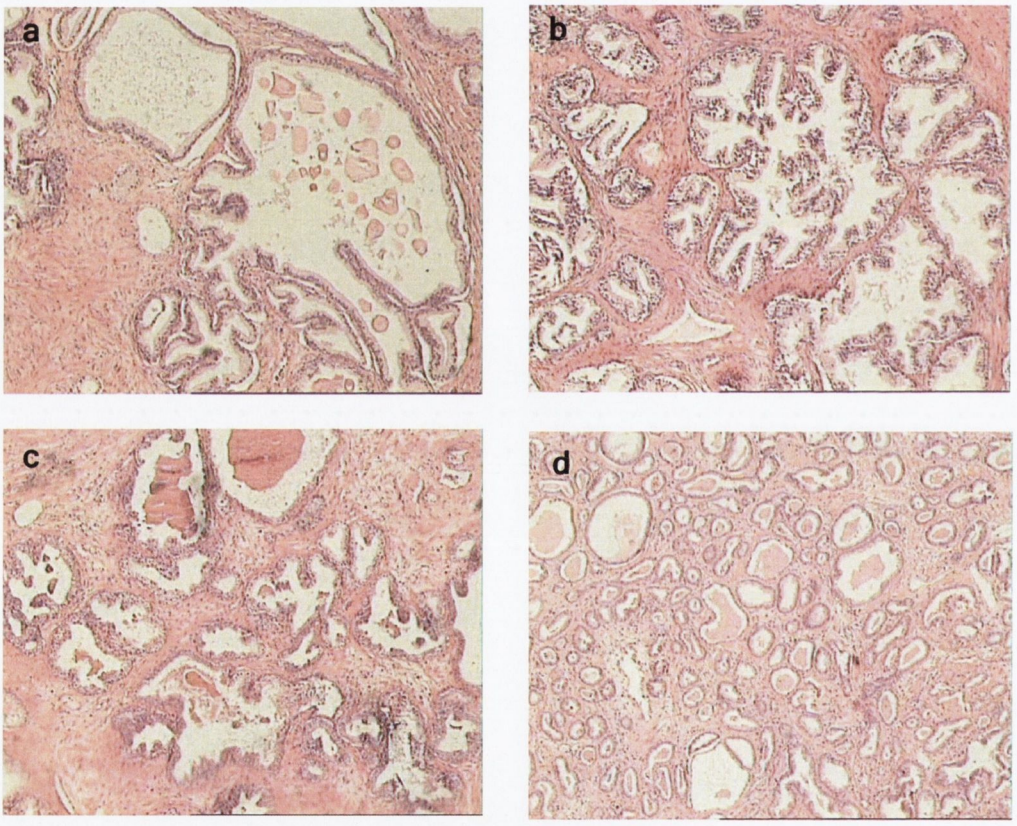

Figure 1.4
Prostate tissue specimen. H&E stained prostate tissue sections. a) normal prostate contains glands consisting of 2 epithelial cell layers, and is composed of a greater stromal content relative to the tumour tissue. b) BPH, c) HGPIN and d) prostate cancer. 4X objective used in all photographs (Image obtained from Perry AS, PhD Thesis: Investigating novel targets if DNA methylation for the early detection of prostate cancer, Oct 2006).

1.3.2.2 Pathophysiology and natural history of prostate cancer

Almost all cases of prostate cancer are adenocarcinoma (Scardino, 2000). Approximately 4% of prostate cancer cases display transitional cell morphology and are believed to originate from the urogenital lining of the prostatic urethra. A relatively small number of cases exhibit neuroendocrine morphology, and are thought to derive from neuroendocrine stem cells normally present in the prostate (Crawford, 2009). Prostate cancer occurs primarily (70%) in the peripheral zone, while the remaining develop in either the transitional or central zones (Crawford, 2009).

Prostate cancer is often multifocal in nature and lesions are frequently present in different zones and are typically of different grades (Bostwick, 1999). Prostatic adenocarcinomas usually consists of a proliferation of small acini with multiple patterns (Bostwick, 1999). Diagnosis relies heavily on the architecture and cytologic features of the prostate, such as irregular glandular contours, variation in gland size, nuclear and nucleolar enlargements. The basal cell layer is key in the diagnosis of adenocarcinoma, whereby an intact basal cell layer is located at the periphery of benign glands, but is entirely absent in carcinoma (Figure 1.4) (Bostwick, 1999).

Asymptomatic prostate cancer is common, largely due to the majority of adenocarcinomas arising in the periphery of the gland, distant from the urethra. However, the following symptoms may be an indication of the disease: problems with urination, hematuria (blood in the urine), bone pain (often indicative of metastatic disease), constant fatigue, weight loss and chronic-severe back pain.

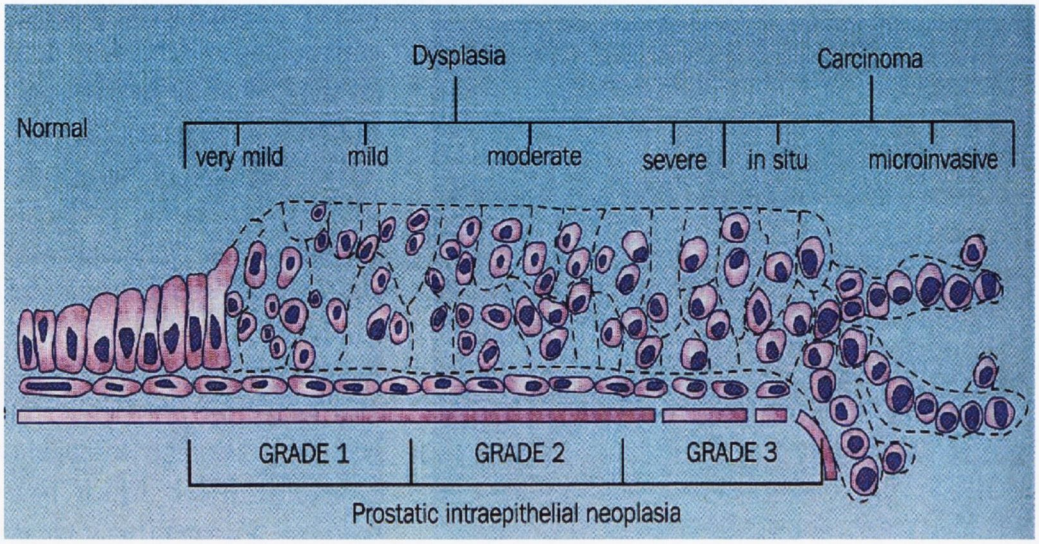

Figure 1.4

Prostate cancer development. From very mild to severe stages of abnormal development, changes occur to the spatial arrangements of the luminal cells and to their nuclear size and shape. In carcinoma, there is an enlargement of the nucleus and disappearance of the basal cellular layer, one of the hallmarks of prostate cancer. Kirby R: Prostate Cancer, 2nd ed. London, Mosby, 2001, pg 14.

Our understanding of the natural history of prostate cancer is far from complete. This is partly a result of the heterogeneous behaviour of the disease from both a morphological and clinical perspective (Scardino, 2000). Prostate cancer grows slowly and often does not manifest itself during the lifetime of an individual. Hence, most men die **with** prostate cancer rather than **from** prostate cancer (Bostwick, 1999). Men under the age of 40 rarely present with prostate cancer. However the incidence rate increases dramatically in the fifth decade of life to 40%, and to 80% by the age of 80 (Bostwick, 1999). A study by Chodak et al, found that patients with lower grade tumours, exhibiting highly to moderately differentiated tumour cells, had a 10 year disease free survival rate of 87%. In contrast, high-grade or poorly differentiated tumours were associated with a 34% survival rate (Chodak et al., 1994). Johansson and colleagues examined the natural history of prostate cancer and determined the potential for survival by analyzing survival following watchful waiting in a

large patient cohort (n=223) (Johansson et al., 2004). Overall, 89 patients (40%) experienced progression of disease. Of these, 39 (17% of the total cohort) developed advanced disease. Similar disease free survival rates observed in the Chodak study were also reported here after 15 year follow-up period. However, further follow-up from 15 to 20 years revealed a decrease in cumulative progression-free survival (45% to 36%) and survival without metastases (76.9% to 51.2%). These findings suggest that clinically localised prostate cancer may result in tumour progression and metastases in the long term; this data supports early, radical treatment, particularly among patients with an estimated life expectancy exceeding 15 years.

1.4 EPIDEMIOLOGY

1.4.1 Prostate cancer incidence rates

Worldwide, prostate cancer is highly prevalent and is the most common noncutaneous cancer in men (Jemal et al., 2008). Estimations suggest that 782,600 new cases and 254,000 deaths attributable to prostate cancer occurred in 2007 (Dominguez et al., 2003). Prostate cancer incidences increase with age (Zhang et al., 2007). Cases are extremely rare in men under the age of 45 years and with >90% of cases occurring in men over the age of 55 years. Thus, ageing populations in developed countries is likely a contributing factor to the overall increase in prostate cancer incidence rates.

Prostate cancer incidences and mortality rate are known to vary dramatically among different geographic regions (Figure 1.5). High incidences occur in areas such as the US, Northern\Western Europe and Australia with relatively low incidences in Asian countries (Parkin, 2001). Prostate cancer is now the most frequent cancer diagnosis of men in Europe (Ferlay et al., 2007). The variation in incidence rates is likely influenced by differences in PSA screening methods employed in individual countries, diet and better awareness and detection methods in more developed countries and therefore incidence rates must be interpreted with care. It is important to note, that since the introduction of PSA testing, the incidence of clinically localised disease has increased, whereas the incidence of metastatic disease has decreased (Hankey et al., 1999)

(Han et al., 2001). The relevance of reported incidence rates can be accessed from examination of age-adjusted mortality rates (Freda, 1999).

1.4.2 Prostate cancer mortality rates

Mortality rates, which represent a clearer guide to the risk of invasive prostate cancer, also vary in different populations. Studies show that mortality rates are high in the Caribbean, Southern and Central Africa, North and West Europe, Australia/New Zealand and North and South America and low in Asian and North Africa. In Europe, prostate cancer is the third most common form of cancer death in males (Ferlay et al., 2007).

Interestingly, mortality rates differ significantly between racial and ethnic groups within individual countries (Figure 1.6). In the US for example, death rates from prostate cancer among African Americans are twice those than in whites and five times that of Asian Americans (Jemal et al., 2008). Observations in Japanese immigrants to the US show rates intermediate between original and host communities (Dunn, 1975). Such data clearly demonstrates that risk of progressive prostate cancer is dependent upon ethnic group and/or country of residence, suggesting a prominent role of both genetic and environmental factors in disease epidemiology.

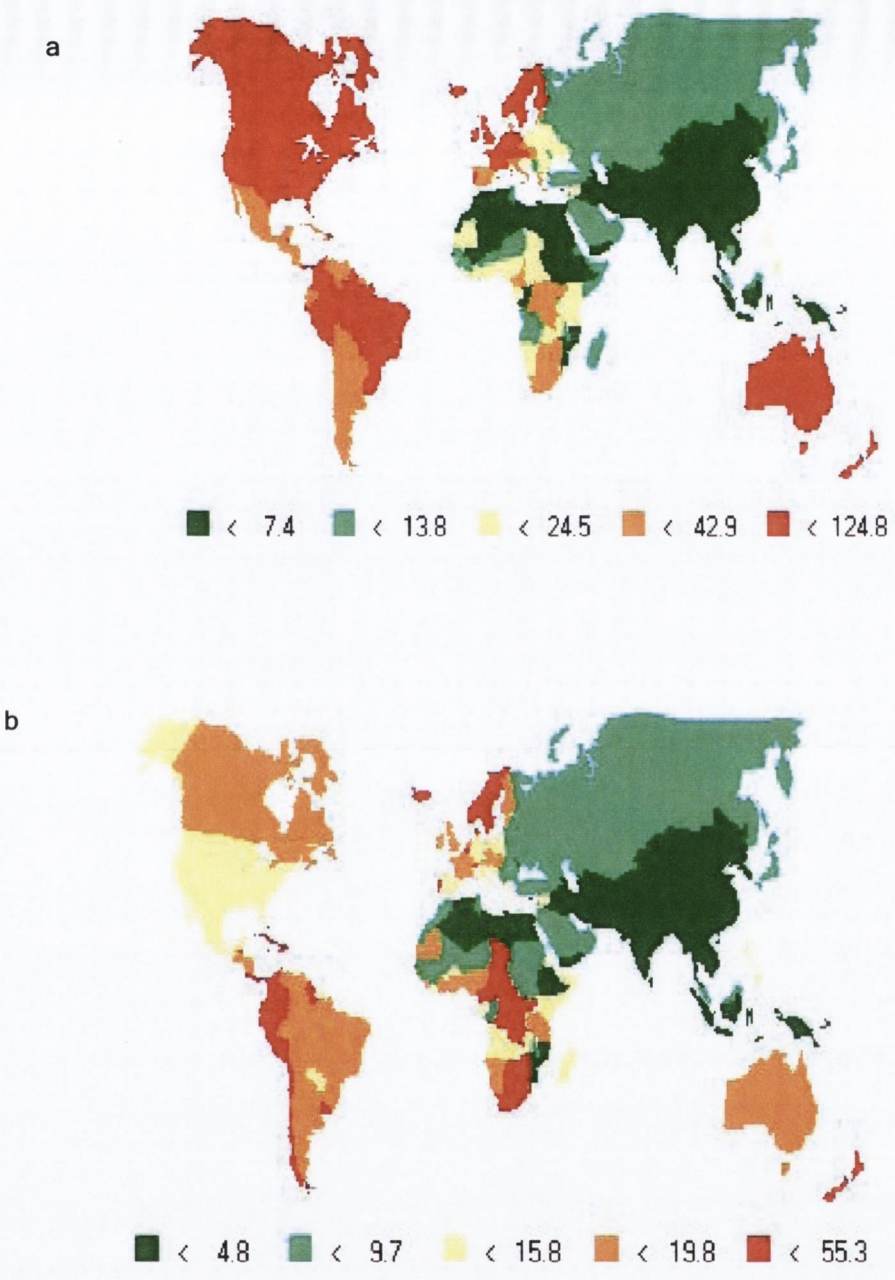

Figure 1.5

Worldwide view of prostate cancer. a) age-standardised incidence of prostate cancer per 100,000. b) age-standardised mortality from prostate cancer. Images obtained from Globocan 2002, the International Agency for Research on Cancer http://www-dep.iarc.fr/.

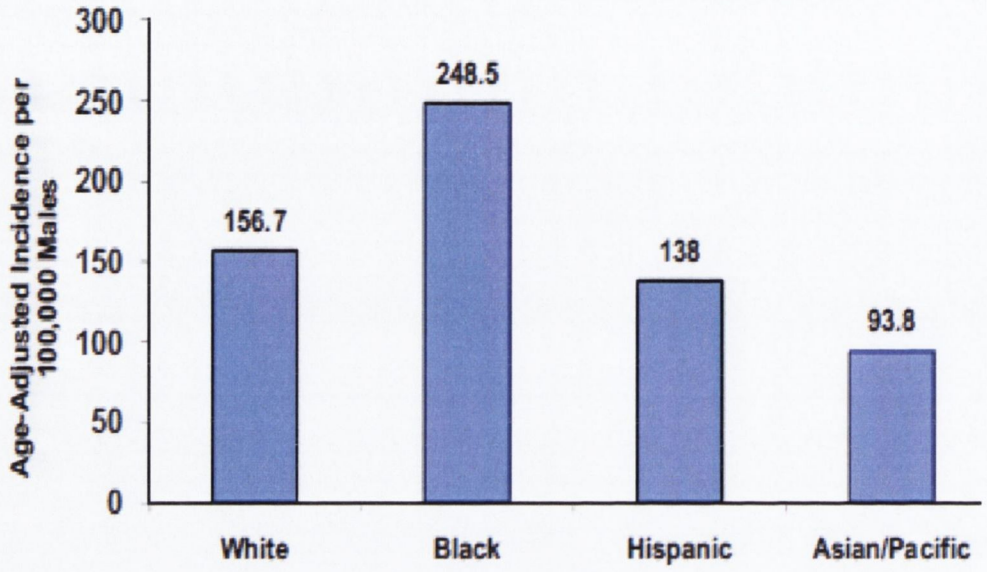

Figure 1.6

Age-adjusted incidence of prostate among men of different racial and ethnic populations (2001-2005). Image obtained from (Crawford, 2009).

1.4.3 Prostate cancer in Ireland

In Ireland, an average of 2,750 cases of prostate cancer and 745 deaths attributable to the disease were reported per year, between 2000 and 2004. Prostate cancer is the most frequently diagnosed noncutaneous cancer in men and the second most common cause of cancer death (after lung) in Ireland (Donnelly, 2009) (Figure 1.7). Prostate cancer incidence rates have increased by an average of 8.3% per year between 1994-2004 (Figure 1.8), which is likely a result of population growth and ageing. Mortality rates have decreased by 1% per year between 1994 and 2004 (Figure 1.9). Prostate cancer incidence rates were lower in Northern Ireland but higher in the Republic of Ireland compared to the EU and the UK but lower than Canada, Australia and the United States rates (Donnelly, 2009) (Figure 1.10).

a

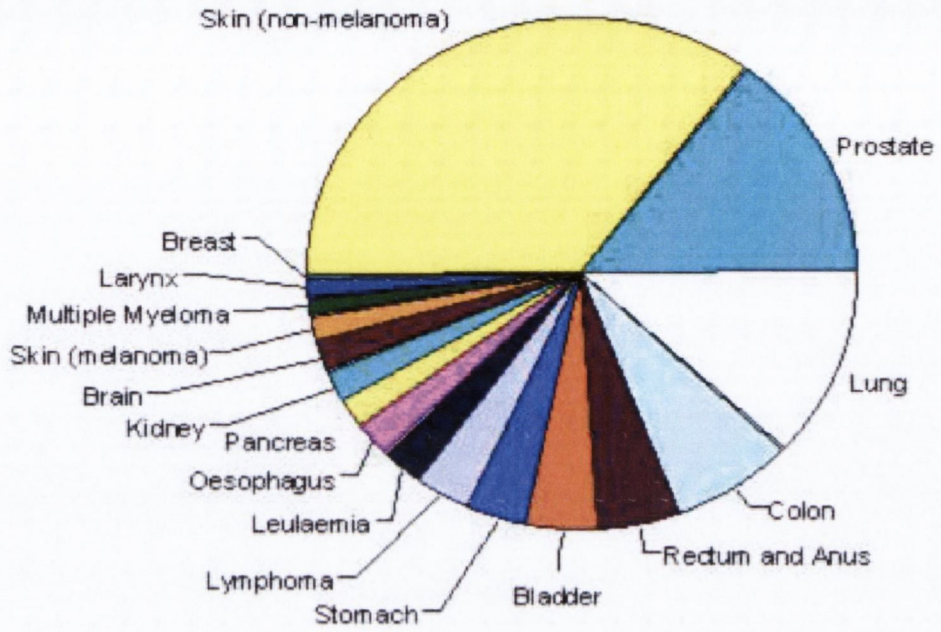

b

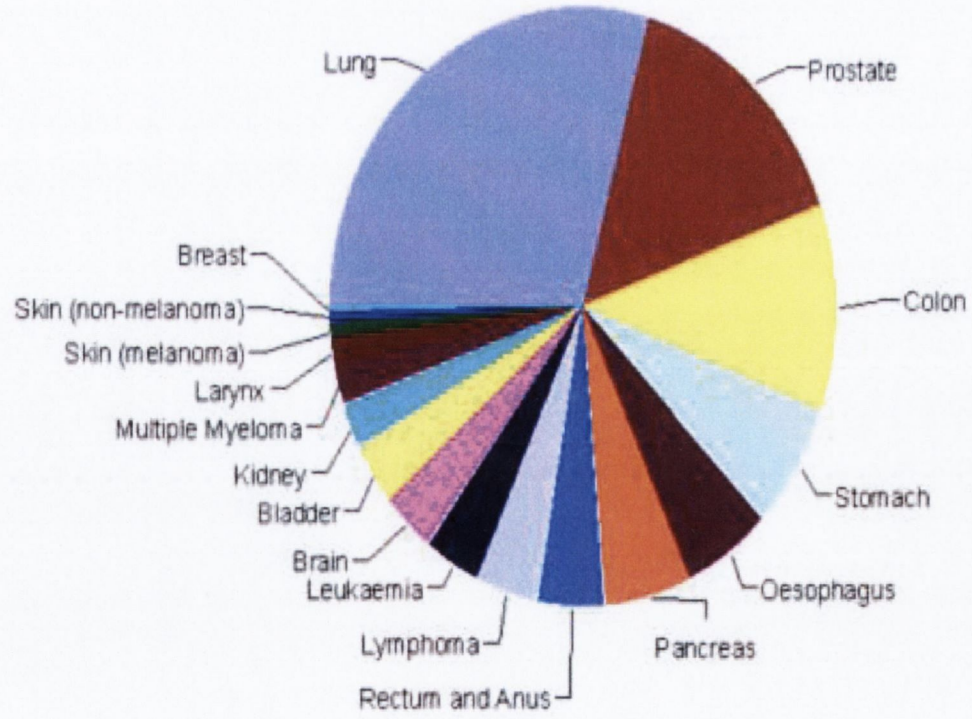

Figure 1.7

(a) Incidence and (b) mortality rates of different cancers among Irish men. Image obtained from the Irish Cancer society, accessed at: http://www.irishcancer.ie/.

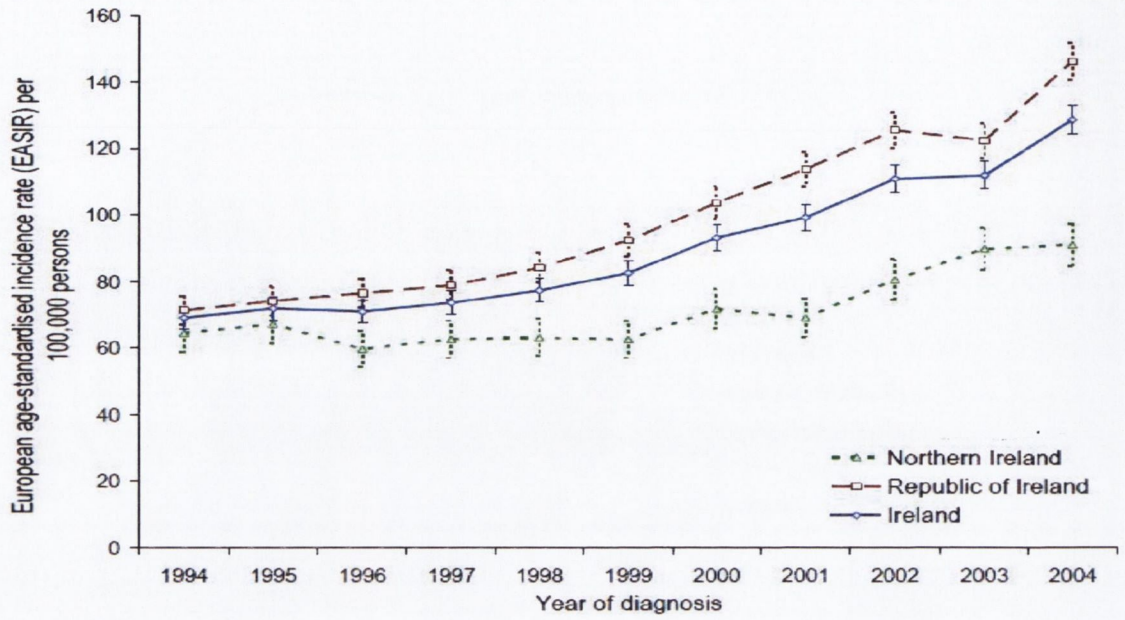

Figure 1.8

Incidence and mortality rates. Trends in European age-standardised incidence rates for prostate cancer by country:1994-2004. Image obtained from NICR/NCRI http://www.allirelandnci.com.

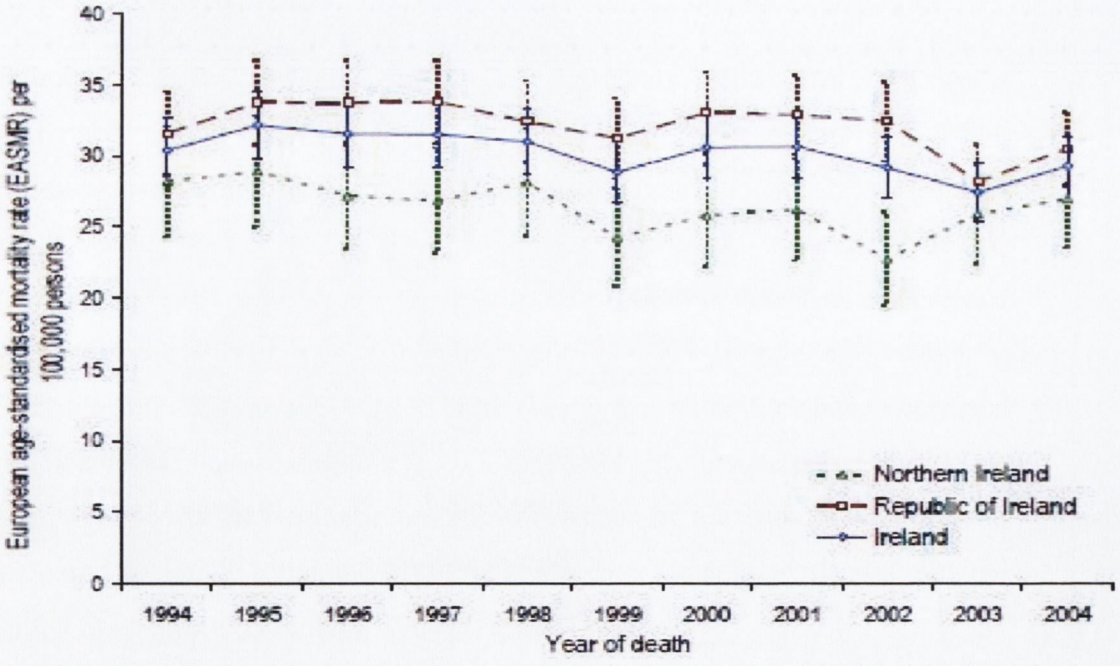

Figure 1.9

Trends in European age-standardised mortality rates for prostate cancer by country:1994-2004. Image obtained from NICR/NCRI http://www.allirelandnci.com.

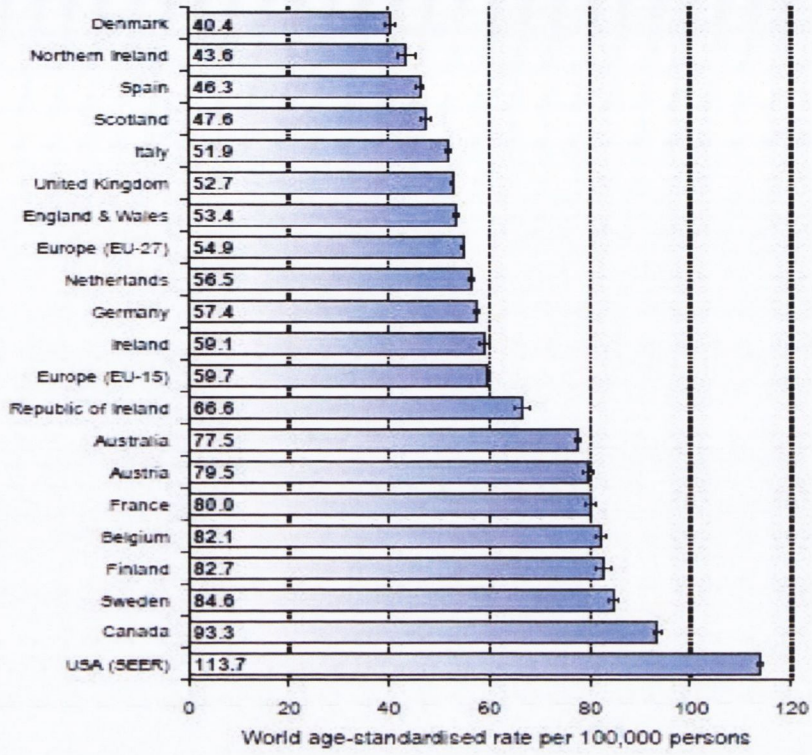

Figure 1.10

International comparison of world age-standardised incidence rate for prostate cancer: 1998-2000. Image obtained from EUROCARE IV, http://www.allirelandnci.com.

Differences between cancer rates between the Republic of Ireland and Northern Ireland is likely due to more extensive use of PSA testing in the Republic of Ireland. In addition, the Republic of Ireland also had higher mortality rates for prostate cancer than Northern Ireland (Figure 1.11) (Donnelly, 2009).

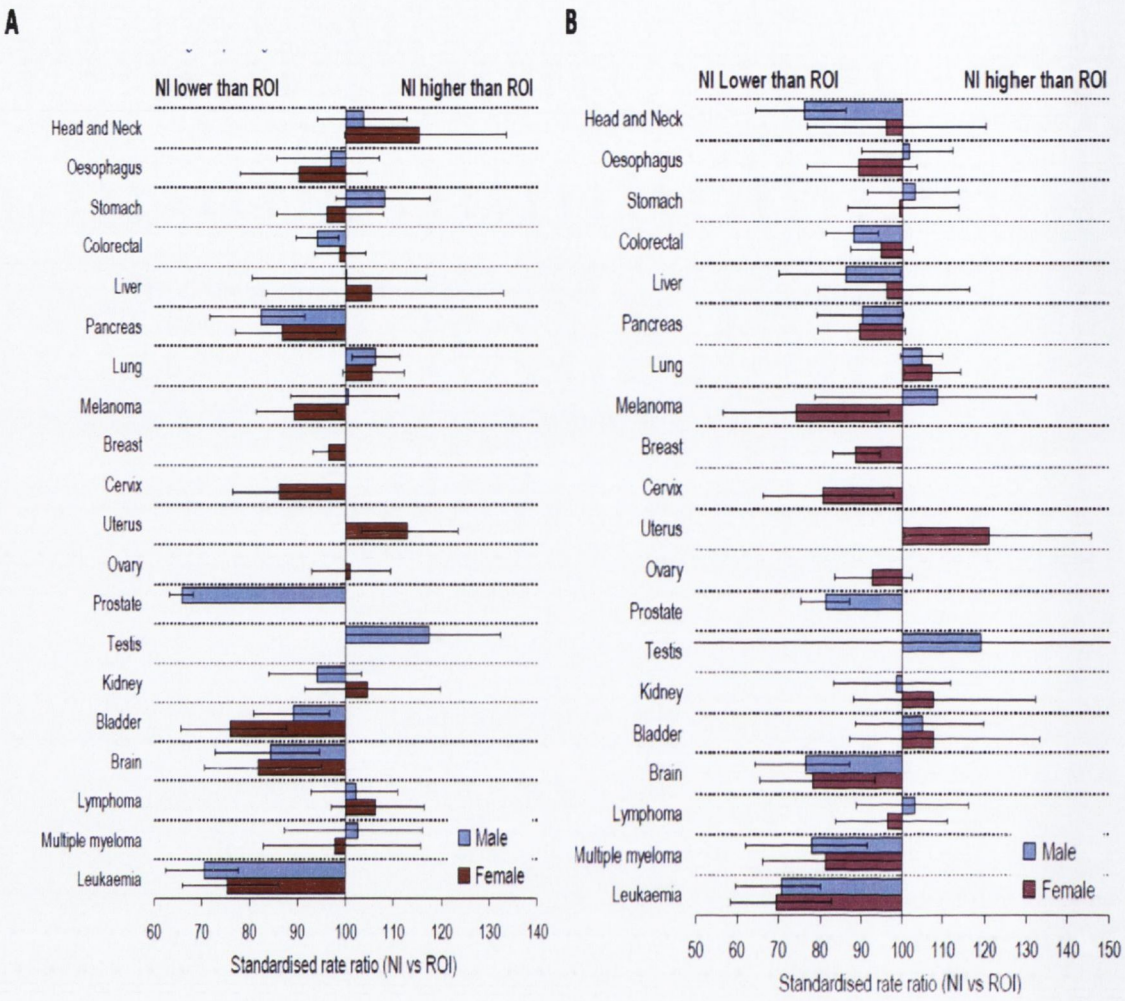

Figure 1.11

Prostate cancer incidence (A) and mortality rates (B) in Northern Ireland (NI) and the Republic of Ireland (ROI). Image obtained from NICR/NCRI http://www.allirelandnci.com.

1.4.3.1 Prostate Cancer Research Consortium

Created in October 2003, with funding from the Irish Cancer Society, the Prostate Cancer Research Consortium (PCRC) is a multi-disciplinary trans-institutional (University College Dublin, Trinity College Dublin, Royal College of Surgeons and Dublin City University), research initiative. Fundamental to the consortium is the development of the first prostate cancer Bio-Resource which was initially developed in the Mater Misericordiae University Hospital and St James's Hospital. The primary focus of the PCRC is to identify novel

disease biomarkers that allow earlier detection and more reliable prognosis of prostate cancer and identification of putative therapeutic targets. This research programme aims to:

1) Establish a prostate cancer tumour bank to support ongoing research and evaluate patient attitudes to tumour banking

2) Apply genomic and proteomic technologies to identify novel biomarkers allowing early detection and prognosis of prostate cancer

3) Correlate these molecular characterisations with disease progression phenotypes

4) Evaluate novel therapies in pre-clinical & potentially Phase I/II studies

Standard Operating Procedures (SOPs) for patient consent, sample collection and sample preparation for genomic, transcriptomic and proteomic analysis have been established and validated at all sites. The Bio-Resource currently has >500 tissues with matched serum/plasma samples and >90 urine samples. All samples have comprehensive clinical information and follow up (https://pcrc.tchpc.tcd.ie, Figure 1.12). Hence, this vital resource is critical for ongoing prostate cancer research in Ireland.

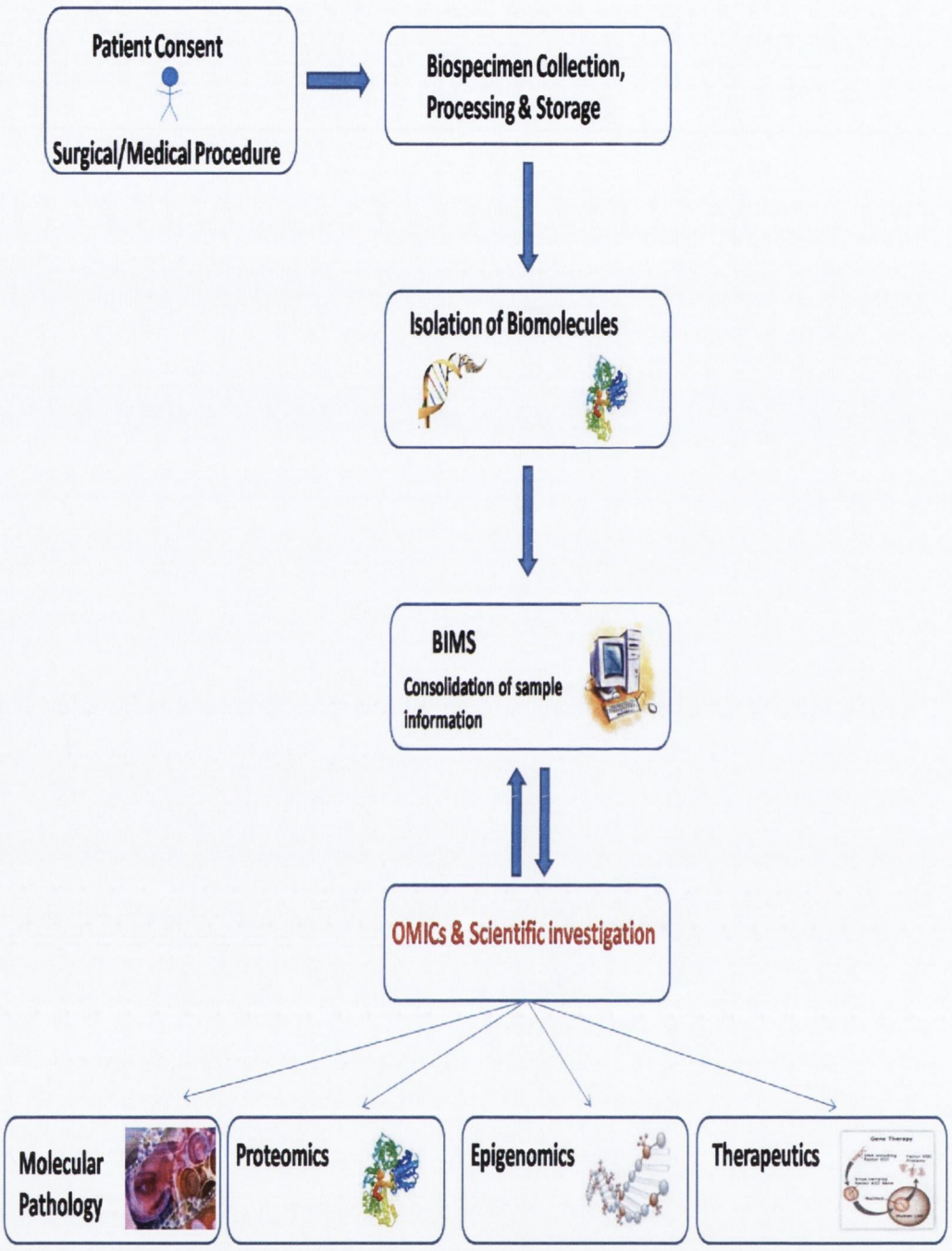

Figure 1.12:

Schematic representation of the workflow utilised in the PCRC from patient consent to scientific investigation.

1.5 DIAGNOSIS AND PROGNOSTIC MEASURES IN PROSTATE CANCER

Transrectal ultrasound (TRUS) guided prostate needle biopsy is currently the most reliable method of histologic diagnosis of prostate cancer. In most cases, prostate cancer rarely presents with symptoms until it is advanced. Thus, recommendation of prostatic biopsy is most often raised by abnormalities identified during routine Digital Rectal Examination (DRE) and serum Prostate Specific Antigen (PSA) elevation (Carter, 2007).

1.5.1 Prostate Specific Antigen (PSA)

PSA is a member of the human kallikrein gene family and was first recognized in the late 1970s, but it was over a decade until PSA testing became widespread in clinical urology (Kuriyama et al., 1980). PSA is a 33kD glycoprotein with similar properties to serine proteases. PSA functions to liquefy semen via its action on the gel-forming proteins semenogelin and fibronectin within the semen following ejaculation (Christensson et al., 1990).

Seminal fluid contains high concentrations of PSA, whereas serum contains relatively low concentrations. Serum PSA circulates as both bound (complexed) and unbound (free) forms, which are easily detected using pre-approved assays (Carter, 2007). PSA is produced by both normal and cancerous prostate cells and a high PSA value can be indicative of cancer. Serum PSA levels vary with age, race and prostate volume (Stamey et al., 1987). Normal PSA levels are between 0.6-0.7 ng/ml in men in their 40's and 50's (Catalona et al., 2004). Elevated PSA levels may occur as a result of benign prostatic disease such as BPH, prostate cancer and prostate manipulation such as biopsy.

In 1991, a PSA threshold of 4ng/ml was demonstrated as a screening test for prostate cancer (Brawer et al., 1992; Catalona et al., 1991). Looking at the link between prostate cancer occurrence and PSA test results, 12%, 15-25%, 17-32% and 43-65% of men with PSA Level between 0-2ng/ml, 2-4ng/ml, 4-10ng/ml and >10ng/ml, respectively, will have concurrent prostate cancer.

However not all these cancers will represent clinically significant disease (Carter, 2007).

1.5.2 Limitations of PSA as a prostate cancer biomarker

Measurement of serum PSA is now widely used as a first step in the detection of prostate cancer and in the staging and follow-up to treatment of prostate cancer (DeVere White et al., 1992; Kim et al., 2006). However, the efficacy of PSA as a prostate cancer biomarker is highly controversial. Firstly, elevated PSA is not cancer specific and as discussed previously can be indicative of a range of prostatic diseases or manipulation. Moreover, a quarter of men with prostate cancer have a PSA level below 4 ng/ml, thus, would not be identified exclusively by a PSA test (Eeles et al., 2008; Schroder et al., 2000). This led to a revised threshold of 2.5 ng/ml being proposed (Catalona, 2004). Indeed, lowering the cut-off value may improve detection at least for younger men, who would potentially benefit more from early detection (Carter, 2007). However, lowering PSA cut-off levels will inevitably increase the number of clinically indolent prostate cancer diagnoses, resulting in unnecessary biopsies and anxiety in men with elevated PSA levels with little clinical significance. The PSA threshold that can lead to detection of life-threatening cancers while avoiding unnecessary testing and over diagnosis is not known (Carter, 2007).

The efficacy of using different PSA thresholds is dependent on both age and ethnicity (Catalona et al., 1994). Adjustments of the PSA from total prostate volume (PSA density) (Gjengsto et al., 2005) and evaluation of PSA velocity (Fang et al., 2002) have been explored to improve sensitivity and specificity of PSA testing. In addition, the measurement of the different forms of PSA: total, free and complexed may improve the discrimination between prostate cancer and BPH (Hernandez and Thompson, 2004).

1.5.3 PSA screening: Decreasing mortality rates or over-diagnosis?

Reducing prostate cancer mortality by routine PSA screening, earlier detection and treatment in asymptomatic men remain highly controversial topics (Eeles et al., 2008). In 2009, the European Randomized Study of Screening for

Prostate Cancer (ERSPC) was published, which formally addressed the role of PSA screening and mortality rates (Schroder et al., 2009) .

The ERSPC was initiated in the early 1990s to evaluate the effect of screening with prostate-specific-antigen (PSA) testing on death rates from prostate cancer. 182,000 men between the ages of 50 and 74 years resident in seven European countries were included in the study. Men were randomly assigned to a group that was offered PSA screening at an average of once every 4 years or to a control group that did not receive such screening. The predefined core age group for this study included 162,243 men between the ages of 55 and 69 years.

Results, of a median follow-up of 9 years, showed that the cumulative incidence of prostate cancer was 8.2% in the screening group and 4.8% in the control group. Results concluded that PSA-based screening reduced the rate of death from prostate cancer by 20% but was associated with a high risk of over diagnosis in the screening population. The report estimated that for every prostate cancer death prevented, 1,410 men have to undergo screening, while 48 are needed to be treated in excess of the control group population to save one prostate cancer death.

The European Association of Urology (EAU) has taken into consideration the recent scientific information of this randomised screening study on prostate cancer and suggests that current published data are insufficient to recommend the adoption of population screening for prostate cancer as a public health policy due to the large overtreatment effect. The EAU urge that before screening is considered by national health authorities, the level of current screening, over diagnosis, overtreatment, quality of life, costs and cost-effectiveness should be investigated further (www.uroweb.org/professional-resources/guidelines/).

It is clear, therefore, that current screening methods are inadequate due to a lack of specificity and selectivity for aggressive cancers which require treatment. The development of novel diagnostic and prognostic markers and

imaging modalities is urgently required to enhance the predictive value of screening tools (www.uroweb.org/professional-resources/guidelines/).

1.5.4 TRUS biopsy and Gleason grading

At present Transrectal Ultrasound (TRUS)-guided sextant needle biopsy is the most reliable method to ensure sampling of prostatic tissue (Durkan and Greene, 2000). The sensitivity and specificity of TRUS-biopsy in detecting prostate cancer is reported as 60% and 100% respectively (Durkan and Greene, 2000). However, prostate cancer is extremely heterogeneous in nature, which can render tumour diagnosis of biopsies difficult. Moreover, TRUS-guided needle biopsies may fail to detect microscopic foci of cancer resulting in false negative results (Epstein, 2009). As a result, repeat biopsies are often required for patients whose PSA levels continue to rise.

Histologic grade is the most informative observation from a needle biopsy. The Gleason grading systems is the most commonly used classification system for histological grading of prostate cancer (Gleason, 1977). Gleason grading is based on microscopic examination of tumour architecture (Figure 1.13). The predominant pattern in the tumour specimen is given a Gleason score between 1 and 5 and this score is then added to the score assigned to the second most predominant pattern. These two scores are summed to give a Gleason score, which can range from 2-10 (Carter, 2007). Good correlation between Gleason sum and prognosis has been demonstrated in long-term follow up studies (Epstein, 2009; Gleason, 1977, 1992; McNeal et al., 1990; Sogani et al., 1985). The presence of a Gleason grade ≥ 4 or a Gleason sum of ≥ 7 is highly predictive of a poor prognosis. Moreover, Gleason score 4+3 tumours have a worse prognosis than those with Gleason score 3+4. Gleason score of a biopsy specimen is central when considering the most appropriate treatment choice, with a score of >6 suggesting advanced disease (Gleason and Mellinger, 1974). Therefore, the Gleason score of a biopsy specimen along with age and PSA level are important factors in considering the most appropriate treatment options.

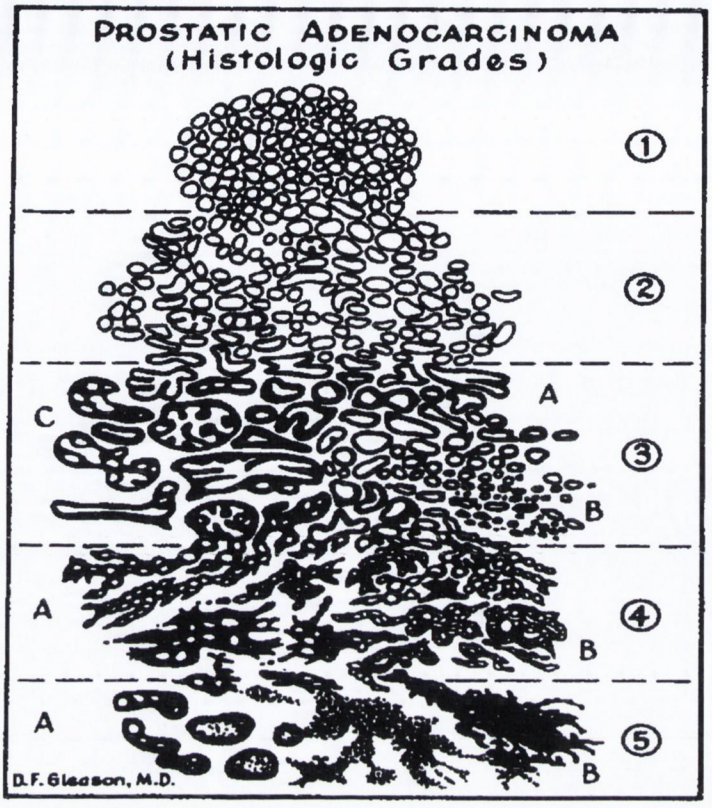

Figure 1.13

The appearance of cancer cells according to the Gleason system, which grades the cancer according to its ability to form gland like structures. Image obtained from (Epstein, 2009).

Such diagnostic tools fail however to predict accurately the outcome for individual patients. Consequently, prognostic based methods are required to help distinguish between clinically indolent prostate cancers, which will be asymptomatic and aggressive prostate cancers with the potential to kill the patient (Hughes et al., 2005).

1.6 TREATMENT OF PROSTATE CANCER

1.6.1 Early and locally advanced prostate cancer

The treatment options for primary localised and primary progressive prostate include active monitoring without treatment (depending on the age and overall health of the patient), radical prostatectomy, radiotherapy and/or hormonal therapy. Early prostate cancer often grows slowly and with limited adverse symptoms and may not require treatment immediately. Traditionally deferred

treatment has been reserved for men with low grade prostate cancer and a life expectancy of >10 years. However, in recent years, research has focussed on active monitoring for the management of younger patients with low volume or intermediate-grade tumours (Catalona, 2007). A prospective, randomised clinical trial in Scandinavia reported a significantly increased rate of local cancer progression, metastases, mortality and a shorter cancer-specific and overall survival for patients with clinically localised prostate cancer managed by watchful waiting than patients treated with radical prostatectomy (Bill-Axelson et al., 2005).

Young healthy patients most often are encouraged to undergo radical prostatectomy and older patients are steered toward radiotherapy. Radical prostectomy is the "gold standard" of prostate cancer treatment and has been utilised for more than 100 years by Kuchler and Young. Healthy men who present with prostate cancer and have a life expectancy >10 years are good candidates (Catalona, 2007). A number of complications are associated with prostatectomy, including damage to the urinary sphincter and penile nerves during surgery can result in postoperative urinary incontinence and impotence (Naitoh et al., 1998).

Treatment of prostate cancer with external beam radiotherapy involves directing gamma radiation beams at the prostate and surrounding tissue. Radiotherapy can also have significant side effects. It is associated with severe bladder irritation (urgency, pain and frequency) in as many as 5 percent of patients. Rectal irritations (diarrhoea, urgency, tenesmus and bleeding) occur in 3 to 10 percent of patients who receive radiotherapy for prostate cancer, and impotence is a problem in 40 to 50 percent of patients receiving this treatment (Shipley et al., 1994). An alternative to traditional radiotherapy is brachytherapy, whereby radioactive seeds or needles are implanted directly into the prostate gland. As a result, the tumour receives high dose radiation localised to the prostate while having a less severe impact on the bladder and the rectum (Naitoh et al., 1998). This method is popular for localised prostate cancer but seldom implemented for tumours with a larger volume and high-risk cancers.

Both radical prostectomy and radiotherapy have comparable cure rates, with a five-year relative survival rate close to 100% (Jani and Hellman, 2003; Jemal et al., 2006). Patients with a high PSA level, high Gleason score and/or larger tumour volume benefit from combined radiotherapy and androgen deprivation therapy (Hanks et al., 1994).

1.6.1.2 Pathologic staging of prostate cancer

Clinical staging in prostate cancer aims to utilise pre-treatment parameters to predict disease progression. Moreover, pathological stage is the most steadfast means of predicting the outcome of traditional treatment methods in men with clinically localized cancer (Catalona, 2007). The tumour, node, metastases (TNM) system for staging prostate cancer was adopted in 1975 and has since undergone several modifications (Table 1.1). The finding of seminal vesicle invasion or lymph node metastases on pathologic evaluation after radical prostatectomy is associated with a very low probability of total eradication of tumour and a high probability of treatment failure (Jani and Hellman, 2003).

Table 1.1 Tumour Node Metastases (TNM) classification of prostate cancer	
Classification	**Description**
T-Primary Tumour	
TX	Primary tumour cannot be assessed
T0	No evidence of primary tumour
T1	Clinically in apparent tumour not palpable or visible by imaging
T1a	Incidental histological finding in <5% of tissue resected by TURP
T1b	Incidental histological finding in >5% of tissue resected by TURP
T1c	Tumour identified by needle biopsy (e.g. because of elevated PSA)
T2	Tumour confined within the prostate
T2a	Tumour involves < half of one lobe
T2b	Tumour involves > half of one lobe
T2c	Tumour involves both lobes
T3	Tumour extends through the prostatic capsule (invasion into but not beyond the prostatic apex)
T3a	Extracapsular extension (unilateral or bilateral)
T3b	Tumour invades seminal vesicle(s)
T4	Tumour is fixed or invades adjacent structures other than the seminal vesicles: bladder neck, external sphincter, rectum, levator muscle, and/or pelvic wall.
N-Regional lymph node status	
NX	Regional lymph nodes cannot be assessed
N0	No regional lymph nodes metastases
N1	Regional lymph node metastases
M-distant metastases status	
MX	Distant metastases cannot be assessed
M0	No distant metastases
M1	Distant metastases
M1a	Non-regional lymph node(s)
M1b	Bone(s)
M1c	Other site(s)
Table adapted from TNM classification of prostate cancer (Fleming *et al*, 1997)	

1.6.2 Metastatic disease

Treatment failure and death for prostate cancer patients is largely a result of tumour metastasis, which is the ability of tumour cells to spread via the lymphatic and blood circulations to distant loci and form secondary tumours. Androgen ablation therapy is the primary treatment option for metastatic prostate cancer, when surgery or radiotherapy are no longer options. Androgens play a critical role in prostate cancer cell proliferation and androgen ablation therapy aims to lower levels of androgens (mainly testosterone) or block androgen receptor function by anti-androgens. Androgen depletion may contribute to reduction of the tumour mass. The adrenal gland is a minor source

of nontesticular androgen, hence luteinising hormone-release hormone analogues have been utilised in combination with anti-androgens to block both testicular androgen production and residual androgen stimulation of the prostate from the adrenal gland (Partin and Rodriguez, 2002).

Initially most advanced tumours respond favourably to ablation therapy. However, the response is short lived and the cancer ultimately recurs as an androgen independent tumour, which is difficult to treat. Subsequently new therapeutic therapies are required for the treatment of prostate cancer. Understanding the molecular pathology of prostate cancer is essential to discover potential novel therapeutic targets and design adequate prevention strategies.

1.7 RISK FACTORS AND AETIOLOGY

The aetiology of prostate cancer is complex and has not fully been elucidated (Nelson et al., 2002). The primary predictors for prostate cancer are age, race, geographical location and a positive family history. Hence, both genetic and environmental factors are likely risk factors for prostate cancer development.

1.7.1 Environmental influences on Prostate cancer

Analysis of differences in diet between low and high incidence/mortality regions has lead to a number of insights. Prostate cancer mortality rates correlate highly with the average level of saturated fat consumption around the world (Gann et al, 1994). Further studies have shown that a diet rich in fruit, vegetables, fish and low in saturated fats (a typical Asian diet) correlated with a reduced risk of prostate cancer (Andersson et al 1996, Gann et al 1999, Clinton & Giovannucci 1993.).

The Health Professional follow-up study, a prospective cohort study involving 51,529 men found that increased total fat intake, animal fat intake, and consumption of red meat were risk factors for prostate cancer (Giovannucci et al., 1993). In addition, the level of red meat consumption was correlated with prostate cancer risk in the Physicians' health study (Gann et al., 1994) and a large cohort study in Hawaii (Le Marchand et al., 1994). The component of red

meat that promotes prostate carcinogenesis is unknown. However, evidence suggests that meats cooked at high temperatures or on charcoal grills results in the formation of potent carcinogens, which have been shown to cause prostate cancer when fed to rats (Shirai et al., 1997). Alcohol consumption has also been associated with increased risk of prostate cancer, whereby alcohol consumers are at risk compared to abstainers and occasional drinkers (Benedetti et al., 2009). In addition to the diet, evidence suggests that sexually transmitted diseases may also confer an increased risk of prostate cancer. A specific pathogen has so far not been identified, and studies suggest that prostatic inflammation associated with sexually transmitted diseases may play an important role in the carcinogenetic phenotype (Strickler and Goedert, 2001).

In contrast, vegetable intake may have a protective effect against prostate cancer development (Hsing and Devesa, 2001). A number of studies have identified tomatoes and its active ingredient, lycopene, to have a protective affect against prostate cancer. Lycopene is a potent anti-oxidant and can scavenge for reactive oxygen species in cells. thereby preventing oxidative cellular stress and DNA damage (Clinton, 1999). Of interest, a clinical trial, whereby men were given tomato sauce based pasta dishes for three weeks prior to radical prostectomy had increased lycopene levels in prostate cells and a reduction in PSA serum levels (Navone et al., 1993). Other antioxidants such as Vitamin E and selenium may also reduce the risk of prostate cancer (Loeb and Partin, 2009). Interestingly, a key component of Asian diets, green tea, has also been implicated in attenuating prostate cancer progression (Pandey and Gupta, 2009). Green tea is a rich source of polyphenols, in particular epigallocatectin 3-gallate (EGCG), a powerful antioxidant. Green tea polyphenols have been shown to induce apoptosis in prostate cancer cell lines reduce the rate of tumour development in a mouse model of prostate cancer (Caporali et al., 2004) and preliminary studies report chemopreventative activity of polyphenols in patients with HGPIN (Bettuzzi et al., 2006). Moreover, EGCG has been demonstrated to inhibit DNA methyltransferases *in vitro*. This inhibitory activity has been associated with demethylation of the promoter CpG islands of a number of tumour suppressor genes in prostate

cancer (Fang et al., 2003). The role of green tea catechins in prevention of prostate cancer is currently under investigation in clinical trials in the United States.

It is noteworthy that a diet low in red meat and saturated fats and rich in cruciferous green vegetables and fish is typical of Asian men, who experience among the lowest rates of prostate cancer in the world. Furthermore, the particularly interesting point about the relationship between diet and prostate cancer is that diet is easily modifiable and could be adapted as a chemopreventative measure to protect against prostate cancer.

1.7.2 GENETICS OF PROSTATE CANCER

1.7.2.1 Inherited prostate cancer

The molecular pathology of prostate cancer is complex; epidemiological studies have demonstrated familial clustering of prostate cancer suggesting that hereditary factors are important in the development of the disease (Porkka and Visakorpi, 2004). Linkage analyses have indicated several chromosomal loci that may harbour high-penetrance prostate cancer susceptibility genes, such as X chromosomes and a region on chromosome 1q (Eeles et al., 2008; Xu et al., 1998). Estimates of 9-10% of all prostate cancer cases are believed to be inherited (Hughes et al., 2005). Linkage studies have however had limited success, largely due to the fact that prostate cancer is a common disease and it is often hard to distinguish between truly heritable and sporadic cancers Moreover, susceptibility genes may only confer disease risk in the correct dietary or environmental background (Hughes et al., 2005).

1.7.2.2 Chromosomal alterations in prostate cancer

A number of chromosomal abnormalities have been identified in prostate cancer. One of the most common events in early prostate cancer is loss of specific regions of chromosome 8p, which has been identified in 80% of prostate tumours (Chang et al., 1994). The most promising tumour suppressor gene in this region is prostate specific homeobox gene, *NKX3.1*. Studies have shown that *NKX3.1* is downregulated in 20% of PIN lesions, 6% low stage cancer and 78% of cancer metastases (Bowen et al., 2000). Loss of

chromosome 10q is also a frequent (50-80%) event in prostate carcinogenesis (Abate-Shen and Shen, 2000). Interestingly, potent tumour suppressor gene phosphotase and tensin homologue (*PTEN*) maps to 10q23. *PTEN* encodes a lipid phosphotase which is essential for cell cycle regulation. In prostate cancer, *PTEN* is often downregulated, particularly in higher grade cancer (McMenamin et al., 1999). Chromosome 13q is lost in ~50% of prostate tumours. Of interest, the retinoblastoma gene (*RB*) maps to this region (Li et al., 1998). *RB* is an important tumour suppresser gene and is aberrantly expressed in a large number of cancers. *RB* is vital for regulation of G1 phase of the cell cycle (Phillips et al., 1994). Moreover, *RB* negative prostate cancer cells lose their carcinogenetic phenotype when transfected with wild-type Rb (Bookstein et al., 1990).

In more advanced stage prostate cancer and metastatic disease, 17p chromosomal loss is frequently observed (Saric et al., 1999). Interestingly, the gene, which encodes the "gatekeeper of the genome" p53, lies in this region. Aberrant p53 expression has been associated with bone metastasis, androgen independent disease and a reduced survival rate after radical prostectomy (Grignon et al., 1997).

1.7.2.3 Polymorphisms and susceptibly to prostate cancer

Polymorphisms or single nucleotide polymorphisms (SNPs) are genetic variants that appear in at least 1% of the population. Genetic polymorphisms may contribute to risk of prostate cancer development by altering the response of the patient to certain environmental factors or by interacting with their genes. A number of studies have associated genetic polymorphisms with prostate cancer risk. *CYP17* for example encodes cytochrome P-450c17alpha, an enzyme responsible for the biosynthesis of testosterone. A variant *CYP17* allele has been shown to be associated with both hereditary and sporadic prostate cancer. The allele is believed to increase the transcription rate of the gene, resulting in increased androgen production hence increasing the risk of prostate cancer (Stanford et al., 2002).

A polymorphism in the vitamin D receptor (*VDR*) has been associated with advanced prostate cancer. Vitamin D has been shown to have an anti-proliferative effect on prostate cancer cells, via induction of growth arrest (Skowronski et al., 1993). Polymorphisms in *VDR* gene have been associated with variation in VDR activity (Eeles et al., 2008). Particular *VDR* alleles have been associated with risk of prostate cancer progression (Ingles et al., 1997). Other SNPs have been identified in a number of genes with wide ranging functions, such as *TLR4* (Zheng et al., 2004), androgen receptor (Giovannucci et al., 1997) and *CDKN1B* (Kibel et al., 2003).

Recently, genome wide association studies (GWAS) have identified a number of susceptibility loci for prostate cancer. In one large scale study ~1900 prostate cancer cases and controls were genotyped at over 500,000 SNPs. Seven susceptibility loci were identified as associated with prostate cancer on chromosome 3,6,7,10,11, 19 and X. Moreover, they found that 3 of the newly identified loci contain candidate susceptibility genes microseminoprotein, beta (*MSMB)*, lemur tyrosine kinase 2 (*LMTK2)* and the gene which encodes PSA, kallikrein-related peptidase 3 (*KLK3)* (Eeles et al., 2008).

1.7.2.4 Androgen independent prostate cancer and the role of genetics

Androgen-ablation therapy is the most common treatment for advanced prostate cancer and in the short term causes tumour regression. However, ablation therapy ultimately leads to tumour recurrence, which is androgen independent, often highly aggressive and /or metastatic in nature (Abate-Shen and Shen, 2000). There are several possible mechanisms for acquisition of androgen independence, including alterations in androgen receptor (AR) activity, function and/or specificity (Figure 1.14) (Abate-Shen and Shen, 2000)
.

The *AR* is frequently mutated within the hormone binding domain, which renders it more susceptible to accommodating binding of and activation by other steroid hormones (Harada et al., 2002). Gene amplification also can occur and hence prostate cells become hypersensitive to small amount of androgen

(Koivisto et al., 1998). Furthermore, hormone requirement may be bypassed by acquiring alternative growth regulation pathways (Figure 1.14).

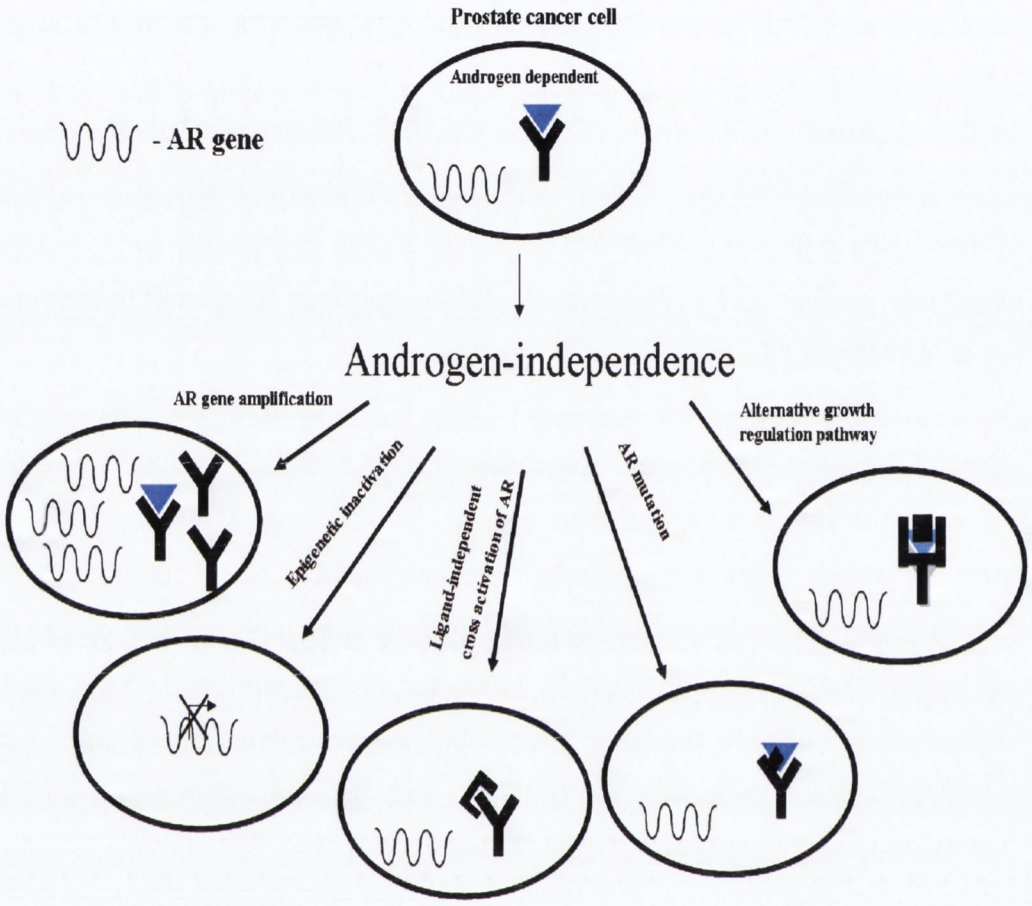

Figure 1.14:

Development of androgen independence. Evidence has been found for a number of possible molecular mechanisms for development for androgen independence; including gene amplification, AR (Androgen receptor) mutations, cross-activation of AR in the absence of androgen, AR signalling via alternative growth pathways and epigenetic inactivation. Image adapted from (Foley et al., 2004).

1.7.2.5 Alterations of gene expression patterns in prostate cancer versus normal prostate

With the era of microarray technology well and truly upon us, understanding which genes are aberrantly expressed in prostate cancer is achievable. Utilising microarray technologies, examination of gene expression patterns of multiple genes have been examined in large cohorts of prostate cancer tissue samples and benign prostate. Genes such has *HEPSIN* (Magee et al., 2001), *AMACR*

(Luo, 2002), *PIM1* (Dhanasekaran et al., 2001) and the polycomb regulatory gene, *EZH2* (Varambally et al., 2002) have been identified as up-regulated in prostate cancer compared to normal prostate. In addition, a number of tumour suppressor gene have been identified utilising microarray expression analysis, such as *PTEN, E-CADERIN* (Dhanasekaran et al., 2001), *EPHB2* (Huusko et al., 2004) are frequently downregulated in prostate cancer compared to normal tissue.

1.8 EPIGENETICS AND PROSTATE CANCER

In addition to classical genetic abnormalities, epigenetic modifications have emerged as a central driving force in the molecular pathology of prostate cancer (Perry et al., 2006). The concept of epigenetics was first introduced by C.H. Waddington in 1939 to name "the casual interactions between genes and their products, which bring the phenotype into being" (Waddington, 1939), epigenetics was later defined as the mechanisms that initiate and maintain heritable patterns of gene expression without altering the sequence of the genome (Holliday, 1987).

There are several layers of epigenetic complexity including histone modifications, chromatin remodelling, micro RNAs, antisense regulation, polycomb genes and DNA methylation, the later being the most thoroughly studied to date (Esteller, 2006). Our group and others have hypothesised that epigenetic modifications, specifically DNA hypermethylation, play an important role in the down regulation of genes important for protection against prostate cancer.

1.8.1 The "Prima Donna" of Epigenetics: DNA methylation

DNA methylation has been described as the "Prima Donna" of epigenetics, highlighting its central importance in epigenetic inheritance (Scarano et al., 2005). DNA methylation refers to the covalent addition of a methyl group to the carbon at position 5 of the cytosine ring, by a family of DNA methyltransferase (DNMT) enzymes, resulting in 5-methylcytosine (Figure 1.15) (Razin and Riggs, 1980). In mammalian DNA, 5-methylcytosine is found in approximately 4% of genomic DNA, primarily at cytosine-guanine

dinucleotides (CpGs) (Baylin, 2005a). These CpG sites are non-randomly dispersed throughout the genome, concentrated in hot spots or CpG rich regions known as CpG islands. Approximately half of all human genes are estimated to contain a 5' or promoter CpG island (Larsen et al., 1992; Wang and Leung, 2004). CpG methylation is a key regulatory mechanism of the genome and plays a central role in diverse biological processes. Mice knock-outs of the *DNMT* genes are lethal, suggesting a vital role for DNA methylation in normal mammalian development (Li et al., 1992; Okino et al., 2007). DNA methylation plays a significant role in suppressing parasitic repetitive elements such as Alus and LINEs (both rich in CpGs), which have been incorporated into many transcriptional units of active genes (Yoder et al., 1997). As a general rule, CpG islands are usually unmethylated in normal tissue (Esteller, 2005). There are, however a number of exceptions; genomic imprinting for example requires DNA hypermethylation at one of the two parental alleles of a gene to ensure monoallelic expression (Feinberg et al., 2002), similarly promoter regions of genes on the inactive X chromosome are hypermethylated in females (Reik and Lewis, 2005). Promoter hypermethylation is a regulatory mechanism for expression of certain germline-specific genes, such as MAGE genes, which are hypermethylated and silenced in all tissues except cancerous tissue (Bodey et al., 2002) and certain tissue specific genes, such as MASPIN, a member of the serum protease inhibitor family (Futscher et al., 2002).

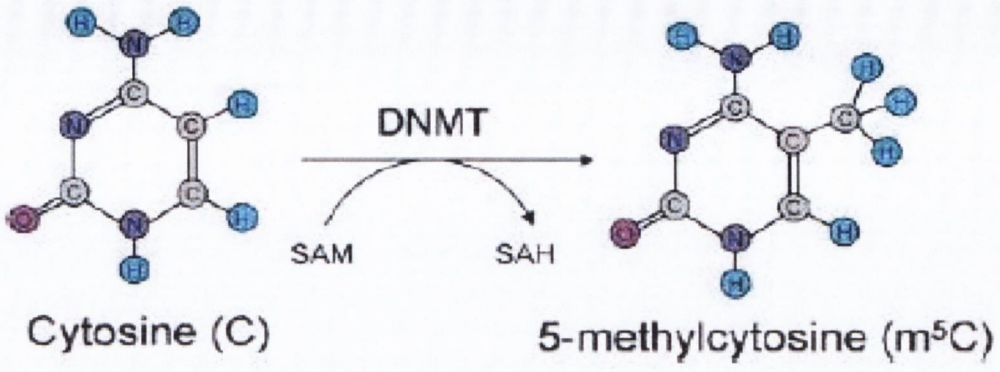

Figure 1.15

Methylation of cytosine. DNA methylation refers to the transfer of methyl group (CH_3) from the universal methyl donor S-adenosylmethione (SAM) to the carbon at position 5 of the cytosine ring (m^5C). This reaction is catalysed by a group of enzymes known as DNA methyltransferases (DNMT). Image obtained from (Gronbaek et al., 2007).

1.8.2 DNA methylation and transcriptional repression

DNA methylation inhibits transcriptional initiation through (i) directly blocking transcription factor binding to the promoter: *NFκB* for example, is a transcription factor whose binding has been shown to be inhibited by DNA methylation (Bednarik, 1993) and (ii) indirectly by promoting histone deacetylation resulting in chromatin condensation (Bird, 2002). The latter is more complex and deserves some discussion. Active genes usually lack promoter methylation and are generally associated with histone lysine (K) acetylation and histone methylation at H3K4, H3K36 and H3K79. Chromatin condensation and transcriptional repression of genes is marked by promoter methylation and histone deacetylation (Figure 1.16) (Thiagalingam et al., 2003). Histone methylation at H3K9, H3K27 and H4K20 (Klose and Zhang, 2007) residues can also have repressive effects on gene expression. There is evidence that H3K9 methylation can serve as a DNA methylation signal (Fuks, 2005). A recent study by Smallwood *et al* reports that heterochromatin protein 1 (HP1) mediates communication between histone modifications and DNA methyltransferase. This study supports a model whereby HP1 is attracted to euchromatic genes in regions where H3K9 has been methylated by the histone methyl transferase G9a. The HP1 molecule appears to act as an adaptor, which

binds to DNMT1 and enhances its DNA methyltransferase activity, resulting in increased cytosine methylation of the surrounding DNA (Brenner and Fuks, 2007). Studies have also shown that G9a activity can be enhanced by DNMT1 (Esteve et al., 2006). Smallwood and colleagues argues that the evidence suggests a mechanism whereby DNMT1, HP1 and G9a form a positive feedback loop, which helps control the silencing of genes (Smallwood et al., 2007).

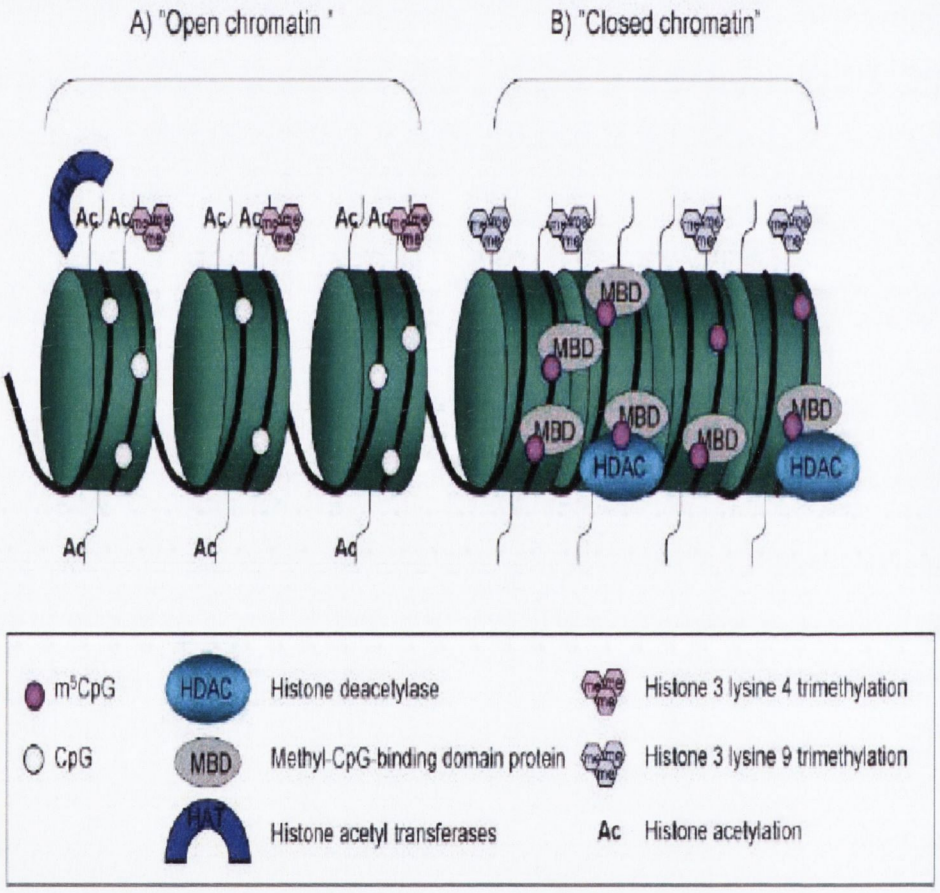

Figure 1.16

Chromatin structure of active and inactive promoters. A) Open chromatin is transcriptional active and is characterised by unmethylated cytosines and acetylation of histone tails. Lysin 4 on histone H3 is trimethylated. B) Methylation at cytosine molecules attract and bind to MBDs that in return attract HDACs, which remove acetyl groups for histone tails. A closed chromatin structure results, whereby the DNA becomes coiled and carries the silencing mark histone H3 lysine 9 trimethylation. Image obtained from (Gronbaek et al., 2007)

1.8.3 Gene methylation in cancer

1.8.3.1 DNA hypomethylation in cancer

During oncogenic transformation, simultaneous gain (hyper) and loss (hypo) of methylation occurs. In general, cancer cells exhibit global genomic hypomethylation (Gronbaek et al., 2007). DNA hypomethylation may lead to increased expression of certain oncogenes, such as *MDR1* (Nakayama et al., 1998) or cause upregulation of oncogenic microRNAs (Cowland et al., 2007). Moreover, global hypomethylation can activate proviral and transposon sequences leading to the disruption of their surrounding genes (Chalitchagorn et al., 2004; Yoder et al., 1997). The main carcinogenic effect of global hypomethylation is its ability to destabilize the genome and promote loss of heterozygosity in regions containing tumour suppressors (Ehrlich, 2002). Loss of methylation can result in aberrant recombination leading to chromosomal breaks, translocations and/or allelic loss (Hoffmann and Schulz, 2005). Furthermore, studies have shown that DNA hypomethylation in the pericentromeric regions of chromosomes is a hallmark of many cancers and contribute to breakage in the region (Ehrlich, 2002). Such alterations are reminiscent of those observed in patients with Immunodeficiency, Centromere instability and Facial anomalies (ICF) syndrome, whereby they are deficient in the methyltransferase enzyme DNMT3b (Gronbaek et al., 2007).

1.8.3.2 DNA hypermethylation and cancer

The major focus of epigenetic research in human cancer over the past decade has been promoter hypermethylation. In fact, it is now thought that hypermethylation-driven gene inactivation is at least as common as, if not more frequent than, traditional mutational events in the development of certain cancers (Fraga and Esteller, 2005). The large numbers of genes found to undergo hypermethylation in a wide variety of cancer types suggests a key role for DNA methylation changes in the initiation and progression of cancer (Esteller, 2006). How does DNA hypermethylation contribute to carcinogenesis? In the past decade, a significant amount of information has emerged on how and where these methylation changes occur. Methylation which occurs at or near tumour suppressor genes is associated with gene silencing (Figure 1.17). In contrast, methylation at further downstream gene

sequences has no effect on gene expression (Eeles et al., 2008). DNA methylation can be viewed as another "hit" in Knudson's two hit hypothesis of tumour suppressor inactivation (Knudson, 2001). Indeed, many of the causative tumour suppressor gene mutations observed in inherited cancers are frequently inactivated by methylation in sporadic tumours, such as in *P16, BRCA1* and *VHL* (Dobrovic and Simpfendorfer, 1997; Furukawa et al., 2005; Herman et al., 1994).

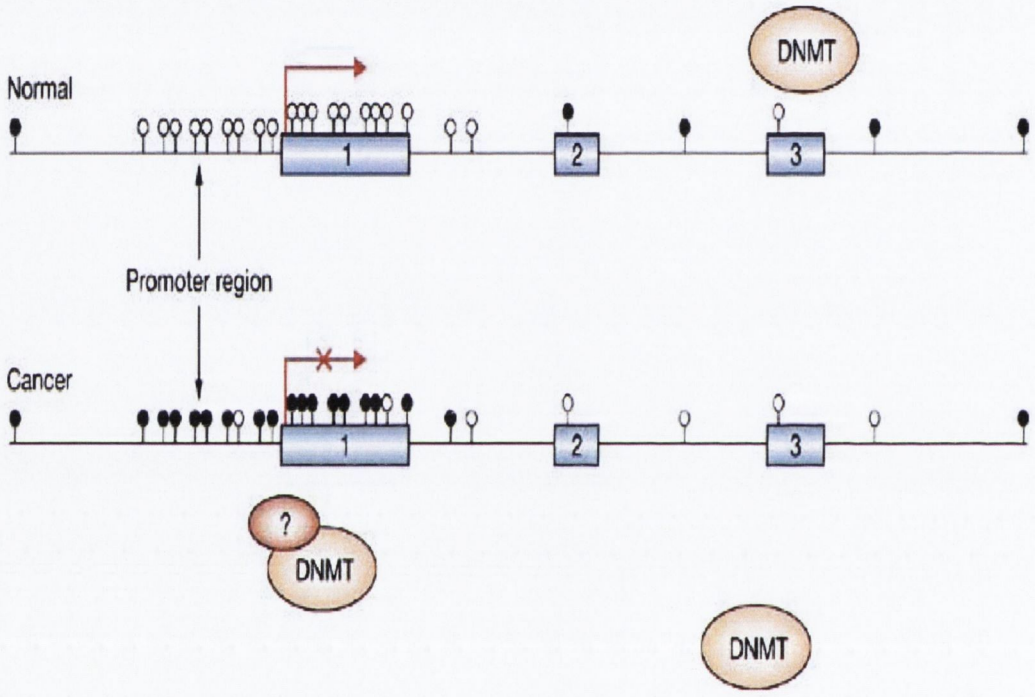

Figure 1.17

DNA methylation in normal and cancer cells. White circles represent CpG sites; Black circles represent hypermethylated CpG sites. Exons are labelled 1, 2, and 3. Transcriptional repression by DNA methylation in cancer cells is depicted by X. Image obtained from (Baylin, 2005b).

Promoter hypermethylation and silencing of the associated genes is widespread in prostate cancer. Many of the genes that are targeted by the cells methylation machinery play a vital role in regulating important cellular functions such as cell growth, differentiation, DNA repair and apoptosis, while others are implicated in tumour metastasis and angiogenesis (Figure 1.17 Perry et al., 2006). The most significant gene that has been described is *GSTP1*, which has been found to be methylated in >90% of prostate cancers (Lin et al., 2001;

Maruyama et al., 2002). In our own laboratory, we have focused on the IGF pathway and have recently identified *IGFPB3* as a novel target of methylation in prostate cancer (Perry et al., 2007).

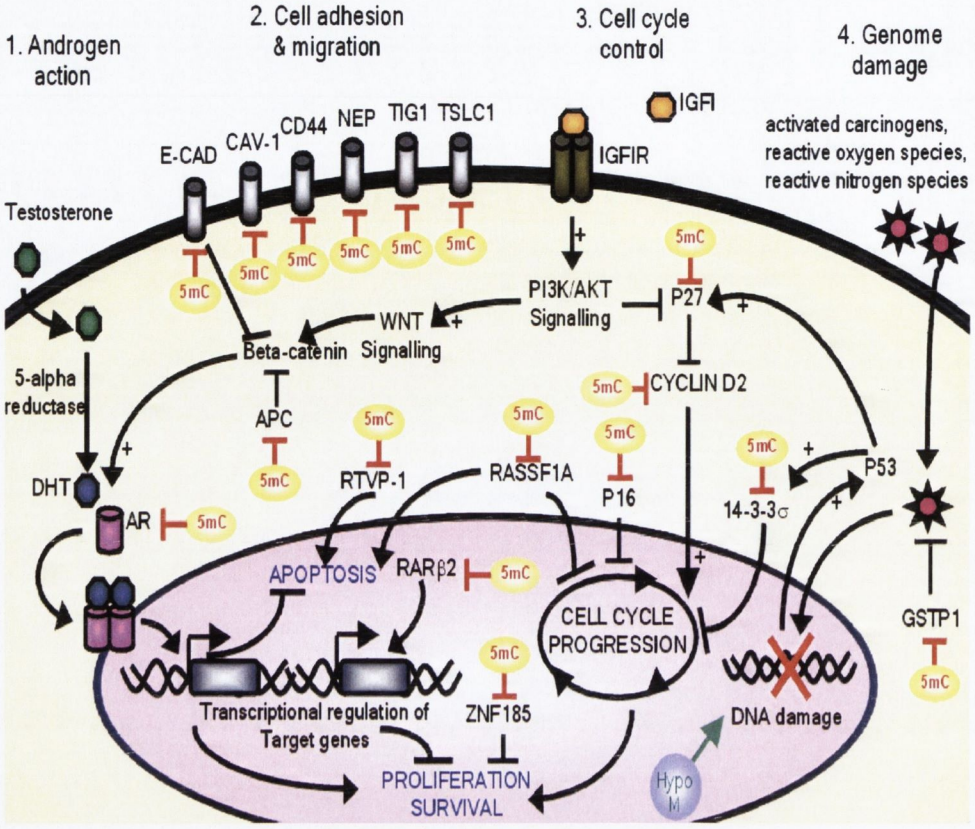

Figure 1.18

An overview of some of the pathways affected by hypermethylation (oval containing 5 mC) in prostate cancer. (1) Conversion of testosterone to the more potent DHT permits transactivation of the *AR*. This facilitates transcriptional regulation of target genes, which leads to enhanced cellular proliferation and reduced apoptosis. Hypermethylation-associated *AR* gene inactivation in a proportion of hormone-refractory prostate cancers may confer a growth advantage through alternative pathways that are capable of 'bypassing' the need for AR (reviewed by Feldman & Feldman 2001). (2) The functions of cell adhesion proteins such as E-cad, CD44 and TSLC1 become abrogated by promoter hypermethylation during invasion and metastases of prostate cancer. (3) Hypermethylation-driven loss of function of key cell-cycle regulators such as p16, p27 and RASSF1A, allows uncontrolled proliferation. (4) Promoter methylation (of intracellular detoxification enzyme GSTP1) and global hypomethylation (Hypo M) promote genome damage. PI3K, phosphoinositide 3-kinase; IGFI, insulin-like growth factor I; IGFIR, insulin-like growth factor I receptor. Image obtained from (Perry et al., 2006).

1.9 APOPTOSIS

Programmed cell death or apoptosis is an evolutionary conserved and genetically regulated biological process that plays an important role in the development and homeostasis of multicellular organisms (Creagh et al., 2003). Apoptosis is classically defined by a characteristic set of morphological changes that occur in cells, including blebbing of the plasma membrane, cell shrinkage, condensation and fragmentation of the nucleus, formation of apoptotic bodies and DNA fragmentation (Kerr, 1972).

A major component of the mammalian cell death machinery is the caspase (**c**ysteine **as**partate-specific prote**ases)** family of proteases. Currently, fourteen mammalian members of this family (caspase-1 through to caspase-14) have been identified. All known caspases contain an active site cysteine (*cys*) residue and cleave after aspartate acid (*asp*) residues. Caspases are typically synthesised in normal cells as enzymatically inert zymogens (enzymes containing an N- terminal prodomain, a P20 and P10 domain) (Hengartner and Bryant, 2000), which require autoproteolytic cleavage or cleavage by other caspases at specific *asp* residues to achieve their active configuration (Vermeulen et al., 2005). Caspases important for apoptosis can be further divided into two sub groups (initiators and effectors) on the basis of the lengths of their prodomain and relative position in the apoptotic caspase cascade (Creagh and Martin, 2001). Upon activation, caspases with long prodomains (caspase 2, 8, 9 and 10) function upstream in the signal transduction pathway, as initiators, proteolytically activating downstream effector caspases 3, 6 and 7, which contain a short prodomain (Vermeulen et al., 2005). These downstream executioner caspases have been shown to be chiefly responsible for the majority of the intracellular caspase-induced cleavage that results in cell death (Earnshaw et al., 1999).

1.9.1 Death Receptor Pathway: caspase activation

Two main pathways of cell death have now been elucidated: a death-receptor-mediated pathway and a mitochondrial mediated pathway. The death receptors are a subset of the tumour necrosis factor (TNF) receptor family of cell surface molecules that possess a common motif within their cytoplasmic tails, called death domains. Receptor death domains are thought to be intimately involved

in the recruitment of adaptor molecules, which in turn, enlist caspases to the receptor complex. Upon ligand binding, death receptors such as Fas aggregate and form membrane-bound signalling complexes (Figure 1.19). These complexes recruit through adaptor proteins (e.g. Fadd), several molecules of pro-caspase 8. The induced proximity, together with a weak protease activity of procaspase-8, is sufficient to allow mutual cleavage and trans-activation (Hengartner and Bryant, 2000). It is believed that caspase-8 propagates the death signal by direct processing of other caspases (Slee et al., 1999). Caspase-3 is a putative substrate for caspase-8. Once activated, caspase-3 can further propagate the cascade by activation of caspase-6 and caspase-7.

1.9.2 Mitochondrial apoptotic pathway: caspase activation

The mitochondrion is not only the cell's powerhouse but is a key player in programmed cell death (Figure 1.19). The signal for the mitochondrial mediated pathway can arise from a number of signals including DNA damage caused by ionizing radiation and from cytotoxic agents (Kim et al., 2006; Vousden and Lu, 2002).

The bcl-2 family of proteins plays a key role in mitochondrial-mediated apoptosis. The family consists of both pro- and anti-apoptotic proteins, the members of which can be classified based on four conserved regions known as bcl-2 homology (BH) domains into three main subclasses (Cory and Adams, 2002). Anti-apoptotic proteins like bcl-2, bcl-xl, mcl-1, A1 and bcl-w are characterised by the presence of the four known BH domains. This class of anti-apoptotic proteins appears to exert control over mitochondrial permeability by stimulating ADP/ATP exchange, stabilising the mitochondrial inner transmembrane potential and preventing the opening of a permeability transition pore that enables release of a plethora of pro-apoptotic molecules including cytochrome c (Miller, 1999).

The bcl-2 family also contains a number of pro-apoptotic members, which can be separated into two subclasses, the BH 1-3 domain containing members (Bax and Bak) and members that contain only one BH domain (The BH3 only class: Bim, Bik, Bad, Hrk, Noxa and Puma) (Cory and Adams, 2002). A number of

the latter class of molecules are up-regulated by P53 induction in response to intracellular damage (Huang and Strasser, 2000). With the exception of Bid, they are thought to, upon stimulation, translocate to the mitochondria and block the protective regulatory activity of anti-apoptotic bcl-2 members (Miller, 1999). The presence of either Bax or Bak seems to be essential for apoptosis in many cell types. Bax and Bak are thought to trigger or contribute to permeabilisation of the outer mitochondrial membrane, allowing efflux of apoptotic proteins such as cytochrome c out of the mitochondria into the cytosol. The mechanism of Bax/Bak mediated cytochrome c release is controversial and a number of models have been proposed and reviewed elsewhere (Cory and Adams, 2002). A dynamic equilibrium exists between pro-apoptotic and anti-apoptotic bcl-2 family members, whereby the relative concentrations of pro/anti apoptotic bcl2 members may decide life or death of the cell (Cory and Adams, 2002).

The release of cytochrome c into the cytosol has dramatic consequences for the cell on two levels. Firstly cytochrome c is an integral part of the mitochondrial electron transport chain that is required for ATP synthesis and secondly, cytochrome c binds to and activates cytosolic Apaf-1 (apoptotic protease activating factor-1). Apaf-1 controls the activation of caspase-9. To enable caspase activation, Apaf-1 must first bind cytochrome c and undergo dATP dependent oligomerization prior to caspase-9 binding (van Noesel et al., 2003). With cytochrome c and dATP bound, Apafl and caspase 9 assemble into a high molecular weight complex that has been termed the "apoptosome" (Ranger et al., 2003). The apoptosome facilitates the cleavage and hence activation of caspase 3, 6 and 7.

Cross talk occurs between the two pathways at the level of caspases. For example, caspase-8 can catalyse the cleavage of Bid into two fragments, the C-terminal portion, which can then translocate to the mitochondria where it integrates into the outer membrane and promotes cell death by activating Bax and Bak, and it may also play a role in the inactivation of its pro-survival relatives (bcl-2 and bcl-xl) (Cory and Adams, 2002).

Caspase activation appears to be the preferred executer of cell death, however in its absence or failure can be compensated for by many other default pathways. Some of the mitochondrial proteins released as a result of mitochondrial outer membrane potential (MOMP) (AIF, HtrA2/Omi, endonuclease G) can promote caspase-independent death via a number of mechanisms (Kroemer and Martin, 2005). For example, AIF and endonuclease G, upon release from the mitochondria, can relocate to the nucleus, where they are believed to cooperate and induce caspase-independent nucleosomes DNA fragmentation (Cande et al., 2004; Niikura et al., 2007).

Alternative mechanisms of cellular fate also exist such as autophagy and cellular senescence. Autophagy can be defined as the process of degrading proteins and organelles and recycling materials in response to cellular stress (Apel et al., 2009). A number of key members of the apoptotic machinery are also implicated in control and regulation of autophagy. For example, potent pro-apoptotic molecule bcl-2 is known to interact with and inhibit autophagy-related protein beclin1 (Pattingre et al., 2005). Cellular senescence, a state of irreversible growth arrest, can be triggered by three key mechanisms; telomere loss, the accumulation of DNA damage and derepression of the *INK4a/ARF* locus (Collado et al., 2007). The mechanisms underlying cellular senescence are important in the protection against cancer and are involved in aging of an organism (Collado et al., 2007).

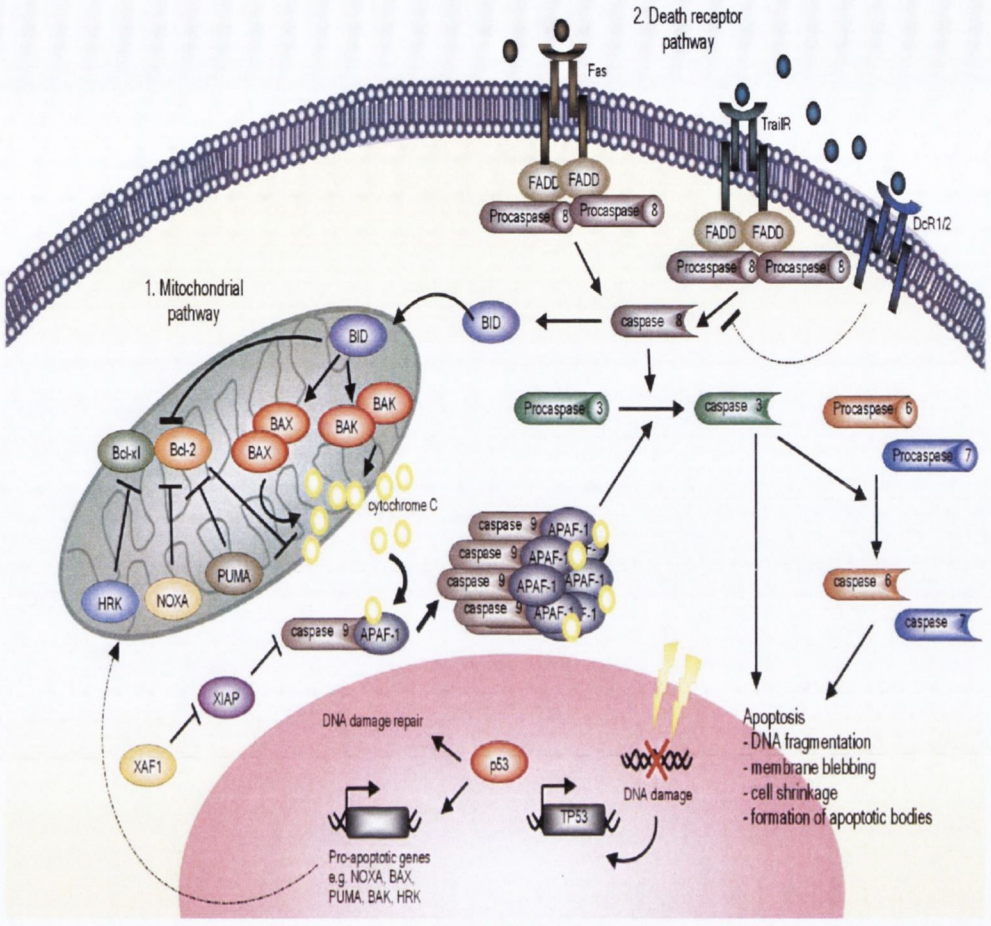

Figure 1.19

Apoptosis Pathways. An overview of the common apoptotic pathways found to be defective in cancer. **(1) Mitochondrial Pathway:** A number of stimuli, such as DNA damage can induce transcription of P53, which modulates transcription of a number of members of the Bcl2 family BH3 only proteins. These proteins translocate to the mitochondria where they promote the release of cytochrome c and/ or inhibit anti-apoptotic Bcl-2/Bcl-xl. Cytochrome c then binds to Apaf-1, which further complexes with caspase 9 to form the apoptosome and promotes cleavage of effector caspases. **(2) Death receptor pathway:** Upon Ligand binding, Fas/Trail receptors aggregate and recruit via FADD adaptor molecules, which attract a number of caspase 8 molecules, whose close proximity allows for mutual cleavage resulting in their activation. Caspase 8 can cleave effector caspases such as caspase 3 resulting in a caspase cleavage cascade. Decoy receptors DcR1/DcR2 compete with trail receptors for Trail binding. DcR1/DcR2 do not propagate the caspase-signalling cascade due to non-functional or absent intracellular domains. Cross talk between pathways occurs at the caspase level. Caspase 8 can cleave Bid, whereby its C-terminal translocates to the mitochondria and promotes cell death via activation of Bax and Bak. Cleavage of effector caspases (by either pathway) results in apoptosis induction and its associated phenotype (DNA fragmentation, membrane blebbing, cell shrinkage and the formation of apoptotic bodies).

1.9.3 The deregulation of apoptosis in prostate cancer

Disruption of normal apoptotic pathways contributes to carcinogenesis via a number of mechanisms including loss of function of tumour suppressor genes (e.g. *TP53, APAF1, FAS*), epigenetic inactivation of members of different apoptotic signalling cascades (e.g. *CASP8, APAF1, BAX*), defects in execution pathways (e.g. caspase 3, caspase 6) and up-regulation of anti-apoptotic proteins (e.g. bcl-2, bcl-xl) (Hanahan and Weinberg, 2000).

In prostate cancer, a number of molecular changes have been identified that target different components of the apoptotic cascade. For instance, *in vivo* studies have demonstrated that bcl-2-overexpressing prostate carcinoma cell lines are associated with a reduced apoptotic response following treatment with various chemotherapeutic agents and ionizing radiation (Kyprianou et al., 1997). In patients with locally advanced or metastatic prostate cancer receiving hormonal therapy, bcl-2 over-expression is an adverse prognostic indicator (Colombel et al., 1993; Shabaik AS, 1995).

P53 induces cell cycle arrest or apoptosis in response to DNA damage, hypoxia, heat shock and many other cellular stresses (Wang et al., 2004). P53 controls the expression of several pro-apoptotic genes such as *BAX*, the cyclin-dependent kinase inhibitor *CDKN1A* and *MDM2*. *TP53* mutations are uncommon in early invasive prostate carcinoma but occur frequently in advanced stages of disease (Navone et al., 1993). A number of studies have indicated that co-staining for p53 and bcl-2 is a potential biomarker for prostate cancer progression, poor prognosis and recurrence (Matsushima et al., 1997; Moul et al., 1996).

Aberrant expression of a number of promiscuous members of apoptotic pathways (both intrinsic and extrinsic) have been implicated in prostate cancer. Tissue microarrays of normal and cancerous prostates have identified *BCL2*, *CLU*, *SMAD4*, *DAP* and *PERP* as downregulated in prostate cancer (Ernst et al., 2002; Yu et al., 2004b). Such data highlights the importance of both pro- and anti-apoptotic molecules in prostate carcinogenesis.

Human prostate cancers often present as heterogeneous tumours, with a mixture of androgen-dependent and independent tumour cells. Androgen ablation therapy is the primary treatment for metastatic prostate cancer. However this treatment alone does not eliminate the androgen-independent cells. Several lines of evidence suggest that progression to androgen independent disease is associated with resistance to apoptosis and altered expression of caspases and expression of inhibitor of apoptosis proteins (IAPs) (McEleny et al., 2002). Understanding which apoptotic pathways become altered and by what mechanism, for example genetic or epigenetic, may provide a rationale for targeting the cell death machinery in hormone refractory prostate cancer.

Manipulation of apoptotic pathways is an attractive therapeutic approach for the treatment of prostate cancer. Investigation into the differential expression of key apoptotic genes, such as *BCL2* and *TP53*, in normal prostate versus prostate cancer has provided valuable insights into the apoptotic profile of prostate cancer cells. Such a profile may act as an important feature of tumour pathology that could influence diagnosis, prognosis, therapeutic response and disease progression. The challenge now is to further dissect the molecular mechanisms underlying the atypical expression of key apoptotic genes.

1.10 DNA METHYLATION OF APOPTOTIC GENES: A KEY SURVIVAL MECHANISM IN PROSTATE CANCER

Evasion of cell death is a key feature of cancer cell survival, whether the cell is proliferating, metastasising or developing resistance to chemotherapeutic drugs (Eeles et al., 2008). Studies suggest that DNA methylation in human cancer cells can help inactivate apoptotic pathways at several points. To date, the majority of methylation studies on apoptotic genes have focused on cancers of the bladder, stomach, colon and breast. In prostate cancer, limited data exists on the methylation status of apoptotic genes.

Studies have shown that pro-apoptotic genes, X-linked mammalian inhibitor of apoptosis protein (*XIAP*)-associated factor 1 (*XAF1*), Cellular retinol binding proteins (*CRBP1*) and Reprimo (*RPRM*) have a moderate methylation

frequency in prostate cancer (35-65%) (Lee et al., 2006; Suzuki et al., 2006), while pro-apoptotic genes fragile histidine triad (*FHIT*) and *FAS* (Maruyama et al., 2002; Santourlidis et al., 2001) have a low methylation frequency in prostate cancer (12.5-15%). Interestingly, anti-apoptotic decoy receptor genes *DCR1* and *DCR2* (Shivapurkar et al., 2004) are methylated in approximately 50% of prostate tumours examined. Further validation of the methylation profile of these targets is necessary in order to investigate their potential as prostate cancer biomarkers and to understand their role in prostate carcinogenesis. In the case of *FHIT, RPRM* and *DCR1/2* there are no reports of gene expression analysis in prostate cancer cell lines or tissue. To determine if DNA methylation is associated with gene silencing it would be important to examine the mRNA levels of these genes.

1.11 HYPOTHESIS

The aims of this study were to implement a combined *in silico* and DHPLC screening strategy to identify novel apoptotic-related gene targets of promoter methylation in a panel of prostate cancer cell lines. The promoter CpG islands of each gene of interest were further characterised in order to identify biologically significant regions of the island. Correlation between promoter methylation at specific gene loci and transcriptional repression was examined utilising quantitative methylation specific PCR and quantitative real-time PCR. Finally, the methylation levels of genes of interest were examined in a prostate cancer biorepository including a range of grades and stages of prostate cancer, BPH, HGPIN and benign adjacent prostate tissue, with a view to generate an "apoptotic methylation signature" of prostate cancer. Detection of an "apoptotic methylation signature" could have potential as a diagnostic and prognostic biomarker and aid early detection and treatment choice for prostate cancer.

CHAPTER 2
MATERIALS AND METHODS

2.1 IDENTIFYING POTENTIAL TARGETS OF PROMOTER HYPERMETHYLATION

2.1.1 Searching a methylation candidate gene bank

An *in silico* approach to identify potential targets of promoter hypermethylation in prostate cancer was employed by Dr. Antoinette Perry in our laboratory. This approach identified a methylation candidate gene bank. This gene bank was searched for apoptotic gene targets of methylation.

2.1.2 Identifying biological role in apoptosis

Key genes involved in important apoptotic cascades were chosen and apoptotic function delineated using the following online resources: Information Hyperlinked Over Proteins (iHOP;http://www.ihop-net.org/UniPub/iHOP/); |http://www.biocarta.com}) and by review of literature searching the biomedical journal literature via PubMed (http://pubmed.gov/).

iHOP is a large-scale information system, which converts information in PubMed into one navigable information resource. Every gene/protein is allocated one page containing all sentences that associate the gene/protein with other gene /proteins. Gene synonyms within these sentences serve as hyperlinks to their corresponding pages. The concept of iHOP is to allow researchers to move between sentences taken from a large volume of abstracts, allowing control over the reliability of the information they obtain. Ease of scanning through associated sentences allow the user to identify incorrectly identified symbols and recognise whether the information offered in a sentence is of interest (Hoffmann and Valencia, 2004). The navigation trail of iHOP is illustrated in Figure 2.1.

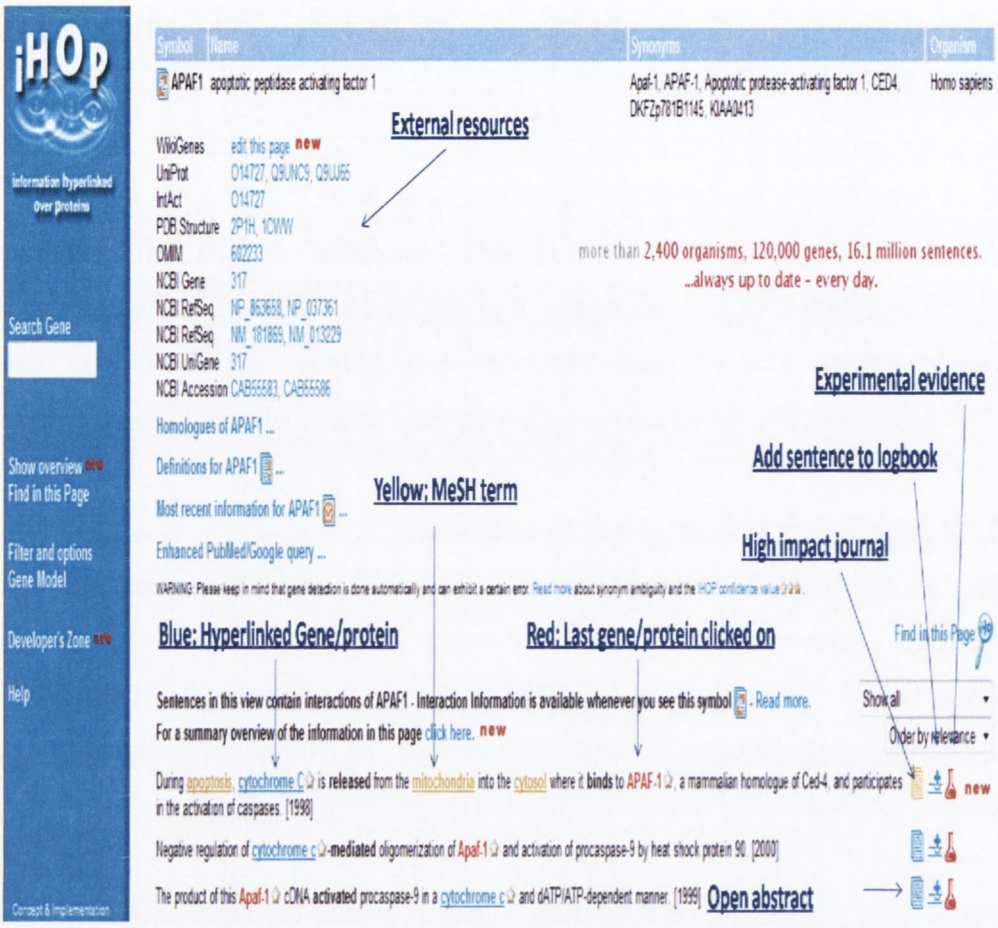

Figure 2.1

Navigation of iHOP. The starting point for the literature search is a gene or protein (e.g. *APAF1*) of interest. A link to all external resources is given for the gene/protein of interest. Information pertaining to *APAF1* and its interactions is provided in the form of sentences taken directly from their source abstracts. Gene names in blue are hyperlinked to their corresponding pages in iHOP. Terms in yellow are hyperlinked to the Medical Subject headings (MeSH) definition of the term. Sentences which include proteins whose interaction is experimentally supported is highlighted and ranked higher in order. All sentences are linked to their abstracts for further investigation. Adapted from (Hoffmann and Valencia, 2004).

BioCarta is a leading developer, supplier and distributor of reagents and assays for biopharmaceutical and academic research. Furthermore, the BioCarta website serves as an interactive web-based resource for life scientists, providing information on gene function, proteomic pathways, ePosters and research reagents. This website allows you to observe how genes interact in

dynamic graphical models. A gene/protein of interest can be entered into the search facility of the website and signalling pathways, for which this gene/protein participates in, can be viewed. This website offers an excellent way to unravel complicated apoptotic signalling pathways and gene function.

2.1.3 Screening genes for 5' CpG Islands

Selected genes were screened for the presence of a CpG island in their promoters using the March 2006, Human Genome Browser at the University of California Santa Cruz (UCSC) (http://genome.ucsc.edu). The browser is a rapid and reliable web-based tool for exploring human genome sequences and is used daily by thousands of biomedical researchers worldwide. The UCSC genome browser was developed and is maintained by the genome bioinformatics group at UCSC (Kent et al., 2002) .

The CpG island track, utilised by the UCSC human genome browser, is a modified version of a program developed by G. Miklem and L. Hillier. CpG islands are predicted by applying a scoring system, whereby each CG dinucleotides scored +17 and all other dinucleotides are scored –1, whilst searching the gene sequence base by base. The maximum scoring segments are identified and each segment is evaluated for the following criteria:

GC content ≥50%

Length >200bp

Ratio >0.6 of observed number of CG dinucleotides to the expected number of Gs and Cs present in the segment.

Obs/Exp CpG = Number of CpG * N / (Number of C * Number of G)

Where N = Length of sequence (Gardiner-Garden and Frommer, 1987) (http://genome.ucsc.edu/cgi-bin/hgTrackUi?g=cpgIslandExt&hgsid=114645567)

2.1.4 Identifying genes with susceptibility to hypermethylation and/or reduced expression in prostate cancer.

2.1.4.1 Microarray studies

A number of published microarray studies that compared gene expression between different stages and grades of prostate cancer were examined for selection of genes with evidence of decreased gene expression levels in prostate cancer (Cho-Vega et al., 2005; Ernst et al., 2002; Yu et al., 2004a).

2.1.4.2 Literature review

Meta-analysis and extensive review of the literature was performed using PubMed (http://pubmed.gov/), iHOP (http://www.ihop-net.org/UniPub/iHOP/) and Google (www.google.ie) to 1) identify apoptotic genes, which show evidence of promoter hypermethylation in both prostate cancer and/or additional cancers and 2) review the literature of individual genes of interest for evidence of downregulation of gene expression in both prostate cancer and/or additional cancers.

2.1.5 Candidate prioritising

Apoptotic-related genes containing 5' CpG island(s) identified from our *in silico* approach were pooled with genes identified from searching the candidate gene bank. Firstly, genes were organised by predicted function and importance in apoptosis. Candidate genes with evidence of decreased gene expression in prostate cancer and/or evidence of susceptibility to promoter hypermethylation in prostate cancer or other cancers were selected.

2.2 CELL CULTURE

2.2.1 Solutions and media

A class II laminar flow cabinet (Clean Air Techniek, Woerden, Netherlands) was utilised for all cell culture work. All reagents were purchased from Invitrogen, Cambridge, UK, unless otherwise stated.

Complete medium (for culture of LNCaP, PC-3, 22RV1, RC58 and DU145 cell lines):

500 ml RPMI 1640 with Glutamax

50 ml foetal calf serum (FCS)

5 ml penicillin-streptomycin

Serum free medium (for culture of PWR-1E and RWP1E cell line):

500 ml keratinocyte, serum free medium with EGF (Bovine pituitary extract)

5 ml penicillin/streptomycin

2.2.2 Prostate cell lines

LNCaP and 22RV1 androgen-dependent prostate cancer epithelial cell lines, DU145 and PC3 androgen-independent prostate cancer epithelial cell lines and normal prostate epithelial cell lines (RWPE1 and PWR1E) were all obtained from the American Type Culture Collection (ATCC, Manassas, VA, USA). Prostate cancer epithelial cell line RC58T was a kind gift from Yutaka Yasunaga, Centre for Prostate Disease Research, Uniformed Service University of Health Sciences, Bethesda, MD, USA. All cell lines are adherent. Prostate cancer cell lines LNCaP, PC-3, DU145, 22RV1 and RC58T were derived from human prostate carcinoma xenograft, primary tumour with telomerase, prostate cancer bone metastatic sites, lymph node, bone, and brain, respectively. Normal cell lines RWPE1 and PWR1E were both established from normal prostate basal epithelial cells. Doxetaxel resistant PC3-D12 cell line and an age-matched control were generated by Dr. Amanda O'Neill (Conway Institute, University College Dublin, Dublin, Ireland).

2.2.3 Colon Cancer cell lines

Colon cancer cell pellets from four cell lines (HCT116, RKO, LoVo and HT-29) were a kind gift from Dr. Daniel Longley (Queen's University, Belfast, Northern Ireland). HCT116, RKO, LoVo and HT-29 were derived from colorectal carcinoma, colon carcinoma, colorectal adenocarcinoma derived from a left supraclavicular region metastatic site and colorectal adenocarcinoma respectively.

2.2.4 Thawing cells

Cells were stored in liquid nitrogen until required. Frozen cells were thawed at room temperature and transferred to a 20 ml sterile tube on ice. Complete medium was added, slowly, until twice the original volume. Medium was added to a final volume of 10 ml is reached. Cells were centrifuged for 5 minutes at 1200 rpm in a Centra GP8 centrifuge (IEC, USA). The supernatant was discarded and cells resuspended in 10 ml medium (complete or serum free, depending on cell type) and transferred to a 75cm^3 culture flask.

2.2.5 Culturing cells

LNCaP, PC3, DU145, 22RV1, RC58T, PC3-D12 and PC3 age-matched control cell lines were cultured in 20 ml complete medium. PWR1E and RWPE1 cells were cultured in 20 ml keratinocyte, serum-free medium with EGF. All Cells were cultured in 75 cm^3 flasks (NalgeNunc, UK) and incubated at 37°C, 5% CO_2 (Forma Scientific, USA). Medium was replaced twice/week as required with 20 ml fresh medium. Colon cancer cell lines HCT116, RKO, LoVo and HT-29 were cultured in 20ml of complete medium.

2.2.6 Passaging cells

Cells were passaged when they reached 70% confluence and were split into new 75cm^3 flasks. This was performed by removing spent medium and washing the cells twice with 2mls of d-PBS (GIBCO d-PBS, contains $CaCl_2$, $MgCl_2$, Invitrogen, Cambridge, UK). 5ml of trypsin, 1:250 dilutions, in GIBCO solution A (Invitrogen, Cambridge, UK) was added to each flask. Cells were incubated at 37°C for 2-5 minutes. The flasks were swirled gently to minimise clumping during cell detachment. Trypsin was inactivated with 5ml of complete medium. Trypsinised cells were transferred to new 50ml tubes and centrifuged (Thermo Fisher Scientific Inc, IEC Centra GP8, Waltham, MA, USA,)) at 1500rpm for 3 minutes. The supernatant was discarded and cell pellets resuspended in 10 ml of fresh medium and split either 1:3, 1:4 or 1:5 into new 75 cm^3 flasks, depending on confluency/cell count. The medium was brought to a final volume of 20 ml with fresh medium. All medium, trypsin and PBS was pre-warmed to 37°C before use.

2.2.7 Freezing cells

Cells were trypsinised as outlined in 2.2.6. Cell pellets were resuspended in 3.6 ml complete medium. The medium was split into 2 cryovials (NalgeNunc, Rochester, NY, USA) and placed immediately on ice. While on ice, 200 µl of dimethyl sulfoxide (DMSO) was added. Cells were immediately stored at -80°C in a polystyrene box (previously at room temperature), to allow cooling at -1°C per minute. For long-term storage, cells were stored in liquid nitrogen.

2.2.8 Drug Treatment to induce DNA hypomethylation

PC3 cells (1 x 10^6) were seeded in 75 cm^3 culture flasks. 24 hours after plating (day 1), the cells were treated with 1 µM 5aza2'deoxycytidine (5-Aza-CdR) (Sigma, Dublin, Ireland) to induce demethylation. Treatment was repeated on day 3 and day 5. Cells were harvested on day 6.

2.2.9 Preparation of cells for nucleic acid extractions

To harvest cells for DNA and RNA isolation, cells were first washed twice with 1X PBS. Cells were trypinsinised as described previously and subsequently centrifuged at 1500 rpm for 5 minutes. The supernatant was discarded and the pellet resuspended in 10 ml of complete media. Cells were counted using ethidium bromide acridine orange (ETAO). 100 µl of cells were diluted 1:3, 1:5 or 1:10 (depending on confluency) with ETAO and placed immediately on ice. 7 µl was transferred onto a haemocytometer glass slide (volume: 1 x 10^{-4} cm^3) and viewed under a Leitz Dialux 20 EB fluorescent microscope (Leitz Instruments). Using the 20X objective, living cells were visualised by the green fluorescent stain of acridine orange. Dead cells were stained orange by ethidium bromide, which cannot enter viable cells. Viable cells were counted in four different grids of the haemocytometer. A mean viable cell count was calculated by multiplying the number of viable cells by the volume of the haemocytometer (1 x 10^{-4}), which gives the number of cells/ml. This number is multiplied by the dilution factor (3, 5 or 10); this gives the number cells/ml in our stock solution (10ml).

In order to isolate DNA and RNA from the same culture, the cell suspension was divided in two and centrifuged at 1,500 rpm for 5 minutes. Supernatant was discarded and resuspended in 50µl of PBS for DNA isolation. For the purpose of RNA isolation, 10 volumes of RNA*later* RNA stabilization reagent (QIAGEN Ltd., West Sussex, UK) were added to cell pellets resuspended in 50 µl PBS/ 5 x 10^6 cells. Cells were stored at -80°C for future nucleic acids extractions.

2.3 PROSTATE TISSUE SAMPLES

2.3.1 Ethical approval

A proposal requesting the collection of retrospective patient prostate material for the purpose of our epigenetic research was submitted to St. James's Hospital (SJH) Pathology Department. Ethical approval for use of patient material in prospective genetic and epigenetic research had been previously granted by the St James's Hospital and Adelaide and Meath incorporating the National Children's Hospital (AMNCH) Tallaght Ethics Committee.

2.3.2 Retrospective sample collection

2.3.2.1 Patient Selection

Prostate tissue samples were sought from patients:

1) Treated by radical prostatectomy for primary (either clinically localised or locally advanced) prostate cancer.

2) With BPH who underwent transurethral resection (TURP) of the prostate and who had no histological diagnosis of prostate cancer.

3) With a histological diagnosis of HGPIN, with or without prostate cancer.

The Biobank Information Management System (BIMS) was utilised to identify patients within the Prostate Cancer Research Consortium (PCRC) which met the above criteria. The BIMS consists of a central biobank data repository for the storage of clinical, pathology, sample information and analytical research data from consenting patients diagnosed as having prostate cancer. The purpose of the BIMS is to facilitate research into prostate cancer. Data are held

in the BIMS for each patient in relation to some or all of the following categories:

- Patient Information
- Pre-op/Biopsy
- Radical prostatectomy
- Pre/post operational PSA
- Patient outcome
- Sample collection blood, plasma, serum, DNA, RNA
- Sample collection (tissue)
- Sample collection (urine)

Data held in the BIMS are made available to the hospitals and research institutes participating in the PCRC.

Pathology reports were sourced through the PCRC with the help of Dr. Linda Sullivan and Dr. Antoinette Perry to collect information regarding disease stage, grade, TNM classification, age of diagnosis, gland confinement, pre- and post- procedure PSA levels and family history. Four patients (IMM0001, IMM0058, IMM0075, IMM0084) had a positive family history of prostate cancer (with a least one first degree relative also having a diagnosis of prostate cancer).

2.3.2.2 Specimen retrieval

Tissue specimens from radical prostatectomy, TURP procedures carried out at AMNCH and SJH are formalin-fixed and paraffin-embedded (FFPE) and are archived within the pathology department. Pathology numbers and medical record numbers were obtained from pathology reports and used together to retrieve all of the histology slides for the FFPE surgical specimens.

The slides were reviewed by pathology registrar Dr. Ciara Barrett, SJH to identify areas of tumour, normal prostate glands, HGPIN and BPH respectively, which were then marked on the slides. The Gleason grades were also marked on each slide. The corresponding paraffin blocks for these slides were recovered from the pathology archives. Nine serial 5 μm sections were

cut from blocks on a microtome by an experienced technician. The first and last tissue section from each block was stained with haematoxylin and eosin (H&E), cover-slipped and compared with the pathologically evaluated slide, to ensure a consistent percentage of target cells. All slides were labelled with their PCRC code and contained no patient identifiers.

In addition, additional patient material was available from AMNCH, from a cohort of patients previously collected by Dr. Antoinette Perry, in the laboratory. This cohort consists of 40 cases of prostate cancer (with histologically benign tissue available in 39/40 cases and HGPIN available in 14 cases) and 37 cases of BPH. H&E slides were reviewed by Dr. Perry with consultant histopathologist Dr. Barbara Loftus (AMNCH) to identify and mark out target cells (Tumour, benign, BPH or HGPIN). AMNCH tissue samples were anonymised with a unique 4-element laboratory code, to protect patient confidentiality and to facilitate rapid sample identification. Each code started with the letters AM, which identified the source of the tissue as AMNCH, followed by two digits, which identified the year the procedure was carried out (-98 to –03), a unique 3 digit number, which was used for all samples from an individual case (for example, tumour, normal and HGPIN) and finally a single letter, which identified the type of sample as either tumour (T), normal (N), BPH (B) or HGPIN (P).

The PCRC bio-resource collects prostate tissue from patients with suspected organ-confined or locally advanced prostate cancer who are undergoing a radical retropubic prostatectomy. Specimens are also collected from patients with benign prostatic hyperplasia who are undergoing a transurethral resection of the prostate. The PCRC has put in place Standard Operating Procedures (SOP) for the collection, handling, processing and storage of biospecimens which are consistently followed across all sites to generate uniformly high quality biospecimens and to avoid introducing variables into research studies. Sample information including time of collection; time elapsed from collection to processing and sample usability are recorded on the consortium's Bio-resource Information Management System (BIMS). Each sample aliquot is labelled with a unique alphanumeric code and transferred to a local cryogenic

storage facility. The precise physical location of each sample is mapped and documented on BIMS.

In collaboration with the surgical staff, the prostate gland is collected from theatre and transported to the hospital pathology department, (by the research nurse), as rapidly as possible to minimise warm ischemic time and maintain the integrity of the DNA/RNA. As prostate cancer develops as independent foci within the gland and is usually not visible macroscopically, the patient biopsy report is used to inform the most likely site of tumour and normal tissue. Prostate tissue that is surplus to diagnostics, as determined by the pathologist, is then excised from the gland and immersed in RNA*later*, for nucleic acid preservation, and stored at -80°C until further use. Prior to DNA/RNA extraction from fresh tissue, additional pathology characterisation of suspected tumour and normal prostate tissue is required.

2.4 NUCLEIC ACID ISOLATION

2.4.1 Nucleic acid isolation from cultured cell lines

Prostate cancer cell lines were cultured for the purposes of DNA and RNA extraction, as described in section 2.2.6.

2.4.1.1 DNA extraction

Total DNA was isolated from cell lines by use of a QIAamp DNA blood mini kit (QIAGEN Ltd., West Sussex, UK), according to the manufacturer's instructions. Briefly, 5 x 10^6 cells were digested with 20 µl QIAGEN protease. Appropriate binding conditions were achieved by adding 200 µl of buffer AL and incubated for 10 minutes at 56°C, followed by the addition of 200 µl of 100% ethanol. The lysate was transferred to the QIAamp spin column, whereby the DNA becomes adsorbed onto the silica-gel membrane during centrifugation. The DNA was washed to remove protein and other contaminants with Buffer AW1 and AW2. DNA was eluted in 300 µl Buffer AE (10 mM TrisCl, 0.5 mM EDTA; pH 9.0) and stored at -20°C until required. The concentration (absorbance at 260 nm) and purity (ratio of absorbance at

260 nm to absorbance at 280 nm) of DNA was measured using a NanoDrop ND-1000 spectrophotometer (NanoDrop Technologies, Inc.).

2.4.1.2 RNA extraction

Total RNA was isolated using the RNeasy mini kit (QIAGEN Ltd., West Sussex, UK), following the manufacturers protocol. Briefly, 5 x 10^6 cells were disrupted in a guanidine isothiocyanate- containing buffer (Buffer RLT and β – Mercaptoethanol), to inactivate RNases, which can result in RNA degradation. Disrupted cells were homogenized by pipetting the lysate directly into a QIAshredder spin column and centrifuged for 2 minutes at full speed. To ensure appropriate RNA binding conditions to the silica-gel membrane one volume of 70% ethanol was added to the homogenized lysate and the sample was mixed by pipetting. Residual DNA was removed by addition of an on-column DNase I digestion step. Two centrifuge wash (with Buffer RW1 and RPE) steps were added to remove any remaining contaminates. Purified RNA was eluted into 60 µl DNase and RNase-free molecular grade water (Sigma-Aldrich, Dublin, Ireland) and stored at -80°C until further use. The concentration (absorbance at 260 nm) and purity (ratio of absorbance at 260 nm to absorbance at 280 nm) of RNA was measured a NanoDrop ND-1000 spectrophotometer.

2.4.1.3 cDNA Synthesis

After RNA isolation, reverse transcription was performed to generate cDNA for real-time PCR. cDNAs were synthesised from between 2.5-5 µg of RNA using the applied biosystems High-Capacity cDNA Reverse Transcription kit. Between 2.5- 5µg of RNA was diluted into a final volume of 25µl in RNase free water and incubated at 70°C for 10 minutes to remove any secondary structures, and cooled immediately on ice. The 2X reverse transcription master mix was prepared as follows.

Reagent	Volume/ reaction (µl)
10X RT Buffer	2
25X dNTPs Mix (100mM)	2
10X RT Random primers	5
Multiscribe Rev. Transcriptase	2.5
Nuclese-Free H2O	10.5
Total	25

Table 2.1: 2X Reverse Transcription master mix

The denatured RNA was added to the mixture and vortexed gently. The reaction was placed in a DNA engine Peltier Thermal Cycler-200 (MJ Research) and cDNA synthesis performed under the following cycling conditions; 25°C for 10 minutes, 37 °C for 2 hours, followed by 5 seconds incubation at 85 °C. Synthesised cDNA was stored at -20°C until required.

2.4.2 Nucleic acid isolation from formalin fixed paraffin embedded (FFPE) tissue

2.4.2.1 Deparifinization of FFPE tissue

In a fume hood, a Shandon staining station (Thermo Electron Corporation, Cheshire, UK) was prepared with three troughs of xylene (Sigma-Aldrich, Dublin, Ireland), two of 100% ethanol, two of 95% ethanol, 1 with 70% ethanol and 1 with PBS. Slides were deparaffinised by placing in xylene with gentle agitation in each solution for five minutes and then rehydrated in the decreasing concentrations of ethanol, by gentle agitation in each solution for two minutes, and 30 seconds in the 70% ethanol wash. Finally, slides were washed in PBS for 3 minutes. Slides were air dried in the fume hood. A sterile razor blade was used to scrape off tissue from within the pathologically marked areas. Using the blade together with a 20 µl pipette tip, the tissue was transferred to a 2 ml microcentrifuge tube with screw-top lid.

2.4.2.2 DNA extraction

DNA was extracted using Recover All Total nucleic acid isolation kit (Applied Biosystems, Warrington, UK) according to manufactures instructions. In brief, 200 µl of Digestion Buffer and 2 µl protease was added to each sample. The tube was swirled gently to mix. Half the sample was removed after 3 hour incubation at 50˚C (stored at -80ºC for RNA extraction at a later date) and the remaining sample was incubated for 72 hours for DNA isolation. Samples were topped up with 10 µl of Qiagen protease after 24 hours following incubation. 240 µl of isolation additive was added to each tube and vortexed. 550 µl of 100% molecular grade ethanol (Sigma-Aldrich, Dublin, Ireland) was also added to each sample and mixed by pipetting. A filter cartridge was placed in a pre-labelled collection tube. 500 µl of the sample/ethanol mixture was pipetted onto the filter cartridge and the lid closed. To prevent clogging of the filter, pipetting large pieces of undigested tissue onto the filter cartridge was avoided. The tubes were centrifuged at 10,000 x g for 60 seconds to pass the mixture through the filter and the flow through discarded. This was repeated until all the mixture had passed through the filter.

700 µl of Wash 1 was added to the filter cartridge and centrifuged for 30 seconds at 10,000 x g to pass the mixture through the filter and the flow through was discarded. 500 µl of Wash 2 was added to the filter cartridge and centrifuged for 30 seconds at 10,000 x g. This was repeated with Wash 3. A master mix of 10 µl RNase A and 50 µl of Nuclease-free water was prepared. 60 µl of the mix was added to the centre of each filter cartridge and incubated for 30 minutes at room temperature. 700 µl of Wash 1 was added to the Filter Cartridge and incubated for 30–60 seconds at room temperature. The tubes were centrifuged for 30 seconds at 10,000 x g. Two more wash steps were performed with Wash 2 and 3 as described above. The tube was centrifuged for 1 minute at 10,000 x g to remove residual fluid from the filter. The Filter Cartridge was then transferred to a fresh collection tube and labelled. 25 µl of pre-heated (95ºC) nuclease-free water was applied to the centre of the filter and the cap closed. The sample was incubated at room temperature for 1 minute and centrifuged for 1 minute at maximum speed to pass the mixture through the filter. This step was repeated with a second 25 µl aliquot of elutant. The

DNA yield and quality was assessed using the Nanodrop spectrophotometer. The DNA was stored at –20°C.

2.5 METHYLATION TECHNIQUES

2.5.1 Methylation Controls

A fully methylated positive control (CpGenome Universal Methylated DNA) and fully unmethylated negative control (CpGenome Universal Unmethylated DNA A, CpGenome Universal Unmethylated DNA B) (Chemicon International, Temecula, CA, USA) were used for PCR, DHPLC and sequencing analysis. CpGenome Universal Methylated DNA (MC) is enzymatically methylated human male genomic DNA. Two separate unmethylated genomic DNA controls were used to ensure that each assay had a negative methylation control. CpGenome Universal Unmethylated DNA A (UMA) represents unmethylated human genomic DNA. CpGenome Universal Unmethylated DNA B (UMB) is genomic DNA isolated from a human fetal cell line. In the case of certain genes, such as *TMS1* (see Section 4.4.1), where both unmethylated controls were methylated, a cell line (RWPE1) which was unmethylated for *TMS1*, was employed as an alternative negative methylation control.

2.5.2 Partial Methylation Control

A partial methylation control (PMC) was made by treating CpGenome UMA DNA with varying concentrations of *SSs*I methylase (New England Biolabs, London, England). Briefly, in order to generate a fully methylated, unmethylated and two partially methylated controls (varying levels of methylation), a *SSs*I methylase mix was prepared as follows, 10 µl 10X NEBuffer 2, 640 µM/160 µM of S-Adenosyl methionine, 4, 2 ,1 or 0 units of *SSs*I methylase, 5 µg DNA to a final volume of 100 µl. The reaction was incubated at 37°C for 2 hours and heat inactivated for 20 minutes.

2.5.2.1 Restriction digestion of SSsI methylase treated DNA

The *SSs*I methylase treatment of unmethylated DNA was analysed by restriction digestion. Utilising the freely available NEBcutterV2.0

(http://tools.neb.com/NEBcutter2/index.php) the restriction enzyme *BsiE*1 (New England Biolabs, London, England) was identified to analyze *SSs*I methylase treated DNA. BsiE1 cuts the DNA at unmethylated cytosines but is blocked by the presence of a 5-methyl-cytosine in its restriction site 5'...CGRYCG...3', where R and Y represent ambiguous nucleotides (see Appendix 4, table A4.6) and therefore will not cut a fully methylated DNA sequence, allowing comparison of the fully methylated and unmethylated sequence to the PMC. The restriction digest was performed according to manufacturer's instructions.

2.5.3 Bisulfite modification

Bisulfite modification of genomic DNA was first employed for the detection of varying methylation patterns in individual strands of particular genomic sequences (Frommer et al., 1992). In this reaction, a bisulfite ion is added to the 5-6 double bond of the cytosine molecule, which is converted to a uracil-bisulfite derivative by hydrolytic deamination. The final alkali treatment of the DNA removes the sulphonate group to give uracil (Shapiro et al., 1973; Shapiro et al., 1974; Wang et al., 1980). Under these conditions, 5-Methylcytosine (5-mC) remains unchanged. During PCR amplification, with primers designed to anneal with bisulfite-converted DNA only, all uracil and thymine nucleotides are amplified as thymine, whereas only 5-mC is amplified as cytosine (Figure 2.2).

Bisulfite modification was performed according to a protocol kindly provided by Dr Karen Woodson (National Cancer Institute, MD, USA). This method was adapted from the EZ DNA methylation kit (Zymo Research, Orange, USA) and all components were used from this kit unless otherwise stated. All bisulfite reactions were performed in 0.2 ml PCR strip tubes (Axygen Scientific, Union City, CA, USA). Up to 2 µg of DNA was denatured (double stranded DNA prevents cytosine dinucleotides from reacting with sodium bisulfite) by adding 5 µl M-dilution buffer (contains NaOH), 1 µg salmon sperm DNA as a carrier and molecular grade dH_20 (both supplied by Sigma, St. Louis, USA) to a final reaction volume of 50 µl, and incubated at 37°C for 15 minutes in a DNA engine Peltier Thermal Cycler-200 (MJ Research, Waltham,

MA, USA). Meanwhile, the bisulfite reagent was prepared by adding 210 µl of M-dilution buffer and 750 µl dH_2O to 1 vial of Ct conversion reagent (contains hydroquinone and sodium bisulfite) and mixed for 10 minutes using a Vortex Genie 2 (Scientific Industries Inc., Bohemia, NY, USA). 100 µl of freshly prepared bisulfite reagent was added to each DNA sample and incubated in a DNA engine Peltier Thermal Cycler-200 (MJ Research) for 12 -16 hours.

The bisulfite treated reactions were purified using microcon ym-100 filters (Millipore, Cork, Ireland). Filters were labelled and placed into a Microcon-96 filtrate assembly 96 well plate (Millipore, Ireland). A counter balance was prepared by adding 300 µl into the lower chamber of a Microcon-96 filtrate assembly plate, which had been set up similarly to our sample plate. 150 µl of dH_20 was added to the upper chambers of our sample plate. The bisulfite reaction was added to the filters. The sample plate and counter balance was centrifuged at 500 x*g* for 20 minutes at 25°C. The filtrate was discarded and the sample washed with 300 µl of dH_20. The plates were centrifuged at 500 x*g* for 20 minutes at room temperature. This wash step was repeated and filtrate discarded after each wash. Next, an alkali treatment was performed to remove the sulphonate group to give uracil. 300 µl of freshly prepared 0.1M NaOH was applied to the filter and centrifuged and filtrate discarded as before. The bisulfite treated DNA was eluted first adding 50µl 1x Tris EDTA (Sigma, St. Louis, MO, USA) to the filter and gently mixing on a STR6 platform shaker (Stuart Scientific, UK) for 1 minutes and then allowed to stand at room temperature for 5 minutes. The filter columns were carefully removed from the tray and placed with the reservoir upside down in a newly labelled 1.5 ml microcentrifuge tube. The filter columns were centrifuged at 1000xg for 3 minutes in order to transfer the concentrate to the vial.

Successful bisulfite conversion was determined by one or both of the following methods 1) bisulfite treated DNA was amplified with primers designed to amplify bisulfite-converted DNA only, using unmodified DNA template as a control as per protocol in section 2.5.3 and 2) bisulfite sequencing, outlined in section 2.5.5.

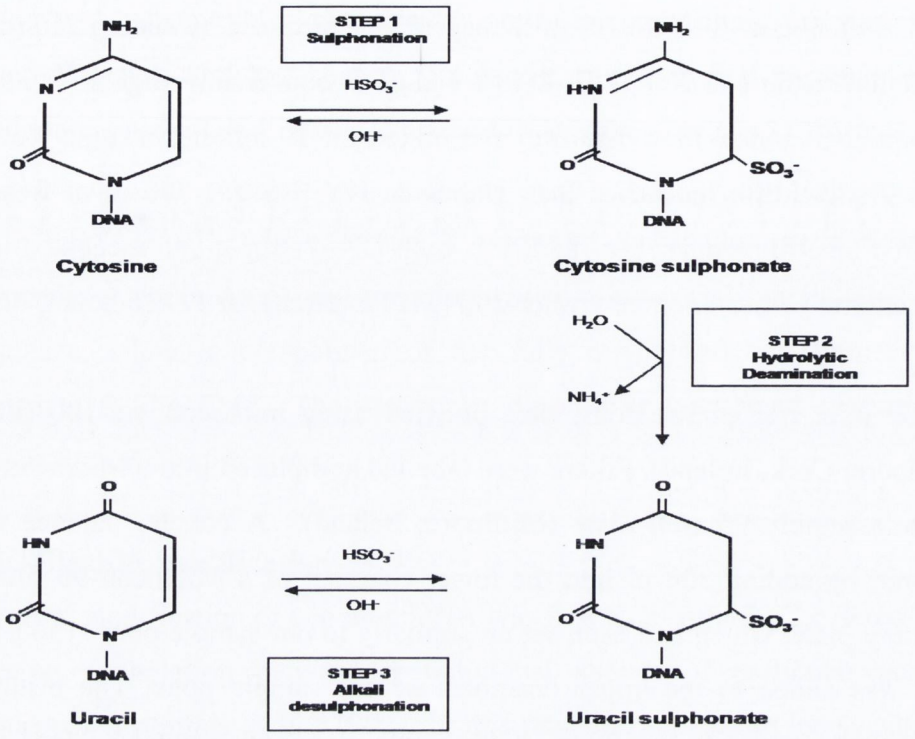

Figure 2.2.

Bisulfite conversion reaction of DNA. The initial step involves the addition of bisulfite to the 5-6 double bond of cytosine. In step 2, cytosine sulphonate undergoes hydrolytic deamination to give uracil sulphonate. Step 3 involves treatment with an alkali to remove the bisulfite adduct, resulting in uracil. A slow reaction within 5-mC and bisulfite can occur, however the equilibrium favours 5-mC rather than the deaminated product thymine (Adapted from Clark et al., 1994).

2.5.4 Bisulfite Polymerase chain reaction

A total of 47 PCR assays were designed to screen part of or the entire promoter CpG island of the 22 apoptotic-related genes identified through the *in silico* screen. Each gene contained only one 5' CpG island (the target of promoter hypermethylation) except *CFLAR*, which contained two distinct islands. Primers were designed as follows:

- Avoid CpG dinucleotides within the primer oligonucleotide hybridisation sites, to ensure amplification of bisulfite modified DNA irrespective of methylation status.

- Sequences to contain a maximum number of non-CpG cytosine nucleotides to bias amplification against incompletely modified DNA.
- All PCR assays were designed to be less than 500bp, since bisulfite modification can cause DNA strand breakage (Li and Dahiya, 2002) .

A list of all primers is given in Table 2.2. Primers (synthesised by MWG-Biotech, Ebersberg, Germany) were rehydrated in molecular grade water (Sigma, St. Louis, USA) to a stock concentration of 100 µM and 1/10 dilution made to generate a working stock concentration of 10 µM.

HotFIREPOL Hotstart PCR reactions (Solis Biodyne., Tartu, Estonia) were performed according to the manufacturer's instructions. Each primer set was optimised by an $MgCl_2$ concentration curve (final concentration: 1.5 mM to 3 mM) and an annealing temperature curve (55°C to 62°C). Briefly, a 50µl PCR reaction of 10x Buffer BD (detergent free), 10 µM each primer (MWG-Biotech, Ebersberg, Germany), 10mM dNTPs (Promega, Hampshire, UK), 1.5mM- 3mM $MgCl_2$ and 1 unit of HotFIREPOL *Taq* polymerase was prepared in 0.2 ml strip tubes (Axygen Scientific, Union City, CA, USA). All reactions were performed in a DNA engine Peltier Thermal Cycler-200 (MJ Research, MA, USA) under the following thermal cycling conditions: 95°C for 15 minutes, followed by 35 cycles of 95°C for 30 seconds, AT°C (Table 2.2) for 30 seconds, 72°C for 1 minute, and a final extension step at 72°C for 10 minutes. After amplification, samples were analysed by gel electrophoresis.

Table 2.2: PCR primer sets and assay conditions					
Gene	Forward primer (5'- 3')	Reverse Primer (5'- 3')	Annealing Tm (°C)	Location of Assay*	Denaturation Tm (°C)
APAF1					
Assay 1	GTGGGAGTTTAAATAGTAGGGGGTT	CCACCTCTCCTAAAAAAACTATAAAACTAAC	58	-1418 to -960	56
Assay 2	AGTTGTTAGTTTTATAGTTTTTTTAGGAGAGGTGG	ACCCAAACTCCCCACCTCTAATT	58	-995 to -553	58
Assay 3	AATTAGAGGTGGGGAGTTTGGG	TCCACCAAAAATTAAAAATACAAAACTC	55	-525 to -138	57
BAD					
Assay 1	GGAGTAGTTAATTAGTAGTAGTTATTATGGAGG	CTTCCCCTACCCAAATTCCTATC	NA	+185 to +485	NA
Assay 2	GATAGGAATTTGGGTAGGGGAAG	CAATAAATCTTTCTAAAACAAAACCC	NA	+462 to +957	NA
BCL2	GTGGGATGAGGGAGATGTGG	TCCCTAAAAAACTCCTCCACCAC	NA	+83 to +416	NA
BIK					
Assay 1	GATAAAATAAGTTTGTAGAATAGTAGGGGGTAG	CAAAAAAACCACCCCATTACACA	56	-13491 to -12940	57
Assay 2	TGTGTAATGGGGTGGTTTTTTTG	CACCTCCAATTTACCAAACAAAAT	52	-12963 to -12532	60
Assay 3	ATTTTGTTTGGTAAATTGGAGGTG	AAAACTACAACAATAACATCAACAACCA	56	-12556 to -12334	NA
BNIP3	AGGTTTTTACGTTAGGTTGGTTTTTA	AAACCCTTCTTTCCATCCTACTAAT	51	-1037 to -536	55
CASP3					
Assay 1	GGGGTTTAGTTTGGGGTTGG	CCTCTCCCTAAATCAAAAACCTTAAC	55	+197 to -251	61
Assay 2	GTTAAGGTTTTTGATTTAGGGAGAGG	TTTCCCAACTTACCTCTACCTTC	NA	+462 to +684	NA
CASP8	GGGGTTGTTTTGTGTGTATAGATAAGGTAT	AACAACCACCAATCACCTTCTTC	58	+534 to +198	52
CASP9	GGTAGGTTTTGGGGAGGGG	TCTCCAAATCTATAATCAACTACCTAACCTAA	NA	-99 to +187	NA
CDKN2A					
Assay 1	GTTTTTTTAGAGGATTTGAGGGATAGG	CCCAAAAAAACCTCCCCTTTTT	52.3	+162 to -267	60
Assay 2	GTTTTTTTAGAGGATTTGAGGGATAGG	CCCAAAAAAACCTCCCCTTTTT	NA	-163 to +267	NA
CFLAR (cFLIP)					
CpG1 assay 1	GATTAAGGGAGGAGGTGTAGGAGAG	AAACCTACAAAACTAAATCAAATTCCAAA	55	-13554 to -13155	56
CpG1 assay 2	TTTGGAATTTGATTTAGTTTTGTAGGT	ACCCCAAAAATTAAACTCTCAAAATC	52	-13184 to -12854	55.5
CpG2 assay 1	TAGTTTTTAGTAGGTGGTGGGGG	CAAACCAAAATTAAAAATACTCCAAATAAA	53	-11486 to -11090	55.5
CpG2 assay 2	TTTATTTGGAGTATTTTTAATTTTGGTTTTG	CCTCTAAAAACTCAAAAAAACCTAAAACC	54	-11081 to -10817	54.5
DAPk					
Assay 1	GAGGGTAGTTTAGTAATGTGTTATAGGTGG	CCCTCCTCGAAAAAAACAAAATC	NA	-648 to -279	NA
Assay 2	TTTGTTTTTTTCGCGGAGGGGAT	AACCCCCTCATACATCAATCTCC	NA	-302 to -81	NA
Note:* base pairs from ATG start site, NA = Not applicable: These Primer sets/ Denaturing temperatures could not be optimised					

Table 2.2: PCR primer set and assay conditions. A list of all primers, annealing temperature, location relevant to ATG start site and denaturing temperature of assay for DHPLC analysis.

Table 2.2 Contd.: PCR primer sets and assay conditions					
Gene	Forward primer (5'- 3')	Reverse Primer (5'- 3')	Annealing Tm (°C)	Location of Assay*	Denaturation Tm (°C)
DCR1					
Assay 1	TAGGGATGTTTGGTTTTGGTTATTT	ATAAATTCCACCTTAACTCCCTCCC	NA	-281 to +334	57.5
Assay 2	TAGGGATGTTTGGTTTTGGTTATTT	ATAAATTCCACCTTAACTCCCTCCC	55	+133 to +343	NA
DCR2					
Assay 1	AATTAGATTATGGTTTTTGGATTTTAAGATT	CTATTCTAAAACTTCCTCTAAAACAACTCAAT	NA	-194 to +108	56.5
Assay 2	AATTAGATTATGGTTTTTGGATTTTAAGATT	CTATTCTAAAACTTCCTCTAAAACAACTCAAT	55	+77 to +423	NA
DR4					
Assay 1	ATTTTAGTTATTTAGGAGGTTGAGGTAGGA	CTATTAACTAACCCTAAACTTCCTTCCTCTA	NA	-559 to -111	NA
Assay 2	TAGAGGAAGGAAGTTTAGGGTTAGTTAATAG	AACTCTCCCAAAAAACTATATTCCCA	NA	-127 to +387	NA
DR5					
Assay 1	GTTTTTGGGAAGGGGAGAAGA	CAAATCCAATATACAACTACAAATTCCAC	54	-532 to -202	57
Assay 2	GTGGAATTTGTAGTTGTATATTGGATTTG	CAAACTCAACTAAAACCAACAACAAAAC	NA	-231 to +153	NA
FADD					
Assay 1	GTAATTTTGGTTATTAATAGATGTGAGGGT	ACCTACACTCCTATACCTAATTCACTACAAA	56	-497 to -106	55
Assay 2	TTTGTAGTGAATTAGGTATAGGAGTGTAGGT	CTACACACAAATCTTCTTCCCCAA	NA	-129 to +158	NA
FAS	TTTGAAGTGAGTATGTTAGTTATTGTAGGAA	CCAAAAATAAAAAAATCCAAATACCC	NA	-445 to +31	NA
HRK					
Assay 1	ATTTAGGAAAAGGGGAAGGAGAA	CCTCCTCTCCCTCCTACCTCTA	NA	+124 to -308	NA
Assay 2	TAGAGGTAGGAGGGAGAGGAGG	CCAACCCAACTTCTCCAATACC	NA	-286 to -429	NA
PAR4					
Assay 1	TAAAAGGAAGAGTGGTGGGAGAAG	AACTCCAAACAATCCCAAAACAA	NA	+703 to +263	NA
Assay 2	TTGTTTTGGGATTGTTTGGAGTT	CTTCCACTCCTCCAAAAAATCTATAATAC	NA	+286 to -69	NA
Assay 3	GTATTATAGATTTTTTGGAGGAGTGGAAG	TTCATCATCTTCTTACTCATCTAAACACTCT	NA	-40 to - 540	NA
PIGPC1					
Assay 1	AAATAAGTGTATATGTTGGTGAGTTAGGAAG	ACCCCACCTAAATTCCTATAACTCAA	56	-378 to -156	55.5
Assay 2	TTGTAGTTGGATTTTGTTTTTGT	CAAACATTCTAAAAAACACTAACTCCCC	53	-181 to +49	56
Assay 3	TTGAGTTATCGGAATTTAGGTGGGGT	ACAAAAACAAAATCCAACTACAA	53	+27 to +335	56
TMS1					
Assay 1	AATTGTGGGAGAGGATTTTAAGGTT	CCTTCCTCCCACTCTAATCTCC	57	-451 to -92	55
Assay 2	GGAGATTAGAGTGGGAGGAAGG	ACAAAACATCCAACAACCACTCA	NA	+228 to +349	NA
XIAP					
Assay 1	TGGTTTTGAAGAATTGTTGGGA	AAAAATTAAAACCATCCTAACCAACAC	NA	-2175 to -1664	NA
Assay 2	GTGTTGGTTAGGATGGTTTTAATTTTT	CCTTCTAACCCTCACTACCCACTC	NA	-1691 to -1219	NA
Assay 3	GAGTGGGTAGTGAGGGTTAGAAGG	CCTCCAAACAAACTCTAAAATTCAAAC	NA	-1243 to -744	NA
Assay 4	GTTTGAATTTTAGAGTTTGTTTGGAGG	CCCTCACCCTAACTAACTAACTTCTCTC	NA	-771 to -298	NA
Note:* base pairs from ATG start site, NA = Not applicable: These Primer sets/ Denaturing temperatures could not be optimised					

Table 2.2 Contd: PCR primer set and assay conditions. A list of all primers, annealing temperature, location relevant to ATG start site and denaturing temperature of assay for DHPLC analysis.

2.5.5 Denaturing High Performance Liquid Chromatography (DHPLC)

DHPLC was first described for the detection of DNA sequence variation by (Oefner and Underhill, 1995). DHPLC allows for the detection of single base substitutions and small insertions/deletions based on denaturing temperature differences between mutant (heteroduplex) and wild type (homoduplex) sequences. DHPLC has been reported as a highly sensitive and specific tool in detecting mutations (O'Donovan et al., 1998).

Recently, DHPLC has been used to discriminate between differentially methylated regions of genes subject to parental imprinting (Baumer, 2002; Couvert et al., 2003). Following PCR amplification of bisulfite modified DNA, a methylated template has a dramatically higher GC % and therefore a higher melting temperature than an unmethylated form of the same sequence. This results in different column retention time under partially denaturing (DHPLC) conditions. More recently, DHPLC has been developed as a methylation screening platform, whereby CpG islands can be rapidly screened for methylation (Perry et al., 2007).

In contrast to SNP detection, which uses heteroduplex analysis, here we perform homoduplex analysis only. As a result a heteroduplex step, whereby the DNA is denatured and cooled rapidly to allow reannelling of single stranded (ss)DNA resulting in heteroduplex formation, was not added. Using homoduplex analysis, 100%, 0% and various intermediate levels of partial methylation can be detected.

DHPLC was performed on an automated DHPLC instrument (WAVE®, Transgenomic Inc, Cambridge, MA, USA) and the column was a Transgenomic DNASep® cartridge. The DNASep® cartridge is composed of alkylated non-porous polystyrene-divinylbenzene particles 2-3 microns in diameter and allows for nucleic-acid separation via ion-pair reversed-phase liquid chromatography (Couvert et al., 2003). After the PCR product was analysed by gel electrophoresis (described in Section 2.5.4), the remaining PCR product was stored at –20°C, until required for DHPLC analysis.

2.5.5.1 Optimisation of DHPLC assay: Choosing the best partially denaturing temperature.

The partially denaturing temperature of the fully methylated and fully unmethylated sequence for each assay was determined using the Stanford DHPLC Melt Program (http://insertion.stanford.edu/melt.html). This melt program uses parameters obtained by the simple simulated annealing algorithms used to fit melting temperature predictions to experimental data for 10 mutations. Temperatures 1 and 2 degrees lower than the temperature(s) predicted by the DHPLC Melt program for the methylated template and 1 and 2 degrees higher than the temperature(s) predicted for the unmethylated template were selected for assay optimisation. These predicted temperatures were optimised using methylated and unmethylated controls. The partially denaturing temperature that gave the best separation of unmethylated and methylated sequences was chosen.

2.5.5.2 Analysis of PCR products using DHPLC

Prior to sample analysis, a series of standards (supplied by Transgenomics) were run on the DHPLC according to manufactures guidelines to ensure accuracy of the DHPLC DNASep cartridge. Furthermore, a daily maintenance program was performed according to the manufacturer's instructions.

A volume of 10 µl of PCR product was analysed. The samples were run at a linear gradient of 2% buffer B (a mixture of 25% acetonitrile and 100 mM triethyl ammonium acetate) at 0.9 ml per minute flow rate over 16 minutes starting at 40% buffer B. Results were analyzed using Client Software supplied by Transgenomics.

2.5.6 Bisulfite sequencing

Bisulfite sequencing is the "gold standard" for methylation studies and utilises traditional sequencing methods on bisulfite-modified genomic DNA to determine methylation status at individual CpG dinucleotides. Primer sets used for amplification of CpG islands of interest, outlined in section 2.5.4, were also used to amplify our template DNA for bisulfite sequencing. In some cases (CpG1 cFLIP, CpG2 cFLIP, DCR1 and DCR2), the number of PCR assays

required could be lowered by amplification of the whole CpG island using the forward primer of assay 1 and the reverse primer from its final assay.

In order to obtain unambiguous data on methylation patterns, PCR assay products were cloned prior to bisulfite sequencing.

2.5.6.1 Cloning PCR products

Agar Plates with Ampicillin:

16g of lucia agar (Sigma, St. Louis, USA) was dissolved into 400µl of distilled water and autoclaved. Agar was melted in the microwave and allowed to cool to 60°C. In a sterile laminar flow cabinet, 400µl of Ampicillin (50mg/ml) was added to the warm agar. Approximately 25mls of agar/Ampicillin was poured into sterile plates and allowed to set for 30 minutes. The plates were stored upside down at 4°C, until required.

Prior to cloning, PCR products were purified using a PCR purification Kit (QIAGEN Ltd., West Sussex, UK) according to manufactures instructions. Purified PCR products were cloned using TOPO TA cloning kit for sequencing (Invitrogen, Cambridge, UK). All reagents were supplied with this kit unless otherwise stated. In order to ensure the presence of 3′ poly A-overhangs on PCR products prior to cloning, the following step was performed. 0.5 units of Solis Biodyne HotFIREPOL taq and 0.4µl of 10µM dATP (Promega, Southampton, UK) was added to 3.5 µl of PCR product and incubated at 72 °C for 15 minutes.

The PCR product was first ligated into a plasmid vector (Figure 2.3). The following ligation reaction consisted of 4 µl PCR product (with 3′ A-overhangs), 1 µl salt solution, 1 µl pCR4-TOPO vector; this was set up in the laminar flow cabinet and gently mixed and incubated at room temperature for ten minutes. In addition, a vector only control reaction (with no DNA) was performed in parallel. The ligation reaction was used for transformation directly or stored at -20 °C overnight.

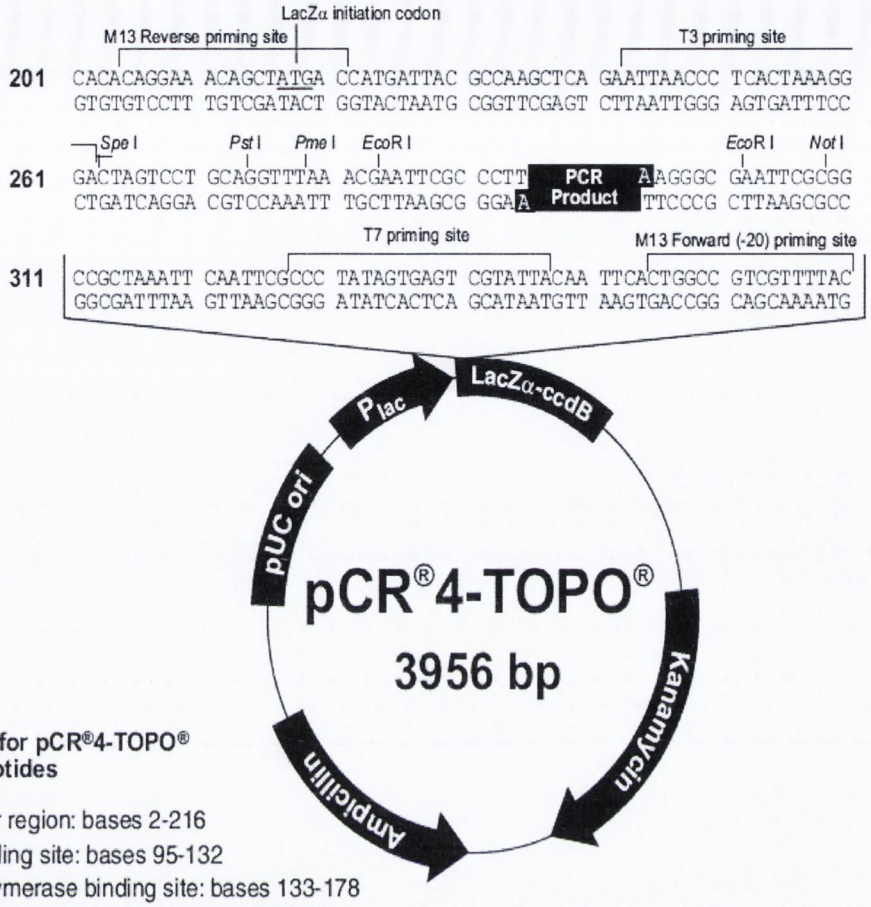

Comments for pCR®4-TOPO®
3956 nucleotides

lac promoter region: bases 2-216
CAP binding site: bases 95-132
RNA polymerase binding site: bases 133-178
Lac repressor binding site: bases 179-199
Start of transcription: base 179
M13 Reverse priming site: bases 205-221
LacZα-*ccdB* gene fusion: bases 217-810
LacZα portion of fusion: bases 217-497
*ccd*B portion of fusion: bases 508-810
T3 priming site: bases 243-262
TOPO® Cloning site: bases 294-295
T7 priming site: bases 328-347
M13 Forward (-20) priming site: bases 355-370
Kanamycin promoter: bases 1021-1070
Kanamycin resistance gene: bases 1159-1953
Ampicillin (*bla*) resistance gene: bases 2203-3063 (c)
Ampicillin (*bla*) promoter: bases 3064-3160 (c)
pUC origin: bases 3161-3834
(c) = complementary strand

Figure 2.3:

Genetic map of vector pCR4-TOPO. Map of pCR4-TOPO and the sequence surrounding the TOPO cloning site. Restriction sites and gene loci are listed. The arrows indicate the start of transcription for the T7 polymerase. Image obtained from Invitrogen (http://www.invitrogen.com).

The pCR4-TOPO plasmid was transformed into TOPO 10 one Shot chemically competent *E.Coli* cells. Cells were thawed on ice and SOC medium was warmed to room temperature. 2µl of the ligation reaction was added to one vial of competent *E.Coli* cells and mixed gently. Similarly, 2µl of the vector-only ligation control reaction was added to one vial of competent *E.Coli* cells. A positive transformation control was also carried out by transforming 1 vial of cells with 10 pg of pUC19 plasmid. The cells were incubated on ice for 10 minutes and heat shocked for 30 seconds at 42 °C in a water bath. Cells were immediately placed back on ice and 250 µl of SOC medium was added to each tube of cells. The tubes were secured in a rack and shaken horizontally at 200rpm at 37 °C for 1 hour in G25 shaker incubator (New Brunswick Scientific Co., Edison, NJ, USA). In the laminar hood, 50 µl of each transformation was spread onto a pre-warmed selective agar plate (1% Amp). Plates were wrapped in parafilm and incubated upside down at 37 °C overnight.

The following day, the plates were removed from the incubator. The vector-only control was analysed for absence of colonies. The pCR4-TOPO vector contains a lethal *E.Coli* gene, *ccd*B, which is fused to the C-terminus of the LacZα fragment (Figure 2.3). Ligation of the PCR product disrupts expression of the *lacZα-ccd*B gene fusion, permitting growth of only positive recombinants upon transformation in cells. We would expect the vector-only ligation control to contain no colonies. The transformation efficiency was calculated by comparing the total number of colonies/plate with that of the pUC19 plate.

Between four and ten colonies were selected for sequencing. A "patch-plate" was prepared using a sterile agar plate (1% Amp) with a 10 square-grid drawn on the base. Using a 20 µl Gilson pipette tip, individual colonies were picked from the plate and transferred firstly to a square in the "patch-plate" and secondly into a 20 µl prepared PCR master mix (according to the protocol outlined in 2.5.4, substituted with an M13 primer set; M13 Fwd 5'-ACACAGGAAACAGCTATGA-3'; M13 Rev 5'-GTAAACGACGGCCAG-3'). Patch plates were incubated upside down at 37°C overnight to allow the

colonies to grow. PCRs were performed under the following thermal cycling conditions: 95°C for 15 minutes, followed by 35 cycles of 95°C for 1 minute, 55°C for 1 minute, 72°C for 1 minutes, with a final extension step at 72°C for 10 minutes in a DNA engine Peltier Thermal Cycler-200 (MJ Research). Gel electrophoresis of PCR products was performed to determine if colonies contained the ligated plasmid.

The following day, positive clones were selected from the patch plates and transferred into 20 µl of dH_20. The bacteria were lysed by incubation at 98°C for 20 minutes. Lysed samples were stored at –20°C, until required for sequencing.

2.5.6.2 Bisulfite Sequencing

Bisulfite sequencing was performed using the ABI Prism BigDye Terminator v3.1 Cycle Sequencing kit (Applied Biosystems, Warrington, UK) according to manufacturer's instructions. The sequencing reactions and pGEM control sequencing reaction were set up as shown in Table 2.3. Samples were sequenced using both the M13 forward and M13 reverse primer to obtain a consensus sequence.

Reagents	**Samples (µl)**	**Control (µl)***
Template (~35ng)	3	1
Primer (2 pmoles)	0.4	2
Big Dye terminator Mix v3.1	2	2
Buffer (5 X)	4	4
dH2O	10.6	13
Total Volume	**20**	**20**
*Control reaction used pGEM as a template and forward M13 Primer		

Table 2.3: Bisulfite Sequencing Reaction

Reactions were amplified on the GeneAmp PCR System 2400 (Applied Biosystems, Warrington, UK) as follows: 94°C for 30 seconds, followed by 25 cycles of 96°C for 10 seconds, 50°C for 10 seconds and 60°C for 4 minutes.

Removal of unincorporated dye terminators directly from sequencing reactions was performed using DyeEx 2.0 spin kit (QIAGEN Ltd., West Sussex, UK). Briefly, the sequencing reaction (20µl) was gently applied to the resuspended gel-filtration resin in the spin column and centrifuged at 3000rpm for 3 minutes. The flow-through (containing the purified DNA) was collected in a 1.5 ml microcentrifuge tube. The column was removed and sample dried in a DNA 100 SpeedVac (Savant, UK) at medium heat. The pellet was resuspended in 10µl of HiDi formamide. (Applied Biosystems, Warrington, UK) and transferred to a 96-well reaction plate in a vertical direction and sealed with a septa strip (Applied Biosystems, Warrington, UK). All empty wells, in multiplies of 16 wells, were filled with HiDi Formamide. HiDi is a highly deionised formamide used to resuspend samples prior to electrokinetic injection in a capillary array.

Sequencing was performed on an automated ABI PRISM 3100 DNA Sequence Detection System (Perkin-Elmer, Foster City, USA). The samples were passed through the 50 cm capillary array with Pop7 polymer (Applied Biosystems, Warrington, UK). Operation of the instrument is described in detail in its manual (ABI Prism 3100 Genetic Analyser Users manual, Applied Biosystems).

The sequencing data were analysed by Mutation Surveyor™ (SoftGenetics, PA, USA). Methylation was analysed at individual CpG sites by the presence of a cytosine (methylated site) or a thymine (unmethylated site) compared to methylation controls. Percentage methylation at individual CpG sites was calculated by analysis of multiple clones (4-10).

2.5.7 Quantitative methylation specific PCR

Eads and colleagues first introduced the high-throughput technology known as MethyLight or quantitative methylation specific PCR (QMSP) for the analysis of DNA methylation that utilises fluorescence-based real-time PCR (TaqMan®) technology (Eads et al., 2000).

2.5.7.1 Real-Time (TaqMan) PCR

Bisulfite treated genomic DNA is amplified by fluorescence-based real-time quantitative PCR using PCR primers flanking a probe with a 5'flourescence reporter dye (6FAM) and a 3' non-fluorescent quencher dye with a minor-groove binding (MGB) moiety, which enhances the melting temperature disparity between matched and mismatched probes. The Taq polymerase 5' to 3' nuclease activity cleaves the probe, thereby releasing the reporter, whose fluorescence can be detected by a laser (Figure 2.4). The initial template quantity can be derived from the cycle number (threshold cycle, C_T) at which the fluorescent signal crossed a threshold in the exponential phase of the PCR reaction. The higher the starting copy number of the nucleic acid target, the earlier in the reaction (as judged by Cycle number) a significant increase in fluorescence is observed (Figure. 2.5).

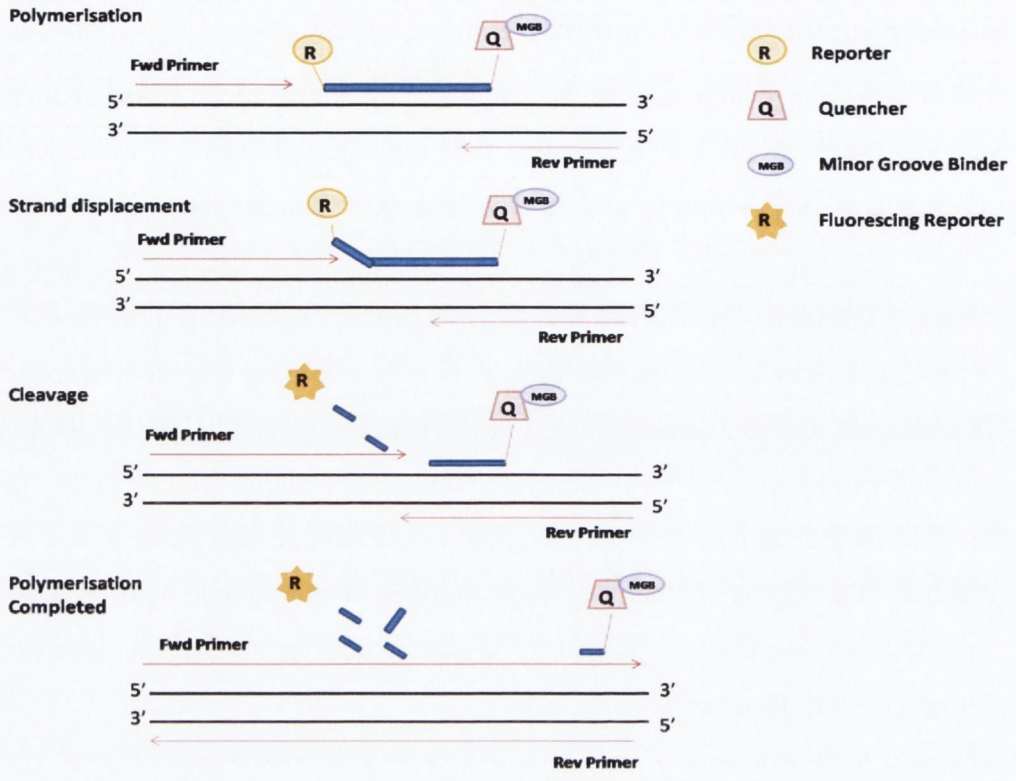

Figure 2.4.

Chemistry of Taqman Real-time PCR. Once the probe remains intact, the location of the quencher significantly reduces the fluorescence emitted by the reporter dye by fluorescence resonance energy transfer (FRET). If the target sequence is present, the probe anneals downstream of the forward primer site. The probe is then cleaved by the 5' to 3' nuclease activity of the Taq polymerase as primer extension continues. Finally, probe cleavage results in release of the reporter dye from the quencher dye, hence increasing the reporter dye signal. The probe is also removed from the target strand allowing primer extension to finish. With each subsequent cycle, additional reporter dye molecules are cleaved from their probes resulting in an increase in fluorescence intensity, which is proportional to the amount of amplicon produced. Adapted from (http://www3.appliedbiosystems.com/AB_Home/index.htm), Applied Biosystems essentials of Real-Time PCR.

A passive reference dye ROX, which does not take part in the PCR reaction, is used to normalise the reporter dye signal, by correcting for fluorescence fluctuations that result from changes in reaction concentration or volume; this

normalised reporter is known as the Rn. After each experiment, the cycle number at which an increase in fluorescence was first detected (baseline) was set by examining the linear view of the amplification plot. ΔRn is the normalization of the Rn obtained by subtracting the baseline (ΔRn = Rn - baseline). The threshold (a level of ΔRn used for the C_T determination) was selected for each experiment by adjusting the level within the exponential phase, to give the best slope (~3.32) and R^2 (>0.98) using the absolute standard curve. The quantity of unknown samples was automatically interpolated from the standard curve by the ABI Prism Sequence Detection software.

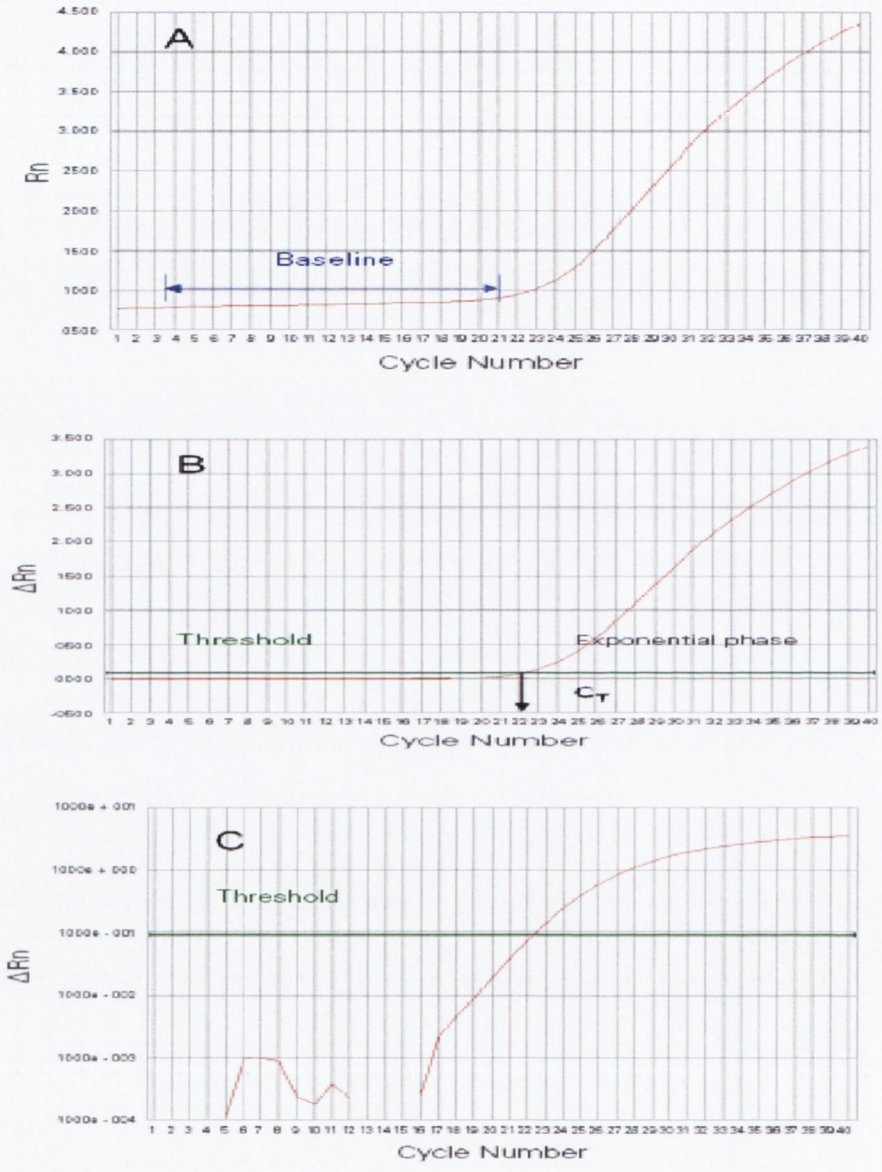

Figure 2.5.

Real-time TaqMan PCR A: Illustrates Rn versus cycle number. Rn is the reporter signal normalised to the fluorescence signal of ROX. The baseline is highlighted, this is the point at which an increase in fluorescence was first detected B: ΔRn versus the cycle number, whereby Rn is normalised by subtracting the baseline to give ΔRn. The threshold is also illustrated and is the line whose intersection with the amplification plot defines the C_T (threshold cycle.) The C_T is the fractional cycle number at which the fluorescence passes the threshold. C: Amplification plot shows the Log (ΔRn) graphed versus cycle Adapted:AppliedBiosystems (http://www3.appliedbiosystems.com/AB_Home/index.htm) Applied Biosystems Real-Time PCR: Understanding C_T.

Relative quantitation using the standard curve method was employed to quantify differences in methylation levels of a target gene between samples. A quantity of product for each reaction was calculated by interpolating from a standard curve, constructed from five reference samples representing fold dilutions (10 ng/µl, 1 ng/µl, 0.1 ng/µl, 0.05 ng/µl, 0.01 ng/µl) of bisulfite modified, universal methylated DNA (Chemicon International, Temecula, CA, USA).

Designing primers and probes to target and amplify small regions of fully methylated bisulfite-modified DNA of the promoter CpG island of interest and analysing the ratio between this reaction and an endogenous control reaction (*ACTB*), which is impartial to methylation status, provides a measure for the frequency of methylated molecules at a given locus.

2.5.7.2 QMSP primer and probe design

Oligonucleotides were custom designed using Primer Express software version 2.1 (Applied Biosystems, Warrington, UK) and tailored to conventional TaqMan primer and probe assay development guidelines:

- Amplicon length between 50 and 150bp
- Melting temperature of probe 10°C higher than that of primers (58 - 60°C).
- No guanine on the 5' end of the probe due to the ability of a guanine residue adjacent to the reporter dye to quench the reporter fluorescence, even after cleavage.
- In addition, QMSP primers and probes were designed to amplify bisulfite modified DNA specifically and to permit sequence discrimination (between methylated and unmethylated target) to occur at both the PCR amplification and the probe hybridisation according to the guidelines below:
- Target to contain a maximum number of non-CpG cytosine nucleotides to bias amplification against incompletely modified DNA.

- Assess a number of CpGs, with at least one CpG dinucleotide at the 3' end of each primer to facilitate maximum discrimination between methylated and unmethylated DNA.

A primer/probe optimisation experiment was completed to determine the appropriate concentration of primer/probe required to yield the highest ΔRn value and lowest C_T value. Six combination optimisation assays were set up at the following concentrations: Combination 1: 900 [Primer (nm)], 100 [Probe (nM)]

Combination 2: 900 [Primer (nm)], 200 [Probe (nM)]

Combination 3: 900 [Primer (nm)], 300 [Probe (nM)]

Combination 4: 300 [Primer (nm)], 100 [Probe (nM)]

Combination 5: 300 [Primer (nm)], 200 [Probe (nM)]

Combination 6: 300 [Primer (nm)], 300 [Probe (nM)]

Each assay was optimised on methylated control DNA and assessed for the best primer/probe concentration combination. QMSP primers and probes and their relative concentrations are listed in Table 2.4.

Table 2.4: QMSP primers and probes

Gene	Forward Primer (5'-3')	Reverse Primer (5'-3')	Probe (6FAM5'-3'MGB)	Location of Assay*	[Primer], [Probe] (nM)
ACTB	GGTGGAGTAGTTAGGGTTTATTTGTA	CCACACCACAAAATCACACTTAACCTCATTT	CACTTTTATTCAACTAATCTC	+3370 to +3468	300,100
BIK	ACGTTCGTGTTGGGCGTAG	GAACGCGAAATCCCGAACTA	AGCGACGTACGGGATA	-13483 to -13327	900,200
BNIP3	CGTTTATCGTAGGATTCGTTTCG	CACAAAACAAAACGAAACCGAA	CGTACGTGTTATACGTATTT	-285 to -150	900,200
CDK2NA	TTATTAGAGGGTGGGGCGGATCGC	GACCCCGAACCGCGACCGTAA	AGTAGTATGGAGTCGGCGGCGGG	-171 to -35	300,300
CFLIP CpG 1	TCGCGAATAGCGATCGTTTAG	GCGACCGAACTCTCCTACCG	GTTCGTTTTTAGGTTTTCGG	-13524 to -13393	300,100
CFLIP CpG 2	GGGTCGTACGTAACGGTTTTG	AATCCTATCTACGAAATTCCCCG	GTCGTTTGATTACGTATGG	-11383 to -11248	900,100
DCR1	TTACGCGTACGAATTTAGTTAACGAT	CGCACCCTACCTCGACCA	AGAGCGTTTCGGTCGTT	-179 to -96	900,100
DCR2	CGGAGGAGTACGTTTTATTTTGGT	GCTCGAAACGATCGAAACG	TGTACGCGTATAAATTACGG	-116 to 36	900,200
TMS1	TTGGCGTTTTTCGACGGT	TCTAATCTCCCGACTCCCCG	GGAGGGTAACGGATCG	-228 to -104	300,100

Genomic co-ordinates are given in relation to the ATG start site. Abbreviations: FAM: 6-carboxyfluorescein, MGB: minor groove binder

The primer and probe set for the endogenous control *ACTB* were kindly provided by Dr K. Woodson (National Cancer Institute, USA). Since neither the primers nor the probe overlie any CpG dinucleotides, this reaction

represents unbiased amplification and serves to normalise results for the differing amounts of bisulfite modified DNA between samples.

2.5.7.3 QMSP reactions

Real-time PCR assays were performed in a reaction volume of 10 µl, consisting of 1µl bisulfite-modified DNA, primers (concentration calculated from optimisations reactions, see Table 2.4) (MWG Biotech, Ebersberg, Germany), fluorescent labelled probe (concentration calculated from optimisations reactions, see Table 2.4) (Applied Biosystems, Warrington, UK) and 2 X TaqMan® Universal PCR master mix, no AmpErase Uracil N-Glycosylase (Applied Biosystems, Warrington, UK). Each assay was performed in triplicate in a 96 well plate under normal real time cycling conditions on a 7500 Real-Time PCR System (Applied Biosystems, Warrington, UK) for both primer/probe optimisation and for QMSP analysis in prostate cell lines.

The large number of patient samples analysed necessitated the use of the 7900 to allow high through-put analysis of methylation using 384-well plates. For QMSP analysis of FFPE prostate tissue samples, each assay was performed in a 384 well plate on a 7900 Real-Time PCR System (Applied Biosystems, Warrington, UK) with the aid of the Matrix HydraII (Thermo Fisher Scientific Inc., Waltham, MA 02454, USA).The Matrix Hydra II is a syringe-based liquid handling system that provides high-speed aspirating and dispensing of microliter volumes into 96-well or 384-well format plates. Bisulfite modified DNA from primary tumour, normal prostate, HGPIN and BPH were randomised, plated and stored in 96 well plates (Figure. 2.6). These plates were utilised with the matrix HydraII for accurate pipetting of DNA of the 96 well sample plates in triplicate into 384-well optical reaction plates for real-time PCR analysis.

A set of standards, representing fold dilutions (10 ng/µl, 1 ng/µl, 0.1 ng/µl, 0.05 ng/µl, 0.01 ng/µl) of bisulfite modified, universal methylated DNA, were

run in triplicate on each TaqMan plate. In addition, each plate contained reference samples to verify plate-plate consistency, multiple water blanks and non-template controls (NTCs).

PROSTATE PLATE 1: AMNCH/IMM												
	1	2	3	4	5	6	7	8	9	10	11	12
A	WATER	AM02026T	AM02037N	WATER	WATER	AM02027P	AM02045T	WATER	IMM0011N	IMM0017T	WATER	IMM0032T
B	AM03029T	AM02026N	AM03016P	AM03009P	WATER	AM01010P	AM03014T	AM02006P	IMM0013T	IMM0017N	WATER	STN10
C	AM02058B	AM99038N	AM03052B	AM02004N	AM01010N	WATER	WATER	AM02007N	IMM0013P	IMM0018T	IMM0022T	STN 1
D	AM02059B	AM02001P	AM00066B	AM03082B	AM03085N	AM03086B	WATER	AM02047T	IMM0013N	IMM0018N	WATER	STN0.1
E	AM02012N	AM01065B	AM02081B	AM01072B	AM01023N	AM03020N	AM01028T	WATER	IMM0014T	IMM0019T	IMM0022N	STN0.05
F	WATER	AM00032P	AM00054B	AM02025N	AM02012T	AM00027N	WATER	AM03013P	WATER	IMM0019N	IMM0025T	STN0.01
G	AM02075B	WATER	AM01022P	AM02004T	AM03029N	AM01028N	AM99038T	AM02036T	IMM0014P	WATER	IMM0025B	IMM0032N
H	AM02040T	AM02036N	WATER	AM03009N	AM02030N	AM02018T	WATER	IMM0011T	IMM0014B	WATER	WATER	IMM0031T

PROSTATE PLATE 2: IMM												
	1	2	3	4	5	6	7	8	9	10	11	12
A	IMM001T	IMM005B	IMM020N	IMM0018B	IMM0056T	IMM0056N	IMM0076B	WATER	IMM0084B	IMM0083B	IMM0084T	WATER
B	IMM001N	IMM007T	IMM036T	IMM0052B	IMM0056P	IMM0072B	WATER	IMM0070N	WATER	IMM0085T	AM02045N	WATER
C	IMM001B	IMM007B	IMM036B	IMM0052N	IMM0019B	WATER	IMM0058B	IMM0075B	IMM0078T	WATER	AM02042P	STN10
D	IMM002T	IMM008T	IMM072T	IMM0037T	WATER	IMM0068P	IMM0068B	IMM0068T	IMM0078N	IMM0085N	WATER	STN 1
E	IMM002P	IMM009N	IMM0022B	WATER	IMM0038B	IMM0075P	IMM0070T	IMM0072N	IMM0082T	IMM0085B	AM02031T	STN0.1
F	IMM005T	IMM009T	WATER	IMM0037B	IMM0011B	IMM0076N	IMM0056B	IMM0058T	IMM0082N	IMM0086T	AM02037T	STN0.05
G	IMM005N	WATER	IMM0037N	IMM0038N	IMM0052T	IMM0076T	IMM0075T	AM02007T	IMM0083T	IMM0086N	AM02039T	STN0.01
H	WATER	IMM020T	IMM0037P	IMM0013B	IMM0020B	IMM0075N	IMM0058N	AM01023T	IMM0083N	IMM0038T	IMM0084N	WATER

Figure 2.6.

Layout of 96-well tissue sample plate. 96 well plate plans for bisulfite modified DNA from prostate cancer, normal prostate, HGPIN, BPH. Abbreviation: STN = Standard, IMM = Samples from Institute of Molecular Medicine section of bioresource, AMNCH = Samples from Adelaide and Meath National Children's Hospital section of bioresource.

2.5.7.4 Quantitation of methylation levels

The target and endogenous control mean quantities and standard deviations for each unknown sample for target and endogenous control (*ACTB*) are automatically interpolated from the standard curves by the ABI PRISM Sequence Detection software.

The level of methylation of target genes was determined by calculating the normalised index of methylation (NIM), defined as the ratio of the normalised amount of methylated target template to the normalised amount of the endogenous control (*ACTB)* in any given sample (Yegnasubramanian et al., 2004). The NIM was calculated by applying the formula:

[(mean *Target* quantity$_{(Sample)}$/ mean *Target* quantity$_{(Methylation\ Control)}$ / (mean *ACTB* quantity$_{(Sample)}$ / mean *ACTB* quantity$_{(Methylation\ Control)}$) * 1000].

A normalised target value is calculated by dividing the average target value (mean of replicate target results) by the average endogenous control value (mean of replicate endogenous results): **Target $_{mean\ quantity}$ /Reference $_{mean\ quantity}$**

The standard deviation of the normalised target value is calculated from the standard deviations of the target and endogenous control mean quantities. The coefficient of variation (cv) must be calculated for both target and endogenous controls. Firstly, the standard deviation is divided by the mean quantity:

cv_1 = endogenous control $_{standard\ deviation}$ / endogenous control $_{mean\ quantity}$
cv_2 = target $_{standard\ deviation}$ / target $_{mean\ quantity}$

The cv of the quotient is next calculated by applying the formula:

$$cv = \sqrt{(cv_1^2 + cv_2^2)}$$

Finally, since the cv and mean are known, the standard deviation of the quotient is calculated:

cv = standard deviation / normalised mean target value

Therefore,

Standard deviation = (cv)(normalised mean target value)

If the mean target quantity could not be normalised, an alternative score for methylation quantification was utilised known as the relative methylation score (RMS) (Jeronimo et al., 2004b). The RMS is calculated by applying the formula:

(Target $_{\text{mean quantity} \pm \text{cv}}$: Reference $_{\text{mean quantity} \pm \text{cv}}$) x 1000

2.6 EXPRESSION ANALYSIS IN PROSTATE CANCER CELL LINES

2.6.1 Relative quantitation using the comparative C_T method

Expression levels of target genes were measured by real-time TaqMan PCR (described in *2.5.7.1*). Relative quantification by the comparative C_T method was performed according to the manufacturer's instructions (Applied Biosystems, User Bulletin 2; (Livak and Schmittgen, 2001)). This method applies arithmetic formulas to determine gene expression. As a result, the use of standard curves for relative quantification is eliminated, providing the PCR efficiencies between target and endogenous control are equivalent. The amount of target, normalised to an endogenous control and relative to a calibrator, is given by: $2^{-\Delta\Delta C_T}$, whereby ΔCT is defined as the difference in C_T values for target and endogenous control, $\Delta\Delta C_T$ is the value obtained by subtracting the ΔC_T of the calibrator from the ΔC_T of our target gene. The full derivation of the formula is outlined in User Bulletin #2: ABI Prism 7700 sequence detection system.

2.6.2 Quantitative RT-PCR assay design

Phosphoglycerate kinase 1 (*PGK1)* TaqMan Pre-Developed Assay was employed as an endogenous control in relative quantitation gene expression studies. *PGK1* was analysed for consistent expression in cell lines, comparing the C_T levels across identical amounts of cDNA from different samples.

TaqMan gene expression assays for mRNA transcripts of interest and *PGK1* are summarized in Table 2.5. Where possible, assays were selected that detected all gene transcripts and spanned exon-intron boundaries. Non-inventoried gene expression assays (*TMS1* and *CDKN2A*) were designed using

primer express software 3.0 (Applied Biosystems, Warrington, UK), *TMS1*; Forward primer 5'-caccgggctgcgctta-3', reverse primer 5'-agcatccagcagccactca -3', probe 6FAM 5'-cgcgagggtcacaaa-3'; *CDKN2A*; Forward primer 5'-cctccgagcactcgctca-3', reverse primer 5'-cttcctccggtgctggc-3', probe 6FAM 5'-agataccgcggtccct-3'. Primers (synthesised by MWG-Biotech, Germany) were rehydrated in molecular grade water to a concentration of 100 µM. The optimal primer and probe concentrations for each gene were determined as outlined in section 2.5.6.1. The efficiencies of non-inventoried assays were determined prior to analysis of gene expression by real-time PCR by a validation experiment, to ensure that the efficiencies of the target and endogenous control assay are approximately equal. The target assay efficiency was calculated by using relative quantification using the standard curve method similar to the standard curve method used for the methylation analysis. The efficiencies are automatically calculated by the ABI 7500 software. Once the efficiencies are determined they can be manually set and corrected for during design of experiment.

Table 2.5: TaqMan Gene Expression assays

TaqMan Assay ID	Entrez Gene Symbol	Gene Name	Assay size (bp)
Hs00969289_m1	BNIP3	BCL2/adenovirus E1B 19kDa interacting protein 3	85
Hs00609635_m1	BIK	BCL2-interacting killer	97
Hs00182570_m1	TNFRSF10C	tumor necrosis factor receptor superfamily, member 10c, decoy without an intracellular domain	81
Hs00388742_m1	TNFRSF10D	tumor necrosis factor receptor superfamily, member 10d, decoy with truncated death domain	93
Hs00354474_m1	CFLAR short	CASP8 and FADD-like apoptosis regulator	69
Hs00236002_m1	CFLAR long	CASP8 and FADD-like apoptosis regulator	104
Hs99999906_m1	PGK1	phosphoglycerate kinase 1 (Endogenous control)	75

Table 2.5

Taqman Gene expression assays. Inventoried TaqMan assays are listed with there ID number, gene symbol, gene name and size of assay.

2.6.3 Quantitative RT-PCR reactions

cDNA (100ng) was used as a template for real-time TaqMan reactions. Real-time PCR assays were performed in a reaction volume of 20 µl, consisting of 9µl cDNA (100ng) and RNAase free water, 1 µl 2X TaqMan® Gene Expression Master Mix (Applied Biosystems, Warrington, UK) and 10 µl

TaqMan® Universal PCR Master Mix (Applied Biosystems, Warrington, UK). Each assay was performed in triplicate under normal real time cycling conditions on a 7500 Real-Time PCR System (Applied Biosystems, Warrington, UK). The target and endogenous control reactions were performed in separate wells of the same plate along with a non-template control for each assay.

2.7 STATISTICAL ANALYSIS

Statistical analysis was performed using MINITAB 15 statistical software. A paired T test was performed to determine if the changes in gene expression observed in PC3 cells and PC3 cells treated with a methylation inhibitor was significant for each gene with evidence of methylation in its PC3 cells (*BIK, CDKN2A, DCR1, DCR2* and *TMS1*).

QMSP analysis yielded relative methylation scores (RMS). For each gene, the frequency of methylation, as well as the median and range of the RMSs for each groups of tissue samples, was determined. Differences in frequencies of methylation between prostate cancer, HGPIN, normal and BPH tissue groups were assessed using Fisher's Exact Test. Association of methylation status of our gene panel and clinicopathological features of prostate cancer, including Gleason score, PSA levels and TNM stage were also assessed using the Fisher's exact T test. The p-value from Fisher's exact test is accurate for all sample sizes, whereas results from the chi-square test that examines the same hypotheses may be inaccurate when cell counts are small.

The RMSs for each gene were compared between the four groups of tissue samples (prostate cancer, HGPIN, histologically benign prostate and BPH) using the nonparametric Kruskal-Wallis alternative to one-way ANOVA test. In addition, the Tukey all-pairwise test was used to perform multiple comparisons to assess the significance of differences among means. The multiple comparisons are presented as a set of confidence intervals rather than as a set of hypothesis tests. This allows examination of the practical significance of differences among means, in addition to statistical significance.

Prior to analysis, an Anderson-Darling normal probability plot was performed to determine if age and PSA levels of prostate cancer patients and BPH patients were normally distributed. An Unpaired 2 sample T Test was used to calculate the differences in age and PSA between patient groups.

For all of the tests, significance was ascribed at $P < 0.05$.

CHAPTER 3

IN SILICO IDENTIFICATION OF POTENTIAL APOPTOSIS-RELATED GENE TARGETS OF PROMOTER HYPERMETHYLATION IN PROSTATE CANCER.

3.1 INTRODUCTION

Cancer cells exhibit a number of genetic defects in their apoptotic machinery that impair programmed cell death. Downregulation or loss of expression/activity of pro-apoptotic genes during prostate carcinogenesis may be involved in the evolution of an apoptotic-resistant pro-survival carcinogenic phenotype. We hypothesised that silencing of important apoptotic genes in prostate cancer, through epigenetic changes such as DNA methylation, could affect pathways integral to the apoptotic cascade. Furthermore, understanding which apoptotic pathways become altered and deciphering the molecular mechanisms underlying the atypical expression of key apoptotic genes may provide valuable insight into disease progression and therapeutic responses in prostate cancer.

Recent studies strongly support a role for DNA hypermethylation in deregulating programmed cell death in cancer. To date, the majority of methylation studies on apoptotic genes have focused on cancers of the bladder, stomach, colon and breast. The information available on the methylation status of apoptotic genes in prostate cancer is limited (Reviewed in Murphy et al., 2008). The challenge is to rapidly identify novel targets of methylation in prostate cancer and rigorously evaluate these potential markers using standardised techniques and to test their limit of detection and specificity for prostate cancer over other cancers and benign urological diseases.

Here we employed an *in silico* strategy to identify a bank of potential apoptotic-related gene targets of promoter hypermethylation for methylation screening in prostate cancer cell lines with a view to generate a "methylation signature" for early detection of prostate cancer.

3.2 EXPERIMENTAL STRATEGY

In this study, the upstream regions of genes important for apoptosis regulation were screened for the presence of a 5' promoter CpG island utilising the UCSC human genome browser, identifying genes which are potentially deregulated in cancer as a result of promoter hypermethylation. Meta-analysis of published methylation and microarray studies, which compared gene expression between

different stages and grades of prostate cancer (Cho-Vega et al., 2005; Ernst et al., 2002; Yu et al., 2004a) identified a number of apoptotic-related genes with evidence of promoter hypermethylation and/or downregulation in prostate and other cancers. A bank of gene candidates for methylation analysis, previously generated by Antoinette Perry (Ph.D Thesis, Investigating novel targets of DNA methylation for the early detection of prostate cancer, Oct 2006) was searched for candidate apoptotic gene targets of methylation (Figure 3.1). In total, a bank of 22 apoptotic-related genes was identified as possible targets of promoter hypermethylation in prostate cancer (Table 3.4).

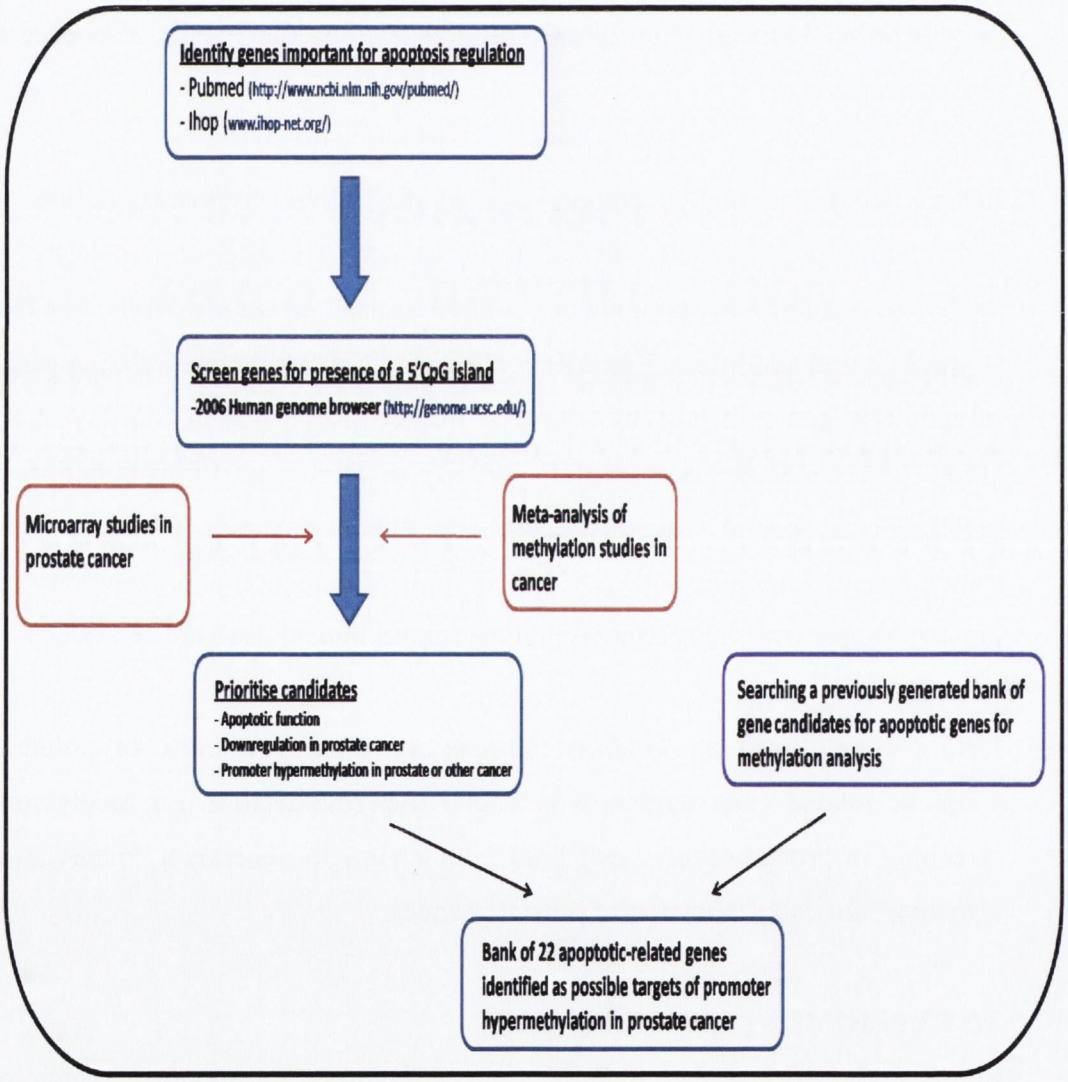

Figure 3.1

In silico selection of apoptotic-related gene targets of promoter hypermethylation in prostate cancer.

3.3 IDENTIFYING APOPTOTIC GENE TARGETS OF HYPERMETHYLATION IN PROSTATE CANCER.

3.3.1 Searching a methylation candidate gene bank

An *in silico* approach to identify potential targets of promoter hypermethylation in prostate cancer was employed by Dr. Antoinette Perry in our laboratory. This approach yielded a methylation candidate gene bank (N=338). Within this bank, genes were sorted based on their known or predicted function. A total of 9 candidate gene targets of methylation, whose predicted function was listed as apoptosis, were selected from this gene bank (Table 3.1).

Table 3.1. Apoptotic gene identified from a methylation candidate gene bank.

Gene Symbol	Gene description
BCL2	B cell CLL/lymphoma 2
CFLAR	CASP8 and FADD-like apoptosis regulator
CLU	Clusterin
SMAD4	Mothers against DPP homolog 4
DAP	Death associated protein
RAGA	Ras-related GTP binding protein
IER3	Immediate early response 3
PIGPC1	p53-induced protein PIGPC1
SPHK2	Spinosine Kinase 2

3.3.2 Identifying key apoptotic genes

A number of freely available online resources; (PubMed (http://pubmed.gov/), Information Hyperlinked Over Proteins (IHOP; http://www.ihop-net.org/UniPub/iHOP/) and BioCarta (http://www.biocarta.com)) were exploited to identify key genes involved in apoptosis regulation. A list of genes deemed important for apoptosis regulation was compiled (n= 30). (Table 3.2)

Table 3.2 List of Key Apoptotic genes

Intrinsic pathway	Gene description (full name)	Extrinsic pathway	Gene description (full name)	Cross talk	Gene description (full name)
BIM	Bcl2-interacting mediator of cell death	**FAS**	Fas (TNF receptor superfamily, member 6)	**IAP**	Integrin-associated protein
BID	BH3 interacting domain death agonist	**FASL**	FAS ligand	**CASP3**	Caspase 3
BAD	BCL2-associated agonist of cell death	**CASP8**	Caspase 8	**CASP7**	Caspase 7
PUMA	p53 up-regulated modulator of apoptosis	**CFOS**	v-fos FBJ murine osteosarcoma viral oncogene homolog	**CDKN2A**	Cyclin-dependent kinase inhibitor 2A
PMAIP1	Phorbol-12-myristate-13-acetate-induced protein 1	**CAD (DFF40)**	Carbamoyl-phosphate synthetase 2, aspartate transcarbamylase, and dihydroorotase		
BAX	BCL2-associated X protein	**ICAD (DFF45)**	Inhibitor of CAD		
DIABLO	Diablo homolog (Drosophila)	**FADD**	Fas (TNFRSF6)-associated via death domain		
CYCS	Cytochrome C	**TRADD**	TNFRSF1A-associated via death domain		
AIF	Apoptosis inducing factor				
		TNFSF10	Tumor necrosis factor (ligand) superfamily, member 10		
APAF1	Apoptotic peptidase activating factor	**PAR4 (PAWR)**	Prostate apoptosis response 4 protein (PRKC apoptosis WT1 regulator)		
CASP9	Caspase 9	**TMS1**	Target of methylation-induced silencing 1		
HRK	Harakiri	**SPHK2**	Sphingosine kinase 2		
XAF1	XIAP Inhibitor of apoptosis factor 1	**DAPk**	Death-associated protein kinase 1		

3.3.3 Screening for 5'CpG islands

The thirty selected genes were screened *in silico* for the presence of a CpG island 1000bp upstream of the transcriptional start site using the March 2006,

UCSC Human Genome Browser (http://genome.ucsc.edu) (described in section *2.1.2)*. For example, *FAS* was successfully screened for a 5' promoter CpG island shown in Figure 3.2. A total of 25/30 apoptotic-related genes contained a 5' promoter CpG island (Table 3.3).

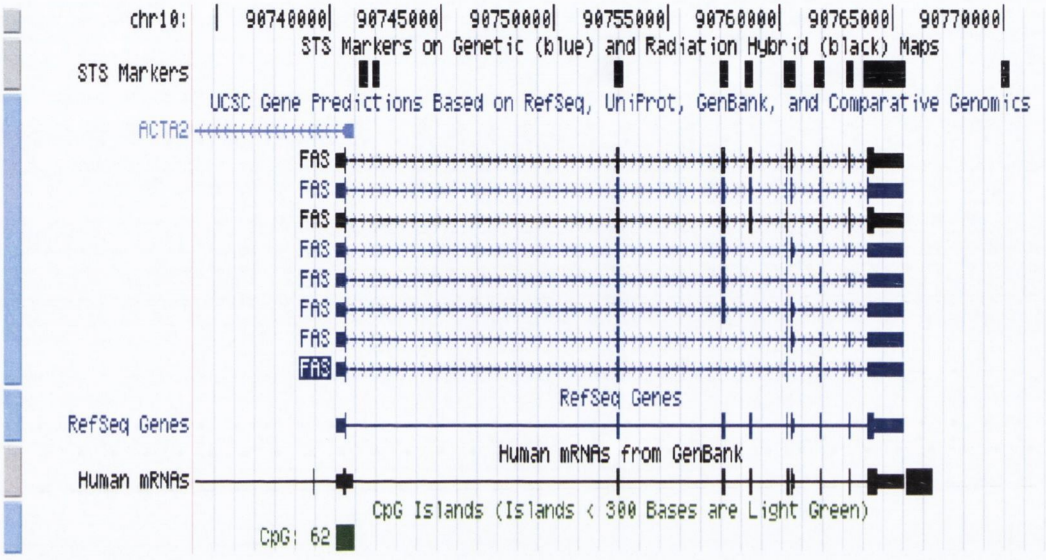

Figure 3.2

UCSC Human genome Browser graphical representation of *FAS*. A number of annotation tracks can be displayed. NCBI RefSeq genes, human mRNA prediction based from GenBank are illustrated. Coding exons are illustrated by the thickest part of the Refseq and GenBank tracks, the thin lines with arrowheads represent introns and the direction of transcription and the UTRs are represented as thinner portions at 3' and 5' end of the track. The CpG island track shows the position of the CpG island in the genome (green box). The number of CpG dinucleotides in the island is displayed to the left of the green box.

Table 3.3. List of apoptotic genes with a 5' promoter CpG island

Intrinsic pathway	Extrinsic pathway	Cross talk
BIM	FAS	CASP3
BID	MAPK8	CASP7
BAD	CAD (DFF40)	CDKN2A
PUMA	ICAD (DFF45)	
PMAIP1	FADD	
BAX	TRADD	
CYCS	PAR4 (PAWR)	
AIF	TMS1	
APAF1	SPHK2	
CASP9	DAPk	
HRK	CFOS	
XAF1		

3.3.4 Identifying genes with susceptibility to hypermethylation and/or reduced expression in prostate cancer.

3.3.4.1 Microarray studies

Literature review of published microarray studies that compared gene expression between different stages and grades of prostate cancer were examined for possible selection of apoptotic genes with evidence of decreased gene expression levels in prostate cancer compared to normal prostate and benign prostatic hyperplasia (BPH) (Cho-Vega et al., 2005; Ernst et al., 2002; Yu et al., 2004a). Two genes, *CFOS* and *FAS* were identified from our literature search.

3.3.4.2 Literature review

Apoptotic genes identified to contain at least one CpG island (identified from Section 3.23) were investigated for evidence of methylation in 1) prostate cancer and 2) other cancers using PubMed (http://www.pubmeth.org/) and iHOP (http://www.ihop-net.org/UniPub/iHOP/). Next, a literature review of methylation studies in cancer was performed using PubMed and Google (www.google.ie) to identify apoptotic genes, which show evidence of promoter hypermethylation in cancer but may not have a CpG island as predicted by

UCSC human genome. In this way, *CASP8* and *XAF1* were identified as candidate apoptotic gene targets of methylation. Using the criteria set in the UCSC human genome browser, both genes did not contain a CpG island, however the literature suggested its promoter region was a target of hypermethylation in certain cancers (Byun et al., 2003; Hopkins-Donaldson et al., 2003).

Individual genes of interest were investigated for evidence of downregulation in both prostate cancer and/or additional cancers using extensive review of the literature via PubMed.

3.3.5 Candidate prioritising

Apoptotic-related genes containing 5' CpG island(s) identified from our *in silico* approach (n=25) were pooled with genes identified from searching the candidate gene bank (n= 9). Firstly, genes were organised by predicted function and importance in apoptosis. Candidate genes with evidence of decreased gene expression in prostate cancer and/or evidence of susceptibility to promoter hypermethylation in prostate cancer or other cancers were selected. Upon further investigation, 3/9 genes identified from the candidate gene bank (*BCL2, CFLAR* and *PIGPC1*) were selected for further studies. Finally, genes without a predicted USCS CpG island but with evidence of promoter targeted methylation as determined from our literature search (n=2) were also added. A short list of 22 apoptotic-related genes was complied (Table 3.4).

Table 3.4: In silico identification of potential apoptotic-related gene targets of promoter hypermethylation in prostate cancer.

Gene symbol	Gene description (full name)	NCBI UniGene	Apoptotic Function	Methylation in cancer	References
Intrinsic pathway					
BCL2	B-cell CLL/lymphoma 2	NP_000624.2	Anti-apoptotic molecule; control mitochondrial permeability by stimulation ADP/ATP exchange	Bladder cancer; Non-Small Cell Lung cancers	Friedrich et al, 2004; Friedrich et al, 2007; Nagatake et al, 1996
PIGPC1	PERP, TP53 apoptosis effector	Hs.520421	p53 effector gene (initiates apoptosis involved in DNA damage to the cell)	Not found	
BAD	BCL2-antagonist of cell death	Hs.370254	Binds to BH3 domain of BCL2	Multiple Myeloma KAS-6/1 cells	Pompeia et al, 2004
APAF1	Apoptotic peptidase activating factor	Hs.708112	Part of the apoptosome; complex comprising of cytochrome c and ATP involved in activation of caspase-9	Acute Leukemia, Bladder cancer, Clear Cell Renal Cell carcinoma, Gastric cancer, AML, CML, ALL	Christoph et al, 2007a; Wang et al, 2007; Christoph et al, 2007b; Furukawa et al, 2005; Fu et al, 2003
CASP9	Caspase 9, apoptosis-related cysteine peptidase	Hs.329502	Part of the apoptosome; complex comprising of cytochrome c and ATP involved in activation of caspase-9	Not found	
XAF1	XIAP-associated factor 1	Hs.441975	Inhibits an inhibitor of apoptosis protein IAP and facilitated apoptosis	Prostate cancer; Colorectal cancer; Renal Cell carcinomas, Gastric cancer	Fang *et al.*, 2006, Lee *et al.*, 2006; Chung et al, 2007; Kempkensteffen et al, 2007; Byun et al., 2003, Jang et al., 2005
BIK	BCL2-interacting killer	Hs.475055	BH-3-only BIK functions at the endoplasmic reticulum to stimulate cytochrome c release from mitochondria.	Renal Cell Carcinoma; Malignant Glioma	Kim et al, 2006; Sturm et al, 2006
BNIP3	BCL2/adenovirus E1B 19kDa interacting protein 3	Hs.144873	Interacts with anti apoptostic Bcl-2 family proteins	Pancreatic, Haematopoietic, Gastric and Colon cancer	Murai *et al.*, 2005a, Murai *et al.*, 2005b, Okami *et al.*, 2004

PERP, p53 apoptosis effector related to PMP-22, ATP, Adeonsine triphosphate, AML, acute myeloid leukeamia, CML, chronic myeloid leukaemia, ALL, acute lymphoblastic leukemia, Trail, tumour necrosis factor (TNF)-related apoptosis-induced ligand, CAD, carbamoyl-phosphate synthetase , ICAD, Inhibitor of CAD, MDM2, Mouse Double Minute 2, BH, Bcl-2 homology, IAP, Inhibitor of Apoptosis Protein, XIAP, X-Linked IAP, PRKC, Protein Kinase C.

Table 3.4 Contd.: In silico identification of potential apoptotic-related gene targets of promoter hypermethylation in prostate cancer.

Gene symbol	Gene description (full name)	NCBI UniGene	Apoptotic Function	Methylation in cancer	References
Extrinsic pathway					
FAS	Fas (TNF receptor superfamily, member 6)	Hs.244138	Death receptor for the Fas ligand and induces apoptosis via indirect cleavage of caspase 8	Prostate and Colon carcinoma	Santourlidis et al., 2001; Petak et al, 2003;
CFLAR (c-FLIP)	CASP8 and FADD-like apoptosis regulator (cellular-Flice Like Inhibitory protein)	Hs.244139	Inhibits FAS initiated cleavage of caspase 8	Neuroblastoma	van Noesel et al, 2003 & Margetts et al, 2005
CASP8	Caspase 8, apoptosis-related cysteine peptidase	Hs.655983	Induces apoptosis via its death receptor pathway upon cleavage activation	Neuroblastoma, Glioblastoma Multiforme, Medulloblastomas, Retinoblastomas, Small Cell Lung cancer cell lines, Hepatocellular carcinoma	Nishida et al, 2008; Michalowski et al, 2008; Martinez et al, 2007; Harada et al, 2002; Hopkins-Donalson et al, 2003
FADD	Fas (TNFRSF6)-associated via death domain	Hs.244139	Adaptor molecule for Fas mediated cleavage of Caspase-8	Not found	
PAR4 (PAWR)	Prostate apoptosis response 4 protein (PRKC apoptosis WT1 regulator)	Hs.643130	Par-4 regulates Bcl-2 through a WT1-binding site on the bcl-2 promoter	Ras-transformed epitheilal cells	Pruitt et al, 2005
TMS1	Target of methylation-induced silencing 1	Hs.499094	Induces apoptosis in caspase-dependent manner	Breast, Colorectal, Gastric cancer, Prostate cancer, Glioblastoma Multiforme, Hepatocellular carcinoma cells, Ovarian, Melanoma	Martinez et al, 2007; Riojas et al, 2007; Kato et al, 2008; Suzuki et al., 2006; Mirza et al, 2007; Zhang et al, 2007; Tam et al, 2007; Guan et al, 2003
HRK	Harakiri	Hs.87247	Pro-apoptotic molecule; inhibits bcl-2 anti-apoptotic behaviour	Gastric and Colorectal, Primary Central Nervous System Lymphomas, Glioblastomas	Higuchi et al, 2008; Nakamura et al, 2006; Nakamura et al, 2005; Obata et al, 2003;
DR4	Tumor necrosis factor receptor superfamily, member 10a	Hs.591834	Receptor for TRAIL	Neuroblastoma, Prostate cancer, Ovarian cancer, Von Hippel-Lindau and Sporadic Phaeochromocytomas.	Suzuki et al, 2006; Horak et al, 2005; Margetts et al, 2005; Van Noesel et al, 2003
DR5	Tumor necrosis factor receptor superfamily, member 10b	Hs.521456	Receptor for TRAIL	Neuroblastoma, Von Hippel-Lindau and Sporadic Phaeochromocytomas.	Van Noesel et al, 2003; Margetts et al, 2005
DCR1	Tumor necrosis factor receptor superfamily, member 10c, decoy without an intracellular domain	Hs.655801	Anti-apoptotic. Decoy receptor which do not induce apoptosis upon TRAIL binding	Ovarian cancer, Prostate cancer, Gallbladder carcinoma and Chronic cholecystitis, Neuroblastoma, Lung	Shivapurkar et al., 2004; Suzuki et al., 2006; Van Noesel et al, 2003; Shivapurkar et al., 2007; Takahashi et al, 2004
DCR2	Tumor necrosis factor receptor superfamily, member 10d, decoy with truncated death domain	Hs.213467	Anti-apoptotic.Decoy receptor which do not induce apoptosis upon TRAIL binding	Ovarian cancer, Prostate cancer, Gallbladder carcinoma and Chronic Cholecystitis, Neuroblastoma, Lung	Shivapurkar et al., 2004; Suzuki et al., 2006; Van Noesel et al, 2003; Shivapurkar et al., 2007; Takahashi et al, 2004
DAPk	Death-associated protein kinase 1	Hs.380277	Involved in apoptosis initiated by TNFalpha	Oral Squamous Cell carcinoma, Bladder cancer, Cervical cancer, Non-Small Cell Lung cancers, Kidney cancer	Leung et al, 2008; Wang et al, 2008; Ellinger et al, 2008; Kulkarni et al, 2004; Christoph et al, 2006

PERP, p53 apoptosis effector related to PMP-22, ATP, Adeonsine triphosphate, AML, acute myeloid leukeamia, CML, chronic myeloid leukaemia, ALL, acute lymphoblastic leukemia, Trail, tumour necrosis factor (TNF)-related apoptosis-induced ligand, CAD, carbamoyl-phosphate synthetase , ICAD, Inhibitor of CAD, MDM2, Mouse Double Minute 2, BH, Bcl-2 homology, IAP, Inhibitor of Apoptosis Protein, XIAP, X-Linked IAP, PRKC, Protein Kinase C.

Table 3.4 Contd.: In silico identification of potential apoptotic-related gene targets of promoter hypermethylation in prostate cancer.

Gene symbol	Gene description (full name)	NCBI UniGene	Apoptotic Function	Methylation in cancer	References
Both Intrinsic & Extrinsic					
CASP3	Caspase 3, apoptosis-related cysteine peptidase	Hs.141125	Cleaves ICAD into CAD allowing translocation to the nucleus and induction of apoptosis	Breast cancer	Mimori et al, 2005
CDKN2A	Cyclin-dependent kinase inhibitor 2A	Hs.512599	Inhibits MDM2 and consequently increases stability of P53	Colorectal, Lung, Breast, Bladder, Hepatocellular carcinomas, Prostate, Kidney, Oral Squamous Cell carcinoma.	Ogi et al, 2002; Noda et al, 2002; Jarmalite et al, 2003; Dominguez et al, 2003, Anzola et al, 2004; Konishi et al, 2002; Cairns et al, 2004;

PERP, p53 apoptosis effector related to PMP-22, ATP, Adeonsine triphosphate, AML, acute myeloid leukeamia, CML, chronic myeloid leukaemia, ALL, acute lymphoblastic leukemia, Trail, tumour necrosis factor (TNF)-related apoptosis-induced ligand, CAD, carbamoyl-phosphate synthetase , ICAD, Inhibitor of CAD, MDM2, Mouse Double Minute 2, BH, Bcl-2 homology, IAP, Inhibitor of Apoptosis Protein, XIAP, X-Linked IAP, PRKC, Protein Kinase C.

3.4 DISCUSSION

Our objective in this part of the study was to employ a bioinformatics strategy, similar to one previously developed in the laboratory, to identify a bank of candidate apoptotic-related gene targets of methylation for investigation in prostate cancer.

We exploited a number of freely available online software to generate a list of candidate genes. Identifying key genes important for apoptosis can prove difficult. Many genes can be indirectly linked to apoptosis, resulting in a large number of genes labelled as apoptotic. We choose genes directly involved in apoptosis regulation by extensively reviewing the function of individual apoptotic genes using PubMed, iHOP and BioCarta bioinformatics research tools.

Once key apoptotic genes were identified, they were screened for the presence of a 5'UTR CpG island using the UCSC Human Genome Browser. The exact definition of a CpG island is somewhat arbitrary (Takai and Jones, 2002). Hence a number of different algorithms can be used to predict CpG islands. We choose the default Gardiner-Garden and Frommer, (2002) algorithm used by the UCSC genome browser, as it is a traditional CpG island prediction algorithm frequently used in methylation studies (Ehrich et al., 2008; Oakes et al., 2007; Perry et al., 2007). However, this algorithm has its limitations,

whereby non-repeat portions of the genome only are searched for presence of CpG islands in order to avoid identifying false positive Alu repeats, which often meet the criteria of a CpG island. The majority of genes for which the algorithm did not predict the presence of a 5' CpG island were eliminated.

An additional step in our selection process was added, whereby a review of the methylation literature of apoptotic genes was conducted, to prevent omission of key apoptotic genes whose promoters are known targets of methylation but do not contain a 5' CpG island according to the algorithm used in the Human Genome Browser. For example, extensive review of the methylation literature identified a 5' promoter region of *CASP8* as a target of methylation in cancer. The *CASP8* gene contains a 5' CG rich regulatory region (Teitz et al., 2000). However, this CG rich region did not meet the Gardiner-Garden and Frommer defined criteria for a CpG island. The 364bp region we investigated in our study had a 49% CG content but the ratio of observed number of CG dinucleotides to the expected number of Gs and Cs present in the segment was only 0.34. Further review of the literature revealed this 5' CG rich region to be a target of methylation in certain cancers (Banelli et al., 2002). As a result, *CASP8* was identified as a potential target of methylation in cancer and included in our study.

Similar to *CASP8*, the USCS human genome browser did not predict a CpG island in the promoter region of *XAF1*. Review of the literature identified two 5' upstream regions of the *XAF1* gene, which encompassed only 200 bp (region I) and 380 bp (region II) and satisfied the Gardiner-Garden and Frommer defined criteria for CpG island. Hence, these two CG rich regions and surrounding CG dinucleotides were included in our study (Byun et al., 2003).

Investigation into the methylation status of individual genes was conducted using PubMed and Google. This work was conducted before PubMeth (http://www.pubmeth.org/) became available. PubMeth contains more than 5000 records, built from over 1000 literature sources and would help to quickly

answer the question we asked "is this gene already described in the literature as methylated and in which cancer types?" (Ongenaert et al., 2008).

A number of microarray studies were analysed to identify apoptotic-related genes downregulated in prostate cancer compared to normal tissue or benign urological diseases. Only a small number of apoptotic genes were identified as being downregulated in prostate cancer tissue. The microarray studies analysed in the study were not specific to apoptotic genes but rather listed genes important in a wide range of important pathways. It was necessary, therefore, to also research genes individually to determine if there was evidence of their downregulation in prostate or other cancers.

A bank of 22 apoptotic-related genes was identified as possible targets of promoter hypermethylation in prostate cancer. The majority of genes identified (18/22) are pro-apoptotic (Table 3.4), cFLIP has dual functionality with evidence suggesting it has both anti and pro-apoptotic action (Chang et al., 2002), while the remainder (*BCL2, DCR1* and *DCR2*) are anti-apoptotic. As anti-apoptotic genes are usually up-regulated in cancer (Hanahan and Weinberg, 2000), their methylation status in prostate cancer is of great interest. We identified 8 genes (*BCL2, PIGPC1, BAD, APAF1, CASP9, XAF1, BIK, BNIP3*) which are intimately involved in the mitochondrial apoptotic pathway (Intrinsic pathway), 12 genes (*FAS, cFLIP, CASP8, TMS1, FADD, DAPk, DR4, DR5, DCR1, DCR, PAR4, HRK*) important in the death receptor pathway (Extrinsic pathway) and 2 genes involved in crosstalk between the two pathways (*CDK2NA* and *CASP3*) (Table 3.4).

To the best of our knowledge, this is the first investigation of the methylation of *CASP9*, *FADD* and *PIGPC1* in cancer. *CASP9* and *FADD* play a central role in apoptosis induction by propagating the mitochondrial and death signal respectively and *PIGPC1* is an important p53 effector gene and is downregulated in prostate cancer (Ashida et al., 2004).

The 22 apoptotic-related gene bank provides the basis of our investigation into the role of methylation as a key controller of aberrant cell death in prostate cancer. Analysis of the methylation status of these genes could help generate

an "apoptotic methylation signature" for early detection and prognosis of prostate cancer, the results of which are presented in subsequent chapters.

CHAPTER 4

DISCOVERY OF APOPTOTIC-RELATED GENE TARGETS OF ABERRANT METHYLATION IN PROSTATE CANCER UTILISING A DHPLC METHYLATION SCREENING STRATEGY

4.1 INTRODUCTION

An *in silico* strategy, applied in the last chapter, identified a bank of 22 potential apoptotic-related gene targets of promoter hypermethylation in prostate cancer. A wide range of methylation techniques are now available, such as bisulfite sequencing, methylation specific PCR (MSP) and Combined Bisulfite Restriction Analysis COBRA, which are effective in detailed methylation studies but have limited merit as a rapid screening technique (Perry et al., 2007). COBRA and MSP for example can only evaluate small regions within the CpG island, whilst bisulfite sequencing can be arduous, hence we require a rapid screening tool for our methylation analysis.

Recently, a denaturing high performance liquid chromatography (DHPLC) approach has been developed in our laboratory as an effective screening platform for detecting DNA methylation in cancer (Perry et al., 2007). DHPLC was first developed as a highly sensitive, highly specific rapid mutation screening tool, based on denaturing temperature differences between mutant and wild type sequences (Lai et al., 2005; O'Donovan et al., 1998). In the last number of years, DHPLC has been successfully used to discriminate between differentially methylated regions of imprinted genes (Baumer et al., 2001). This technology is based on the detection of "multi mutations" in target sequences following bisulfite modification. Bisulfite modification of DNA converts unmethylated cytosine to uracil but leaves 5-methylcytosine unaltered. Following PCR amplification, a methylated template has a significantly greater GC content and therefore a higher melting temperature than an unmethylated form of the same sequence, resulting in different column retention times under DHPLC conditions (Perry et al., 2007) (Figure 4.1).

The primary aim of the current study was to profile the methylation status of apoptotic-related genes in prostate cancer, which may help identify novel diagnostic and prognostic biomarkers and elucidate novel therapeutic targets. Utilising a DHPLC screening strategy, we aimed to identify a number of novel apoptotic-related gene targets of promoter hypermethylation in a panel of prostate cancer cell lines (22RV1, DU145, RC58, LNCaP and PC3) representing different stages of disease progression (Table 4.1).

Table 4.1: Summary of prostate cell lines		
Cell line	**Origin**	**Androgen repsonsive**
RWPE1	Normal basal epithelial	NA
PWR1E	Normal basal epithelial	NA
22RV1	Primary: Human prostate carcinoma xenograft	Androgen Sensitive
Du145	Metastatic: Brain	Androgen Independent
RC58	Primary	Androgen Sensitive
LNCaP	Metastatic:left supraclavicular lymph node	Androgen dependent
PC3	Metastatic: Bone	Androgen Independent
NA= not applicable		

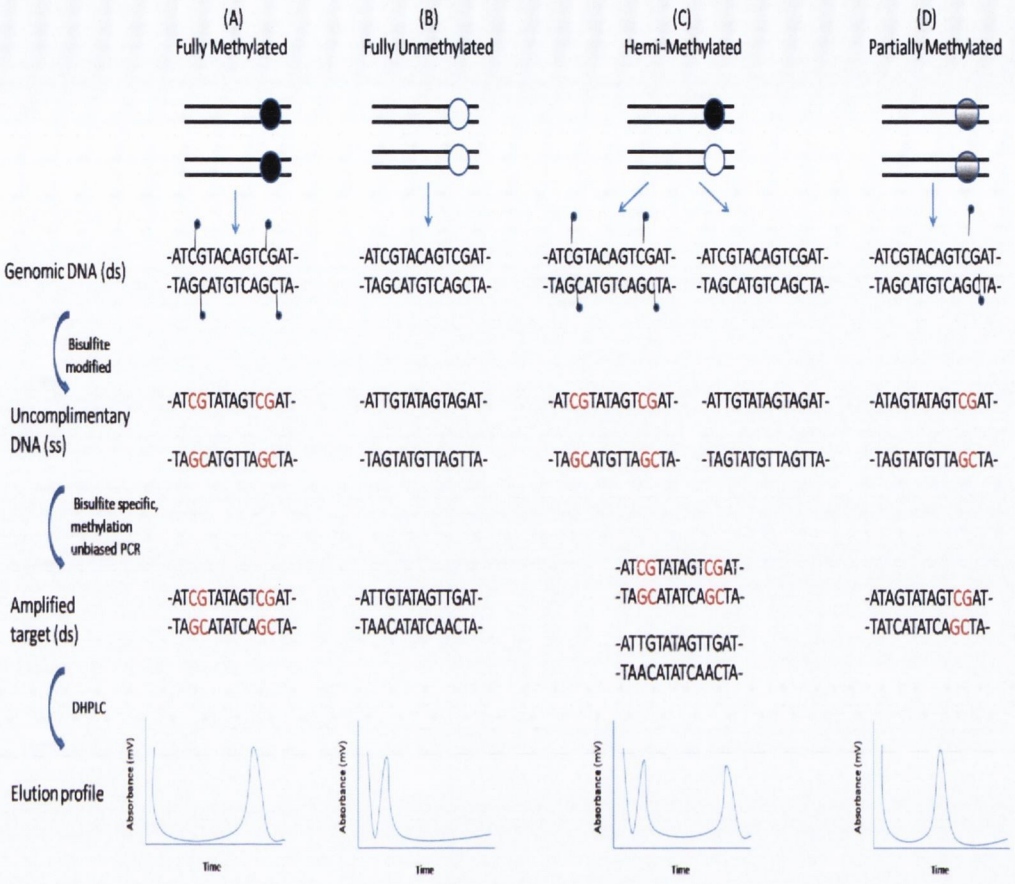

Figure 4.1:
Methylation profiling by DHPLC. Following bisulfite modification and PCR amplification, the methylation status can be determined by the time at which the DNA fragment elutes from the column. A fully methylated template has a significantly higher GC% and therefore a higher melting temperature than an unmethylated form of the same sequence. As a result, a fully methylated sequence will have a later elution time than an unmethylated form of the same sequence (A and B). The DHPLC profile of a hemi-methylated sequence, whereby only one strand is fully methylated and the other is fully unmethylated, has two peaks one which resolves at the same time as the methylation control coupled with a second peak at the elution time of the unmethylated control (C). A DNA sequence which is partially methylated, whereby only some of the CG sites are methylated, resolves at a time-point in between that of the unmethylated and methylated form of the same sequence (D). Adapted from (Perry et al., 2007).

We next validated DHPLC results by bisulfite sequencing of methylated genes and generated promoter methylation maps.

A secondary aim of this study was to utilise our pre-optimised DHPLC screening platform to investigate the underlying epigenetic changes in apoptotic-related genes potentially associated with a docetaxel resistant phenotype in prostate cancer cells.

4.2 METHYLATION UNBIASED PCR

For each gene, the consensus promoter CpG island sequence was downloaded from the UCSC Human Genome Browser (http://genome.ucsc.edu/). The CpG islands were bisulfite modified *in silico* to represent a fully methylated bisulfite modified sequence. Only one promoter CpG island was analysed for each gene except in the case of *cFLIP*. *cFLIP* has a number of splice variants (Irmler et al., 1997). Interestingly, *cFLIP* contains two 5' CpG islands, one which over laps the 5'UTR of the Long (L) *cFLIP* isoform and a second which contains the 5'UTR for the Short (S) *cFLIP* isoform. In order to investigate the role of methylation in *cFLIP* splice variation, both 5'UTR CpG islands were analysed. PCR primers were designed to walk the length of the CpG islands at the 5' end of the 22 apoptotic-related genes. Primers were designed to amplify bisulfite modified DNA irrespective of methylation status (described in section *2.5.4*).

In total, 47 PCR assays were synthesised. PCRs were optimised on methylation controls (MC & UMA) and optimised genes amplified in a panel of prostate cancer cell lines (LNCaP, DU145, PC3, 22RV1, RC-58T) and normal prostate cell lines (PWR1-E, RWPE-1) (Appendix 2.1). Approximately 50% of our PCR assays were successfully optimised; despite primer redesign, the remaining assays could not be optimised (*BAD, BCL2, BNIP3* Assay 2 and 3, *CASP3* assay 2, *CASP9, DAPk, DCR1* assay 1, *DCR2* assay 1, *DR4, DR5* assay 2, *FADD* assay 2, *FAS, HRK, PAR4*, *TMS1* assay 2, *XAF1*).

4.3 METHYLATION SCREEN USING A DHPLC PLATFORM

In this study, we investigated the methylation status of apoptotic-related genes using a DHPLC screening platform. In total, 23 PCR assays were optimised to amplify the 5' CpG islands of 13 apoptotic-related genes identified in the *in silico* analysis. The partially denaturing temperature of the fully methylated and fully unmethylated sequence for each assay was determined using the

Stanford DHPLC Melt Program (http://insertion.stanford.edu/melt.html). Experimentation revealed that the predicted denaturing temperature(s) recommended by the Stanford DHPLC Melt Program were too high for the methylated template and too low for the unmethylated template. Temperatures one and two degrees above and below the temperature(s) recommended for the unmethylated and methylated template were used respectively as starting temperatures for assay optimisation using methylated and unmethylated controls. All 23 PCR assays were successfully optimised on the DHPLC Wave instrument with the exception of *BIK* assay 3. A denaturing temperature, which allowed for adequate separation of the fully methylated and unmethylated *BIK* templates, could not be determined.

4.3.1 Screening genes for methylation in prostate cell lines using DHPLC

We first screened the genes in a panel of prostate cancer cell lines. These are very useful because they are an abundant source of DNA, representing different stages of the disease, primary (22RV1 and RC58) and metastatic (LNCaP, PC3 and DU145) and both androgen sensitive (22RV1 and RC58), dependent (LNCaP) and independent (PC3 and DU145).

The methylation status of the thirteen genes studied is summarised in Table 4.2. Six genes showed no evidence of methylation in prostate cancer cell lines (Figure 4.2). The elution profiles of *APAF1, CASP3, CASP8, BIK* (assay 2), *FADD, PIGPC1* and *DR5* are similar to that of their respective unmethylated control, providing strong evidence that this part of the CpG island of these genes are unmethylated in all prostate cell lines examined. We identified seven genes (c*FLIP, BNIP3, TMS1, BIK, DCR1, DCR2,* and *CDKN2A)* with evidence of full or partial methylation in their promoter CpG island (Figure 4.3).

BIK assay 1 appeared largely unmethylated, except in DNA from the androgen-independent PC3 cell line, which eluted at a time-point in between those of the methylated and unmethylated controls, suggesting "partial" methylation at certain CpG sites within the island (Figure 4.3 Panel A). Similarly, *BNIP3* appeared partially methylated in three prostate cancer cell lines (22RV1, DU145 and LNCaP) (Figure 4.3 Panel B).

CDKN2A showed evidence of methylation in PC3, 22RV1 and LNCaP cell lines (Figure 4.3 Panel K). For *BIK*, *BNIP3* and *CDKN2A,* there was no evidence of methylation in any of the other cell lines examined (Appendix A2.1).

cFLIP, a key controller of death receptor induced apoptosis, contains two 5'UTR CpG islands. DHPLC analysis of the first CpG island revealed lack of methylation in all of the cell lines, except the androgen-dependent LNCaP, which eluted at two time points, corresponding to both the methylated and unmethylated controls, which suggests *cFLIP* is hemi-methylated or methylated on one allele only (Figure 4.3 Panel C and D). In contrast, DHPLC analysis of the second CpG island revealed partial methylation in LNCaP and full methylation in the primary prostate cancer cell line 22RV1 (Figure 4.3 Panel E and F). There was no evidence of methylation in all other cell lines examined (Appendix A2.1). These results demonstrate differential methylation of these CpG islands in prostate cancer cell lines 22RV1 and LNCaP.

For *TMS1* and *DCR1,* all prostate cell lines (except RWPE1 in the case of *TMS1*) showed evidence of full methylation (Figure 4.3 Panel G and H). Analysis of *DCR2* CpG island shows partial hypermethylation in 22RV1 and PC3 cells, with peaks present at both the methylated and unmethylated control (Figure 4.3 Panel J).

Table 4.2: Summary of DHPLC Methylation screen in prostate cancer cell lines			
Gene Symbol	**Chromosomal location**	**Methylation status**	**Prostate Cancer Cell line**
APAF1	12q23.1		
Assay 1		Unmethylated	All
Assay 2		Unmethylated	All
Assay 3		Unmethylated	All
CASP3	4q35.1	Unmethylated	All
CASP8	2q33.1	Unmethylated	All
FADD	11q13.3	Unmethylated	All
PIGPC1	6q23.3		
Assay 1		Unmethylated	All
Assay 2		Unmethylated	All
Assay 3		Unmethylated	All
DR5	8p21.3	Unmethylated	All
BIK	22q13.2		
Assay 1		Partially Methylated	PC3
Assay 2		Unmethylated	All
BNIP3	10q26.3	Partially Methylated	DU145, LNCaP, 22RV1,
CpG1 CFLIP	2q33.1		
Assay 1		Hemi-Methylated	LNCaP
Assay 2		Hemi-Methylated	LNCaP
CpG2 CFLIP	2q33.1		
Assay 1		Partially/ Fully Methylated	LNCaP, 22V1
Assay 2		Partially/ Fully Methylated	LNCaP, 22V1
TMS1	16p11.2	Partially/ Fully Methylated	DU145, LNCaP, 22RV1, PC3, RC58
DCR1	8p21.3	Partially/ Hemi-methylated	DU145, LNCaP, 22RV1, PC3, RC58
DCR2	8p21.3	Fully Methylated	22RV1, PC3
CDKN2A	9p21.3	Partially/ Fully Methylated	PC3, 22RV1, LNCaP

Note: In the case of some genes more than one PCR assay was analysed,
The Chromosomal location of the promoter CpG island under investigation
and the prosate cancer cell lines with evidence of promoter hypermethylation are listed

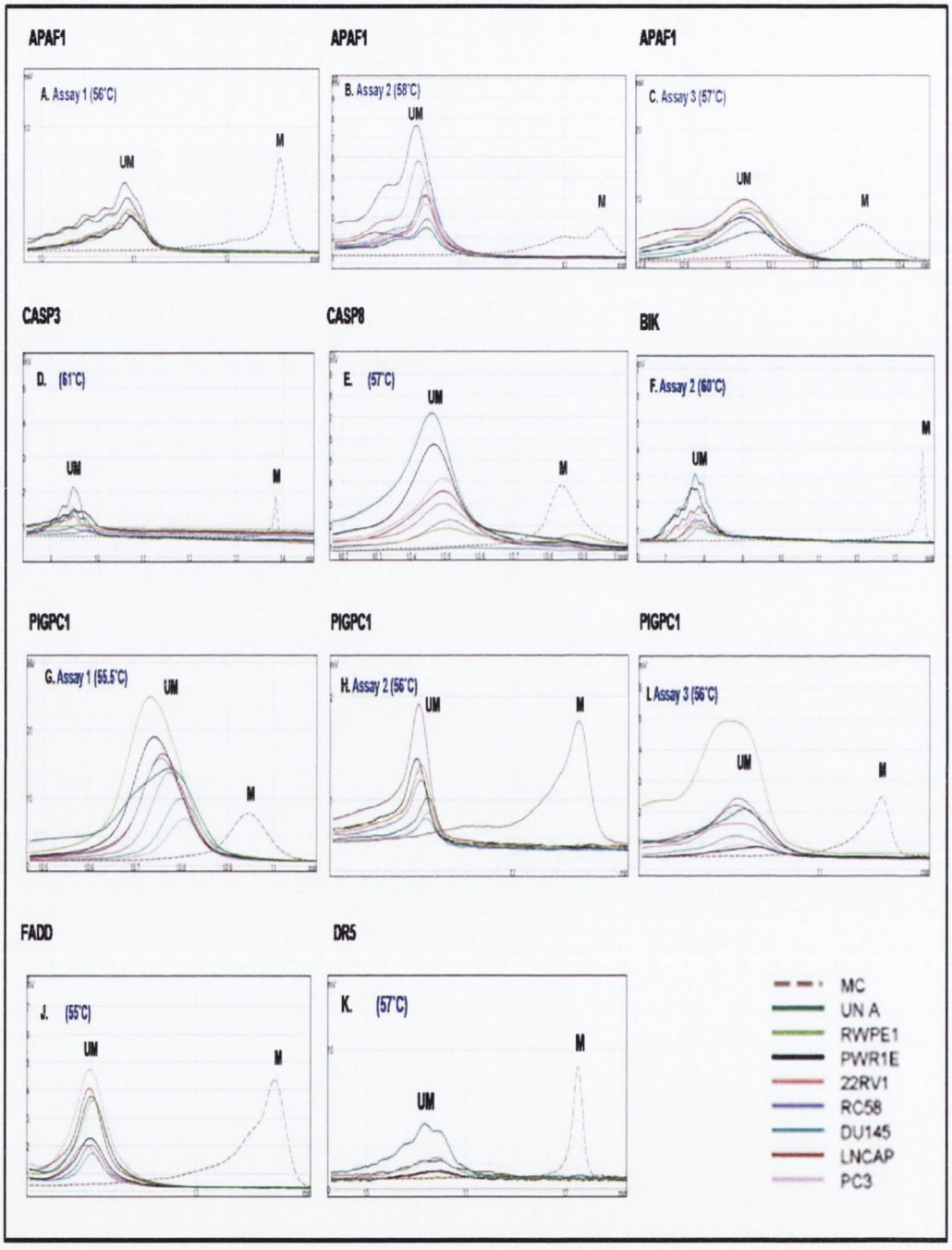

Figure 4.2:

DHPLC chromatograms of promoter CpG Islands of unmethylated genes in prostate cancer cell lines. Methylated control is illustrated by a dashed brown line and the unmethylated control represented by a full green line. Each coloured line represents a prostate cell line, all of which have eluted at the same time as the unmethylated control. An assay-dependant experimentally determined optimal temperature for methylation detection is illustrated in brackets for each assay.

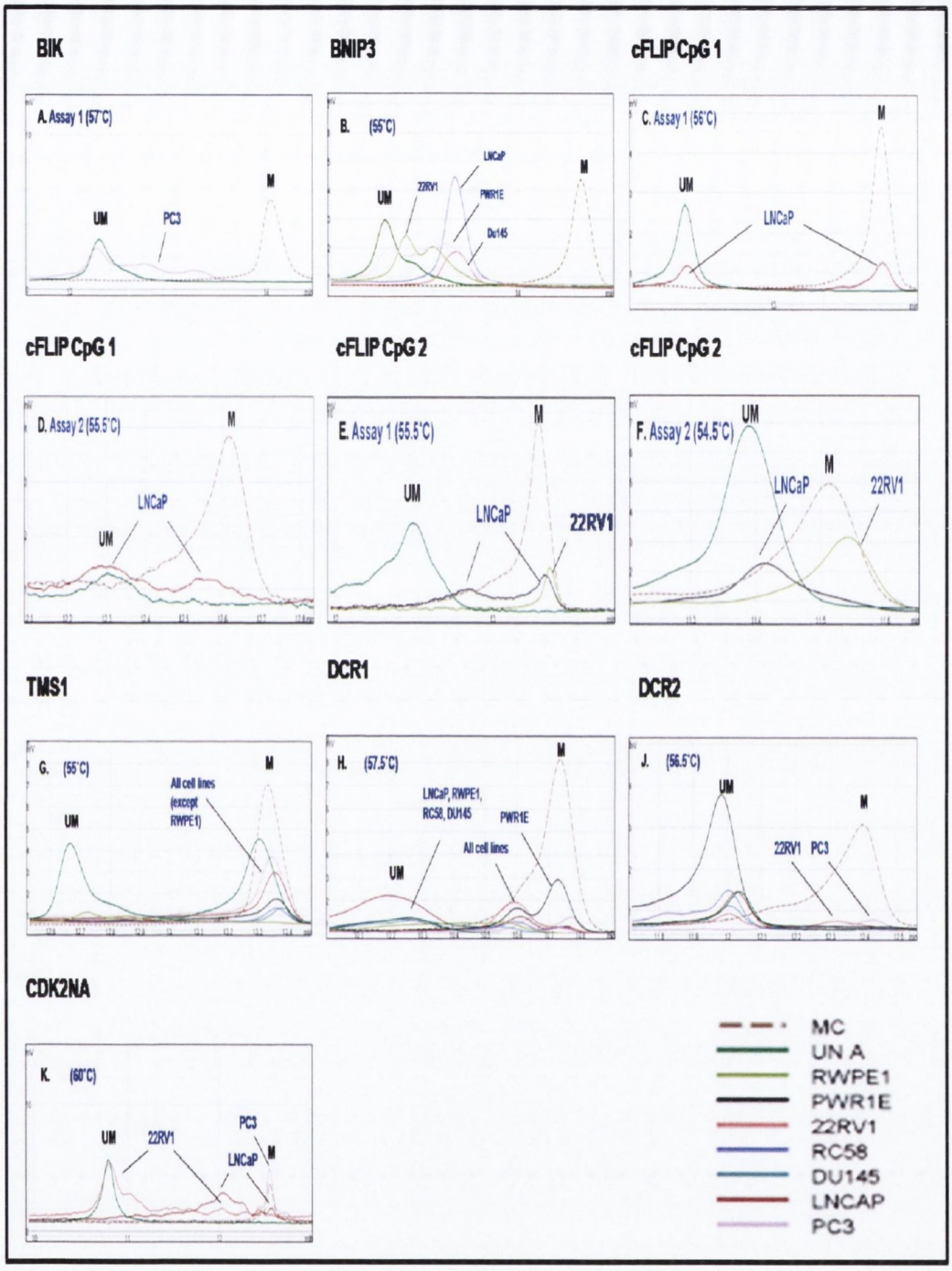

Figure 4.3:

DHPLC chromatograms of promoter CpG Islands of methylated genes in prostate cancer cell lines. Methylated control is illustrated by a dashed brown line and the unmethylated control represented by a full green line. Each coloured line represents a prostate cell line. An assay-dependant experimentally determined optimal temperature for methylation detection is illustrated in brackets for each assay.

4.4 VALIDATION OF DHPLC METHYLATION PROFILES USING BISULFITE SEQUENCING

Previously, it has been demonstrated that DNA methylation is not universal throughout a CpG island and can target specific transcription factor binding sites (Griswold and Kim, 2001; Perry et al., 2007). Therefore, we next sequenced the PCR assays in order to (i) validate our DHPLC screening results and (ii) generate promoter methylation maps and identify methylation hotspots. Fully methylated genes *DCR1* (LNCaP cell line) and *CDKN2A* (PC3 cell line) and partially methylated genes *cFLIP* (CpG1 and CpG2 in LNCaP cell line), *DCR1* (22RV1 cell line), *CDKN2A* (LNCaP and 22RV1 cell lines) were cloned and sequenced. For control purposes, we also sequenced a fully unmethylated gene *cFLIP* (CpG1 in 22RV1 cell line).

Bisulfite sequencing results confirmed our DHPLC methylation screening results in all the cell lines analysed (Figure 4.4- 4.6). In *CDKN2A* for example, the DHPLC profile for PC3 shows a single peak at the same elution time as the fully methylated control, suggesting 100% methylation of this sequence. The corresponding bisulfite sequencing analysis showed ~94% of CG sites methylated for all PC3 clones, hence confirming our DHPLC results (Figure 4.4). In contrast, for more complex DHPLC elution profiles (22RV1 and LNCaP) that showed various levels of methylation present, the corresponding sequencing analysis showed different clones with varying levels of methylation that represented the different peaks observed in the DHPLC elution profile, again showing close correlation between both techniques.

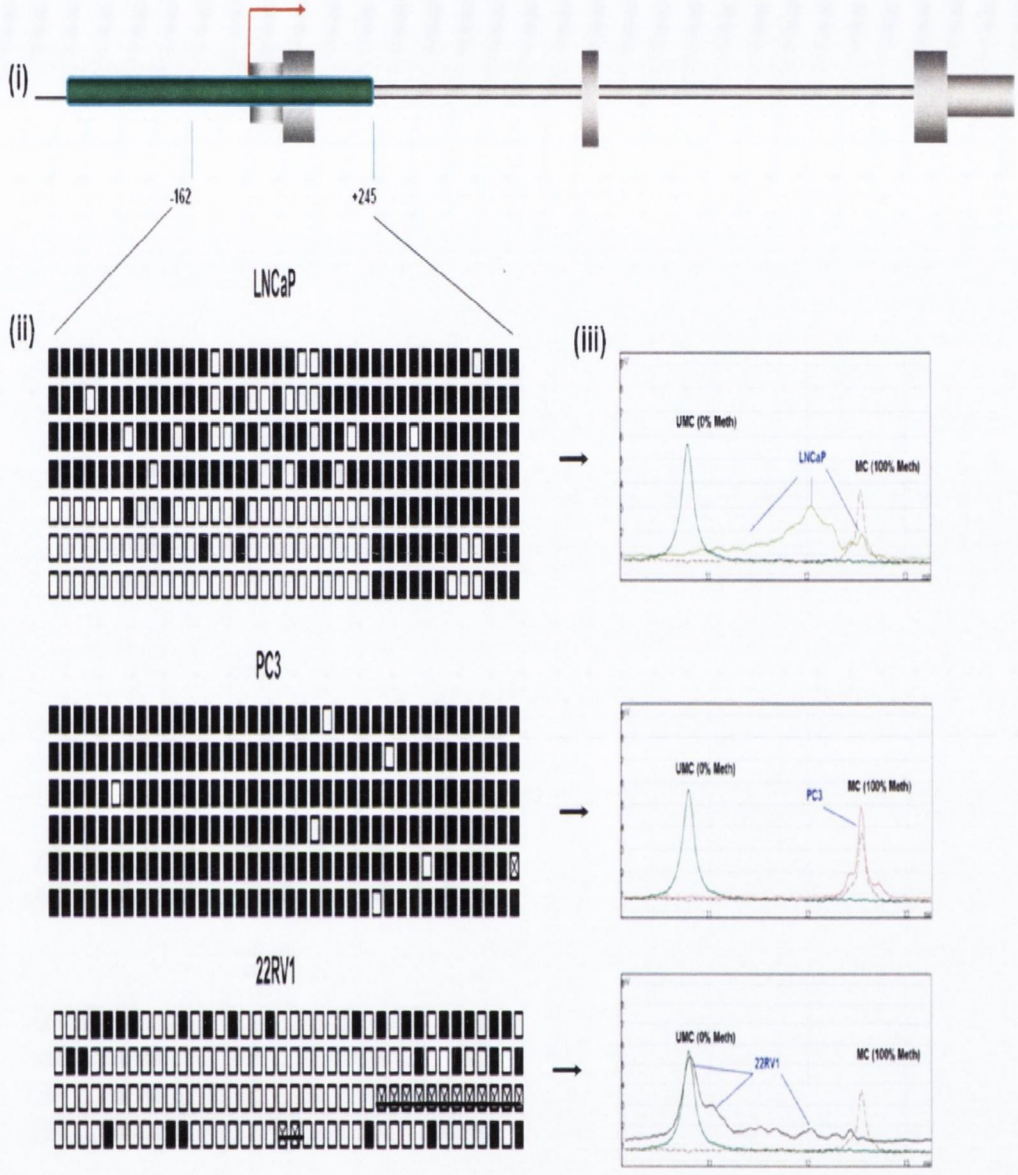

Figure 4.4.
Validation of DHPLC methylation results for *CDKN2A*. (i) *CDKN2A* gene structure, transcriptional start site (red arrow) and CpG island (green bar). **(ii)** *CDKN2A* sequencing results from 3 cell lines (LNCaP, PC3 and 22RV1) with evidence of methylation from DHPLC screening results. Between 4 and 8 clones were sequenced for each cell line. Each line represents an individual clone. Black and white squares signify methylated and unmethylated individual CpG sites respectively. **(iii)** DHPLC chromatogram of *CDKN2A* for 3 cell lines with corresponding sequencing data. The methylated control is indicated by a dashed brown line, labelled M and representing the profile of a fully (100%) methylated sequence. The unmethylated control is represented by a full green line, labelled UMC and is indicative of a profile of a sequence that has 0% methylation. The elution profile of the individual cell lines is illustrated in blue.

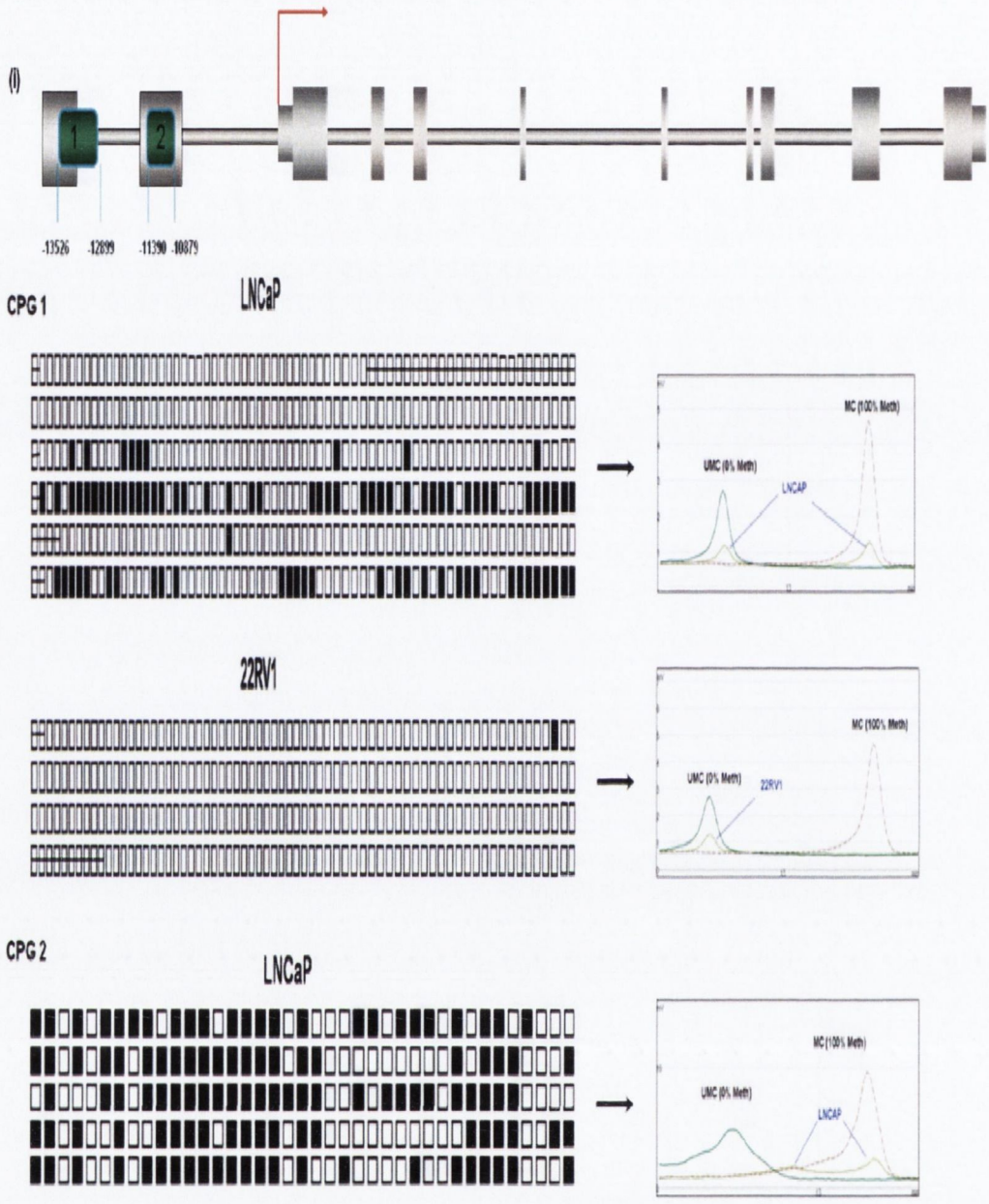

Figure 4.5.
Validation of DHPLC methylation results for *cFLIP*: (i). *cFLIP* gene structure illustrating transcriptional start site (red arrow), exons (grey boxes) and two 5'CpG island (green bars labelled 1 and 2). **(CpG1)** Bisulfite sequencing results of CpG 1 *cFLIP* with evidence of methylation (LNCaP) and with no methylation (22RV1) and corresponding DHPLC chromatogram. **(CpG2)** Bisulfite sequencing results of CpG 2 *cFLIP* in cell line LNCaP and DHPLC chromatogram. Between 4 and 8 clones were sequenced for each cell line. Each line represents an individual clone. Black and white squares signify methylated and unmethylated individual CpG sites respectively. A line through a clone represents unsequenced dinucleotides.

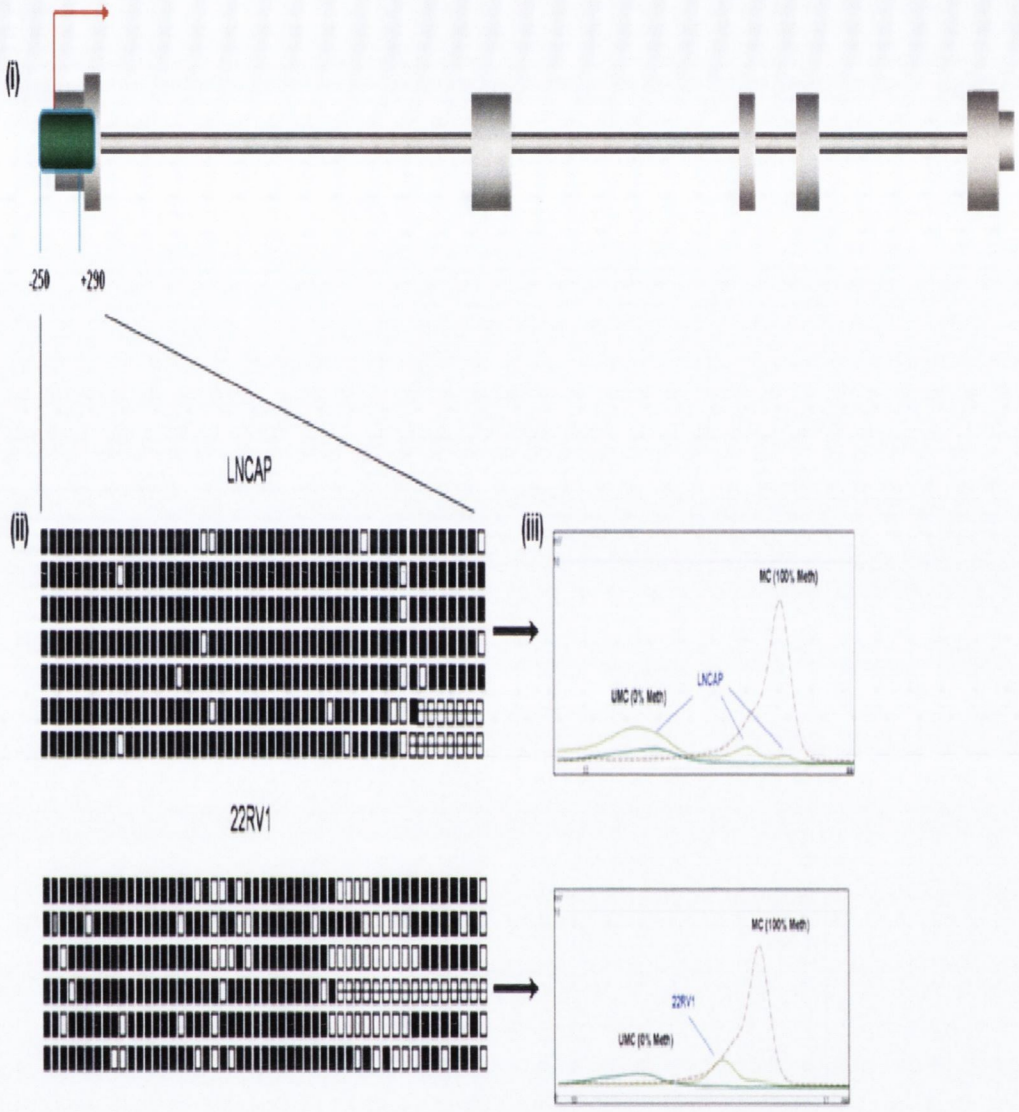

Figure 4.6.
Validation of DHPLC methylation results for *DCR1*: (i) *DCR1* gene structure and (ii) bisulfite sequencing. (iii) DHPLC chromatograms results for cell lines LNCaP and 22RV1. Between 4 and 8 clones were sequenced for each cell line. Each line represents an individual clone. Black and white squares signify methylated and unmethylated individual CpG sites respectively. A line through a clone represents unsequenced dinucleotides.

4.5 GENERATING A PARTIAL METHYLATION CONTROL

In a homogenous population of either methylated or unmethylated DNA, the DHPLC elution profile occurs at single time points. In practice, our sample often represents a heterogeneous population, whereby DNA peaks will elute at multiple time-points. In this way, partial methylation (at certain CpG sites within the island) will produce peak(s) in between that of the fully methylated and unmethylated sequences. As a result, we aimed to generate a partial

methylation control (PMC) for inclusion in our DHPLC screen. Unmethylated human placental DNA was treated with SSsI methylase using decreasing concentrations of the enzyme to generate controls with varying levels of methylation.

Utilising the freely available NEBcutterV2.0 (http://tools.neb.com/NEBcutter2/index.php) the restriction enzyme BsiE1 was identified to analyze SSsI methylase treated DNA. BsiE1 cuts the DNA at unmethylated cytosines but is blocked by the presence of a 5-methyl-cytosine and therefore will not cut a fully methylated DNA sequence, allowing comparison of the fully methylated and unmethylated sequence with the PMC.

We experienced on-going difficulty with optimisation of both SSsI methylase treatment of unmethylated DNA and our BsiE1 restriction digest. After treatment with BsiE1, unmethylated control DNA was partially cut by BsiE1 (Figure 4.7). However, restriction digestion of the SSsI treated PMC was not observed. Furthermore, a SSsI no enzyme control DNA sample, whereby the HPU DNA was treated as normal but without the addition of SSsI methylase, could not be digested by BsiE1 (Figure 4.7). These results suggest that SSsI methylase treatment of the HPU DNA is inhibiting the reaction in some way. Next, the sample was purified prior to restriction digestion. Unfortunately, no improvement of the restriction digest reaction was observed (Figure 4.7)

As a result, we were unable to differentiate between the methylation controls and PMC using restriction digestion. Despite numerous troubleshooting experiments, the restriction digest could not be optimised on the SSsI methylase treated DNA. Unfortunately, the DHPLC methylation screen, which we hoped to have the PMC for, was completed before our PMC was successfully characterised. As an alternative, we validated our DHPLC results by bisulfite sequencing.

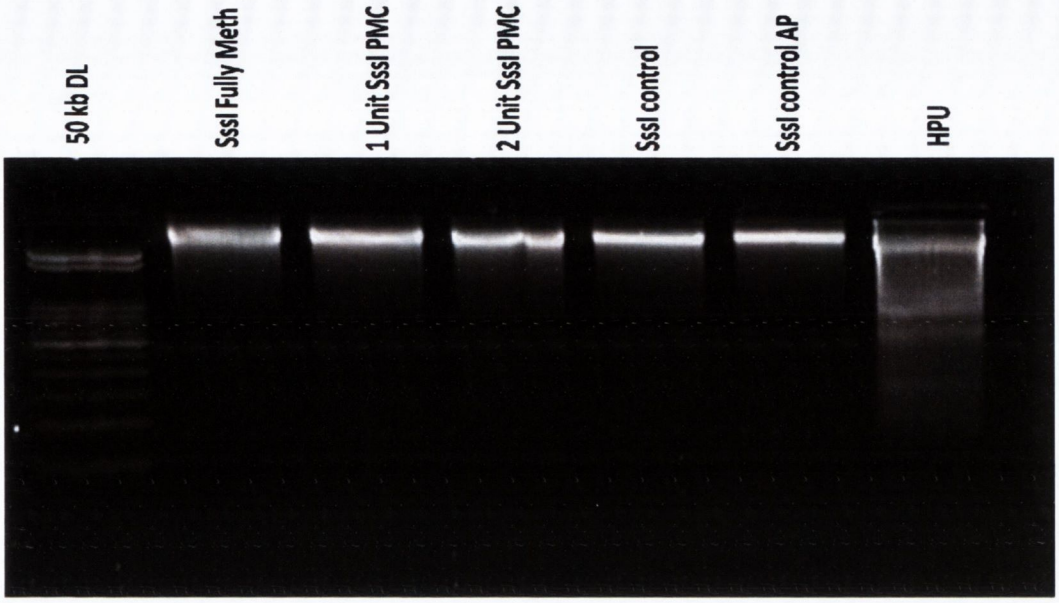

Figure 4.7

Gel electrophoresis of DNA treated with restriction enzyme BsiE1. Untreated human placental DNA (HPU) was partially digested by BsiE1.The following DNA samples were not cut by treatment with BsiE1 overnight HPU DNA treated with 6 units of SSsI methylase (SSsI Fully Meth), HPU DNA treated with 1 and 2 unit of SSsI methylase (1 unit SSsI PMC/ 2 unit SSsI PMC), SSsI non enzyme control (SSsI control) and SSsI non enzyme control after purification (SSsI control AP).

4.6 INVESTIGATING THE METHYLATION STATUS OF *cFLIP* IN COLON CANCER SAMPLES.

Previously, the long and short cFLIP isoforms were shown to be differentially expressed in colon cancer (Longley et al, unpublished data). In collaboration with Dr. Dan Longley and Dr. David Waugh in Queen's University, Belfast, we investigated the possible role of methylation in alternative splicing of both the long and short cFLIP isoforms in both prostate and colon cancer cell lines. We examined the methylation status of *cFLIP* in colon cancer cell lines (HCT116, RKO, LoVo and HT2G), in which Dr. Longley's group had previously obtained isoform specific expression data. Our DHPLC screening results suggest that *cFLIP* is unmethylated in the four colon cancer cell lines analysed (Figure 4.8). Therefore, it is unlikely that methylation plays a significant role in splice variation in colon cancer cells.

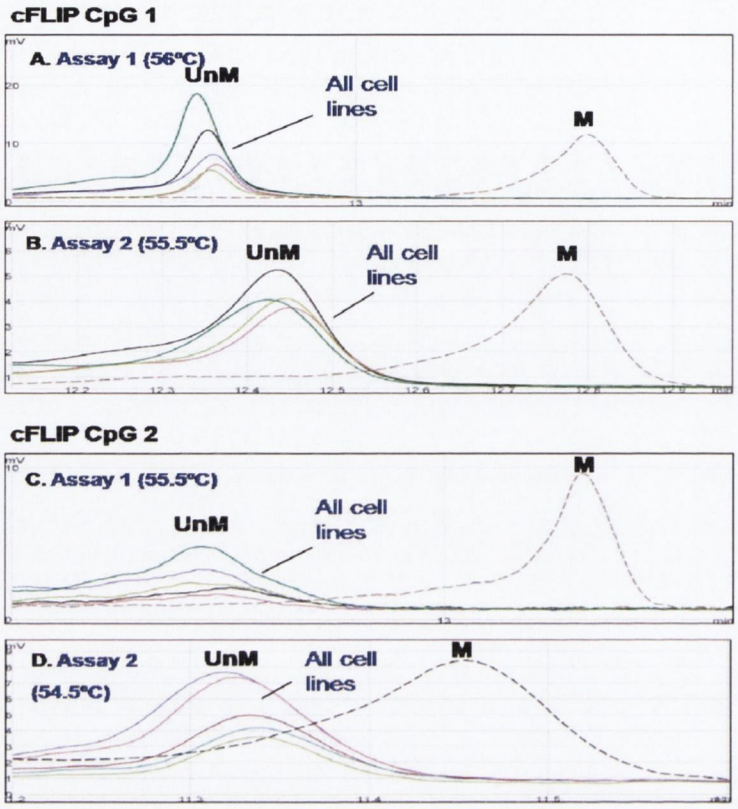

Figure 4.8:

DHPLC chromatogram of the promoter CpG Islands 1 and 2 of cFLIP in colon cancer cell lines. In each chromatogram (A-D) the methylated control is illustrated by a dashed brown line (labelled M) with the unmethylated control represented by a full green line (labelled UnM). Chromatogram A and B illustrates methylation screening results of the first CpG island (CpG 1) in the cFLIP gene. Chromatograms C and D illustrates the methylation screening results of the second CpG island (CpG 2) in the cFLIP gene. Each coloured line represents a colon cancer cell line (RKO, HT29, LoVo and HCT116), all of which have resolved at the same time as the unmethylated control.

4.7 INVESTIGATING THE METHYLATION STATUS OF DOCETAXEL RESISTANT PC3 PROSTATE CANCER CELL LINE (D12-PC3) AND AN AGE-MATCHED PC3 CONTROL.

A docetaxel resistant PC3 prostate cell line was generated by Dr. Amanda O'Neill in Professor Bill Watson's group (University College Dublin, Dublin). Low Density Array (LDA) data was performed by this group on a number of important apoptotic genes in the D12-PC3 and age-matched PC3 control

(AMC-PC3), which was a PC3 cell line grown alongside the D12-PC3 cells. Results showed downregulation of *BIK* in the docetaxel resistant cell line compared to the PC3 age-matched control. In order to investigate whether promoter hypermethylation correlated with the observed downregulation of *BIK* in the resistant cell line, its promoter CpG Island was screened for methylation in both cell lines. Results suggest that *BIK* is methylated in both PC3 and the D12-PC3 cell line. These results are consistent with our previous DHPLC results, where *BIK* appears to be partially methylated in PC3 prostate cancer cell line. Both cell lines resolved at various time points in between that of the unmethylated and methylated control, suggesting partial methylation. However they produced different elution patterns suggesting a slight difference in methylated CG sites, which suggests that the methylation pattern is altered in some way in the docetaxel resistant cell line.

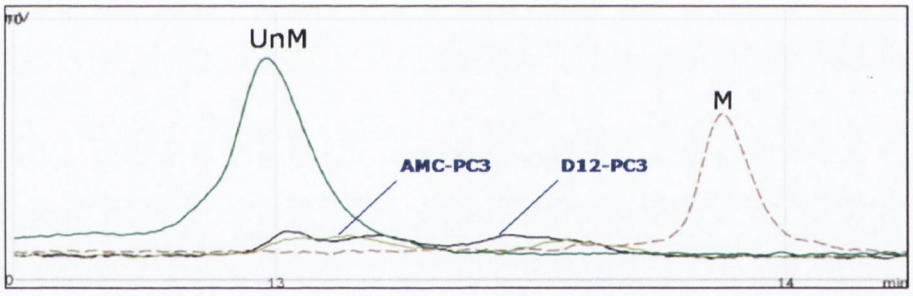

Figure 4.9.

Investigating the methylation status of *BIK* in docetaxel resistant D12-PC3 cells and an age-matched PC3 control (AMC-PC3). The methylated control is illustrated by a dashed brown line (labelled M) with the unmethylated control represented by a full green line (labelled UnM). Both cell lines elute at various time points in between that of the unmethylated and methylated control, suggesting partial methylation.

4.8 DISCUSSION

In total, 23 PCR assays were successfully optimised to amplify the 5' CpG islands of 13 of the 22 apoptotic-related genes identified in the *in silico* analysis (Discussed in Chapter 3). Despite primer redesign, the remaining 24 PCR assays could not be optimised. Often poor reproducibly and low yields of the PCR reactions was observed. A number of reasons may be responsible;

firstly, it may in part be due to the limitations of our primer design options (described in section *2.5.4)*. Due to the strict criteria by which bisulfite specific, methylation insensitive primers are designed, annealing sites are relatively restricted. Selection of primers can be further constrained by the large number of closely spaced CG dinucleotides, resulting in primer sites too short to achieve a desirable T_m. Secondly; regions that are methylated can often contain mutations, especially in cancer derived samples. This can lead to an inability of primers binding to their annealing sites in the DNA. Finally, Poly T sequences in bisulfite converted DNA can result in nonspecific primer annealing and poor amplification due to polymerase slipping (Methylation analysis by bisulfite sequencing: Chemistry, Products and Protocols. Applied Biosystems: http://www.appliedbiosystems.com).

In this study, thirteen genes, integral to apoptosis, were successfully screened for evidence of methylation using DHPLC. Our screen has identified seven genes (c*FLIP, BNIP3, TMS1, BIK, DCR1, DCR2* and *CDKN2A*) methylated in their promoter CpG regions in one or more prostate cancer cell lines. At present, there is no published data on the methylation status of c*FLIP*, *BNIP3*, *BIK, CASP3, CASP8, PIGPC1* and *FADD* in prostate cancer. *APAF1* has been reported to be unmethylated in 3 prostate cancer cell lines (PC3, DU145 and LNCaP) (Lodygin et al., 2005). Suzuki et al, 2006, described methylation of *DR5* at low levels (1%) in prostate tissue, while *TMS1, CDKN2A* and *DCR1/2* have recently been reported methylated in prostate cancer (Suzuki et al., 2006).

Our DHPLC results suggest that *APAF1*, *CASP3*, *CASP8, FADD, PIGPC1* and *DR5* promoter CpGs are unlikely targets of methylation in prostate cancer. However, it is possible that aberrant methylation can indirectly cause atypical expression of these important apoptotic genes. Transactivating regulators, such as enhancers or miRNAs, could be targets of methylation silencing. Such enhancer-related methylation events have been described for the imprinting of *H19* and *Igf2* genes (Bell and Felsenfeld, 2000; Hark et al., 2000). Interestingly, a study by Lodygin et al, 2005 showed that *APAF1* expression was induced by 5-aza-2'deoxycytidine in prostate cancer cell lines PC3 and DU145, suggesting DNA methylation may play a role in *APAF1* expression in

prostate cancer. However, bisulfite sequencing of the promoter CpG of *APAF1* showed no evidence of methylation, which is in accordance with our data. It is possible therefore that a regulatory element is a target of hypermethylation, which indirectly effects the expression of *APAF1*. Such a possibility cannot be ruled out for other genes.

BIK (BCL2-interacting killer)

Bik is a potent pro-apoptotic bcl-2 homology (BH3)-only member of the BCL2 family of proteins and plays a key role in mitochondrial-mediated apoptosis. Loss of Bik appears to be a common feature of renal cell carcinoma (Sturm et al., 2006). It is thought that *BIK* may act as a renal tissue-specific tumour suppressor gene. *BIK* has been reported to be hypermethylated in 59% of primary brain tumours (10/17). Furthermore, hypermethylation of *BIK* correlated with downregulation of *BIK* gene expression (Kim et al., 2006). Our study is the first report on the methylation status of *BIK* in prostate cancer. DHPLC analysis revealed partial methylation in androgen independent cell line PC3. Interestingly, *BIK* CpG island only showed evidence of methylation in its first assay, which encompasses the 5'UTR and a number of transcriptional elements associated with promoter regions. This result suggests that methylation at individual CG sites rather than the entire CpG island may be important for dysregulation of *BIK* in prostate cancer.

BNIP3 (BCL2/adenovirus E1B 19kDa interacting protein 3)

BNIP3 is a pro-apoptotic member of the bcl-2 family of proteins. Bnip3 is not an ubiquitously expressed protein but rather its expression can be induced during hypoxia or hypoxia-like conditions (Lee and Paik, 2006). A number of studies have implicated aberrant *BNIP3* expression in a wide range of cancers (Lee and Paik, 2006). Increasingly, evidence suggests that *BNIP3* promoter hypermethylation contributes to gene silencing in a number of cancers such as pancreatic, haematopoietic, gastric and colon cancer (Abe et al., 2005; Okami et al., 2004). Methylation induced gene silencing is hypothesised to confer a survival advantage to cancer cells by evading hypoxia induced cell death. DHPLC analysis of the *BNIP3* promoter CpG revealed partial methylation in prostate cancer cell lines 22RV1, DU145 and LNCaP.

The promoter of *BNIP3* contains hypoxic inducible factor (HIF)-1α responsive element (HRE), determining whether this HRE was aberrantly methylated in the prostate cell lines would help elucidate the role of aberrant methylation of *BNIP3* in prostate cancer. Bisulfite sequencing of *BNIP3* promoter CpG island would reveal the pattern of methylation within the promoter region and surrounding the HRE. Unfortunately, we were unable to clone the *BNIP3* CpG island for bisulfite sequence due to difficulties incurred during cloning. However, alternative methylation technique, discussed in next chapter, known as quantitative methylation specific PCR (QMSP) will be used to assess the methylation status of the HRE site in the CpG island of *BNIP3*.

CDKN2A

The *CDKN2A* gene encodes proteins important for regulation of cell cycle regulatory pathways p53 and retinoblastoma (RB). The gene contains alternative reading frames and hence encodes two major proteins p16INK4, an important cyclin-dependent kinase inhibitor and P14ARF, which binds the p53 stabilizing protein MDM2 (Robertson and Jones, 1999). Aberrant expression of *CDKN2A* gene has been illustrated in a wide range of cancers. DNA hypermethylation of the *CDKN2A* promoter region is also frequently observed in a wide range of tumours, including prostate cancer (Konishi et al., 2002). Promoter methylation of the *CDKN2A* gene has been illustrated in 3-25% of prostate carcinomas and 0% of normal prostate tissue (Konishi et al., 2002; Yao et al., 2006). DHPLC methylation screening revealed evidence of hypermethylation in the *CDKN2A* promoter region important for expression of P16INK4, in the primary prostate cell line 22RV1 and in two metastatic prostate cell lines LNCaP and PC3. Previous studies have shown promoter methylation in prostate cancer cell lines PC3, 22RV1, PPC1 and TSUPR1 (Jarrard et al., 1997; Yegnasubramanian et al., 2004). In contrast, the Jarrard (1997) study showed no evidence of promoter methylation in LNCaP cells. However, this study utilised methylation sensitive restriction enzyme digests, a technique which only provides information on a small number of CG sites and is less sensitive than DHPLC (Dahl and Guldberg, 2003). Bisulfite sequencing confirmed our DHPLC methylation findings for *CDKN2A*, revealing high

levels of methylation in PC3 and LNCaP cell lines at transcriptional elements, which suggests methylation of *CDKN2A*, may have functional significance.

FLICE-like inhibitory protein (*cFLIP/CFLAR*)

cFLIP has two major splice variants, a short variant (cFLIPS) containing two death effector domains (DED) and a longer (cFLIPL) variant containing an additional caspase-like domain, whereby the active centre cysteine residue is substituted by a tyrosine residue. cFLIPS competes with caspase 8 for binding to adaptor molecule Fadd and inhibits caspase activation (Yang, 2002). The role of cFLIPL has remained one of controversy (reviewed in (Krueger et al., 2001a)). In brief, Chang et al (2002) showed at low expression levels (representative of normal cellular expression) cFLIPL enhances Death Inducing Signalling Complex (DISC) activity, facilitating activation of caspase 8. Interestingly, at intermediate levels (indicative of levels observed in certain tumour cells and macrophages) cFLIPL can inhibit caspase 8 activation by blocking its recruitment to the DISC complex (Chang et al., 2002). Furthermore, $cFLIP^{-/-}$ mice show developmental defects resembling $CASP8^{-/-}$ and $FADD^{-/-}$ mice (Yeh et al., 2000), suggesting complete silencing results in loss of its mild pro-apoptotic function, therefore mimicking an anti-apoptotic phenotype.

cFLIP has been shown to be hypermethylated in 8/22 (36%) of neuroblastoma cell lines and 0/6 (0%) of normal tissues (van Noesel et al., 2003). A study by Margetts et al, 2005 reported *cFLIP* methylation in 3/39 (8%) of phaeochromocytoma and 1/20 (5%) of neuroblastoma tumour samples (Margetts et al., 2005). Curiously, our data indicates differential methylation of the two 5'UTR CpGs in the prostate cancer cell lines 22RV1 and LNCaP. The first CpG island (CpG1) over laps the 5'UTR of the long *cFLIP* Splice variant and the second (CpG2) which contains the 5'UTR for the short *cFLIP* splice variant. Our bisulfite sequencing analysis confirmed our DHPLC results, revealing absence of methylation in the first CpG island in 22RV1 cells and high levels of methylation for the second CpG island in 22RV1 cells, hemi and

partial methylation for the first and second CpG islands, respectively for LNCaP cells.

DcR1 and DcR2

The decoy receptors contain extracellular domains which compete with those of the death receptors DR4 and DR5 for TNF-related apoptosis-inducing ligand (Trail) binding, but fail to propagate the death signal via their non-functional or missing death domains (Ashkenazi and Dixit, 1999). Aberrant methylation of *DCR1* and *DCR2* genes has been reported in a number of tumour types (Takahashi et al., 2004). *DCR1* and *DCR2* were both methylated in 50% of prostate tumours (25/50 and 23/46, respectively) and 60% of prostate cancer samples had either *DCR1* or *DCR2* methylated. Shivapurkar et al, 2004 showed that methylation of either *DCR1* or *DCR2* correlated with improved prognosis in prostate cancer and a subsequent study showed that lack of methylation of both genes predicted a poorer disease free survival rate (Suzuki et al., 2006). Our results indicate that *DCR1* and *DCR2* promoter CpGs are targets of methylation in all prostate cancer cell lines for *DCR1* and in 22RV1 and PC3 for *DCR2*.

TMS1 (target of methylation induced silencing)

TMS1 is a pro-apoptotic tumour suppressor gene. Two reports have implicated methylation as a mechanism of *TMS1* down-regulation in prostate cancer cell lines (Caldas et al., 1994; Collard et al., 2006). Biallelic hypermethylation and silencing of *TMS1* has been shown in the LNCaP prostate cell line. *TMS1* promoter hypermethylation has been implicated as an early event in prostate cancer development, detected at significantly higher frequencies in primary tumours (47-65%) and pre-invasive HGPIN (64% (7/11)) than non-malignant prostate (3-28%) (Caldas et al., 1994; Collard et al., 2006; Suzuki et al., 2006). Our results are consistent with these previous findings; we demonstrated that *TMS1* is fully methylated in all prostate cancer cell lines examined (LNCaP, DU145, RC58, 22RV1 and PC3). It is interesting to note that *TMS1* and *DCR1* were the only genes we examined that were methylated in all prostate cancer

cell lines, suggesting they may have an important role in prostate carcinogenesis.

Of interest, analysis of the chromosomal locations (listed in Table 4.2) of the 13 genes screened for methylation did not support regional spreading of methylation in prostate cancer. For example, *cFLIP* maps adjacent to *CASP8* on chromosome band 2q33.1. These two genes have previously been shown to correlate in their methylation status suggesting clustering of *de novo* methylation (van Noesel et al., 2003). However, our results in prostate cancer indicate absence of methylation in *CASP8* and differential methylation in the two 5'UTR CpG islands of *cFLIP*. Similarly, *DR5*, *DCR1* and *DCR2* co-localise to chromosome band 8p21.3, again these genes show different methylation profiles in the various cell lines examined.

In addition to our methylation profiling of prostate cell lines, we examined the methylation status of one gene, *cFLIP,* in colon cancer cell lines. Interestingly, both 5'UTR CpG islands of *cFLIP* were unmethylated in all four colon cancer cell lines examined, suggesting methylation of *cFLIP* may have a degree of specificity in prostate cancer.

Resistance to chemotherapy, especially to docetaxel, has emerged as a major obstacle in the treatment of advanced prostate cancer (Gopisetty et al., 2006). Deciphering the molecular mechanisms, which disrupt key apoptotic pathways and contribute to chemotherapy resistance, is an important area of research. We first examined the methylation status of *BIK* in a docetaxel resistant cell line and control. Our methylation screen using DHPLC illustrated partial methylation in both cell lines with a slight difference in the elution profile. To establish the actual methylation difference between the cell lines, the CpG island requires bisulfite sequencing. This was not possible due to *BIK* CpG island cloning difficulties encountered.

In summary, this work demonstrates the utility of a DHPLC methylation screening strategy to identify novel targets of aberrant methylation in prostate cancer. Furthermore, our apoptotic methylation profile of prostate cancer cell

lines has identified a panel of apoptotic genes (*BIK*, *BNIP3*, *cFLIP*, *TMS1*, *DCR1*, *DCR2* and *CDK2NA*) showing aberrant DNA methylation. Determining the expression levels of the apoptotic genes, which we have identified as methylated from our DHPLC screen, is required to establish the silencing effect of promoter hypermethylation in prostate cancer. As a result, functional studies are necessary to determine the effect of the methylation status of our 7-gene panel at the mRNA level. This will be investigated in the next chapter.

CHAPTER 5

QUANTIFYING METHYLATION AND GENE EXPRESSION LEVELS OF APOPTOTIC-GENE TARGETS OF METHYLATION IN PROSTATE CANCER CELL LINES

5.1 INTRODUCTION

In the last chapter, we demonstrated the utility of a DHPLC methylation screening strategy to identify novel targets of aberrant methylation in prostate cancer. We identified a panel of apoptotic genes (*BIK*, *BNIP3*, *cFLIP*, *TMS1*, *DCR1*, *DCR2* and *CDK2NA*) showing aberrant DNA methylation. In this chapter, we selected this 7-gene panel for further investigation, with a view to assessing the functional significance associated with methylation of these genes.

We aimed to characterise the promoter CpG islands of each gene of interest in order to identify biologically significant regions of the island and to determine the most relevant areas to locate quantitative methylation specific PCR (QMSP) primers and probes. QMSP is the method of choice for quantitative analysis of methylation in tissue samples and represents a highly sensitive, rapid (does not require gel electrophoresis), high-throughput (can be performed on a 384 well plate) technology. This technology utilises TaqMan fluorescence based real-time PCR (described in section 2.5.7). First, we utilised this high-throughput technology for the semi-quantitative analysis of DNA methylation and to investigate the methylation status at individual CG site for the 7 genes of interest in our panel of prostate cell lines, prior to analysis in tissue samples (Chapter 6).

Promoter hypermethylation is associated with decreases in gene expression. However, methylation alone is often not sufficient to cause transcriptional silencing alone (Bird and Wolffe, 1999). Thus, in order to establish the effect of the methylation status of our 7-gene panel at the mRNA level, quantitative real-time PCR (QRT-PCR) was performed for each gene in prostate cell lines and in PC3 cells treated with a methylation inhibitor using the comparative C_T method (described in section 2.6).

5.2 *IN SILICO* PROMOTER CPG CHARACTERISATION

Studies have shown that methylation at single CG sites within transcription factor binding sites is sufficient to prevent a transcription factor binding to its recognition site, leading to inhibition of gene transcription (Griswold and Kim,

2001; Perry et al., 2007). Hence, methylated CpG islands for each gene of interest were fully characterised for transcription factor binding sites (TFBS) and promoter elements using the freely accessible online software Promoter Scan (http://www-bimas.cit.nih.gov/molbio/proscan/). The software predicts regions of DNA that contain significant numbers of transcriptional elements associated with polymerase II promoter sequences (Prestridge, 1995). Furthermore, each CpG island of interest was screened for the presence of an androgen-response element (ARE) using ConSite (http://asp.ii.uib.no:8090/cgi-bin/CONSITE/consite/), a freely available online resource which allows you to predict various transcription factor binding sites. No ARE sites were predicted in each CpG island except for cFLIP CpG 1, which contains a known ARE (Hsieh et al., 2007).

The transcriptional and translational start sites, exon/intron boundaries and 5'UTR were mapped (if present) onto the CpG island using information from the human genome browser (http://genome.ucsc.edu/) (Figure 5.1). The second CpG island of *cFLIP, DCR1* and *DCR2* contained no predicted transcriptional elements associated with promoter regions. A list of all the transcriptional elements, their binding sequences and position within the CpG island is outlined in Appendix 3.

BIK

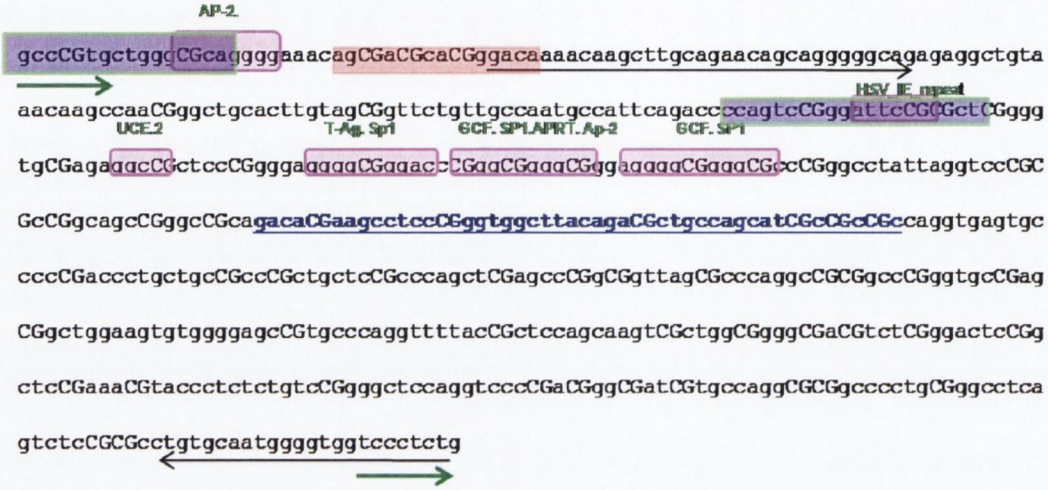

BNIP3



Figure 5.1.

Promoter CpG island characterisation. CpG promoter region are indicated by green arrows. Forward and reverse primers for PCR and bisulfite sequencing are labelled by black arrows. QMSP primers and probes are highlighted in purple and red, respectively. The 5′UTR is underlined in navy text. Translational start site (ATG) is highlighted in blue. Predicted transcriptional elements are marked in pink and labelled in green.

cFLIP CpG 1

caagccatagcaggaaacagCGagcttgcagcctcacCGaCGagtctcaactaaaagggactccCGgagct

aggggtggggactCGgcctcacacagtgagtgcCGgctattggacttttgtccagtgacagctgagacaac

aaggaccaCGggaggaggtgtaggagagaagCCcCGCGaacagCGatCGcccagcaccagtcCGcttccag

gctttCGgtttctttgcctccatcttgggtgCGccttccCGgCGtctaggggagCGaaggctgaggtggca

gCGgcaggagagtccCGgcCGCGacaggaCGgtaCGtgcccCGCGctCGaccccCGCGctggCGgCGcCGga

gctgtcccagaccccaagcccCGaCGccCGgccctgagtcagcattgcagcaggccctgCGcCGcCGCGcc

cCGCGtcccacccCGCGcCGctcctcacagccctgCGctcCGggaaactgcaggtggcCGgcagtggccag

gggatggCGggggCGcttctggaacctgactcagttttgtaggttccttatctCGgttgtttacCGCGggc

tttgCGgaatgccccCGcttcCGttctcCGccCGgctcCGaaccccCGaacccctttctaccCGcaactcCGc

ccCGgattcccagaaagcgggCGacctgggccacagCGgtacaagctgcacccCGatggacctgagagacCG

gaagtaacccttggccaactctggcCGcccctgcagcCGcagccccagaggcccaccCGCGagcttcagt

ggCGggccctcagCGtCGtgtaaactttgcttaaaatgatcttgagagttcaattcttggggt

cFLIP CpG 2

cagctcctagtaggtggtggggCGcagCGgctgtccccactcagtcctggtgggtCGcaC

GtaaCGgtcctgagctatgcataagcCGtttgaccaCGcatggagaattttaccacccagag

acaCGCGagtggccctgtgcaagtttcaactgCGCGgggggCGgggaattcCGcagacagga

ttctagaatttatgtcttgtgtggtaacatttcagcCGgtgggtggCGgggattaggCGtga

agCGgttcagcaggcagaggttctCGgaCGccctcCGgCGaagccacctgttgatgcttttg

actttctgtccttgttcctCGtcccatctggagcatttccaattctggttttgCGgagcagc

aggtctgagcttgtcCGgCGagggtgggagttggtccCGgCGgagatccagtgggaagagcC

GgCGgctgccCGggCGtgagtagacCGagaatcctgccCGatcccCGcccctgggctggtgt

CGccctgggctcctgggaCGtCGgggcactgtccccCGatactggcagaaaaggattgagtc

ctCGcttttggccctaggtctccttgagcctccagag

Figure 5.1.

Promoter CpG island characterisation. CpG promoter region are indicated by green arrows. Forward and reverse primers for PCR and bisulfite sequencing are labelled by black arrows. QMSP primers and probes are highlighted in purple and red, respectively. The 5´UTR is underlined in navy text. Translational start site (ATG) is highlighted in blue. Exons are marked by red arrows. Predicted transcriptional elements are marked in pink and labelled in green.

CDKN2A

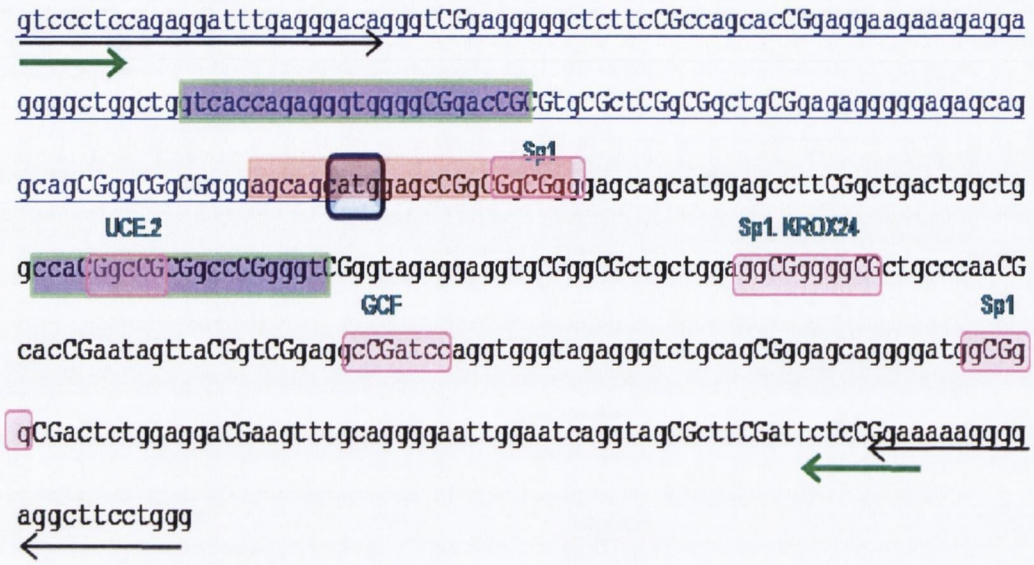

DCR1

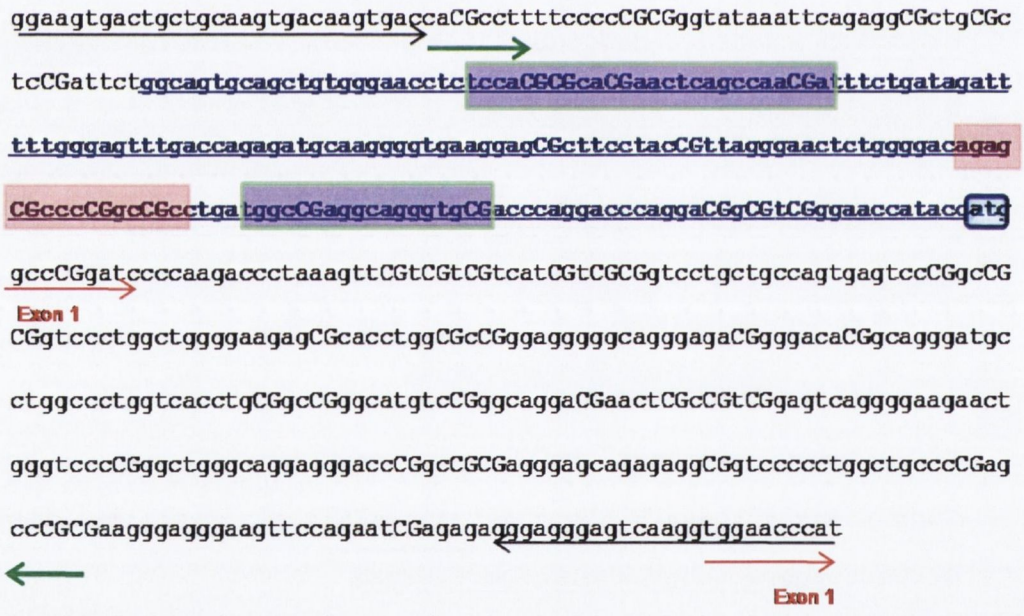

Figure 5.1 Contd.

Promoter CpG island characterisation. CpG promoter region are indicated by green arrows. Forward and reverse primers for PCR and bisulfite sequencing are labelled by black arrows. QMSP primers and probes are highlighted in purple and red, respectively. The 5′UTR is underlined in navy text. Translational start site (ATG) is highlighted in blue. Exons are marked by red arrows. Predicted transcriptional elements are marked in pink and labelled in green.



Figure 5.1 Contd.

Promoter CpG island characterisation. CpG promoter region are indicated by green arrows. Forward and reverse primers for PCR and bisulfite sequencing are labelled by black arrows. QMSP primers and probes are highlighted in purple and red, respectively. The 5´UTR is underlined in navy text. Translational start site (ATG) is highlighted in blue. Exons are marked by red arrows. Predicted transcriptional elements are marked in pink and labelled in green.

5.3 QMSP ASSAY VALIDATION

In addition to data obtained from our bisulfite sequencing analysis (discussed in Chapter 4), the promoter CpG island maps of the 7 genes were employed to design informative quantitative methylation specific PCR (QMSP) assays in order to measure the levels of methylation in prostate cell lines. One QMSP assay was designed for each gene, with the exception of *cFLIP*, where one QMSP assay was designed for each 5'UTR CpG island. All QMSP assays were designed to encompass CG sites overlapping transcriptional elements and/or the 5'UTR.

Primer and probe concentrations for each QMSP assay were optimised using methylated DNA as a control (described in Appendix A4.1), apart from *ACTB*, which was previously optimised by Dr. Antoinette Perry in our laboratory. Assays showed similar efficiencies, defined by the slopes of the standard curves (ranging from: -3.124 to -3.832) (Figure 5.2). Standard curves were generated by plotting C_T versus quantity of methylated DNA using serial dilution (10ng, 1ng, 0.1ng, 0.05ng, 0.01ng) of methylated control DNA. A slope close to -3.32 represents a 2-fold increase in PCR product per cycle during the exponential phase of real-time PCR.

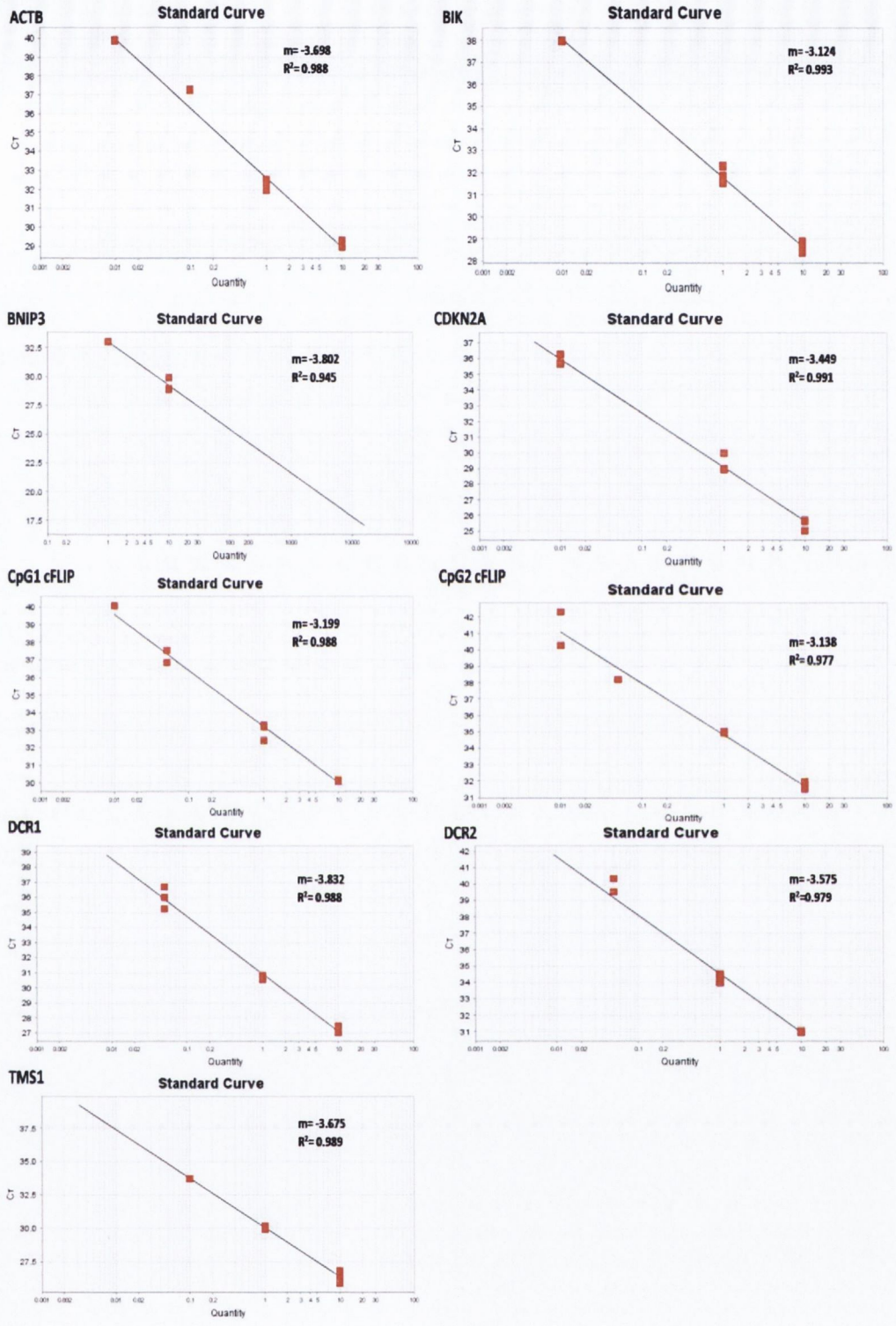

Figure 5.2.

Standard curve of QMSP assays. A standard curve was generated by plotting Ct versus quantity of methylated DNA (10ng, 1ng, 0.1ng, 0.05ng, 0.01ng). m= slope of the standard curve, R2= correlation co-efficient. Red dots represent individual standards (10ng-0.01ng).

The specificity of our QMSP assay was determined using unmethylated DNA (UCA). All QMSP assays, with the exception of *TMS1*, failed to amplify UCA DNA, showing 100% specificity for methylated DNA. *TMS1* was previously shown methylated in our UCA and as an alternative, the normal prostate cell line RWPE1 DNA was used as an unmethylated control for this assay. Our QMSP assay for *TMS1* did not generate a signal for RWPE1 DNA (Table 5.1). In addition, the specificity of each assay for bisulfite modified DNA was tested by using unmodified MC DNA as a template, which did not generate a signal for each of our 7 targets, confirming specificity of the assay.

5.4 QUANTITATIVE METHYLATION ANALYSIS OF A 7-GENE APOPTOTIC PANEL

A TaqMan PCR assay designed to amplify bisulfite modified DNA irrespective of methylation status was designed within the b-actin (ACTB) gene and used to normalise the amount of bisulfite modified template in each cell line. Results are presented in Figure 5.3 and Table 5.1. The level of methylation of a 7-gene apoptotic panel was determined by calculating the normalised index of methylation (NIM). This score reflects the ratio of the normalised amount of methylated target template to the normalised amount of the endogenous control (*ACTB)* in any given sample (Yegnasubramanian et al., 2004).

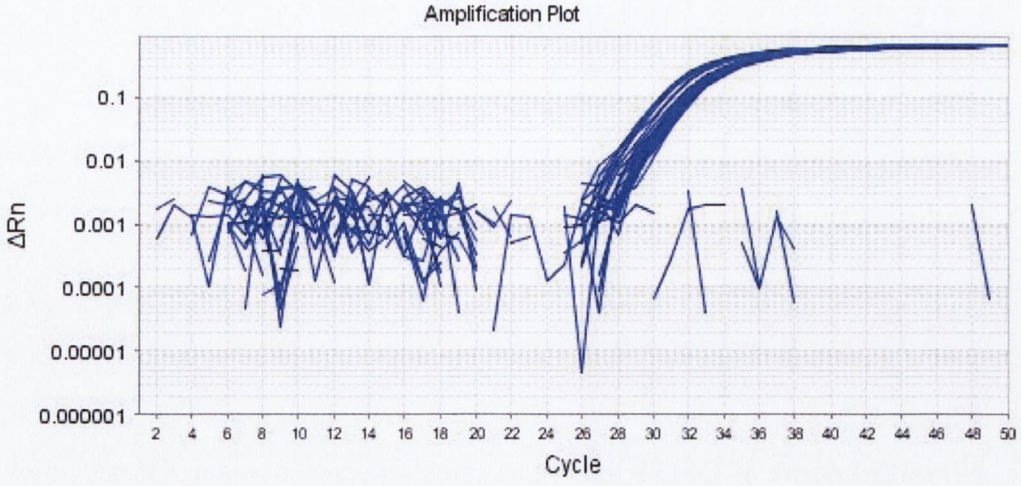

Figure 5.3
Amplification plot of *ACTB*. The amplification plot of ΔRn versus cycle number for endogenous control, *ACTB*, for all prostate cell lines, standards and methylation controls is illustrated. All samples amplified successfully and their

mean C_T values are used to calculate the normalised target value for each assay in individual cell lines.

5.4.1 Methylation frequency of the 7- gene apoptotic panel

Quantifying the methylation levels of the 7-gene panel in various prostate cell lines provides information on the methylation status at individual CG sites, which may be embedded within transcription factor binding sites. Such information is essential for understanding the functional significance of aberrantly methylated promoter CpG islands. Furthermore, our QMSP analysis allows further validation of our DHPLC methylation screening results.

A QMSP summary and heat map of methylation levels for each gene for each of the seven prostate cell lines are illustrated in Table 5.1 and Figure 5.4, respectively. *cFLIP* methylation was detected only in LNCaP (CpG island 1) and LNCaP and 22RV1 (CpG island 2), *BNIP3* was methylated in 3 cell lines (PWR1E, DU145 and LNCaP). Methylation of *TMS1* CpG island was detected in all 5 tumour cell lines and the PWR1E normal cell line. *CDKN2A* was methylated in three prostate cancer cell lines (22RV1, LNCaP and PC3). *DCR1* was also methylated in all cell lines, and showed a very high methylation score in 22RV1 and PC3 cells, indicating very high levels of methylation. Methylation of *DCR2* was detected in 22RV1 and PC3 cell lines and normal cell line RWPE1. A NIM score of >1000 was observed in PC3 cells suggesting high levels of methylation in this prostate cancer cell line.

Our QMSP results largely concurred with our DHPLC methylation results, except for *BIK* and *BNIP3* in 22RV1 cells. QMSP did not detect any *BIK* methylation in PC3 cells, although there was low level partial methylation observed in our DHPLC analysis. A second QMSP assay was designed encompassing different CG site but this also failed to detect methylation in PC3 cells. In the case of *BNIP3*, the QMSP assay was designed to encompass a hypoxic inducible factor (HIF)-1α responsive element (HRE) embedded within the *BNIP3* promoter CpG island. This region of the promoter CpG island was not screened for methylation in our DHPLC screen and may account for the differences observed in QMSP analysis and DHPLC results.

The five tumour cell lines showed varying degrees of methylation across the 7 gene panel. Overall, 22RV1 was methylated at 5 loci, RC58 at 2 loci, DU145 at 3 loci, LNCaP at 6 loci and PC3 at 4 loci. Methylation of certain genes was detected in the "normal" cell lines RWPE1 and PWR1E, although only DCR1 appeared methylated in both.

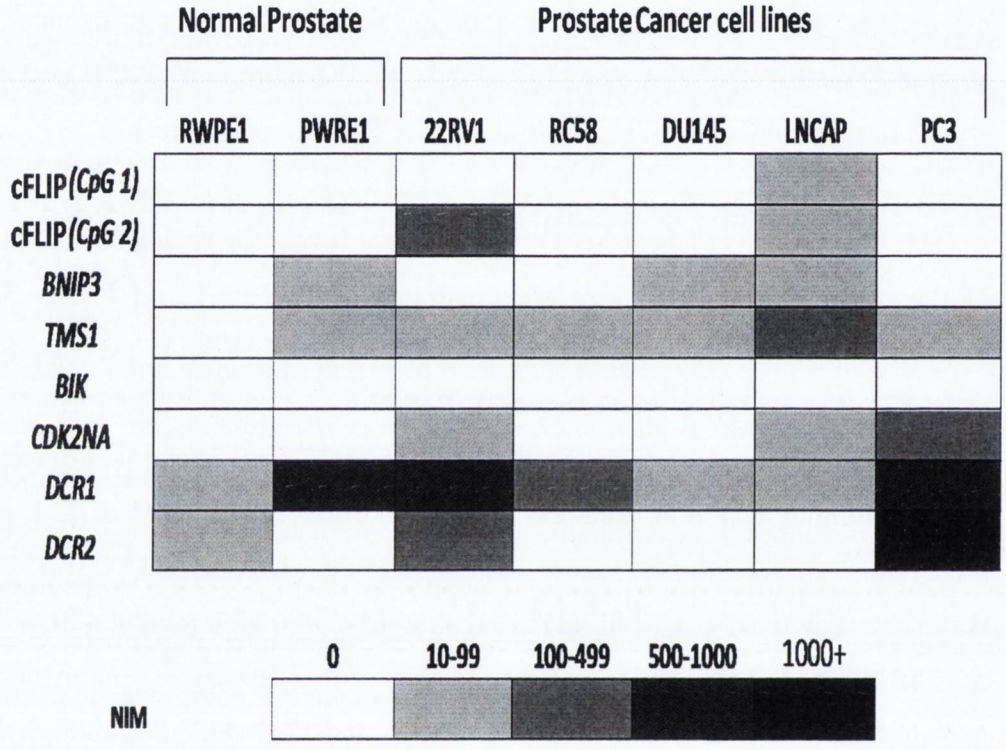

Figure 5.4.

Methylation levels of the 7-gene panel determined by QMSP. A summary of the QMSP results is illustrated as a heat map for our panel of prostate cell lines. The scale represents the normalised index of methylation (NIM).

Table 5.1: Summary of QMSP results

Gene	Cell line	Mean Ct ± SE	Mean quantity ± SE	NIM
ACTB	RWPE1	31.26 ± 0.35	2.34 ± 0.48	N/A
	PWRE1	31.15 ± 0.11	2.47 ± 0.17	N/A
	22RV1	31.18 ± 0.22	2.45 ± 0.35	N/A
	RC58	31.72 ± 0.17	1.74 ± 0.19	N/A
	DU145	31.75 ± 0.15	1.71 ± 0.16	N/A
	LNCAP	31.51 ± 0.05	5.32 ± 0.19	N/A
	PC3	29.92 ± 0.05	1.98 ± 0.07	N/A
CpG1 cFLIP	RWPE1	0	0	0
	PWRE1	0	0	0
	22RV1	0	0	0
	RC58	0	0	0
	DU145	0	0	0
	LNCAP	36.8 ± 0.04	0.09 ± .08	20.31± 0.04
	PC3	0	0	0
CpG2 cFLIP	RWPE1	0	0	0
	PWRE1	0	0	0
	22RV1	34.42 ± 0.48	1.39 ± 0.43	112.83 ± 0.003
	RC58	0	0	0
	DU145	0	0	0
	LNCAP	36.07 ± 0.22	0.23 ± 0.04	36.07 ± 0.004
	PC3	0	0	0
BNIP3	RWPE1	0	0	0
	PWRE1	33.85 ± 0.82	0.04 ± 0.02	5.44 ± 0.11
	22RV1	0	0	0
	RC58	40.23 ± 0.84	0.0005 ± 0.0003	0.04 ± 0.34
	DU145	30.49 ± 0.06	0.37 ± 0.015	34.54 ± 0.002
	LNCAP	32.28 ± 0.28	0.11 ± 0.02	31.58 ± 0.006
	PC3	0	0	0
TMS1	RWPE1	0	0	0
	PWRE1	35.56 ± 0.80	0.034 ± 0.01	10.14 ± 0.05
	22RV1	38.67 ± 0.76	0.0049 ± 0.002	1.46 ± 0.35
	RC58	33.40 ± 0.47	0.13 ± 0.04	53.29 ± 0.006
	DU145	33.40 ± 0.38	0.13 ± 0.03	53.57 ± 0.005
	LNCAP	29.59 ± 0.43	1.38 ± 0.34	188.06 ± 0.001
	PC3	34.32 ± 0.30	0.07 ± 0.02	26.18 ± 0.009

Note: Abbreviations: NIM: Normalised index of methylation, SE: Standard error

Table 5.1 Contd.: Summary of QMSP results

Gene	Cell line	Mean Ct ± SE	Mean quantity ± SE	NIM
BIK	RWPE1	0	0	0
	PWRE1	0	0	0
	22RV1	0	0	0
	RC58	0	0	0
	DU145	0	0	0
	LNCAP	0	0	0
	PC3	0	0	0
CDK2NA	RWPE1	0	0	0
	PWRE1	0	0	0
	22RV1	35.59 ± 0.01	0.013 ± 0.004	2.31 ± 0.13
	RC58	0	0	0
	DU145	0	0	0
	LNCAP	31.68 ± 0.04	0.18 ± 0.04	67.13 ± 0.003
	PC3	27.61 ± 0.42	2.67 ± 0.42	375.30 ± 0.0004
DCR1	RWPE1	37.49 ± 1.23	0.03 ± 0.02	8.34 ± 0.08
	PWRE1	29.57 ± 0.09	2.75± 0.16	810.81 ±0.0001
	22RV1	30.32 ± 0.4	1.77 ± 0.36	526.53 ± 0.0005
	RC58	32.18 ± 0.66	0.59 ± 0.21	247.75 ± 0.001
	DU145	36.13 ± 1.27	0.06 ± 0.05	27.15 ± 0.03
	LNCAP	32.96 ± 0.55	0.37 ± 0.13	50.05 ± 0.007
	PC3	29.62 ± 0.14	2.67 ± 0.23	985.52 ± 0.00001
DCR2	RWPE1	37.93 ± 0.65	0.12 ± 0.04	36.63 ± 0.01
	PWRE1	0	0	0
	22RV1	34.02 ± 0.04	1.39 ± 0.03	412.57 ± 0.0003
	RC58	0	0	0
	DU145	0	0	0
	LNCAP	0	0	0
	PC3	32.90 ± 0.41	2.91 ± 0.73	1071.46 ± 0.0002

Note: Abbreviations: NIM: Normalised index of methylation, SE: Standard error

5.5 GENE EXPRESSION ANALYSIS OF 7-GENE PANEL

Next, we quantified the expression of the 7-gene panel to examine whether promoter hypermethylation is having a functional effect on silencing apoptotic genes in prostate cancer. Gene expression levels were studied in our panel of prostate cancer cell lines and in 5aza2'deoxycytidine treated PC3 cells by QRT-PCR using the comparative C_T method. The amount of target cDNA,

normalised to an endogenous control (*PGK1)* and relative to a calibrator (normal prostate cell line RWPE1) was determined.

5.5.1 Validation of *TMS1* and *CDKN2A* gene expression assays.

All assays were inventoried TaqMan gene expression assays, with exception of *TMS1* and *CDKN2A*, both of which required in house design of primers and probes (described in section 2.6.2). The optimal primer and probe concentrations for each gene were determined (Appendix A4.1.9 and A4.1.10). The efficiencies of non-inventoried assays were defined prior to analysis of gene expression by real-time PCR in a ΔΔCt validation experiment and efficiency test (described in Appendix 4.2.1 and 4.2.2). Once the efficiencies are determined, there is an option to manually adjust the efficiency of a particular target in the ABI 7500 software during design of experiment.

5.5.2 Gene expression analysis in prostate cancer cells

In order to investigate the potential role of methylation in splice variation in the gene *cFLIP*, the expression of both the long and the short isoforms in each prostate cell line were measured and compared to normal cell line RWPE1. Both long (L) and short (S) *cFLIP* isoforms are downregulated in LNCAP and PC3 cells and up-regulated in DU145. In contrast, *cFLIPS* is almost 10 fold up-regulated in RC58 cells (Figure 5.5). These results suggest differential expression of *cFLIP* isoforms in different prostate cancer cell lines.

BNIP3 expression was reduced in all cell lines compared to RWPE1. Both 22RV1 and PC3 cell lines showed the greatest decrease in *BNIP3* expression. Results for *BIK* showed a twofold decrease in gene expression in the androgen independent PC3 cell line and this loss of expression was significantly upregulated (P=0.001, 2 sample T test) by treatment of the PC3 cells with a methylation inhibitor (5aza2'deoxycytidine). Both *TMS1* and *CDKN2A* showed an overall decrease in gene expression in all prostate cancer cell lines examined when compared to RWPE1. A significant up regulation of both *TMS1* and *CDKN2A* gene expression was observed in PC3 cells treated with a methylation inhibitor (P=0.002 and P=0.001, respectively, 2 sample T test) (Figure 5.5 & all statistical analysis is presented in Appendix 5).

Gene expression analysis for *DCR1* showed a decrease in gene expression in all cell lines tested except RC58 and LNCAP. A 0.75 fold upregulation in *DCR1* expression was observed in the methylation inhibitor treated PC3 cells, but this expression change failed to reach significance with a p-value of 0.055. In contrast, *DCR2* showed approximately a four-fold downregulation in PC3 cells ($P<0.0001$) and a smaller decrease (1 fold downregulation) in expression in 22RV1 cells ($P<0.0001$). Strikingly, treatment of PC3 cell with 5aza2'deoxycytidine significantly increased gene expression of *DCR2* approximately three fold ($p<0.0001$).

A comparison between methylation status of all cell lines defined by QMSP analysis and gene expression is illustrated in Figure 5.5, whereby a decrease in gene expression can be identified for a corresponding increase in methylation levels in a particular cell line.

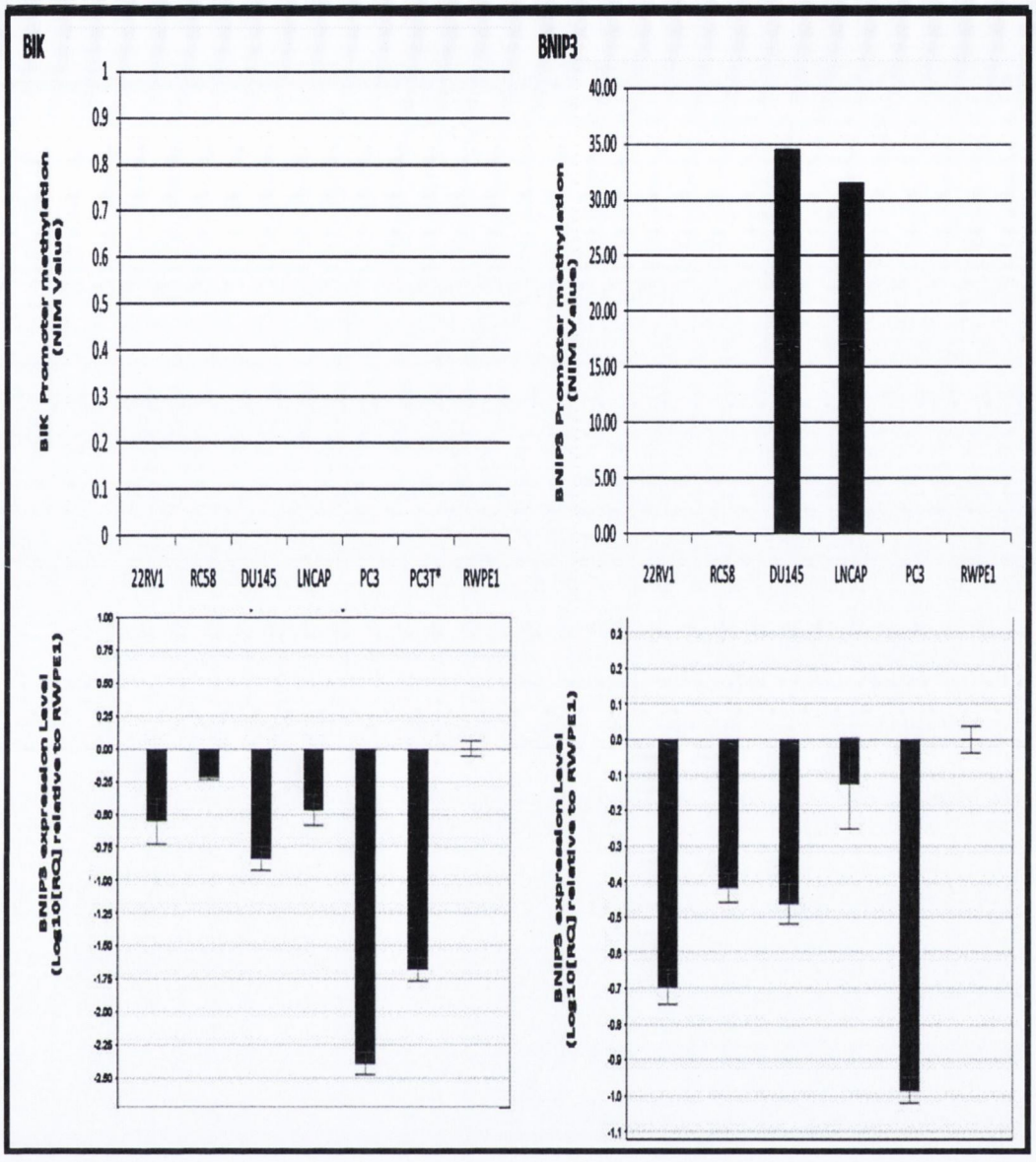

Figure 5.5.

Comparison of promoter methylation and gene expression. (A) Gene promoter methylation status as determined by QMSP for each gene and each cell line tested. The methylation levels are calculated using the normalised index of methylation (NIM). NIM score (vertical axis) is plotted against cell line (horizontal axis). A high NIM score represents a high quantity of methylation in that cell line. (B) Fold changes in gene expression are illustrated for each gene tested in each cell line relative to normal prostate cell line RWPE1. Log10 [RQ] values (Vertical axis) are plotted against Cell lines. A low Log10 [RQ] value represents a decrease in gene expression compared to RWPE1. Methylation levels for our 7-gene panel can be viewed and evidence of a corresponding decrease in gene expression assessed in each cell line. The expression level of genes with evidence of methylation in PC3 cells was also determined in PC3 cells treated with methylation inhibitor 5aza2'deoxycytidine (PC3T).*Methylation levels were not determined for PC3T cells.

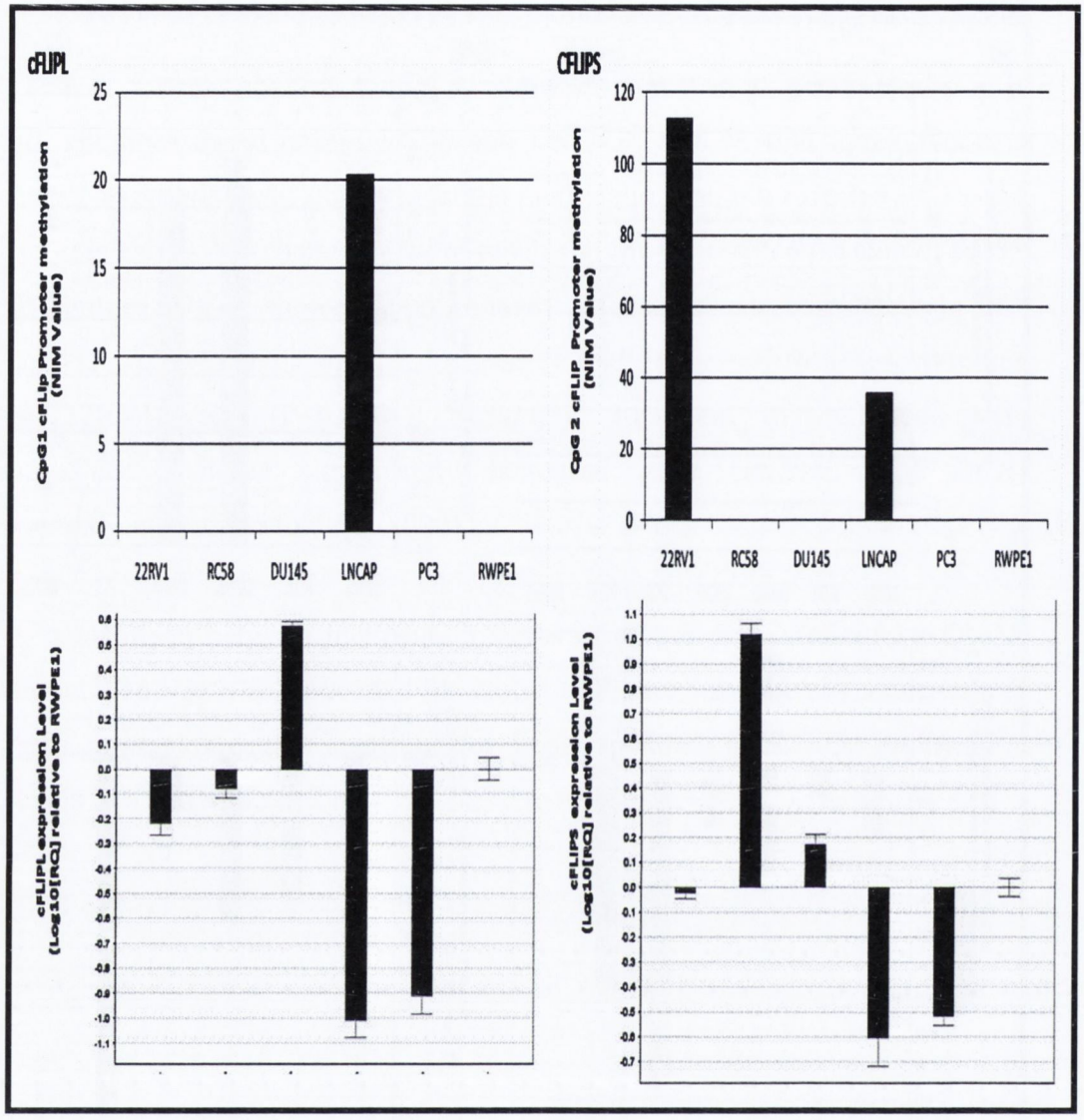

Figure 5.5.

Comparison of promoter methylation and gene expression. (A) Gene promoter methylation status as determined by QMSP for each gene and each cell line tested. The methylation levels are calculated using the normalised index of methylation (NIM). NIM score (vertical axis) is plotted against cell line (horizontal axis). A high NIM score represents a high quantity of methylation in that cell line. (B) Fold changes in gene expression are illustrated for each gene tested in each cell line relative to normal prostate cell line RWPE1. Log10 [RQ] values (Vertical axis) are plotted against Cell lines. A low Log10 [RQ] value represents a decrease in gene expression compared to RWPE1. Methylation levels for our 7-gene panel can be viewed and evidence of a corresponding decrease in gene expression assessed in each cell line. The expression level of genes with evidence of methylation in PC3 cells was also determined in PC3 cells treated with methylation inhibitor 5aza2'deoxycytidine (PC3T).*Methylation levels were not determined for PC3T cells.

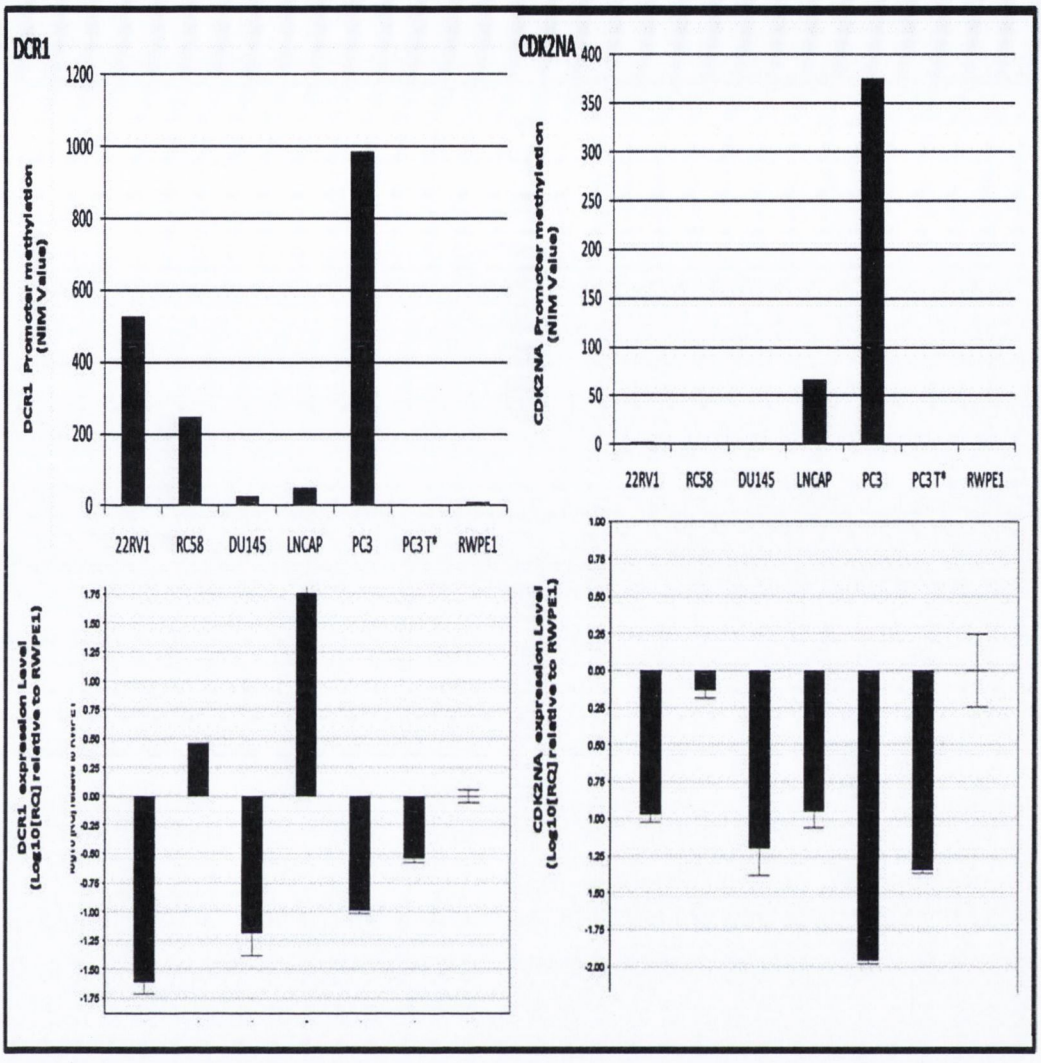

Figure 5.5 Contd.

Comparison of promoter methylation and gene expression. (A) Gene promoter methylation status as determined by QMSP for each gene and each cell line tested. The methylation levels are calculated using the normalised index of methylation (NIM). NIM score (vertical axis) is plotted against cell line (horizontal axis). A high NIM score represents a high quantity of methylation in that cell line. (B) Fold changes in gene expression are illustrated for each gene tested in each cell line relative to normal prostate cell line RWPE1. Log10 [RQ] values (Vertical axis) are plotted against Cell lines. A low Log10 [RQ] value represents a decrease in gene expression compared to RWPE1. Methylation levels for our 7-gene panel can be viewed and evidence of a corresponding decrease in gene expression assessed in each cell line. The expression level of genes with evidence of methylation in PC3 cells was also determined in PC3 cells treated with methylation inhibitor 5aza2'deoxycytidine (PC3T).*Methylation levels were not determined for PC3T cells.

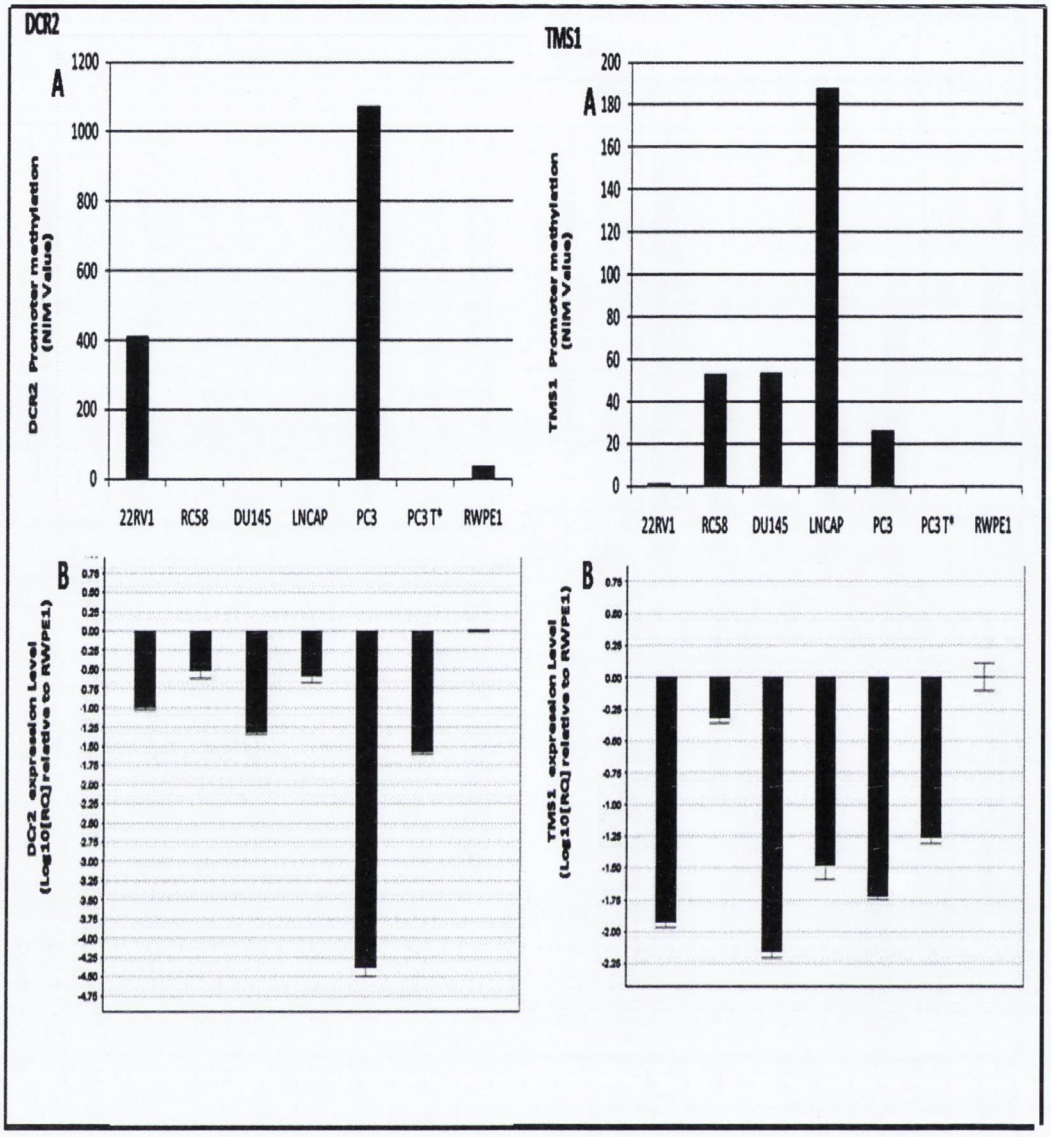

Figure 5.5 Contd.

Comparison of promoter methylation and gene expression. (A) Gene promoter methylation status as determined by QMSP for each gene and each cell line tested. The methylation levels are calculated using the normalised index of methylation (NIM). NIM score (vertical axis) is plotted against cell line (horizontal axis). A high NIM score represents a high quantity of methylation in that cell line. (B) Fold changes in gene expression are illustrated for each gene tested in each cell line relative to normal prostate cell line RWPE1. Log10 [RQ] values (Vertical axis) are plotted against Cell lines. A low Log10 [RQ] value represents a decrease in gene expression compared to RWPE1. Methylation levels for our 7-gene panel can be viewed and evidence of a corresponding decrease in gene expression assessed in each cell line. The expression level of genes with evidence of methylation in PC3 cells was also determined in PC3 cells treated with methylation inhibitor 5aza2'deoxycytidine (PC3T).*Methylation levels were not determined for PC3T cells.

5.6 DISCUSSION

In this chapter, we quantified methylation levels of a 7-gene panel, identified in chapter 4, in prostate cancer cells representing different stages of the disease. The expression levels for each gene were also examined in all cell lines and in PC3 cells treated with a methylation inhibitor.

A detailed map of the promoter CpG regions under investigation was created, which allowed QMSP assays to be designed to encompass CG sites within regions of biological significance. DHPLC analysis of *BIK* revealed partial methylation in androgen independent cell line PC3, however this was not detected by QMSP. *BIK* shows a 2-fold decrease in gene expression in PC3 cells compared with RWPE1 and a significant increase (P=0.001) in gene expression is observed in PC3 cells treated with a methylation inhibitor (5aza2'deoxycytidine). Taken together, these results suggest that low level partial methylation at certain CG sites within the promoter CpG island of *BIK* is sufficient to cause transcriptional silencing of the gene. Sequencing of the *BIK* promoter CpG island is required to identify the methylated CG sites associated with its transcriptional silencing in PC3 cells. Unfortunately, using current cloning and bisulfite sequencing methods, we were unable to successfully sequence the gene. An alternative method known as pyrosequencing is currently under investigation in the laboratory.

BNIP3

QMSP results for *BNIP3* illustrated methylation at a single CG dinucleotide present in a HRE site in both LNCaP and DU145 cell lines, both of which showed evidence of methylation in our DHPLC screen. In contrast, methylation in 22RV1 cells was not detected, despite evidence of promoter methylation from our DHPLC results. However as discussed previously, the QMSP assay designed to encompass the HRE site is downstream of the *BNIP3* promoter CpG region screened using DHPLC.

Our gene expression analysis illustrated a corresponding decrease in *BNIP3* expression in DU145, LNCAP and 22RV1 cells. *BNIP3* is induced by hypoxia and increased levels of HIF-1α (an important transcription factor), and is

important for apoptosis induction in response to prolonged oxygen deprivation (Bruick, 2000). Many solid tumours, including prostate cancer, contain regions of hypoxia, however these cells survive and continue to grow (Semenza, 1999). Here, we hypothesis that promoter hypermethylation of *BNIP3* and in particular the HRE site, may prevent upregulation of *BNIP3* in response to hypoxia, hence conferring a survival advantage to cancer cells by evading hypoxia induced apoptosis. Investigating the levels of *BNIP3* expression in our panel of prostate cell lines under hypoxic conditions and assessing how the methylation status of HRE element effects hypoxia induced *BNIP3* expression may help elucidate the role of promoter hypermethylation and aberrant hypoxia induced cell death. *BNIP3* expression was also downregulated in PC3 and RC58 cells compared to the normal prostate cell line RWPE1, suggesting methylation may not be the only mechanism of *BNIP3* downregulation in prostate cancer.

CDKN2A

QMSP results for *CDKN2A* were consistent with our DHPLC results, showing methylation in 22RV1, PC3 and LNCaP cell lines. Bisulfite sequencing revealed high levels of methylation in the PC3 cell line at transcriptional elements, which is consistent with the dramatic loss of *CDKN2A* expression observed. PC3 cells treated with the methylation inhibitor showed a striking 3-fold increase in *CDKN2A* expression, suggesting a major role of DNA promoter hypermethylation induced gene silencing in the prostate cancer cell line PC3 and perhaps to a lesser extent in LNCAP cells.

cFLIP

To investigate the role of methylation in splice variation of *cFLIP*, we determined the expression of both *cFLIP* variants using QRT-PCR. Both splice variants show the greatest decrease in expression in LNCAP cells compared to RWPE1, which is consistent with partial methylation observed in the promoter CpG of *cFLIP* in LNCAP cells. In contrast, the methylation status of 22RV1 cells does not support our gene expression findings, suggesting DNA methylation may not play a major role in *cFLIP* splice variation in prostate cancer. However, the second CpG island of *cFLIP* contained no predicted

transcription factors or promoter elements and hence methylation at this region may not affect transcription of the *cFLIP* gene. It is interesting to speculate that within this methylated region of the CpG island, regulatory elements (such as miRNAs and/or enhancers) may reside, which could indirectly affect the regulation of other genes. Of interest, expression analysis showed differential expression of the splice variants in various prostate cancer cell lines. Relatively higher levels of *cFLIPL* are observed in DU145 cells with a decrease in expression seen in LNCAP and PC3 cells. In contrast, *cFLIPS* is upregulated in RC58 cells and again downregulated in LNCAP and PC3 cells. These findings provide the impetus for further studies to address the role of differential expression of *cFLIP* splice variants and their role in prostate cancer.

DCR1 and DCR2

Our results illustrate that *DCR1* is methylated in all prostate cancer cell lines and *DCR2* in 22RV1 and PC3 cells. QMSP analysis showed a significantly greater level of *DCR1* methylation in PC3 and 22RV1 cell lines compared to other prostate cancer cell lines. Furthermore loss of both *DCR1* and *DCR2* gene expression was observed in 22RV1 and PC3 cells, which was partially rescued by pharmacological demethylation. Taken together, our findings agree with the literature on a putative role for *DCR1/DCR2* hypermethylation in prostate cancer development.

TMS1

The QMSP assay for *TMS1* encompassed a number of important transcription factor binding sites, UCE.1, T-Ag and Sp1, all of which are important for regulation of gene expression. QMSP analysis suggests therefore that *TMS1* promoter methylation may be associated with transcriptional silencing. Furthermore, a corresponding decrease in *TMS1* gene expression was observed in all prostate cancer cell lines compared to normal and unmethylated cell line RWPE1. It is interesting to note that *TMS1* and *DCR1* were the only genes we examined that were methylated in all prostate cancer cell lines, suggesting they may have a pivotal role in different stages of prostate carcinogenesis.

To the best of our knowledge, concordance between DHPLC methylation analysis and QMSP has not been previously investigated. Our data indicated that methylation status assessed by both techniques were largely in agreement, with the exception of *BIK*. The greatest advantage of DHPLC is that it provides a snapshot of the methylation status of the entire PCR amplified sequence. In the case of *BIK,* the DHPLC assay spans 551bp encompassing 60 CpG sites, whereas the QMSP assay targets 9 specific CpG sites (within the primer/probe hybridisation sites). Thus, it is quite possible that the discrepancy in DHPLC/QMSP results for *BIK* is due to methylation at specific CpG sites not contained within the QMSP oligonucleotides. Furthermore, QMSP will only amplify sequences that are 100% methylated at all of the CpG sites within the primer/probe binding sites, in accordance with the chemistry of this technology (12). This serves to highlight the usefulness and sensitivity of DHPLC as a methylation screening platform, for its ability to detect varying degrees of methylation (i.e. partial methylation) across a large number of CpG sites.

In this study, only PC3 cells were treated with a methylation inhibitor, due to time constraints. Treatment of LNCaP and 22RV1 cell with a methylation inhibitor would help further elucidate the role of DNA methylation and aberrant gene expression in the remaining genes, *cFLIP* and *BNIP3*, neither of which were methylated in PC3 cells. It is important to note, that in some cases, promoter hypermethylation alone is not sufficient for transcriptional silencing. Histone methylation at distinct residues such as H3K9, H3K27 and H4K20 can also have repressive effects on gene expression (Klose and Zhang, 2007). Histone deacetylase (HDAC) inhibitors have been used synergistically with demethylating agents to activate expression of methylated genes (Cameron et al., 1999). Studies suggest that this combined drug administration is more potent than either DMNT inhibitors or HDAC inhibitors alone (Teodoridis et al., 2004a). For example, co-treatment of androgen receptor-negative cell line DU145 with 5-azacytidine (5-aza-CR) and histone deacetylase (HDAC) inhibitor Trichostatin A is most effective in restoring functional expression of the *AR* gene and its downstream targets, compared with either agent alone (Jarrard et al., 1997; Nakayama et al., 2000).

In summary, our apoptotic methylation profile of prostate cancer cell lines has identified a panel of apoptotic genes (*cFLIP*, *BIK*, *BNIP3*, *TMS1*, *DCR1*, *DCR2* and *CDK2NA*) showing aberrant DNA methylation and in some cases concurrent downregulation in gene expression. Three of the genes (*TMS1*, *DCR1* and *DCR2*) identified in our study, have previously shown utility as potential new biomarkers of risk prediction in prostate cancer (Suzuki et al., 2006). *CDKN2A* has previously been identified as aberrantly methylated in prostate cancer but it's utility as a biomarker has yet to be examined, while for the remaining three genes (*cFLIP*, *BIK*, and *BNIP3),* the data presented here is novel, indicating for the first time the potential involvement of methylation of these genes in prostate cancer. Using these pre-optimised QMSP assays, this seven gene panel can be rigorously evaluated for its potential as a biomarker for specific detection of prostate cancer.

CHAPTER 6

INVESTIGATING THE METHYLATION STATUS OF A PANEL OF SEVEN APOPTOTIC-RELATED GENES IN PROSTATE CANCER TISSUE SAMPLES.

6.1 INTRODUCTION

In the previous chapters, we identified a 7-gene apoptotic panel (*cFLIP*, *BIK, BNIP3, TMS1, CDKN2A* and *DCR1/2)* with evidence of aberrant methylation in a number of prostate cancer cell lines, representing different stages of disease progression (Chapter 4 and 5). In accordance with our methylation data, expression of these genes was also reduced in multiple cell lines. Furthermore, treatment of PC3 cells with the methylation inhibitor, 5aza2'deoxycytidine, causes a moderate to strong increase in expression in *BIK, TMS1, CDKN2A* and *DCR1/2*. Thus, we propose that DNA hypermethylation of these genes could be an "apoptotic methylation signature" of prostate cancer.

To verify that methylation of these genes occurs in primary tumours and is not a phenomenon limited to cultured cells, we evaluated a panel of prostate tissue, representing, prostate cancer (n=50), histologically benign prostate (n=43), High-Grade Prostatic Intraepithelial Neoplasia (HGPIN: n=17) and Benign Prostate Hyperplasia (BPH: n=35). Normal tissue adjacent to prostate cancer was included in this study to examine the difference in methylation frequency and levels between normal and tumour prostate tissue and to assess the effect of age-related DNA methylation in normal tissue adjacent to tumour, a phenomenon reported for certain genes such as lysl oxidase (*LOX*), runt-related transcription factor 3 (*RUNX3*) and tazarotene induced gene 1 (*TIM1*) in non-neoplastic epithelial cells (So et al., 2006). HGPIN is a precursor lesion to many intermediate to high grade prostate carcinomas. Hence, inclusion of HGPIN tissue samples (N=17) is necessary to elucidate the role of DNA methylation in early stages of prostate cancer development and progression. In addition, BPH (N=35) samples were included to compare methylation frequencies and levels in prostate cancer to this benign disease of the prostate. Moreover, BPH serves as a very useful control population because it involved proliferation of the stromal and epithelial cells, which rarely progress to malignancy.

Previously optimised QMSP assays were chosen to evaluate the frequency and quantitative level of methylation at each promoter CpG island of the 7-gene

panel in all tissue groups, in order to generate an "apoptotic methylation signature". Methylation differences between each tissue group and correlations with various clinicopathological features were determined utilising multiple statistical tests. Finally, correlation between methylation in this panel of apoptotic genes and *GSTP1*, the most frequently methylated gene in prostate cancer (Jeronimo et al., 2004a), was also examined.

6.2 CLINICAL AND PATHOLOGICAL FEATURES OF STUDY POPULATION

Fifty prostate cancer tissue samples were used in this study (Figure 6.1). The cohort consisted of 33 tumours, sourced through the prostate cancer research consortium (PCRC) and reviewed by pathology registrar Dr. Ciara Barrett and 17 tumours available from the Adelaide and Meath Hospital incorporating the Children's Hospital (AMNCH), a cohort of patients previously collected by Dr. Antoinette Perry in the laboratory. The majority of samples were Gleason score 6 or 7 (n=46), TNM stage T2 (n=33) and from patients with a PSA level >4ng/ml (n=40) (Table 6.1). Due to the small number of individual Gleason scores for patients samples, Gleason scores were divided into two groups, moderately differentiated (Gleason score $\leq$ 6) and poorly differentiated (Gleason score $\geq$7). Moreover, a major prognostic shift is documented between Gleason score 6 and 7 (DeMarzo et al., 2003). To obtain approximately equal numbers in each group, PSA levels were divided into two groups a "low PSA" level ($\leq$8ng/ml) and "high PSA" level (>8ng/ml) for examination of correlations between methylation status of genes and PSA levels. Furthermore, these subgroups of PSA levels have been utilised in studies correlating methylation frequencies of genes with clinicopathological features (Maruyama et al., 2002; Suzuki et al., 2006).

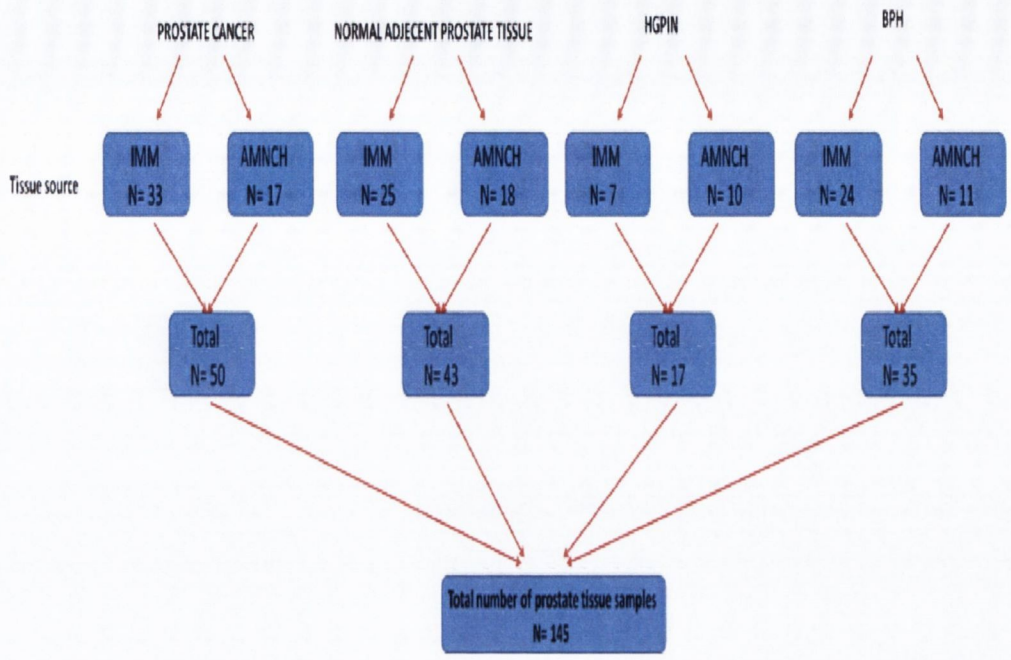

Figure 6.1.

Prostate tissue samples. A workflow and breakdown of the different prostate tissue samples used in the study (Prostate cancer, histologically normal adjecent prostate tissue, HGPIN and BPH). All tissues were sourced from the Institute of molecular medicine, St. James hospital (IMM) or The Adelaide and Meath National Children's Hospital, Tallaght (AMNCH).

Table 6.1. Characteristics of AMNCH & IMM prostate cancer groups

	AMNCH	IMM	Combined Total
Prostate cancer samples,n	17	33	50
Mean age (yrs)	58.35	59.94	59.4
Range	49-69	44-69	44-69
Mean PSA (ng/ml)	6.7	9.2	8.26
Range	2.2-12	3.1-17	2.2- 17
<4ng/ml	4	1	5
4-8ng/ml	8	10	18
>8ng/ml	5	17	22
Gleason score			
5 (3+2 or 2+3)	0	2	2
6 (3+3)	9	4	13
7 (4+3 or 3+4)	8	25	33
8 (4+4)	0	2	2
9 (5+4 or 4+5)	0	0	0
TNM classification			
pT1c	0	1	1
pT2a	0	3	3
pT2b	11	0	11
pT2c	2	17	19
pT3a	3	5	8
pT3b	1	3	4
pT3c	0	0	0

A cohort of 43 histologically normal prostate tissue samples and 17 HGPIN foci were also included in this study. All histologically normal and HGPIN samples were sourced from patients with a concurrent tumour diagnosis. In the case of 10 normal and 10 HGPIN samples however, the corresponding tumour sample was not included, due to removal of several tumour samples from our analysis as described previously. In addition, 35 patients with a diagnosis of BPH were included in our analysis. Due to early diagnosis of prostate cancer as a consequence of increased PSA screening, the mean average age of the prostate cancer cohort was significantly lower than the BPH cohort ($P = 0.024$, $CI = (-7.88, -0.57)$, unpaired two sample T test). Pre-operative PSA levels were not significantly different for the two cohorts ($P < 0.883$, $CI= (-2.44, 2.11)$, unpaired two sample T test). Data is summarised in Table 6.2 and a

comprehensive table of individual patient data and statistical analysis is presented in Appendix 6 and 5, respectively.

Table 6.2. Summary data for patient groups

	Prostate Cancer	HGPIN	Normal Prostate	BPH
Sample, n	50	17	43	35
Mean Age (yrs)	59.4	63.14	59	63.79
Range	44-69	56-70	44-74	44-87
Mean PSA (ng/ml)	8.26	8.34	9.18	7.98
Range	2.2- 17	0.7-14	0.7-13.6	0.7-21
Gleason score				
≤6	15			
≥7	35			
TNM classification				
pT1	1			
pT2	33			
pT3	12			

6.3 METHYLATION STATUS IN PROSTATE TISSUE SAMPLES

Previously optimised QMSP assays used to calculate the methylation levels in prostate cancer cell lines (discussed in chapter 5) were also employed to quantify the methylation levels of a 7-gene apoptotic panel in a cohort of prostate tissue samples (n=145, representing prostate cancer (n = 50), HGPIN (n = 17), normal adjacent prostate (n = 43) and BPH (n=35) prostate tissue samples). A relative methylation score (RMS) was calculated for each sample by normalising the amount of target to the amount of bisulfite modified DNA in the sample. This scoring method has been utilised in a number of studies (Jeronimo et al., 2004b; Perry et al., 2007).

Samples were considered positively amplified when a C_T <50 was detected in at least two of the replicates. A number of problems were encountered with our *CDKN2A* and *DCR1* TaqMan assays. The efficiency of these assays varied and amplification failed on our first tissue sample plate. The assays were both repeated once but unfortunately due to the limited quantity and precious nature of the tissue samples, the assays could not be successfully analysed on plate one. In addition, the initial screening of the 2 QMSP *cFLIP* assays illustrated no evidence of methylation in any prostate tissue samples, consequently these

assays were not examined on the second plate, in order to retain tissue samples for those with evidence of methylation on the first plate. A list of all slopes and R^2 values for standard curves generated for each gene on both plates is presented in Table 6.3.

Table 6.3. Slope and correlation co-efficient of standard curves

Gene		Plate 1	Plate 2
ACTB	*Slope*	-3.67	-2.93
	R^2	0.995	0.96
BIK	*Slope*	-3.59	-5.14
	R^2	0.954	0.99
BNIP3	*Slope*	-4.41	-3.17
	R^2	0.94	0.91
CDKN2A	*Slope*	NA	-2.93
	R^2	NA	0.9
CpG1 cFLIP	*Slope*	-3.43	NA
	R^2	0.97	NA
CpG 2 cFLIP	*Slope*	-3.06	NA
	R^2	0.97	NA
DCR1	*Slope*	NA	-3.43
	R^2	NA	0.94
DCR2	*Slope*	-3.46	-3.03
	R^2	0.92	0.94
TMS1	*Slope*	-3.41	-2.94
	R^2	0.99	0.75

R^2 = *C*orrelation Co-efficient. NA = Not applicable, plate failed.

6.3.1 Methylation frequency of a 7-gene apoptotic panel.

The methylation frequency for all seven genes is illustrated in Table 6.4 and Figure 6.2. Hypermethylation of *BIK* and both CpG island assays of *cFLIP* was not detected in any tumour samples examined (0/50) and (0/22), respectively,

thus results are considered for our remaining 5–gene panel (*BNIP3, CDKN2A, DCR1, DCR2* and *TMS1).*

BNIP3

BNIP3 hypermethylation was detected in 8/50 (16%) of tumour samples and 0% of normal tissue adjacent to prostate cancer, HGPIN and BPH. The difference in methylation frequency between tumour and both normal and BPH tissue groups was statistically significant (P=0.007 (Normal), P=0.02 (BPH); Fisher's exact test). Differences in methylation frequency between tumour and HGPIN failed to reach significance, which may be due to the small HGPIN sample size.

CDKN2A

DNA hypermethylation of *CDKN2A* was detected in 8/29 (27.59%) of tumour samples and 0/28 (0%), 1/13 (6.67%), 2/16 (9.52%) of normal, HGPIN and BPH samples, respectively. 7/17 HGPIN samples had an adjacent tumour sample included in the current study. The HGPIN sample with evidence of *CDKN2A* methylation was also methylated in the adjacent tumour sample. A statistically significant difference in methylation frequency was observed between tumour tissue group and the normal prostate tissue group (P=0.004, Fisher's exact test).

DCR1 and *DCR2*

The methylation frequency of *DCR1* and *DCR2* in tumour samples was 11/29 (37.93%) and 19/50 (38%), respectively. No methylation was detected in the remaining tissue groups for both genes, with the exception of BPH in the case of *DCR2* 2/35 (5.88%). The difference in methylation frequencies between tumour and normal prostate tissue was statistically significant for both *DCR1* and *DCR2* (P<0.0001 and P<0.0001, respectively; Fisher's exact test). In fact, the difference in methylation frequencies between tumour and HGPIN/BPH were also statistically significant for both genes (P=0.009 (*DCR1*), P=0.001 (*DCR2*) and P=0.004, P<0.0001, respectively; Fisher's exact test).

TMS1

TMS1 methylation was detected in 22/50 (44%) of prostate cancer samples and was completely unmethylated in normal prostate tissue. Evidence of methylation was present in both HGPIN and BPH tissue samples 2/17 (11.76%) and 2/35 (2.94%), respectively. One of the 2 HGPIN samples with evidence of *TMS1* methylation had concurrent methylation information on its adjacent tumour, this tumour sample was also methylated. The difference in methylation frequency between tumour and all three tissue groups was statistically significant (P<0.0001 (Normal), P=0.020 (HGPIN), P<0.0001 (BPH); Fisher's exact test).

Approximately, 69% of tumour samples were methylated in at least one of our 5-gene panel (*BNIP3, CDKN2A, DCR1*, *DCR2* and *TMS1).*

All statistical tests are presented in Appendix 5. In addition, methylation levels for *GSTP1* were also determined on the tissue cohort used in this study by Dr. Antoinette Perry in the Laboratory. Combination of this 5-gene panel with *GSTP1* increased the frequency of methylation detected in prostate cancer to 89.4% compared to 80.5% if *GSTP1* was used alone (P=0.259).

Table 6.4. Methylation frequency of a 7-gene apoptotic gene panel in prostate cancer, normal prostate, HGPIN and BPH

	BIK n (%)	BNIP3 n (%)	CDKN2A n (%)	CpG1 cFLIP n (%)	CpG2 cFLIP n (%)	DCR1 n (%)	DCR2 n (%)	TMS1 n (%)
Prostate Cancer	(0/50) 0	(8/50) 16	(8/29) 27.59	(0/22) 0	(0/22) 0	11/29) 37.931	(19/50) 38	(22/50) 44
Normal	(0/43) 0	(0/43) 0	(0/28) 0	(0/24) 0	(0/24) 0	(0/28) 0	(0/43) 0	(0/43) 0
HGPIN	(0/17) 0	(0/17) 0	(1/13) 7.69	(0/11) 0	(0/11) 0	(0/13) 0	(0/17) 0	(2/17) 11.76
BPH	(0/35) 0	(0/35) 0	(2/16) 9.52	(0/13) 0	(0/13) 0	(0/16) 0	(2/35) 5.88	(2/35) 2.94

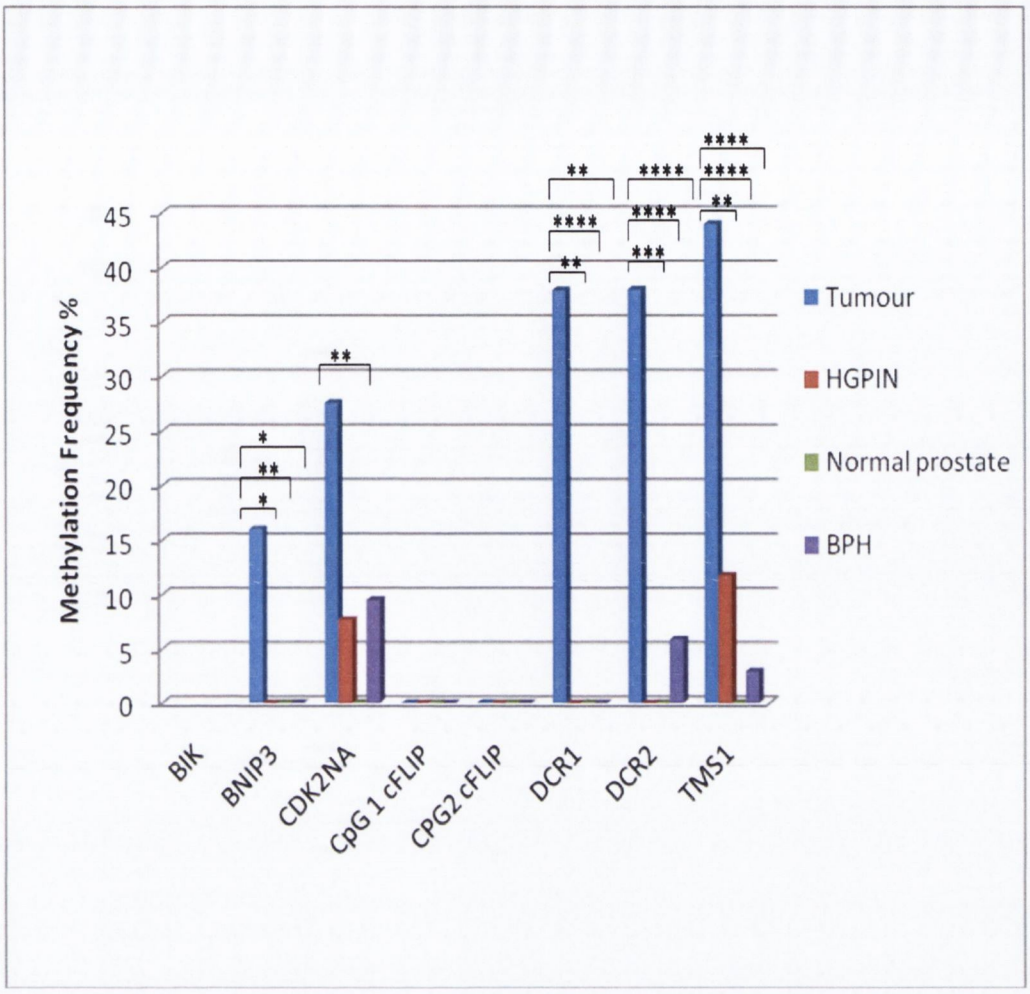

Figure 6.2

Methylation frequencies for 7-gene panel in prostate cancer, HGPIN, Normal adjacent prostate and BPH, illustrated in this order. Methylation was not detected in our 7-gene panel in all normal adjacent prostate tissue samples. Significance levels for differences between prostate cancer and HGPIN, Normal adjacent prostate and BPH are illustrated, respectively. Significance levels are indicated by P<0.1 = *, P<0.05 = **, P<0.001 = ***, P<0.001 = ****. For significance levels not shown between tissue groups the significance level was P>0.1.

6.3.2 Methylation levels in prostate cancer

The quantitative methylation levels for genes with evidence of methylation (*BNIP3, CDKN2A, DCR1, DCR2* and *TMS1*) were also compared between the different tissue sample groups. A comprehensive list of RMS scores is presented in Appendix 7. In the current study, the methylation scores (RMS)

for each gene was compared between different tissue groups using the Kruskal-Wallis test. For all genes, with the exception of *CDKN2A*, differences in RMS scores between tissue groups were statistically significant (all have a P value <0.0001). In addition, a Tukey pairwise multiple comparison test was performed to elucidate which groups are significantly different from one another. In the case of all genes, except *CDKN2A*, the difference between methylation levels in prostate cancer compared to normal and BPH is statistically significant, whereby their confidence interval does not contain zero (all statistical data is presented in Appendix 5). Methylation levels of *DCR2* in prostate cancer were also significantly different from HGPIN samples. No statistically significant differences of methylation levels between other groups were detected.

6.3.3 Correlation between methylation of genes

A methylation heat map of a 5-gene apoptotic panel (*BNIP3, CDKN2A, DCR1, DCR2* and *TMS1*) is illustrated in Figure 6.3. Methylation of both *TMS1* and *DCR2* was detected in significantly more tumours than methylation of *BNIP3* (P=0.004, P=0.023, respectively; Fisher's exact test). The frequency of *TMS1* methylation in tumour samples is higher than all other genes. However, this difference was not statistically significant (P value >0.05, Fisher's exact test, for all comparisons). Methylation frequencies obtained for *DCR1* and *DCR2* in prostate cancer were approximately equal (38%).

Interestingly, methylation of *BNIP3* correlated with methylation of the remaining 4 apoptotic genes, with 8/8 prostate cancer samples hypermethylated in *BNIP3* revealed concurrent hypermethylation in at least one other gene of the 5-gene panel. In addition, correlation between methylation of *DCR2* and *TMS1* was evident, whereby 14/19 tissue samples with evidence of *DCR2* methylation were also methylated in *TMS1*. The 9 prostate cancer samples methylated in *DCR1* also had evidence of methylation in *DCR2* (Figure 6.3). Of interest, 55% (16/29) of prostate cancer samples were methylated in either *DCR1* or *DCR2*.

As discussed previously, methylation levels for *GSTP1* were also determined on the tissue cohort used in this study. Correlation between our 5 gene panel

and *GSTP1*, the most frequently methylated gene in prostate cancer (Henrique and Jeronimo, 2004), was examined. Intriguingly, four prostate cancer samples (IMM0072T, IMM0084T, IMM0018T and IMM0025T) with evidence of methylation in all five apoptotic gene analysed were also methylated in *GSTP1*. Moreover, evidence suggests that two previously investigated genes by our group *IGFBP3* and *SFRP2* (Appendix 8) are also methylated in these four prostate cancer samples. Curiously, 9/46 tumour samples were unmethylated for *GSTP1*, 5 of which were also unmethylated for all apoptotic genes examined (Figure 6.4). Interestingly, 3 of these samples (IMM005, IMM009 and IMM0017) are also unmethylated in *IGFBP3* and *SFRP2* (Appendix 8).

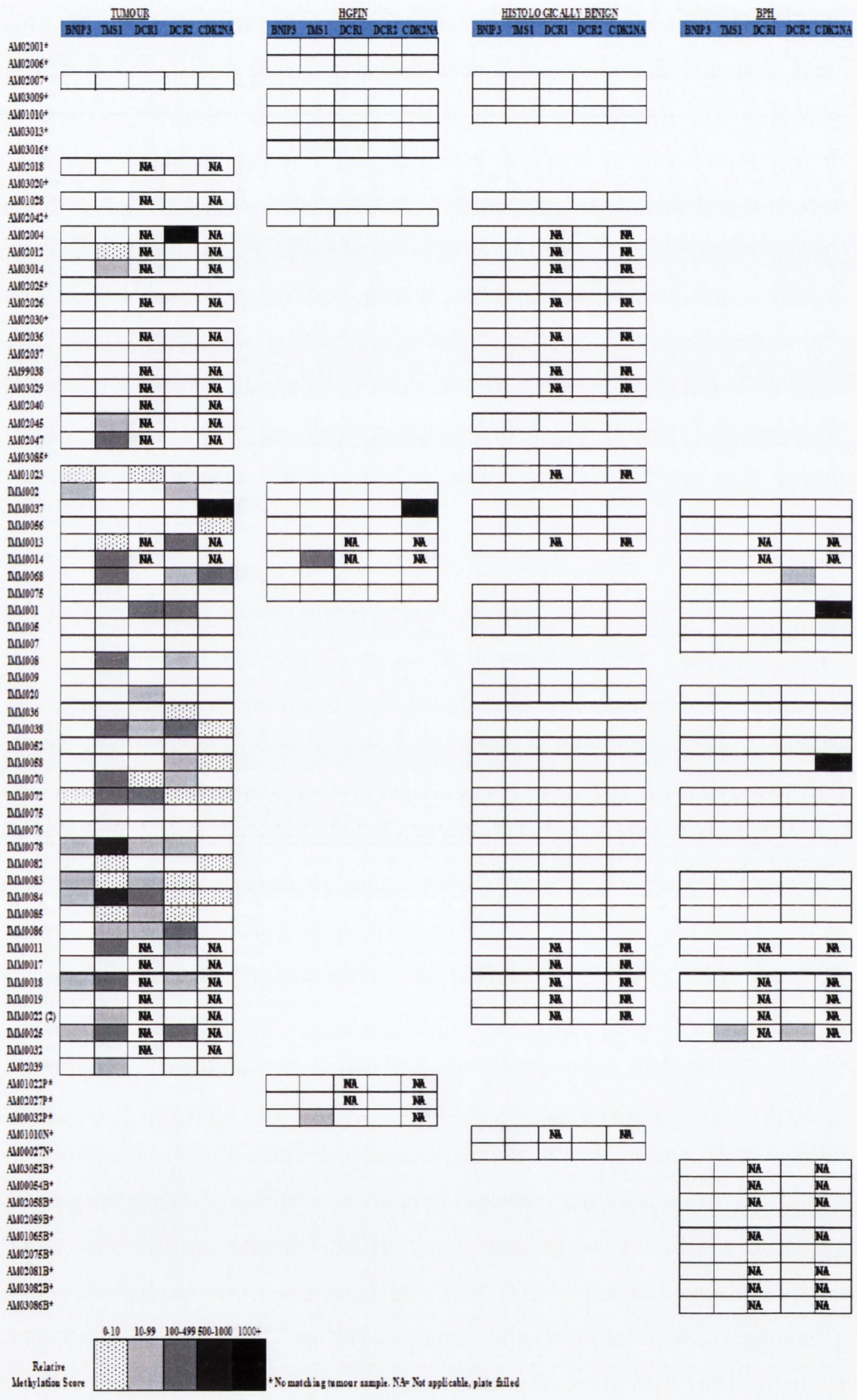

Figure 6.3

Methylation Heat map of 5-gene apoptotic panel in Tumour, HGPIN, Benign prostate and BPH.

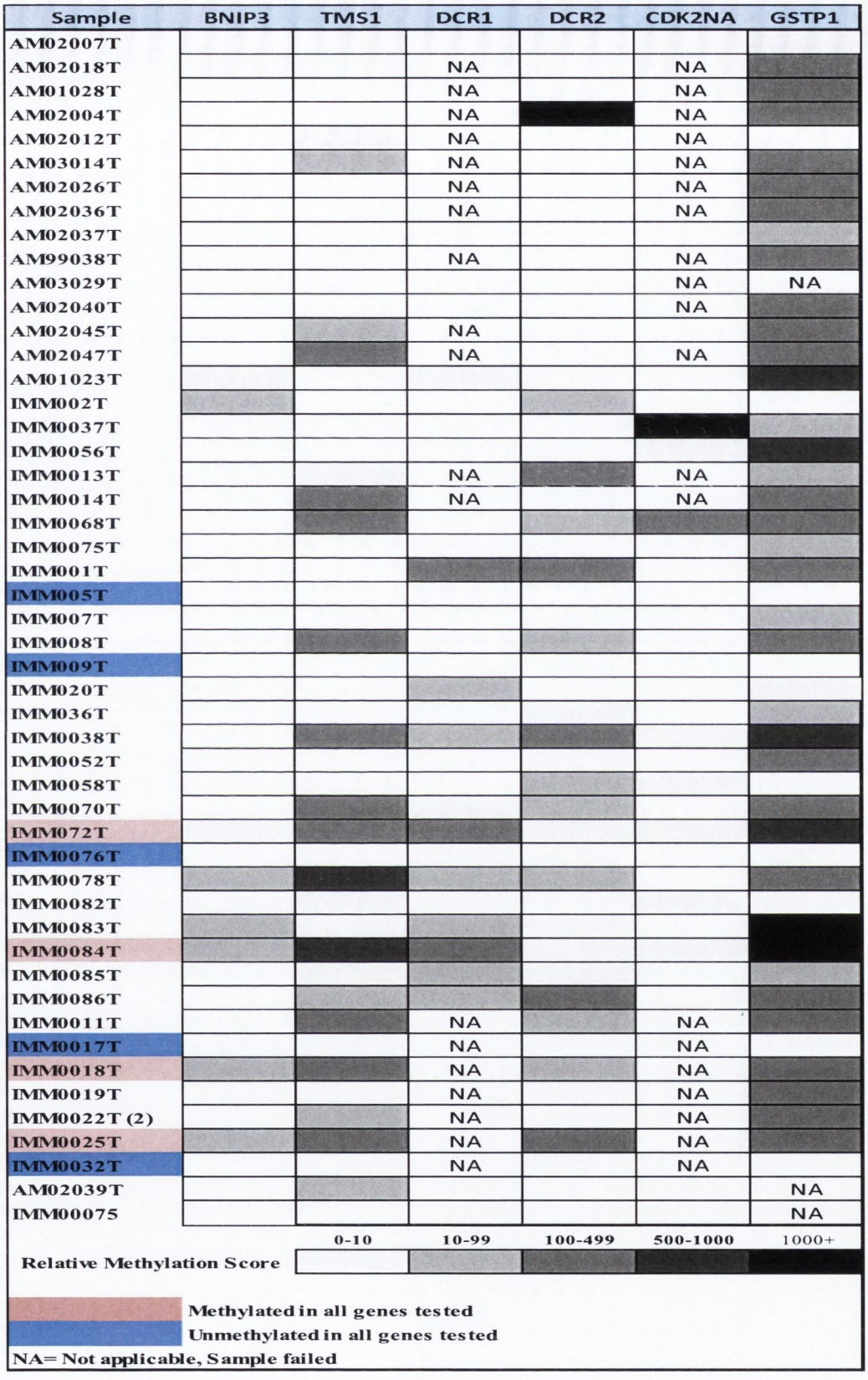

Figure 6.4

Methylation Heat Map of 5-gene apoptotic panel and *GSTP1* in prostate cancer. Tissue samples methylated in all genes analysed are highlighted in pink and samples unmethylated in all genes analysed are highlighted in blue.

6.3.4 Associations with clinicopathologic features

Results for associations between methylation status of our 5-gene panel and clinicopathological features of prostate cancer, including Gleason score, PSA levels and TNM stage are summarised in Table 6.5 and illustrated in Figure 6.5.

All genes, with the exception of *BNIP3,* were more frequently methylated in prostate cancer with a Gleason score ≥7 compared to tumours with a Gleason score ≤6 and TNM stage 2 compared to TNM stage 3. Unfortunately, these observations failed to reach statistical significance, which is likely a result of the small sample size used. All genes, with the exception of *DCR1*, were more frequently methylated in tumours with a high (>8ng/ml) PSA level than those with low (≤8ng/ml) PSA Level. The difference in PSA level was statistically significant for *TMS1* only (P= 0.01, CI (-0.65, -0.138); Fisher's exact test).

Finally, the methylation status of all 5 genes was investigated for correlations with clinicopathological factors (Table 6.5 and Figure 6.6). Upon analysis, 77.3% of prostate cancer samples with Gleason score ≥7 had at least one gene, from our 5-gene panel, methylated compared to only 42.8% of prostate cancer samples with a Gleason score of ≤6 methylated in at least one gene; unfortunately, due to the small number of samples with information on the methylation status of all 5 genes (n=29) statistical significance was not achieved. (P=0.158, Fisher's exact test). Similarly, 76.1% of these prostate cancer samples with TNM staging of 2 were methylated in at least one gene compared to 50% with a TNM staging of 3 (P=0.548, Fisher's exact test). No difference between PSA levels and methylation of our 5-gene panel was observed (P=1.000, Fisher's exact test).

Table 6.5. Summary of methylation status of 5-gene Panel and relationship to clinicopathologic factors

	BNIP3 n (%)	CDKN2A n (%)	DCR1 n (%)	DCR2 n (%)	TMS1 n (%)	All genes n (%)
Prostate Cancer Gleason Score	8/50 (16)	8/29 (27.59)	11/29 (37.93)	19/50 (38)	22/50 (44)	20/29 (68.97)
≤6	3/15 (20)	1/7 (14.29)	2/7 (28.57)	4/15 (26.67)	4/15 (26.67)	3/7 (42.86)
≥7	5/35 (14.29)	7/22 (31.81)	9/22 (40.9)	15/35 (42.86)	17/35 (48.57)	17/22 (77.27)
P	0.683	0.635	0.386	0.351	0.215	0.158
PSA (ng/ml)						
≤8	3/20 (15)	3/13 (23.07)	5/13 (38.46)	5/20 (25)	3/20 (15)	7/14 (50)
>8	4/24 (16.67)	3/11 (27.27)	2/11 (18.18)	10/24 (41.67)	13/24 (54.17)	6/11 (54.55)
P	1	1	0.386	0.342	0.01	1
TNM stage						
pT2	5/33 (15.15)	7/22 (31.82)	10/22 (45.45)	(12/33) 36.36	16/35 (45.71)	16/21 (76.19)
pT3	2/12 (16.67)	1/6 (16.67)	1/6 (16.67)	4/12 (33.33)	4/11 (36.36)	2/4 (50)
P	1	0.64	0.355	1	0.732	0.548

Abberviations: TNM= Tumour, Node and Metstases, PSA= Prostate Specific Antigen.

P= P value, statistical signifcance was set at P< 0.05.

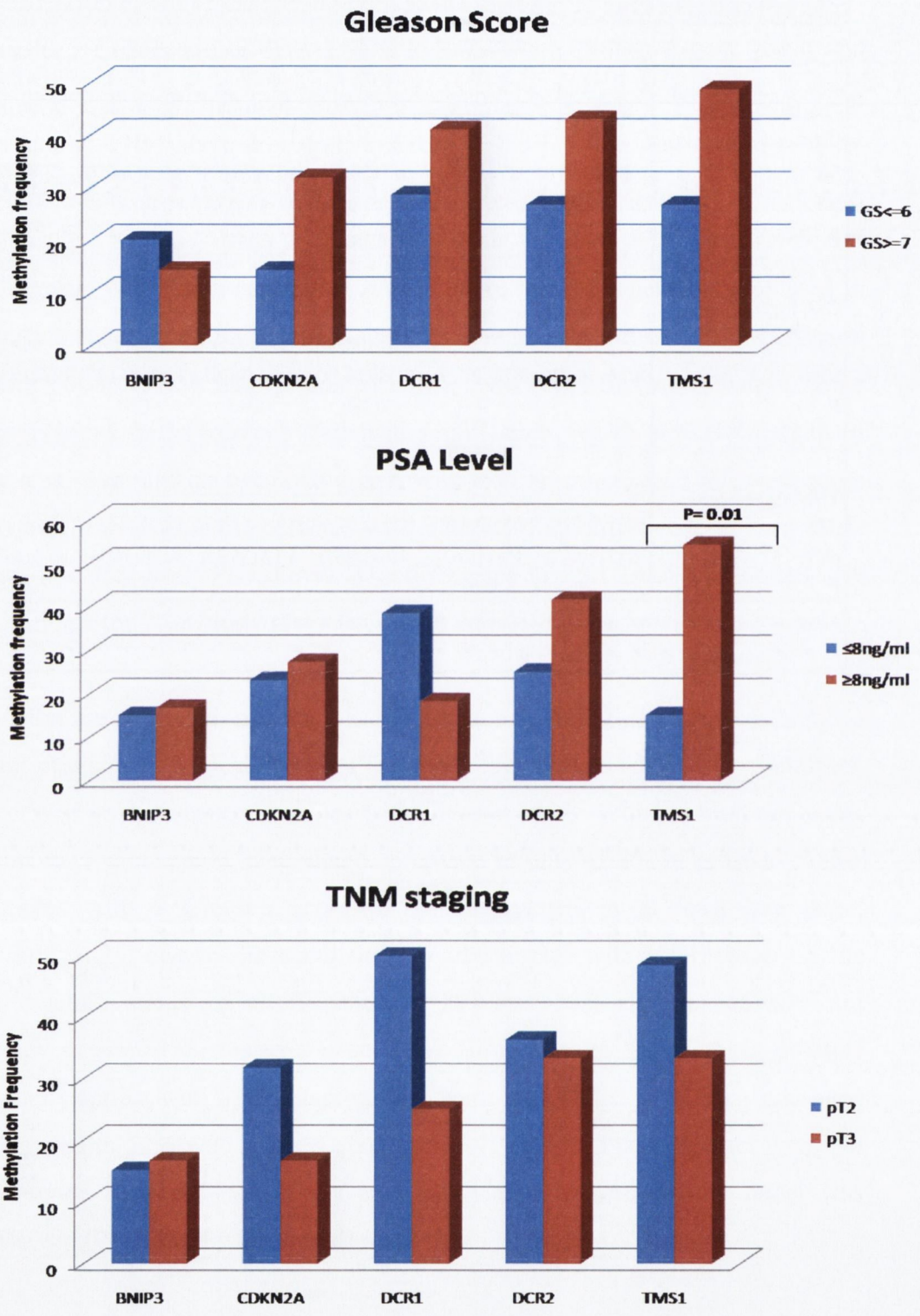

Figure 6.5

Correlation of promoter hypermethylation with clinicopathological features of prostate cancer. Correlation with A) Gleason score, B) TNM stage and C) PSA level.

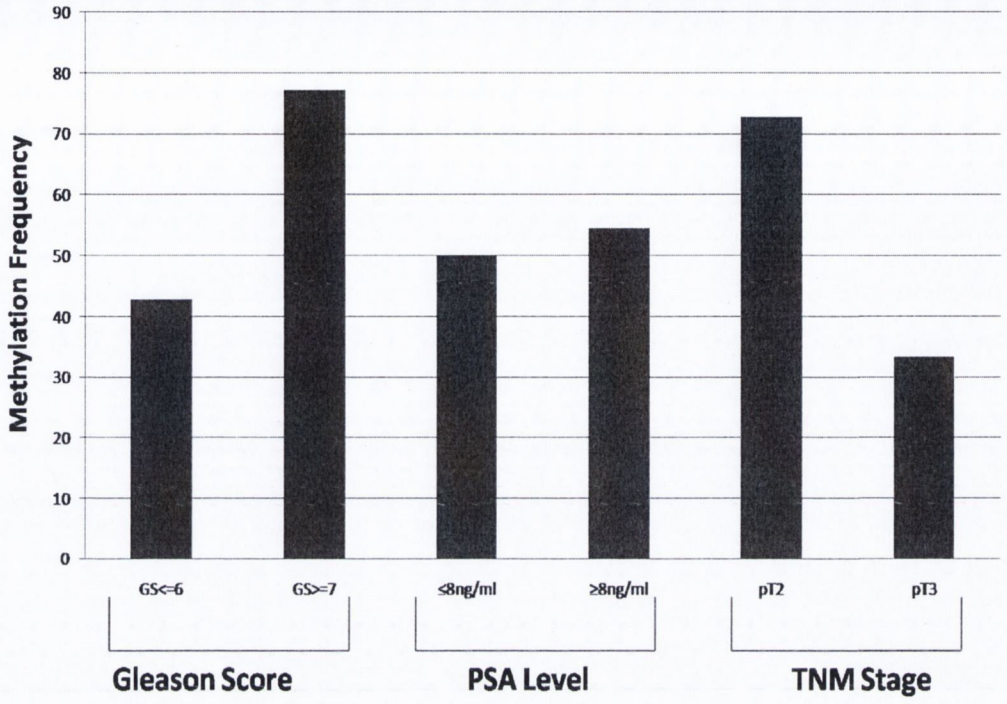

Figure 6.6

Correlation of hypermethylation of all 5 apoptotic gene and clinicopathological features; Gleason Score, PSA level and TNM stage.

6.4 DISCUSSION

In this study, we comprehensively examined the methylation profile of CpG islands at 7 apoptotic-related genes in prostate cancer, HGPIN, normal adjacent prostate and BPH using QMSP. Five genes (*BNIP3, CDKN2A, DCR1, DCR2* and *TMS1*) had a significantly higher frequency of methylation in their promoter CpG islands than normal prostate ($P=0.02$, $P=0.004$, $P<0.001$, $P<0.001$, respectively). *BIK* and both CpG islands of *cFLIP* showed no evidence of promoter hypermethylation in all prostate cancer tissue samples examined.

This is the first report of atypical methylation of *BNIP3* in prostate cancer. *BNIP3* hypermethylation was detected in 16% of prostate cancers but was not detected in any normal, HGPIN or BPH samples. The methylation frequency of *BNIP3* found in prostate cancer is lower than the methylation frequencies observed for primary colorectal (66%) and primary gastric (49%) cancers.

However, the frequencies observed are comparable to the methylation frequencies of *BNIP3* observed in both acute lymphocytic leukaemia (15%) and acute myelogenous leukaemias (17%).

CDKN2A promoter hypermethylation has previously been observed at a moderate frequency in prostate cancers (3-25%) (Noda et al., 2007; Yao et al., 2006; Yegnasubramanian et al., 2004). In the current study, *CDKN2A* was detected at a slightly higher frequency of 27.6%. *CDKN2A* methylation was not associated with any clinicopathological features. Methylation was not detected in normal prostate tissue consistent with previous reports (Maruyama et al., 2002). Moderate levels of promoter hypermethylation of *CDKN2A* were detected in HGPIN and BPH (7.69% and 9.52%, respectively), in contrast to a previous report by Jeronimo et al, 2004, which documented the methylation frequency of *CDKN2A* in 81.6% and 83.4% of HGPIN and BPH samples, respectively. However, in the Jeronimo study, *CDKN2A* methylation is reported in 77% of prostate cancer samples, a significantly higher methylation frequency than reported in ours and other studies (Noda et al., 2007; Yao et al., 2006; Yegnasubramanian et al., 2004). Moreover, the author notes that for all genes analysed (n=9) in their study, a higher methylation frequency is reported than observed in previous studies (Jeronimo et al., 2004a). Taken together, the methylation frequency of *CDKN2A* in both HGPIN and BPH in the Jeronimo study may be over estimated. Of interest, in our study, the adjacent tumour sample to the HGPIN sample with evidence of methylation was also methylated, suggesting *CDKN2A* methylation may be an early event in prostate cancer. However, a larger cohort of tumour and matched adjacent HGPIN is required to test this hypothesis.

The methylation frequencies of *DCR1* and *DCR2* in prostate cancer were approximately equal (~38%) and are consistent with previous reports of *DCR1*/*DCR2* methylation in 37-50% prostate cancers (Shivapurkar et al., 2007; Suzuki et al., 2006). No hypermethylation was detected in normal prostate tissue for both genes. In agreement with the findings in this study, methylation frequencies of between 0-3% and 0-16% have been reported in normal tissue for *DCR1* and *DCR2*, respectively (Shivapurkar et al., 2007; Suzuki et al.,

2006). In the case of both genes, methylation was not detected in HGPIN samples or BPH samples for *DCR1* but was detected in 5.88% of BPH samples for *DCR2*. To the best of our knowledge this is the first report of the methylation status of these genes in HGPIN or BPH.

TMS1 promoter hypermethylation has been implicated as an early event in prostate cancer development, detected at significantly higher frequencies in primary tumours (47-65%) and pre-invasive HGPIN (64% (7/11)) than non-malignant prostate (3-28%) (Caldas et al., 1994; Collard et al., 2006; Suzuki et al., 2006). Methylation of *TMS1* was detected in 44% of prostate cancer samples, which is in keeping with these previous studies, however TMS1 hypermethylation was detected in significantly less HGPIN cases (12%) in our study compared to 64% of HGPIN samples in previous studies. This discrepancy may in part be due to lack of methylation data on adjacent tumour in 10/17 HGPIN samples. Moreover, the HGPIN sample with evidence of methylation was also methylated in the adjacent tumour sample. *TMS1* methylation was not detected in any normal prostate tissues in contrast to previous findings whereby a wide range of methylation frequencies (3-28%) have been observed in non-malignant tissue (Caldas et al., 1994; Collard et al., 2006; Suzuki et al., 2006). Suzuki et al, 2006 found a significant correlation between *TMS1* hypermethylation and Gleason score $\geq$ 7 and PSA level >8. This was validated in the current study, in that *TMS1* methylation was significantly associated with a PSA level >8 and a higher proportion of tumours, with evidence of *TMS1* methylation, had a Gleason score $\geq$ 7, however this difference was not statistically significant.

6.4.1 Cell lines versus prostate cancer: Similar methylation patterns?

The methylation pattern observed in prostate cell lines and primary prostate cancer tissue were similar, whereby only two genes (*BIK* and *cFLIP*) had no evidence of promoter hypermethylation in prostate tissue despite evidence in cell lines. In the case of *BIK*, the QMSP assay utilised in the current study did not detect methylation in PC3 cell lines (discussed in Chapter 5) and therefore it is not unusual that methylation was not detected in primary tissue. The CpG island of *BIK* requires sequencing to elucidate the location of methylation

within the CpG island. This could not be achieved using conventional bisulfite sequencing techniques but may be successful using pyrosequencing, a method currently under investigation in the laboratory. The remaining 5 genes showed methylation levels comparable to those found in the cell line analysis; in the majority of genes the methylation levels observed in cell line analysis varied greatly, this was also the case for the observed methylation levels obtained during primary tissue analysis. The quantitative methylation levels obtained for *BNIP3* in various prostate cancer cell lines (0.04- 34.54) were relatively low and this was also found to be true during analysis of primary prostate tissue (0.04- 48.55). Furthermore, methylation of *TMS1* was detected in all prostate cancer cell lines examined; in keeping with these findings prostate cancer tissue analysis identified *TMS1* as the most frequently methylated gene. These similarities suggest prostate cancer cell lines are a good model system for screening genes for aberrant methylation and have relevancy to prostate carcinogenesis *in vivo*. Our findings are in agreement with a previous report on the similarities of hypermethylation profile between cell lines and prostate cancer tissue (Yegnasubramanian et al., 2004). This study illustrated a striking similarity between prostate cancer cell lines and both primary and metastatic prostate cancer.

6.4.2 The 5-gene panel in a diagnostic and prognostic setting

The methylation status of all 5 genes was investigated for correlations with clinicopathological factors. A higher methylation frequency of 77.3% was observed for prostate cancer samples with a Gleason score ≥ 7 compared to only 42.8% with a Gleason score of ≤ 6, however this association was not statistically significant. The small number of samples with information on the methylation status of all 5 genes (n=29) reduced the power of this study and it is likely that analysis in a larger cohort of prostate tissue samples may detect a statistically significant result. Hence, we introduce the idea that these 5 apoptotic-related gene targets of aberrant methylation may represent an "apoptotic methylation signature" of prostate cancer, which may have utility in a diagnostic and prognostic setting and may also inform us more fully about the biology of the disease.

The correlation between methylation of our 5-gene panel and *GSTP1* was also examined. Interestingly, four prostate cancer samples with evidence of methylation in all five apoptotic gene analysed were also methylated in *GSTP1* and in two other genes *IGFBP3* and *SFRP2*, which have been investigated by our group. This suggests that in these samples, a methylator phenotype may exist. The concept of a CpG island methylator phenotype (CIMP) first emerged in studies on colon cancer (Toyota et al., 1999), whereby a number of sporadic tumours with microsatellite instability (MSI) had increased frequencies of promoter methylation of multiple genes. The definition of CIMP remains controversial (Herman et al., 1995), but two requirements are crucial. Firstly, use of a quantitative method for methylation study and secondly, avoidance of genes with high levels of methylation in benign tissue (Herman et al., 1995). The current study satisfies both requirements. In addition, the methylation status of *CDKN2A*, which is included in our study, is widely used in combination with other genes, to define the CIMP in colon cancer (Riojas et al., 2007). This study therefore provides the impetus for further investigation of a CIMP in prostate cancer, by examining the methylation status of a panel of genes (namely, *GSTP1, BNIP3, CDKN2A, DCR1, DCR2, TMS1, IGFBP3* and *SFRP2*) in a larger cohort of patient samples.

Intriguingly, 9/46 tumour samples lack methylation in *GSTP1*, 5 of which were also unmethylated for all apoptotic genes examined (Figure 6.4). Moreover, 3 of these samples lacked methylation in both *IGFBP3* and *SFRP2*. A number of transcription factors have been shown to convey protection against DNA methylation ((Boumber et al., 2008; Seguin-Estevez et al., 2009). However genes that confer protection against *de novo* methylation have so far not been identified.

The current study had a number of limitations. Firstly, ideally a larger number of tissue samples would help increase the overall power of the study. Furthermore, as only a small number (n=7) of HGPIN samples had adjacent prostate cancer samples included in the study, the role of aberrant methylation of apoptotic-related genes in early stages of disease initiation could not be adequately examined. Therefore, analyses of additional tumour samples would

be beneficial and allow formal assessment of the relevancy of our 5-gene panel during early disease progression.

In summary, approximately 69% of tumour samples and 0% of normal tissues were methylated in at least one of our 5- apoptotic gene panel. Of interest, this 5 gene "apoptotic methylation signature" is more frequently methylated in tumours with a higher Gleason score associated with a worse prognosis (Gleason score ≥ 7; P=0.158). Moreover, combination of this panel of genes with *GSTP1* increased the frequency of methylation detected in prostate cancer by approximately 9% than if *GSTP1* were used alone. Hence, investigation of this "apoptotic methylation signature" is warranted in a larger cohort of patients to further access its role in a diagnostic and prognostic setting.

CHAPTER 7
DISCUSSION & FUTURE DIRECTIONS

7.1 GENERAL DISCUSSION

Cancer cells display a number of acquired genetic defects in their apoptotic machinery that impair programmed cell death. In prostate cancer, tissue microarray studies have determined that a number of central apoptotic molecules such as, *BCL-2*, *CLU*, *SMAD4*, *DAP* and *PIGPC1* (*PERP*) are down-regulated in prostate cancer (Ernst et al., 2002; Yu et al., 2004a). Progression to more aggressive androgen-independent prostate cancer is associated with resistance to apoptosis and aberrant apoptotic-related gene expression (McEleny et al., 2002). Downregulation or loss of expression of proapoptotic genes during prostate carcinogenesis may allow evolution of an apoptotic-resistant pro-survival carcinogenic phenotype (Murphy et al., 2008). Understanding the molecular mechanisms underlying atypical expression of genes integral to apoptosis may provide valuable insight into prostate carcinogenesis and therapeutic responses in prostate cancer. Consequently, a combined *in silico* candidate gene selection approach and a novel DHPLC methylation screening strategy was applied to identify new targets of aberrant promoter methylation in prostate cancer.

7.1.1 *In Silico* analysis and DHPLC screening strategy identifies novel apoptotic gene targets of aberrant promoter hypermethylation in prostate cancer

Our first objective was to employ a bioinformatics strategy to generate a list of candidate apoptotic-related gene targets of methylation, which may have relevancy in prostate cancer diagnosis and disease progression. This comprehensive *in silico* strategy, utilising a number of different approaches and sources, generated a candidate bank of 22 genes which had the potential to undergo promoter hypermethylation in prostate cancer. Next we developed and successfully optimised PCR and DHPLC assays for 13 genes which were then screened for methylation in a panel of prostate cancer cell lines using a high-throughput DHPLC methylation screening platform. Using this approach a panel of genes were identified which showed potential as novel apoptotic methylation biomarkers.

DHPLC offers several important advantages over more conventional techniques, providing a snapshot of the methylation status of a whole PCR amplified sequence. Moreover, DHPLC can detect varying degrees of methylation (i.e. partial methylation) across a large number of CpG sites in a given sequence. In this way, DHPLC surpasses screening techniques based on methylation sensitive restriction enzymes or methylation specific PCR, where only a limited number of CpG sites are amendable to analysis (Perry et al., 2007). DHPLC is significantly more rapid and cost effective than bisulfite sequencing, which involves a number of cloning and optimisation steps. In addition, DHPLC has been shown to be equally sensitive as other methods to small quantities of methylated DNA present within a heterogeneous sample (Perry et al., 2007).

A crucial step required for DHPLC analysis is the need for careful design of primers during PCR amplification of target sequences. Design of successful bisulfite specific, methylation insensitive PCR primers is difficult (discussed in Chapter 4) and can limit the number of sequences under investigation. Furthermore, screening patient tissue samples for methylation using DHPLC requires fresh frozen tissue and not the more readily available paraffin embedded tissues. However, at the time of commencement of this study, DHPLC represented a novel methylation screening platform for screening and thus was employed successfully to identify putative targets of promoter hypermethylation.

Since starting this study, a number of advances in DNA methylation profiling techniques have emerged and as a result a number of alternatives to the methylation screening strategy applied in this study are available. Lodygin et al, 2005 implemented a combined approach of pharmacologic inhibition of DNA methylation and histone deactylation, coupled with gene expression profiling in prostate. Such an approach could be tailored towards profiling of apoptotic genes only, similar to the approach taken in our study. Re-expressed genes containing a promoter CpG island with known function in DNA repair, negative cell cycle regulation, induction of apoptosis, detoxification, differentiation or transcriptional regulation were examined. This yielded 50

genes for methylation screening using bisulfite sequencing, 12 of which were identified as aberrantly methylated in various prostate cancer cell lines.

Our approach yielded 22 candidate gene targets of promoter methylation, 13 of which were subsequently screened for methylation, significantly less than the Lodygin study, however given that our selection process was limited to apoptotic genes only, this is not surprising. The *in silico* selection method applied in this study had a good success rate. Of the 13 genes screened for methylation using DHPLC, 7 genes were identified as aberrantly methylated in prostate cancer cell lines. Furthermore, since this candidate methylation gene bank was generated, 2 out of the remaining 4 genes (*HRK* and *BCL2*), with no information on their methylation status in prostate cancer in the timeframe of our study, have subsequently been identified as targets of methylation in prostate cancer by other groups (Cho et al., 2007; Higuchi et al., 2008), thus illustrating the accuracy of the *in silico* approach used in this study.

In recent years, we have witnessed an explosion of technological advancements in genome-wide approaches to studying DNA methylation. These studies combine global approaches, such as DNA microarrays or high-throughput sequencing, and traditional methylation detection techniques like genomic mapping of methylation sensitive restriction enzyme cleavage sites, bisulfite sequencing, affinity purification with methylcytosine DNA-binding domain (MBD) proteins and MeDIP, a method based on immunoprecipitation of DNA with an antibody that recognises 5-methyl cytosine (Schones and Zhao, 2008).

The choice of methylation technique utilised in a study is greatly dependent on the question the researcher wants to ask or the information they wish to obtain. In this study, we aimed to identify a panel of apoptotic genes with a view to generate an "apoptotic methylation signature" which may have efficacy in a diagnostic and prognostic setting. Our combined *in silico* and DHPLC screening approach allowed relatively inexpensive rapid identification of a panel of apoptotic genes aberrantly methylated in prostate cancer cell lines, which was further investigated for aberrant methylation in a larger cohort of prostate cancer tissue samples (n=50).

Recently, a number of techniques have become available which surpass the rapid and high-throughput capability of DHPLC by generating large amounts of data in only one experiment. *Nimblegen* arrays for example allow for whole genome DNA methylation analysis. This technology is based on MeDIP (Weber et al., 2005; Weber et al., 2007; Zilberman et al., 2007) or the MBD protein method (Rauch et al., 2007). After preparation of DNA samples, using a *Nimblegen* supplied MeDIP or MBD protocol, *Nimblegen* analyse samples on an array design of choice. *Nimblegen* offers a wide range of array designs, such as whole genome analysis, promoter and/or CpG island targeted arrays. There is also an opportunity to customise an array to your specific experimental design. *Nimblegen's* nimblescan software generates a list of methylated regions from the raw data from each array, allowing you to map methylated regions to specific gene promoters. *Nimblegen* is a highly sensitive technique and can readily detect as few as two or three 5-methyl cytosines per CpG island. This technology has been utilised by a number of research groups, the results of which have been published in high impact journals (Rauch et al., 2007; Weber et al., 2007; Zilberman et al., 2007). *Nimblegen* technology is significantly more costly than DHPLC. However, it could be utilised to screen a panel of prostate cancer cell lines and a small cohort of patient samples to identify candidate regions for further investigation, similar to the approach taken in our study.

7.1.2 Quantification of methylation levels using quantitative methylation specific PCR

In this study, we utilised a high-throughput technology, known as quantitative methylation specific PCR (QMSP) for the semi-quantitative analysis of DNA methylation and to investigate the methylation status at individual CG site for the 7 genes of interest in our panel prostate cell lines prior to analysis in a larger cohort of tissue samples (n=145). QMSP represents a highly sensitive, high-throughput (can be performed on a 384 well plate) technology and relies on fluorescence based real-time PCR. This approach allowed us to identify significant promoter hypermethylation levels for a number of our target genes, validating the DHPLC strategy that we employed and allowing us to propose

the existence of a putative apoptosis methylation gene panel which could be tested in primary prostate tissue. Precise mapping of the relevant transcriptional control elements in the different genes also allowed us to pinpoint specific methylation hotspots within genes that could be relevant to abrogating transcription. In addition, the testing of pharmacological demethylation of genes in the PC3 prostate cancer cell line allowed further functional validation of potential epigenetic control in prostate cancer.

One disadvantage of the QMSP technique used is that only the proportion of methylated target and not unmethylated target is quantified. A variation of this technique has been devised, whereby the levels of methylated and unmethylated product for a target sequence are determined (Lo et al., 1999). Furthermore, as discussed in Chapter 5, QMSP will only amplify sequences that are 100% methylated at all of the CpG sites within the primer/probe binding sites, in accordance with the chemistry of this technology (Eads et al., 2000), and thus represents a semi-quantitative assay. A fully quantitative version of QMSP technology can be achieved, whereby separate probes for each sequence variant resulting from different methylation patterns can be designed (Eads et al., 2000). A disadvantage of this technology is the requirement for a greater number of probes, which can be costly.

Very recently, microarray-based DNA methylation profiling using universal BeadArrays has been reported (Bibikova et al., 2006; Martin-Subero et al., 2009). This technology exploits innovations in high-throughput SNP genotyping systems (Fan et al., 2003) for DNA methylation detection, based on genotyping bisulfite modified DNA. Utilising this technology Martin-Subero et al, 2009 characterised the DNA methylation profile of a range of different haematological neoplasm subtypes and identified 220 genes hypermethylated in at least one haematological neoplasm entity (Martin-Subero et al., 2009). This technology represents a high-throughput quantitative measurement of DNA methylation and probes can be specifically designed for most of the CpG sites in the genome. This approach could be utilised to screen the methylation status of hundreds of pre-selected genes simultaneously and to identify methylation signatures that distinguish normal prostate from prostate cancer tissue samples, thus generating information on a wide number of putative

cancer biomarkers. Evaluation of this technique is in its infancy, although this approach leads to less genomic coverage than other array-based techniques (e.g. Nimblegen) it's utility as a cost effective, high-throughput screening method in a large number of samples is promising.

7.1.3 Identification of a 5 gene "apoptotic methylation signature"

In this study, we systematically examined the methylation profile of CpG islands at 7 apoptotic-related genes in a cohort of prostate tissue samples, representing prostate cancer, HGPIN, histologically benign prostate and BPH using QMSP. Employing this approach, we found that *BNIP3, CDKN2A, DCR1, DCR2* and *TMS1* had a significantly higher frequency of methylation in their promoter CpG islands than normal prostate, while *BIK* and both CpG islands of *cFLIP* showed no evidence of promoter hypermethylation in all prostate cancer tissue samples examined. Results demonstrated that 69% (20/29) of tumour samples were methylated in at least one of our 5-gene apoptotic panel. Strikingly, our 5-gene panel was completely unmethylated in all histologically normal tissue. This provides strong evidence that methylation of this 5-gene panel is highly specific to prostate cancer. Moreover, this 5 gene "apoptotic methylation signature" is more frequently methylated in tumours with a higher Gleason score associated with a worse prognosis (Gleason score ≥ 7). Thus our 5 gene panel shows evidence of significant promoter hypermethylation in prostate cancer and merits further study in a larger cohort of patient samples.

To date, a number of studies have highlighted the potential of methylation profiling in a diagnostic and prognostic setting. A large number of these studies have focused on the *GSTP1* gene. The high prevalence of *GSTP1* promoter hypermethylation in early prostate carcinogenesis has lead to the development of a *GSTP1* hypermethylation assay for the detection of prostate cancer (Henrique and Jeronimo, 2004). However, the effectiveness of *GSTP1* alone as an early detection biomarker is limited and increasing evidence suggests that combining *GSTP1* with other genes shown to be methylated in prostate cancer could be more powerful as a diagnostic and prognostic biomarker (Ellinger et al., 2008; Soengas et al., 2001). An extensive study that quantified methylation

of 16 different genes, described a 4 gene panel of *GSTP1*, *APC*, *PTGS2* and *NDR1* that could accurately distinguish primary prostate cancer from benign prostate tissue with 92% specificity (Yegnasubramanian et al., 2004). Thus, we investigated the "apoptotic methylation signature", identified in this study, in combination with the methylation status of *GSTP1*. The frequency of methylation detected in prostate cancer was increased from 80.5 to 89.4%, than if *GSTP1* were used alone. Hence, further examination of this "apoptotic methylation signature" is warranted in a larger cohort of patients to access its role in a diagnostic and prognostic setting.

The present study has a number of limitations, which have been addressed in Chapter 6 but warrant further discussion. Ideally, a larger cohort of tissue samples should be utilised to increase the power of the study. The role of aberrant methylation of apoptotic-related genes in early stages of disease initiation could not be adequately examined, due to the small number of HGPIN samples (n=7), which had concurrent adjacent tumour samples included in the study. Therefore, analyses of these additional tumour samples and the addition of more prostate cancer tissue samples would greatly enhance the power of the current study and allow formal assessment of the relevancy of our 5-gene panel during early disease progression.

In this study, histologically classified tissue was macrodissected, whereby tumour, HGPIN, BPH and histologically normal tissue, as classified and marked by a pathologist, were removed from surrounding tissue. We recognise that in using this method the possibility of admixture of cell types and inclusion of stromal cells cannot be ruled out and hence may obscure the tumour cell-specific methylation profile of these samples. The combination of laser capture microdissection, a microscope based technique that permits the attainment of a homogeneous population of cells from tissue sections in one step (Emmert-Buck et al., 1996) and bisulfite modification would be advantageous. Previously in the laboratory, this technique of tumour acquisition was investigated. However, the technique was unsuccessful when combined with bisulfite modification in formalin fixed paraffin embedded prostate cancer. Currently, more sophisticated techniques of DNA extraction

from small quantities of tissue have become available. We hope in future studies to perform LCM on our retrospective prostate tissue cohort to obtain pure samples of tumour from individual patients.

7.1.3.1 Methylation of 5-gene apoptotic panel in metastatic prostate cancer

Hitherto, our investigation into the frequency and levels of apoptotic-related gene methylation has focused on primary prostate cancer. A major cause of treatment failure and mortality for prostate cancer patients is metastases to lymph nodes and bone and progression from androgen-dependence to androgen-independent growth (Arnold and Isaacs, 2002). Currently androgen ablation therapy is the primary treatment for metastatic prostate cancer. However, ablation therapy alone does not eliminate androgen-independent cells. Several lines of evidence suggest progression to androgen-independent disease is associated with resistance to apoptosis and altered expression of key apoptotic genes, such as Bcl2 and inhibitor of apoptosis proteins (IAPs) (Furuya et al., 1996; McEleny et al., 2002).

There is evidence to support investigation of our 5-gene apoptotic panel in metastatic disease. In a follow-up disease free survival study, Suzuki et al, 2006, found that patients with *TMS1* methylation had a significantly worse disease free survival than patients without *TMS1* methylation. In addition, aberrant expression of both *CDKN2A* and *BNIP3* has been implicated in progression towards a metastatic phenotype in breast and metastatic squamous cell carcinoma of the skin (Kusters-Vandevelde et al., 2009; Manka et al., 2005). Analysis therefore of an "apoptotic methylation signature" in prostate cancer may help elucidate some of the molecular mechanisms underlying progression to androgen resistant disease and metastases and help stratify patients into low and high-risk groups.

7.1.4 Methylation and therapeutic targeting

Could an "apoptotic methylation signature" of prostate cancer help elucidate novel therapeutic targets for drug resistant disease? Recently, evidence suggests that hypermethylation of pro-apoptotic genes may result in conventional chemotherapeutic drug resistance. Methylation of the potent pro-

apoptotic gene *APAF1* for example, in malignant melanoma cells, has been shown to enhance cell survival during chemotherapy (Eeles et al., 2008). *CASP8* represents another gene whose methylation may contribute to chemoresistance. Pharmacological demethylation of cancer cell lines exhibiting aberrant caspase-8 expression due to hypermethylation of the *CASP8* gene, sensitized cells to both death receptor triggered apoptosis and drug-induced apoptosis (Fulda et al., 2001). Methylation of other genes implicated in the control of apoptosis may also have the potential to confer chemoresistance.

Methylation of our 5 gene panel may contribute to altered responses to drug induced apoptosis in a number of ways. Methylation and concurrent silencing of *TMS1* may contribute to inhibition of caspase 8 mediated, death receptor induced apoptosis (Hasegawa et al., 2009). *TMS1* is known to indirectly induce caspase 8 activation (Parsons and Vertino, 2006). In contrast, *BNIP3* inhibition via methylation, is likely to contribute to resistance to hypoxia induced, mitochondria mediated cell death and may have relevance in the therapeutic effect of certain drugs in hypoxic regions of prostate cancer. Loss of *CDKN2A* by aberrant promoter hypermethylation may result in reduction of p53 induced cellular death and increased cell proliferation. Finally, the role of DNA methylation of anti-apoptotic *DCR1* and *DCR2* in cancer progression is not fully understood. Indeed, studies have shown that methylation of these decoy receptors are associated with a better prognosis in prostate cancer patients (Suzuki et al., 2006). Therefore, patients with *DCR1* and *DCR2* promoter methylation may respond better to chemotherapeutic drugs. However, these genes may also be involved in other pro-survival cancer pathways such as NF-κB pathways (Shivapurkar et al., 2004).

In this setting, determining the methylation status of our panel of apoptotic genes could be used to design novel therapeutic strategies for individual patient groups (Teodoridis et al., 2004b). Although our studies in prostate tissue are preliminary, future studies could include stratifying both patient samples and cell lines into 3 subgroups. One group "Group M", would be composed of patient samples and cell lines, which exhibit methylation in all apoptotic genes examined (8% of tumours and prostate cancer cell lines: 22RV1, LNCAP,

PC3) ; the second group "Group Mm" would have less than 5 but greater than one apoptotic gene methylated (61% tumours & prostate cancer cell lines: DU145, RC58), while the 3rd group "Group m" would consist of genes with no evidence of methylation in the 5 apoptotic genes in the panel (31% tumours, no prostate cell lines were unmethylated in all genes but normal cell line RWPE1 had the least number of methylated apoptotic genes) (Figure 7.1).

In this way, the apoptotic phenotype of these 3 subgroups could be further dissected to investigate if they are more sensitive/resistant to apoptosis. From a therapeutic point of view, tumours with greater resistance to apoptosis may respond poorly to chemotherapeutic intervention (Fulda et al., 2001) and thus require more aggressive therapy.

From a treatment point of view, the use of both methylation inhibitors in combination with chemotherapeutic agents may prove beneficial in the treatment of resistant disease (Plumb et al., 2000; Strathdee et al., 1999). Currently a number of studies have focused on the development of small molecular inhibitors of methylation and have produced a number of drugs, such as 5-azacytidine, 5-aza-2′-deoxycytidine, procaine, hydralazine and zebularine (Brueckner and Lyko, 2004). These DNMT inhibitors, once incorporated into DNA, complex with and inactivate all 3 forms of DNA methyltransferase (Teodoridis et al., 2004b). In this way, reversal of the apoptotic methylation phenotype has the potential to render patients more responsive to chemotherapeutic approaches.

However, as discussed, DNA methylation alone is often insufficient for gene silencing, with strong evidence supporting an integral role for histone deacetylation and chromatin remodelling in the silencing process (Bird and Wolffe, 1999). Interestingly, recent studies have identified a compound, known as sulforaphane (SFN) found in cruciferous vegetables, which inhibits HDAC activity in human colorectal and prostate cancer cells. Sulforaphane administration to prostate cells enhanced histone acetylation, derepression of P21 and Bax, and induction of cell cycle arrest and apoptosis.

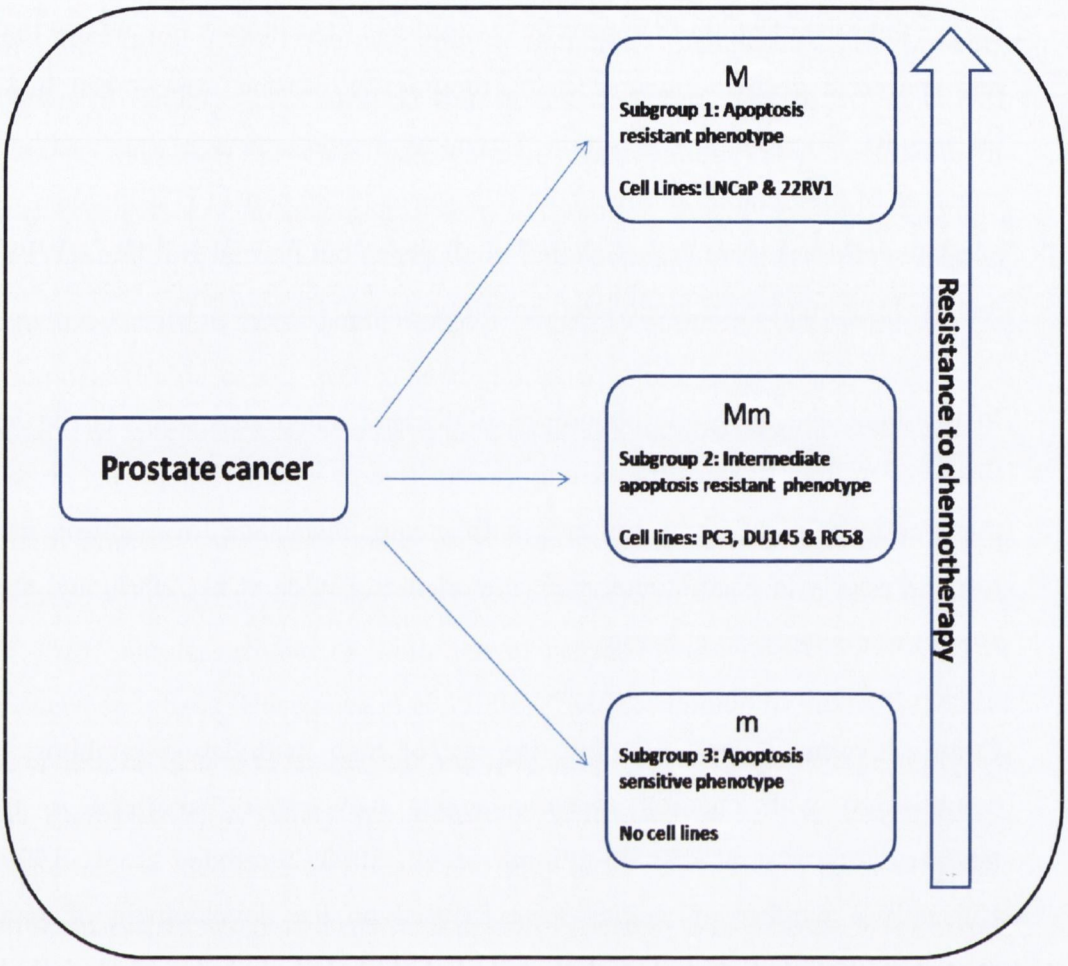

Figure 7.1

Hypothetical sub grouping of prostate cancer by "apoptotic resistant phenotype", based on the methylation status of a panel of apoptotic genes. M represents an "apoptotic resistant" phenotype, which shows evidence of methylation in all apoptotic genes examined; Mm, represents an intermediate apoptotic resistant phenotype, whereby less than 5 but more than 1 apoptotic gene is methylated; m represents an "apoptotic sensitive" phenotype showing no methylation in all apoptotic genes. Accumulation of methylated pro-apoptotic genes contributes to an apoptotic resistant phenotype, thus increasing resistance to chemotherapy.

7.2 FUTURE DIRECTIONS

7.2.1 Future investigation into possible apoptotic-related gene targets of methylation in prostate cancer.

To date, only 13 out of a possible 22 genes from the candidate gene panel have been screened for methylation. Firstly, we would like to update our list of potential apoptotic-related gene targets of methylation, which could be achieved easily by utilising the newly available methylation literature mining tool PubMeth, discussed in Chapter 3. Moreover, genes important for alternative mechanisms of cellular fate, such as autophagy and cellular senescence could also be added. Tumour suppressor genes like *p53*, *PTEN* and *DAP1* kinase have been shown to stimulate autophagy when mutated or epigenetically silenced (Mizushima et al., 2008). Furthermore, a number of key members of the apoptotic machinery are implicated in control and regulation of autophagy. For example, potent pro-apoptotic molecule bcl-2 is known to interact with and inhibit autophagy-related protein beclin1 (Pattingre et al., 2005). Cellular senescence can be triggered by multiple mechanisms including epigenetic derepression of *ink4a/ARF* locus, hence contributing to aberrant cellular proliferation (Collado et al., 2007). Inclusion of genes important in alternative cellular fate pathways would better our understanding of cellular fate in prostate cancer.

Next, the remaining and newly identified candidate genes could be screened for methylation using DHPLC. Alternatively, a custom made apoptosis microarray coupled with universal BeadArrays could be employed to profile methylation of a large number of apoptotic genes in prostate cancer samples. In this way, we intend to develop a larger panel of apoptotic genes aberrantly methylated in prostate cancer, allowing the most appropriate apoptotic candidate methylation bank to be generated.

7.2.2 CpG island methylator phenotype in prostate cancer

In recent years, perplexing data has emerged indicating that in some tumours, groups of genes had consistently increased methylation in their promoter regions (Herman et al., 1995). The phenomenon of a so called "CpG island methylator phenotype" (CIMP) was first proposed by Jean-Piere Issa, based on

his studies in colon cancer (Toyota et al., 1999). Colon tumours with increased microsatellite instability (MSI) had increased frequency of promoter methylation affecting multiple genes, such as *CDKN2A* (Riojas et al., 2007). Subsequent studies showed that CIMP defined a group of cancers with a 3-5 fold increased frequency of aberrant gene methylation (Li et al., 1992). Indeed, 70-80% of sporadic MSI-positive colon cancers could be attributed to CIMP and associated methylation of the DNA repair gene, mutL homolog 1 (MLH1). Thus, sporadic colon cancer could be divided into 4 genetically distinct subgroups ($CIMP^+$ MSI^+, $CIMP^+$ MSI^-, $CIMP^-$ MSI^+, $CIMP^-MSI^-$). Similar "CIMP" phenotypes have been confirmed in various other cancers, such as gastric (Toyota et al., 1999), ovarian (Strathdee et al., 2001) and liver cancers (Shen et al., 2002). On the other hand, some studies have failed to identify CIMP in these cancers. This may result from using less quantitative methylation techniques such as MSP. The definition of CIMP remains controversial, but two requirements are deemed crucial; firstly, use of a quantitative method for methylation study and secondly, avoidance of genes with high levels of methylation in benign tissue (Herman et al., 1995).

To date, a methylator phenotype or "CIMP" has not been identified in prostate cancer. In this study, we examined the correlation between our 5-gene panel and three genes previously investigated in the laboratory (*GSTP1*, *IGFBP3* and *SFRP2)*. Interestingly, four prostate cancer samples with evidence of methylation in all apoptotic genes analysed were also methylated in *GSTP1, IGFBP3* and *SFRP2*. Thus 4/50 (8%) tumours showed methylation in all genes analysed, supporting the existence of a CIMP in prostate cancer. The number of methylated loci which defines CIMP in tumours can vary greatly (Herman et al., 1995). Hence comparison of CIMP frequency between studies and indeed cancers is difficult. Nevertheless the frequency observed in these prostate cancer samples in general is higher than in liver cancer (2%, methylation of $\geq$7 loci) but lower than frequencies reported in colorectal cancer (19%, methylation of $\geq$6 loci) (Ogino et al., 2009; Zhang et al., 2007).

Interestingly, we also identified 3 tumour samples that lacked methylation in all 8 genes, suggesting a $CIMP^-$ subgroup or methylation resistant tumours.

This warrants further investigation, in a larger cohort of patients. In addition, it would be interesting to investigate whether microsatellite instability is a common feature of $CIMP^+$ tumours. It is our hope that, similar to studies in colon cancer, identification of $CIMP^+$ and $CIMP^-$ tumours may help define distinct prostate cancer subgroups allowing further characterisation of the genetic/epigenetic abnormalities associated with these subgroups. In the future, this could have utility in tailoring individual treatments.

7.2.3 The 5-gene "apoptotic methylation signature": putative cancer biomarker?

7.2.3.1 DNA methylation: a promising new cancer biomarker

Identifying biomarkers that can distinguish between clinically indolent and more aggressive prostate cancers is the holy grail of prostate cancer research. CpG hypermethylation has emerged as a biomarker in many cancers, including prostate cancer. DNA hypermethylation at various gene loci has been detected in prostate cancer and other urological malignancies. Furthermore, the unique methylation signatures, which have been identified in specific tumour types (Costello et al., 2000; Soengas et al., 2001) further increases its utility as a biomarker, given that a major concern for an early detection biomarker is its ability to distinguish prostate cancer from other tumour types. Most studies have primarily focussed on prostate tissue, as we have in this study, but some have studied urine with and without prostatic massage (Cairns, 2004; Goessl et al., 2001; Jeronimo et al., 2002) whilst others have successfully detected specific hypermethylation in serum (Ellinger et al., 2008; Roupret et al., 2007). Recent technological advancements in cost effective, high-throughput quantitative measurement of DNA methylation, such as QMSP and DNA methylation profiling using universal BeadArrays may encourage widespread use of methylation analysis in clinical practice. Recently, a methylation technique known as Meth-DOP-PCR, a combination between modified degenerate oligonucleotides primered PCR (DOP-PCR) and traditional MSP, has been identified as a candidate high-throughput methylation analysis of trace amounts of circulating DNA. The authors suggest that coupling this technique with QMSP may prove more effective and hence may represent a cost effective methodology for the development of novel assays for early

diagnosis of many types of cancer and for patient follow-up (Di Vinci et al., 2006).

7.2.3.2 Detection of hypermethylation in biopsies

A problem facing diagnosis of prostate cancer from histological review of biopsy specimens is the false negative rate of ultrasound-guided core-needle biopsy. Methylation markers may complement histological review of biopsies by providing information on the epigenetic signature of the specimen, which could help distinguish between aggressive disease and clinically indolent prostate cancer.

To date most studies have focussed on *GSTP1* methylation to improve the sensitivity of standard histology for prostate cancer detection in needle biopsies. Harden et al, 2003, demonstrated that QMSP analysis of *GSTP1* in conjunction with histological review of needle biopsy specimens improved the sensitivity of tumour detection in pathologically reviewed, resected prostates by 11%, without compromising on specificity (Harden et al., 2003). Investigation of a multi-gene methylation panel identified four loci (*GSTP1*, *APC*, *TIG1* and *RARβ2*) which were aberrantly methylated in prostate cancer. This panel improved the sensitivity of prostate cancer diagnosis by 33% over histology alone (Tokumaru et al., 2004). It would be interesting, therefore, to evaluate the power or our 5-gene apoptotic panel in conjunctions with *GSTP1*, in correctly identifying men with prostate cancer based on biopsy specimens.

7.2.3.3 Detection of hypermethylation in bodily fluids

For a biomarker of prostate cancer to become clinically useful, ideally it should be detectable in easily accessible sites, such as peripheral blood, urine or ejaculate. Peripheral blood specimens are already routinely collected as part of current prostate cancer screening and detection protocols. DNA from prostate cancer can be detected in blood as a result of the presence of cell-free circulating DNA and of phagocytic cells that have ingested prostate cancer cells and/or intravascular apoptosis of prostate cancer cells (Ellinger et al., 2008). Jeronimo and colleagues detected *GSTP1* hypermethylation in the plasma of 36% of men with organ confined prostate cancer (Jeronimo et al.,

2002). Recently, however studies have begun to examine gene-panels for promoter hypermethylation in blood. The methylation status of a panel of genes (*MDR1, EDNRB, CD44, NEP, PTGS2, RASSF1A*, *RAR-β* and *ESR1*) was determined in serum from 192 men with clinically localised prostate cancer and 18 with hormone refractory metastatic disease. Promoter hypermethylation of *MDR1* only was detected in 38.3% of localised prostate cancer. Strikingly, promoter hypermethylation was detected in *MDR1* (83.3%), *EDNRB* (50%), *RAR-β* (38.9%) and both *NEP* and *RASSF1A* in (16.7%) in serum of a different cohort of patients with metastatic disease (Ellinger et al., 2008). This study suggests that promoter hypermethylation may play a pivotal role in the detection of metastatic prostate cancer.

Alternative bodily fluids, such as urine and ejaculate can also be collected and examined for the presence of CpG hypermethylation. DNA is present in fluids of the urinary tract by cellular shedding into the prostatic ducts (Ellinger et al., 2008). A study by Roupret et al, 2007, examined the methylation status of 10 genes (*GSTP1, RASSF1a. ECDH1, APC, DAPK, MGMT, P14, P16, RARβ* and *TIMP3*) in urine samples, collected after prostatic massage, from 95 patients with localised prostate cancer undergoing radical prostatectomy. The methylation frequency for genes ranged from 6.3% (*P14*) to 83.2% (*GSTP1*) in prostate cancer patients. The authors reported that at least one gene was hypermethylated in 93% of cancer patients (Roupret et al., 2007). This begs the question: "What bodily fluid should be routinely tested for aberrant methylation biomarkers?" In 2009, a study by Payne et al, formally addressed this question. Using QMSP they measured four DNA methylation biomarkers, *GSTP1, RASSF2, HIST1H4K* and *TFAP2E* in matched plasma and urine collected from 142 patients with prostate cancer. Analysis of these biomarkers in urine DNA significantly discriminated prostate cancer from biopsy negative patients. *GSTP1* methylation was detected in 81% of urine samples after prostatic massage and in only 39% of plasma samples. Methylation of the remaining three genes, were found in 92-100% of prostate cancer urine samples and in 18-31% of prostate cancer plasma samples (Payne et al., 2009). Taken together, this study suggests that detection of CpG hypermethylation

biomarkers are more readily detected in urine than plasma DNA. However, further studies are required.

The Prostate Cancer Research Consortium (PCRC), from which tissue samples were sourced from in our study, also routinely collect blood and urine samples from patients undergoing radical prostectomy. Furthermore, an initiative to collect urine after prostate massage is underway. It would be interesting to examine the methylation status of the 5-gene apoptotic panel present in this study, in conjunction with other genes tested in our laboratory (*GSTP1, IGFB3, SFRP2*) in both urine and blood and to examine the potential of this panel of genes as a non-invasive novel biomarker in prostate cancer.

7.2.4 The cFLIP paradox: Examining the role of differential expression of *cFLIP* splice variants in prostate cancer

cFLIP has two major splice variants, a short variant (cFLIPS) and a longer (cFLIPL). Intriguingly, expression analysis performed in this study illustrated differential expression of the splice variants in various prostate cancer cell lines. Relatively higher levels of *cFLIPL* are observed in DU145 cells with a decrease in expression seen in LNCAP and PC3 cells. In contrast, *cFLIPS* is upregulated in RC58 cells and again downregulated in LNCAP and PC3 cells.

The apoptotic functionality of cFLIPL has remained one of controversy and is discussed in Chapter 4. Of interest, a study by Shimada et al, 2006, found cFLIPL played an important role in development of metastatic prostate cancer by inhibiting proteasomal degradation of β-catenin. In contrast however, reduction of cFLIPL rendered metastatic cancer cells highly resistant to proteaosome inhibitor MG132-induced growth arrest and apoptosis. The authors report that cFLIPL is stabilised by MG132 and facilitates its mild pro-apoptotic function (Nakamura et al., 2006). Taken together, results suggest that cFLIPL has dual oncogenetic and anti-oncogenetic effects in prostate cancer cells. This dual functionality in prostate cancer may account for the differential expression of cFLIPL observed in prostate cancer cells in this study. cFLIPS does not appear to have dual functionality (Krueger et al., 2001b) and the significance of differential expression observed in prostate cancer cells is

unknown. In colon cancer, studies suggest that cFLIPL may have more significance in cancer progression than cFLIPS. However, this is not the case in all colon cancer cell lines (Wilson et al., 2007), whereby some cell lines may exhibit more efficient recruitment of one splice form over another.

It is clear that cFLIP expression, although hugely complex, is pivotal to cancer progression. Understanding why some cells preferentially express one isoform over another will help further our understanding of this intriguing gene in prostate cancer progression. Elucidating the functionality of both cFLIP isoforms at basal levels observed in normal and cancerous cells is essential to formally establish its contribution to prostate carcinogenesis and progression to metastatic disease.

7.2.5 Investigating the methylation status of Docetaxel resistant PC3 prostate cancer cell line (D12-PC3) and an age-matched PC3 control using a nimblegen array

In collaboration with Professor John O'Leary (IMM, TCD) and Professor Bill Watson (Conway Institute, UCD), we aim to investigate the global methylation status of the D12-PC3 cell line compared to its age-matched control utilising *Nimblegen* technology. *Nimblegen* CpG island-plus promoter methylation analyses would allow for rapid identification of methylated regions and comparisons of methylated patterns between the docetaxel resistant cell line (PC3-D12) and the PC3 age-matched control. We could exploit this high-throughput technique to decipher the underlying epigenetic changes associated with the docetaxel resistant phenotype. CpG island-plus promoter arrays cover all UCSC- annotated CpG island and promoter regions for all known Refseq genes.

It is likely that deregulation of apoptotic genes through aberrant promoter hypermethylation may confer resistance to docetaxel. Thus, elucidating the methylation profile of our 5-gene apoptotic panel would be advantageous. Furthermore, a recent study reported reversal of *TMS1* methylation with 5-azacytidine increased sensitivity to docetaxel treatment in two breast cancer cell lines, indicating that *TMS1* methylation may contribute to docetaxel

resistance in breast cancer (Gordian et al., 2009). In this study, we detected *TMS1* methylation in 44% of primary tissue. Therefore it would be interesting to further elucidate the role of *TMS1* and other apoptotic genes in docetaxel resistance in prostate cancer.

7.2.6 Investigating racial differences among men with prostate cancer

Men of sub-Saharan African ancestry are strongly associated with more aggressive prostate cancer (Burks and Littleton, 1992). African American men have the highest prostate cancer morbidity and mortality rates than any other racial or ethnic group in the US (Burks and Littleton, 1992). It is likely therefore, with an increasing Irish population of African descent and adaptation to a more westernised "Irish" diet, prostate cancer incidences and mortality rates in our population will increase. Understanding the aetiology of the more aggressive disease associated with men of African descent is essential. Indeed, it has been shown that differences in promoter hypermethylation exist for certain genes between different racial groups (Woodson et al., 2004; Woodson et al., 2003). Differences with respect to apoptosis have also been reported whereby apoptosis in malignant prostate cells were significantly higher in African Americans than Caucasian men (Guo et al., 2000). Furthermore, down-regulation of anti-apoptotic Bcl2 expression was observed in prostate tumours from African-American men compared to Caucasians (Guo et al., 2000).

Here we ask the question "are black men of sub-Saharan African decent more susceptible to environmentally induced epigenetic changes that contribute to prostate cancer progression"? Comparing a prostate cancer methylation profile of apoptotic-related genes in Caucasians, Asians and Africans may help to elucidate some of the molecular differences underlying the more aggressive prostatic tumour phenotypes associated with patients of African ethnicity.

7.2.7 DNA methylation, miRNAs and histone modifications: Linking it all together.

Epigenetics can be defined as the mechanisms that initiate and maintain heritable patterns of gene expression without altering the sequence of the genome. There are several layers of epigenetic complexity including histone

modifications, chromatin remodelling, micro RNAs and DNA methylation. DNA methylation has been the most thoroughly studied to date (Esteller, 2006). The focus of this study is deciphering the methylation of apoptotic genes in prostate cancer. However, the role miRNAs and histone modifications are being implicated in different forms of cancer. Increasingly it is also becoming clear that these three modes of epigenetic regulation are intimately linked.

7.2.7.1 Methylation of miRNA

MicroRNAs (miRNAs) represent a class of small non-coding RNAs that regulate gene expression (Filipowicz et al., 2008). MiRNAs are themselves epigenetic regulators (by altering gene expression without changing the genetic code) and interestingly have recently emerged as targets of epigenetic regulation, in that they are subject to promoter hypermethylation in oncogenesis.

Most miRNAs play a crucial role in cell proliferation, apoptosis and differentiation during development (Ambros, 2004; Bartel, 2004). Hence, it is not surprising that deregulation of miRNAs has been observed in many tumours. Advancements in miRNA microarray technology and qRT-PCR have encouraged the analysis of global miRNA expression profiles (Shi and Chiang, 2005). Moreover, miRNA expression profiling in cancer tissue has been utilised to define molecular subgroups in breast cancer (Blenkiron et al., 2007).

A number of miRNAs have been shown to target and regulate genes important for apoptosis. MiR-15/16 targets the Bcl2 protein and is deleted in 65% of chronic lymphocytic leukaemias (Calin and Croce, 2006) and may account for the increased expression of Bcl2 observed in these tumours. In addition, recent studies have identified the miR-34 family as direct p53 targets. Increased levels of miR-34 have been shown to induce apoptosis and cell cycle arrest (Figure 7.2) (Chang et al., 2007; Corney et al., 2007). Intriguingly, a study by Lodygin et al, 2008, identified miR-34 as a target of DNA hypermethylation. CpG methylation of miR-34a promoter was detected in 79.1% of primary prostate carcinomas and at a lower frequency in many other cancers (Lodygin et al.,

2005). This study is an excellent example of how DNA methylation and miRNAs are intimately involved in the deregulation of apoptosis in prostate cancer. To date, a clear prostate cancer miRNA profile has not been established (Coppola et al., 2009). Profiling miRNAs, whose gene targets are integral to control of apoptosis, via epigenetic or genetic mechanisms, would better our understanding of aberrant cell death and its role in prostate carcinogenesis.

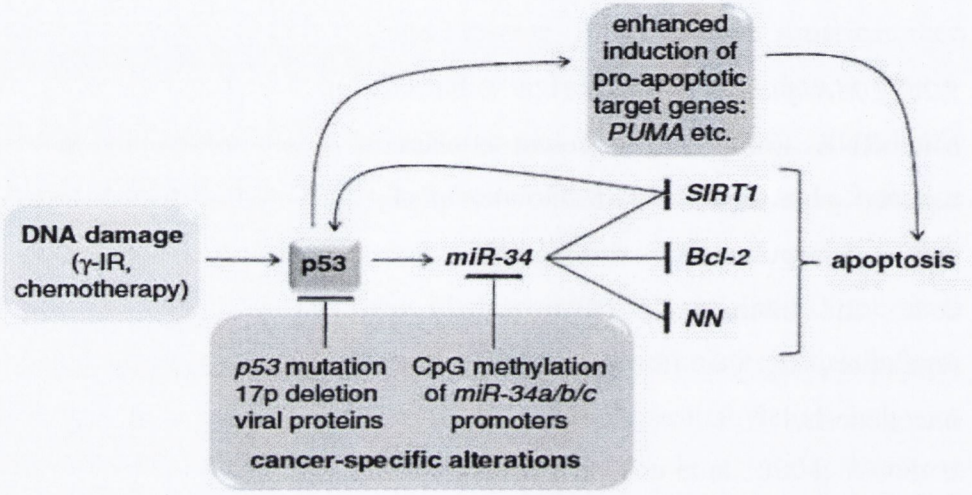

Figure 7.2.

P53/miR-34 pathway regulation of apoptosis. Mir-34 is a p53 target gene. miR-34 activation promotes apoptosis in two ways: 1) Inhibition of SIRT1, decreasing its deacetylation activity leads to increased transcription of p53 and 2) suppression of Bcl-2 and other anti-apoptotic proteins (NN). In cancer, the miR-34 promoter is often hypermethylated. As a result, the induction of apoptosis is diminished in response to p53 and this aids tumour growth and invasion of apoptosis. (Lodygin et al., 2005).

7.2.7.2 Histone modifications

Histone proteins are subject to a number of covalent modification at their N-terminal tails, including methylation, acetylation, phosphorylation, ubiquitylation and ADP-ribosylation (Schones and Zhao, 2008). Major advancements in genome-wide approaches for studying histone modifications have dramatically increased our knowledge about the function of these histone modifications.

The most established technique used to map histone modifications at a genomic scale has been the combination of Chromatin immunoprecipitation (ChIP) technology with DNA microarray, so called (ChIP-chip). Using this technique a number of functional enhancers and regulatory regions have been identified (Roh et al., 2006; Roh et al., 2007). Heintzman and colleagues have identified a signature of enhancers based on the pattern of histone modifications (Heintzman et al., 2007). Recently, utilising ChIP-chip technology, a genome-wide profile of histone H3 lysine 4 and lysine 27 trimethylation, histone modifications associated with transcriptional activation and repression, respectively, identified an epigenetic signature in prostate cancer (Ke et al., 2009). They found that loss and/or gain of these histone modifications were strongly associated with differential gene expression, including numerous miRNAs, between prostate cancer and normal cells.

In prostate cancer, profiling of histone modifications is in its infancy. Profiling a range of modifications, coupled with DNA methylation and miRNA profiling will provide a complete epigenetic picture in prostate cancer and help to further our understanding of coordinate deregulation of gene expression in prostate cancer.

7.3 CONCLUSION

In conclusion, DNA methylation is a rapidly advancing field of research in prostate cancer. While investigation into the methylation status of genes as biomarkers for diagnostic, prognostic and therapeutic approaches are at an early stage, a number of genes have been identified which show significant promise. The work presented in this thesis demonstrates the value of a combined *in silico* candidate gene selection approach and a novel DHPLC methylation screening strategy to identify new targets of aberrant methylation in prostate cancer. This comprehensive approach has identified a panel of apoptotic genes (*BIK*, *BNIP3*, *TMS1*, *DCR1*, *DCR2, cFLIP* and *CDK2NA*) showing aberrant DNA methylation and concurrent downregulation in gene expression. Three of these genes (*BIK*, *BNIP3*, *cFLIP*) are novel in relation to their methylation status in prostate cancer. Three genes (*TMS1*, *DCR1* and *DCR2*) identified in our study have previously shown utility as potential new

biomarkers of risk prediction in prostate cancer (Suzuki et al., 2006), while *CDKN2A* has previously been identified as aberrantly methylated in prostate cancer but whose utility as a prostate cancer biomarker was unknown. Further examination of the methylation profile of these 7 apoptotic-related genes in prostate cancer, HGPIN, normal adjacent prostate and BPH using QMSP identified 5 genes (*BNIP3, CDKN2A, DCR1, DCR2* and *TMS1*) which had a significantly higher frequency of methylation in their promoter CpG islands than normal prostate. Approximately 69% of tumour samples and 0% of normal tissues were methylated in at least one of our 5- apoptotic gene panel. Furthermore, this 5 gene "apoptotic methylation signature" is more frequently methylated in prostate cancer with higher Gleason score associated with a poorer prognosis. Moreover, combination of this panel of genes with *GSTP1* increased the frequency of methylation detected in prostate cancer from 80% to 89% than if *GSTP1* were used alone. Thus, we conclude that future examination of this "apoptotic methylation signature" in a larger cohort of patients to further access its role in a diagnostic and prognostic setting is justified, while study of the functional relevance of promoter hypermethylation "silencing" of these genes may also have relevance to therapeutic targeting in prostate cancer.

APPENDIX 1: PCR PRODUCTS GENERATED AND ANALYSED BY GEL ELECTROPHORESIS FOR EACH OF THE TARGET GENES IN THE PROSTATE CELL LINES

A1.1 PCR agarose gel analysis for the 7 prostate cell lines

APAF1

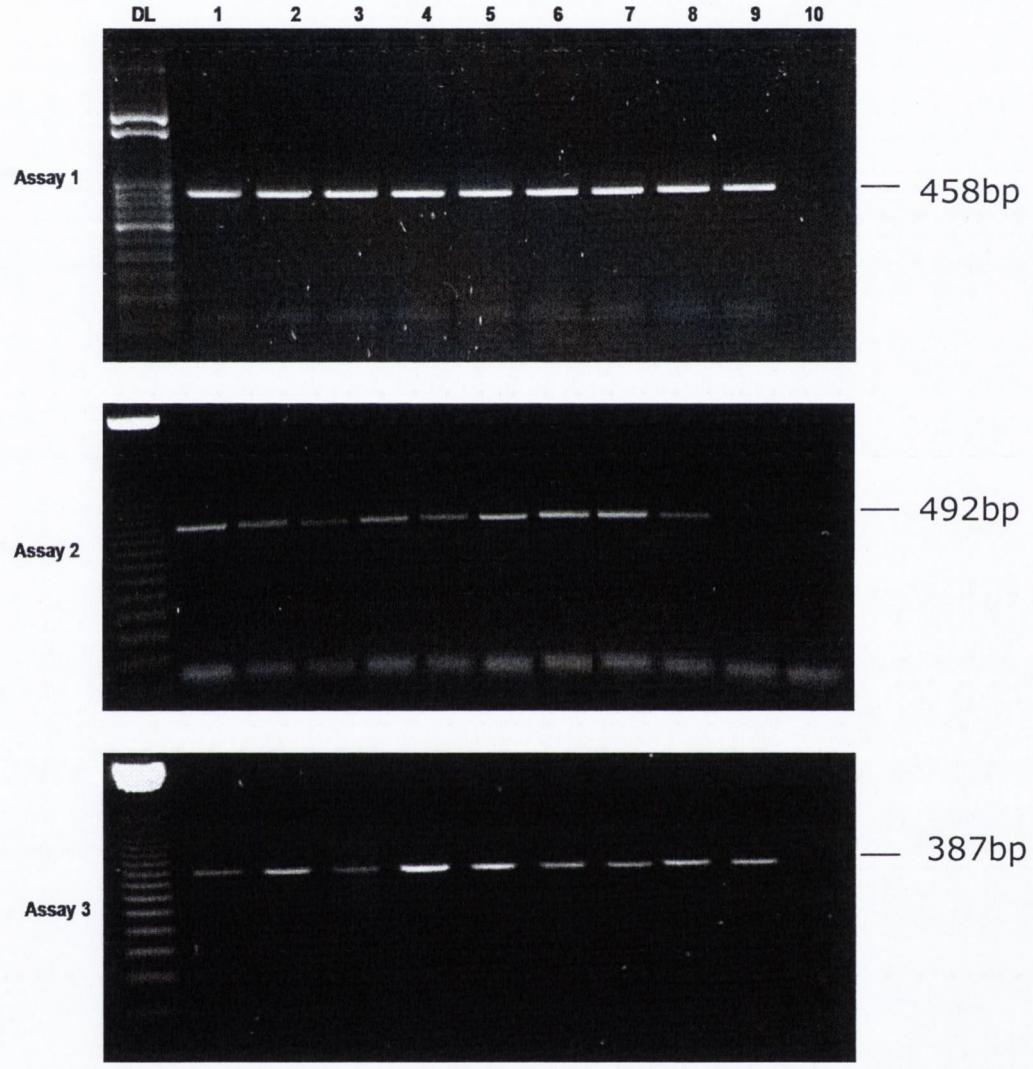

Figure A1.1

Gel analysis of APAF1 PCR products. DL= 50Kb DNA Ladder. Lane 1-10: RWPE1, PWR1E, 22RV1, RC58, DU145, LNCaP, PC3, MC (methylated control), Umeth A (unmethylated control A), water control. Bp= base pairs.

BIK

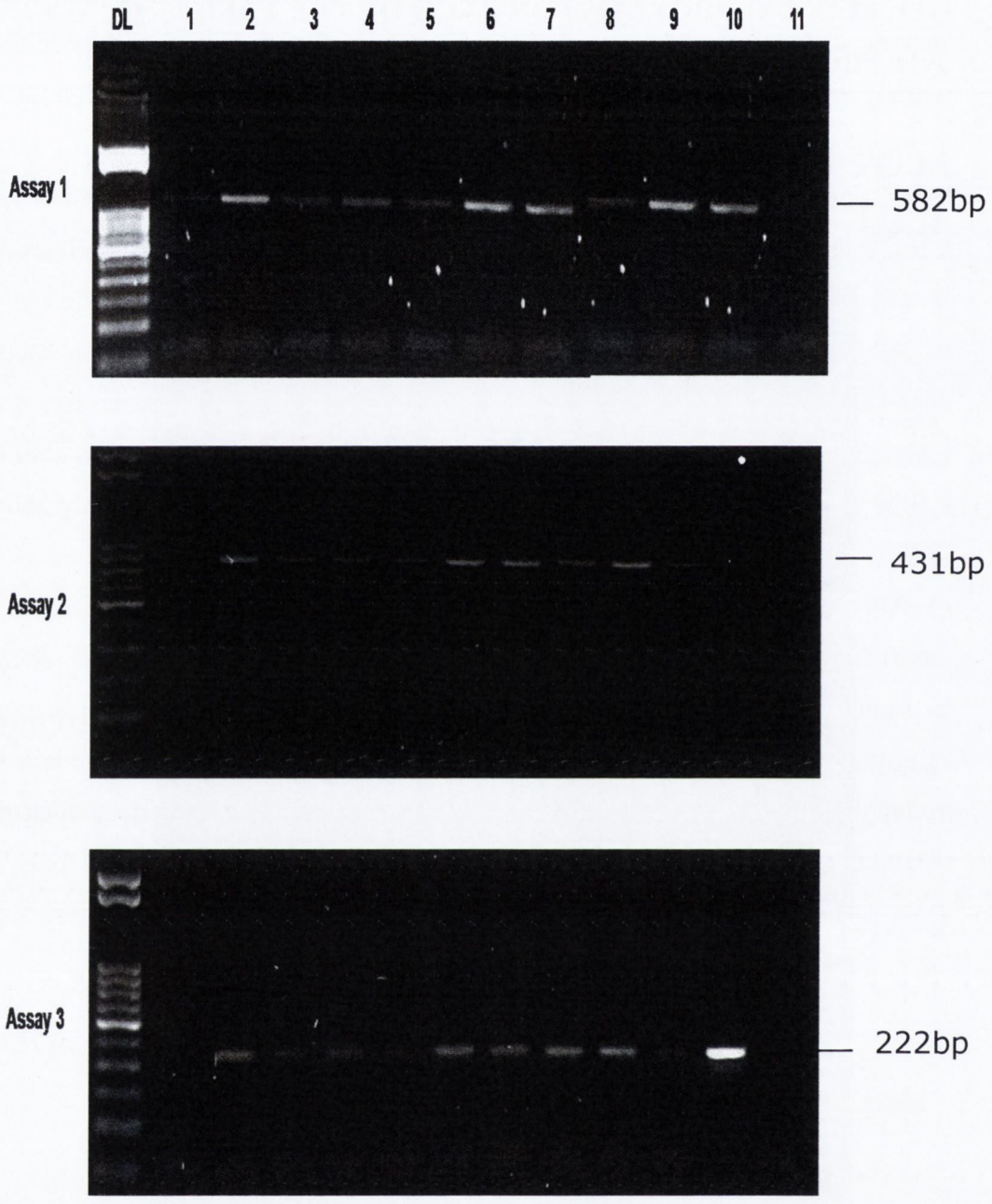

Figure A1.2

Gel analysis of BIK PCR products. DL= 50Kb DNA Ladder. Lane 1-10: RWPE1, PWR1E, 22RV1, RC58, DU145, LNCaP, PC3, MC (methylated control), Umeth A (unmethylated control A), Umeth B (unmethylated control B), water control. Bp= base pairs.

BNIP3

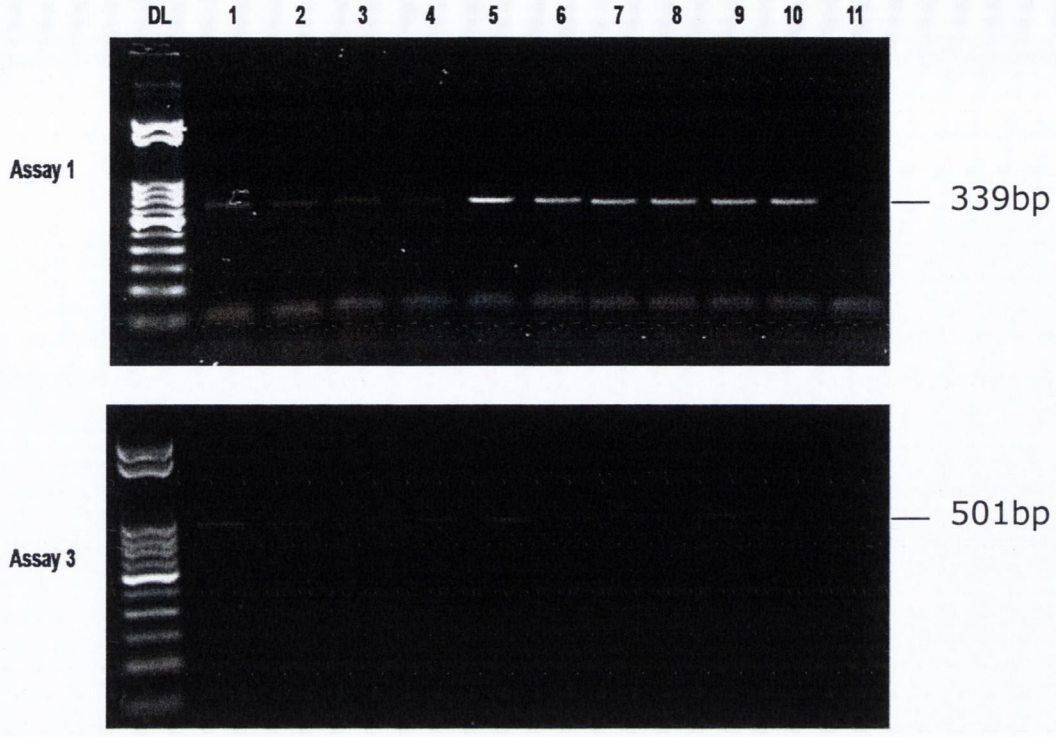

Figure A1.3

Gel analysis of BNIP3 PCR products. DL= 50Kb DNA Ladder. Lane 1-10: RWPE1, PWR1E, 22RV1, RC58, DU145, LNCaP, PC3, MC (methylated control), Umeth A (unmethylated control A), Umeth B (unmethylated control B), water control. Bp= base pairs.

CFLIP

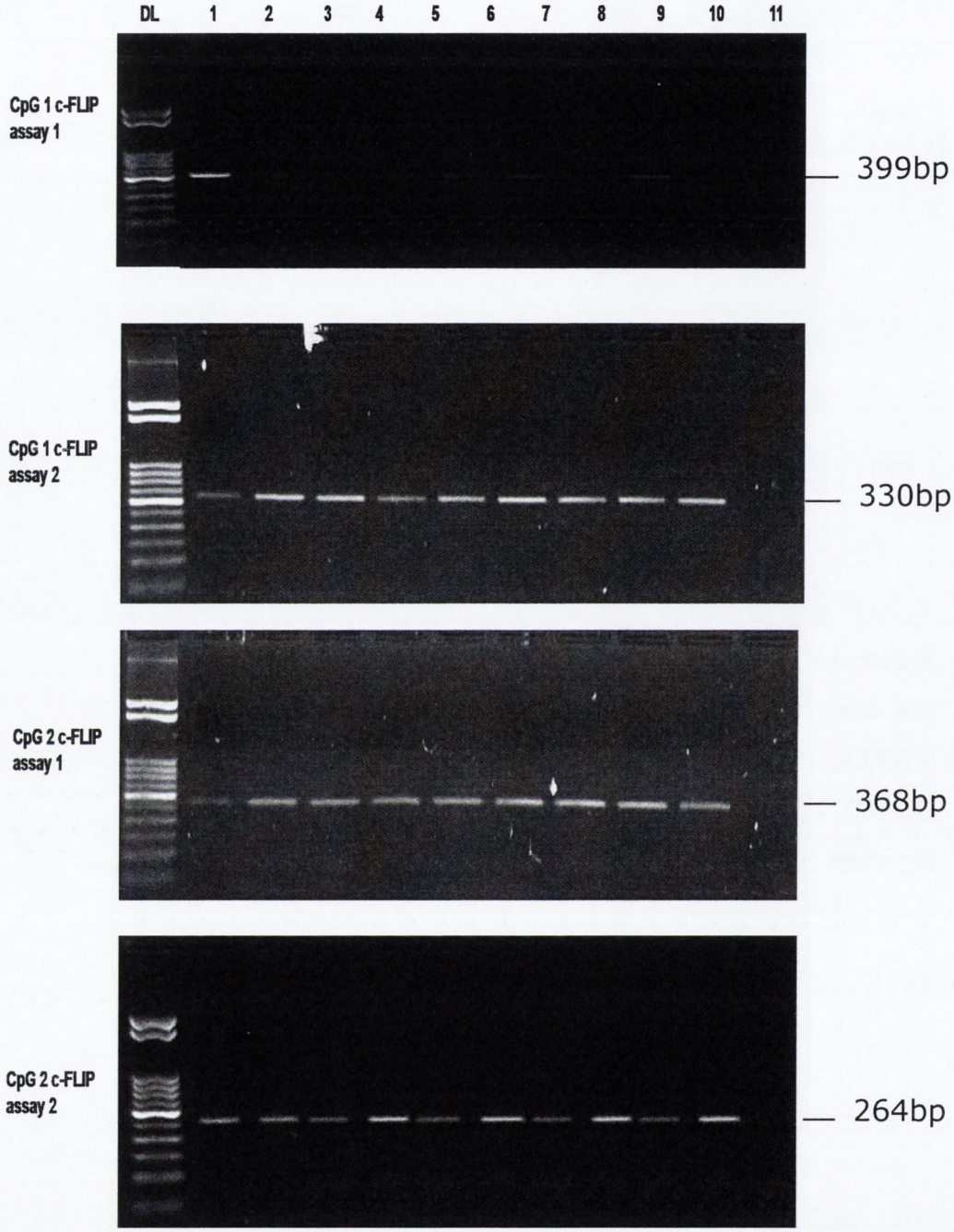

Figure A1.5

Gel analysis of cFLIP PCR products. DL= 50Kb DNA Ladder. Lane 1-10: RWPE1, PWR1E, 22RV1, RC58, DU145, LNCaP, PC3, MC (methylated control), Umeth A (unmethylated control A), Umeth B (unmethylated control B), water control. Bp= base pairs.

CASP8

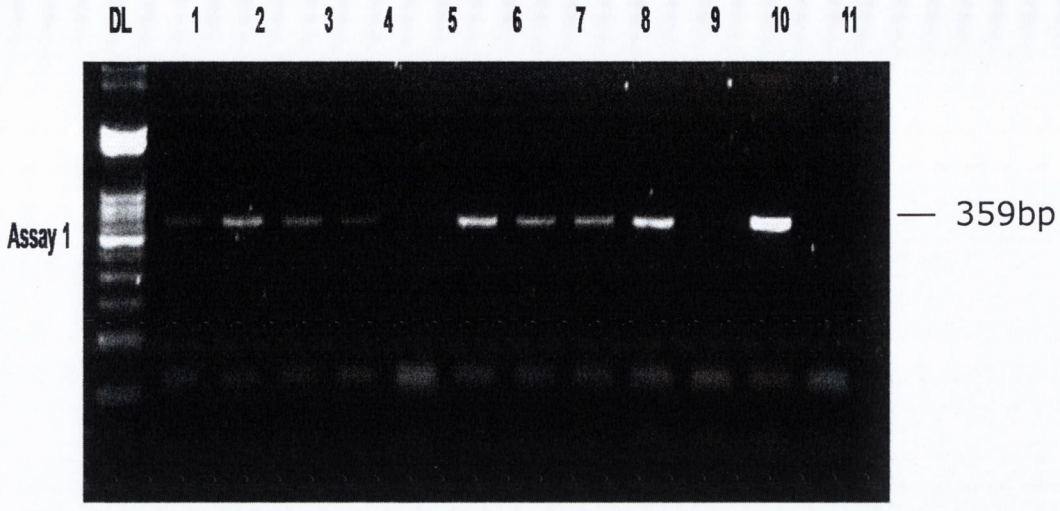

Figure A1.6

Gel analysis of CASP8 PCR products. DL= 50Kb DNA Ladder. Lane 1-10: RWPE1, PWR1E, 22RV1, RC58, DU145, LNCaP, PC3, MC (methylated control), Umeth A (unmethylated control A), Umeth B (unmethylated control B), water control. Bp= base pairs.

CASP3

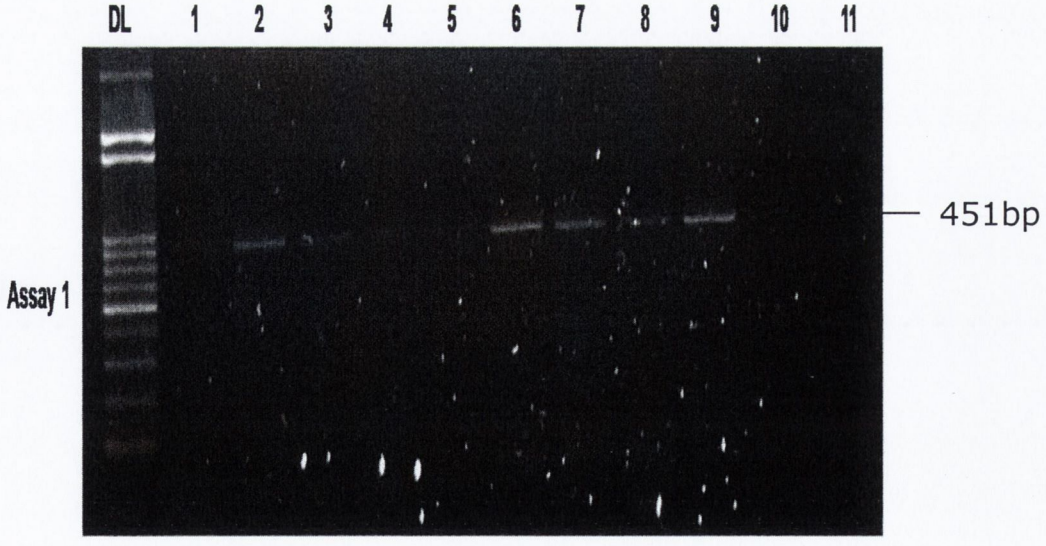

Figure A1.7

Gel analysis of CASP3 PCR products. DL= 50Kb DNA Ladder. Lane 1-10: RWPE1, PWR1E, 22RV1, RC58, DU145, LNCaP, PC3, MC (methylated control), Umeth A (unmethylated control A), Umeth B (unmethylated control B), water control. Bp= base pairs.

DCR1

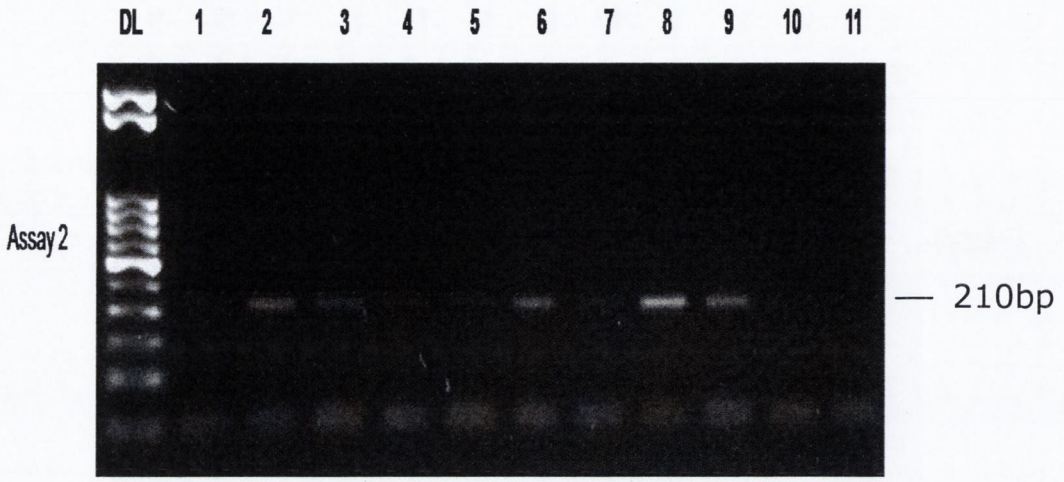

Figure 1.8

Gel analysis of DCR1 PCR products. DL= 50Kb DNA Ladder. Lane 1-10: RWPE1, PWR1E, 22RV1, RC58, DU145, LNCaP, PC3, MC (methylated control), Umeth A (unmethylated control A), Umeth B (unmethylated control B), water control. Bp= base pairs.

DCR2

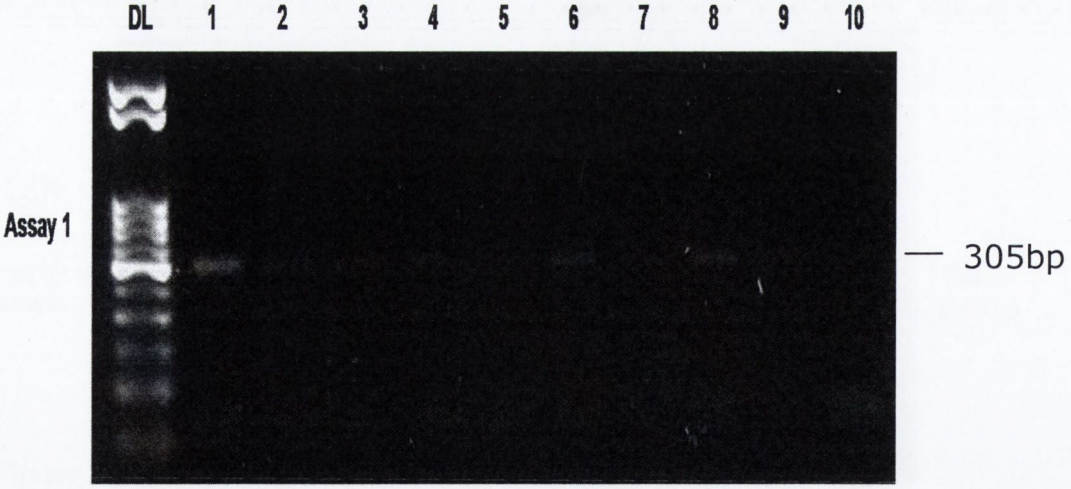

Figure A1.9

Gel analysis of DCR2 PCR products. DL= 50Kb DNA Ladder. Lane 1-10: RWPE1, PWR1E, 22RV1, RC58, DU145, LNCaP, PC3, MC (methylated control), Umeth A (unmethylated control A), water control. Bp= base pairs.

DR5

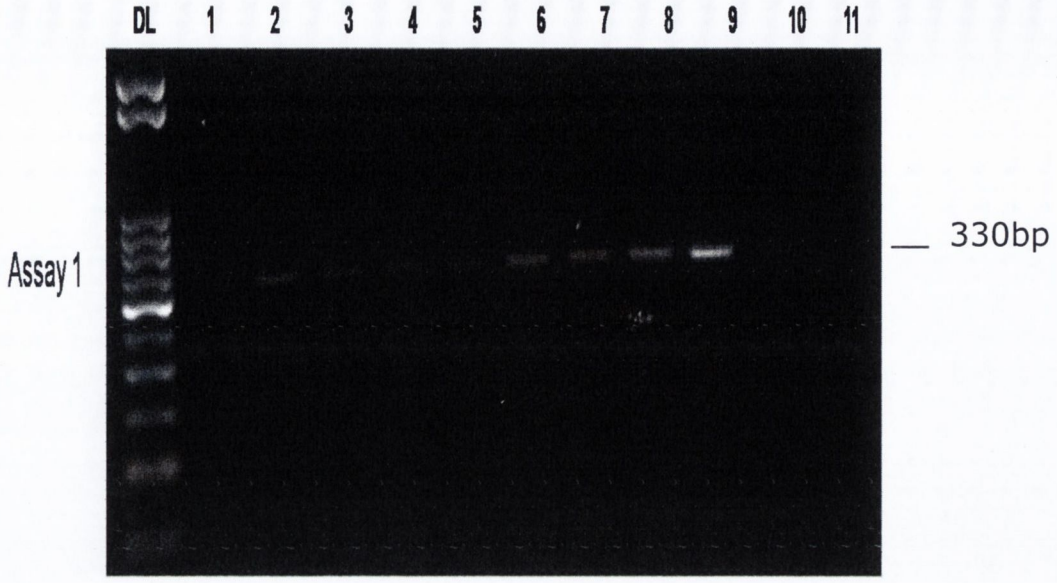

Figure A1.10

Gel analysis of DR5 PCR products. DL= 50Kb DNA Ladder. Lane 1-10: RWPE1, PWR1E, 22RV1, RC58, DU145, LNCaP, PC3, MC (methylated control), Umeth A (unmethylated control A), Umeth B (unmethylated control B), water control. Bp= base pairs.

FADD

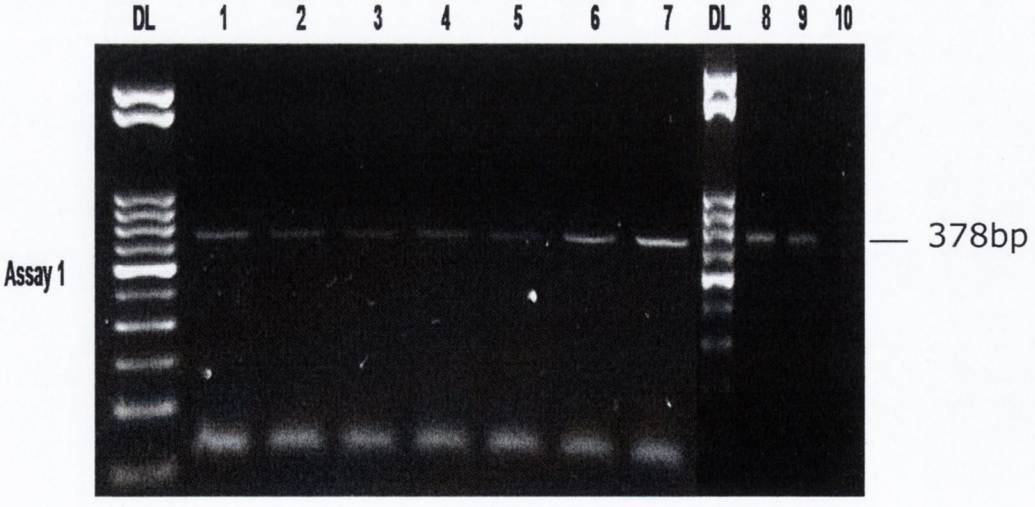

Figure A1.11

Gel analysis of FADD PCR products. DL= 50Kb DNA Ladder. Lane 1-10: RWPE1, PWR1E, 22RV1, RC58, DU145, LNCaP, PC3, MC (methylated control), Umeth A (unmethylated control A), water control. Bp= base pairs.

PIGPC1

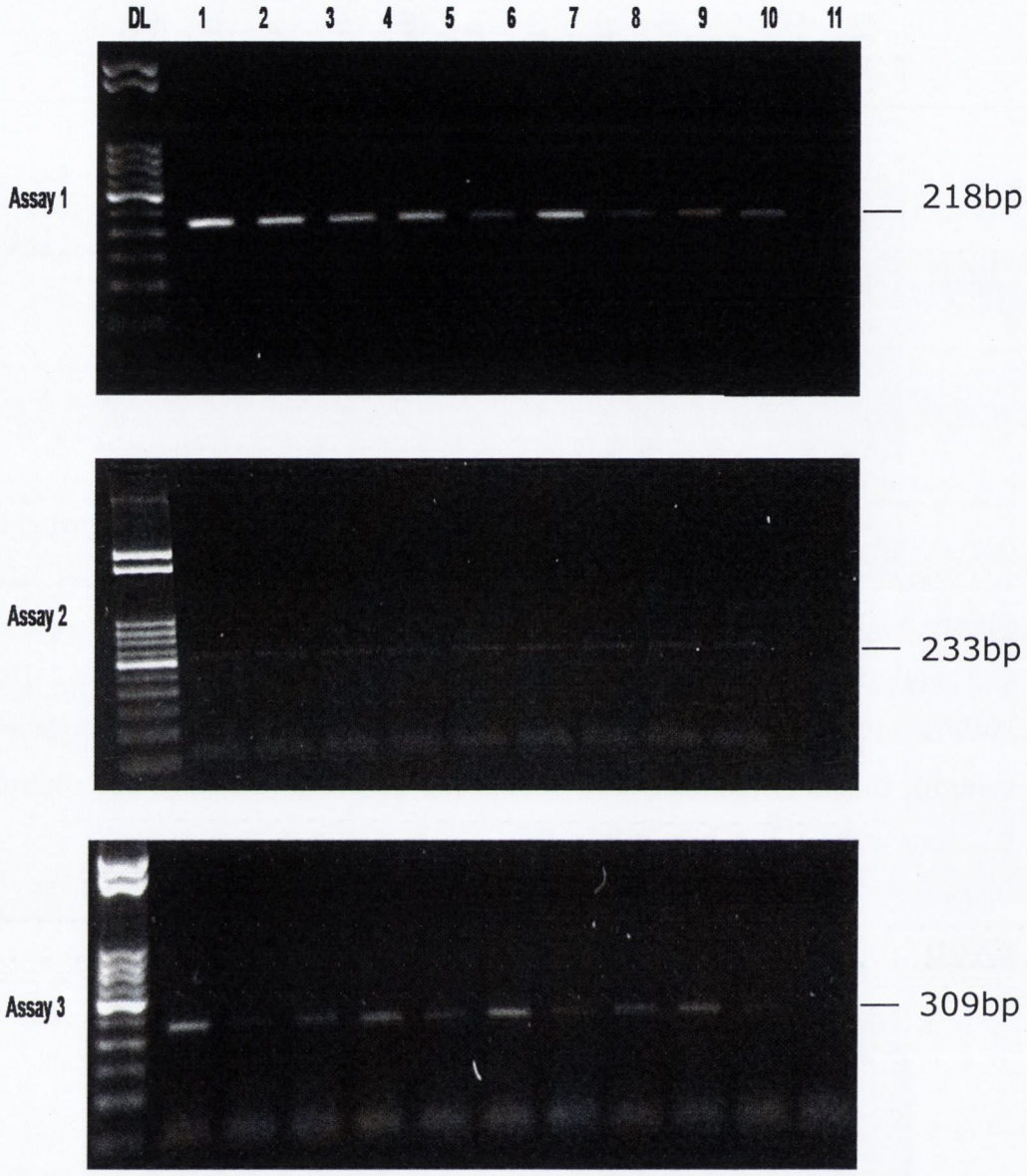

Figure A1.12

Gel analysis of PIGPC1 PCR products. DL= 50Kb DNA Ladder. Lane 1-10: RWPE1, PWR1E, 22RV1, RC58, DU145, LNCaP, PC3, MC (methylated control), Umeth A (unmethylated control A), Umeth B (unmethylated control B), water control. Bp= base pairs.

TMS1

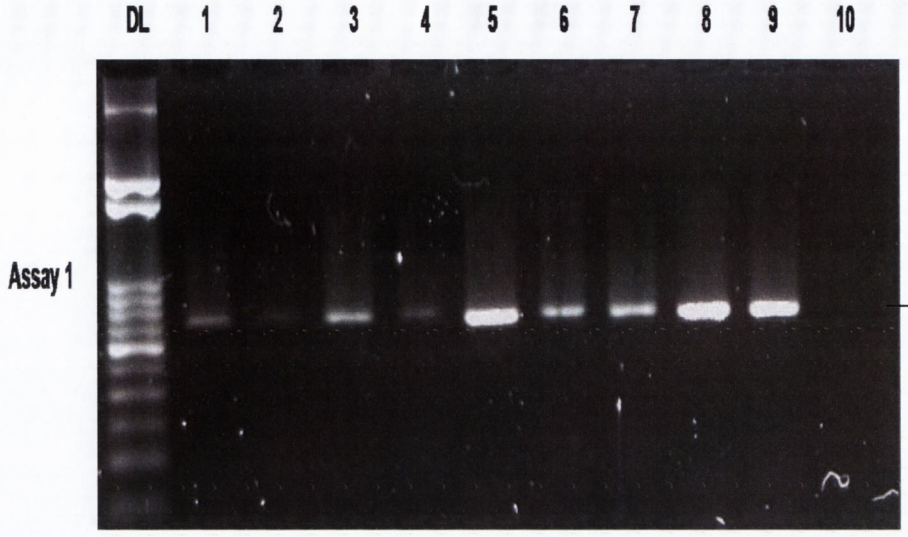

Figure A1.13

Gel analysis of TMS1 PCR products. DL= 50Kb DNA Ladder. Lane 1-10: RWPE1, PWR1E, 22RV1, RC58, DU145, LNCaP, PC3, MC (methylated control), Umeth A (unmethylated control A), water control. Bp= base pairs.

APPENDIX 2. DHPLC CHROMATOGRAMS.

A2.1 DHPLC chromatograms

DHPLC Chromatograms for all cell lines for all genes with evidence of methylation except *DCR1* and *TMS1*, both of which are methylated in all prostate cell lines examined and are illustrated in figure 4.2.

A. BIK assay 1

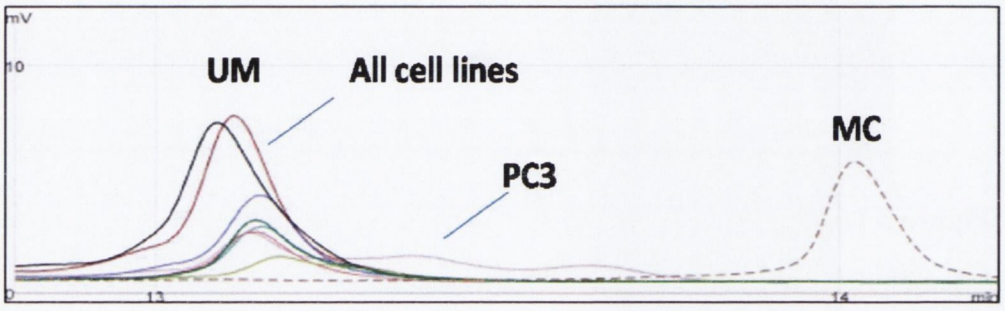

B. BNIP3

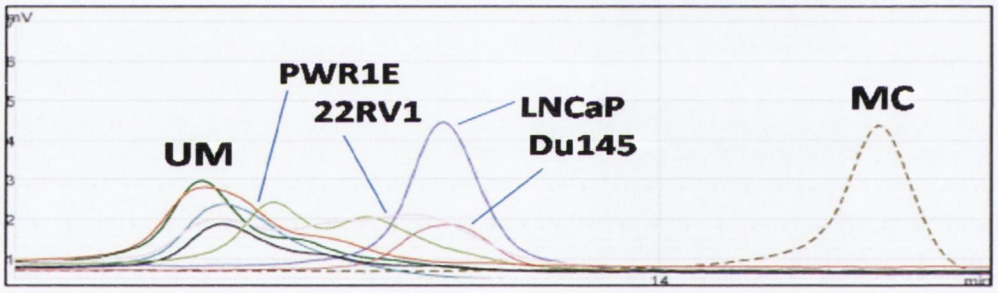

C. CDKN2A

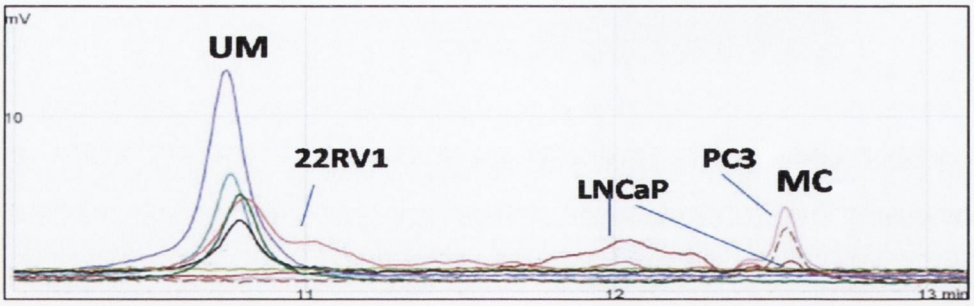

Figure A.2.1

DHPLC chromatograms. (A-H) illustrates chromatograms for all cell lines. The methylated control is labelled by MC and highlighted by a dashed brown line. The unmethylated control is illustrated by a green line. Each coloured line represents individual cell line elution profiles. Cell lines with evidence of methylation are labelled. All other cell lines elute at the same time as the unmethylated control.

D. cFLIP CpG1 assay 1

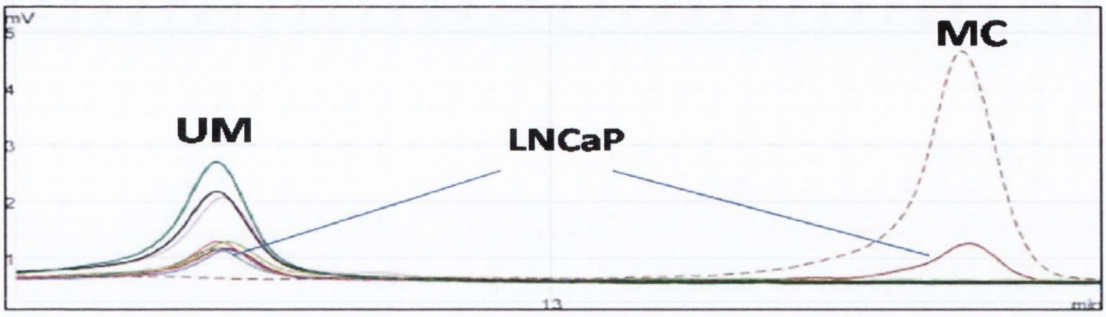

E. cFLIP CpG1 assay 2

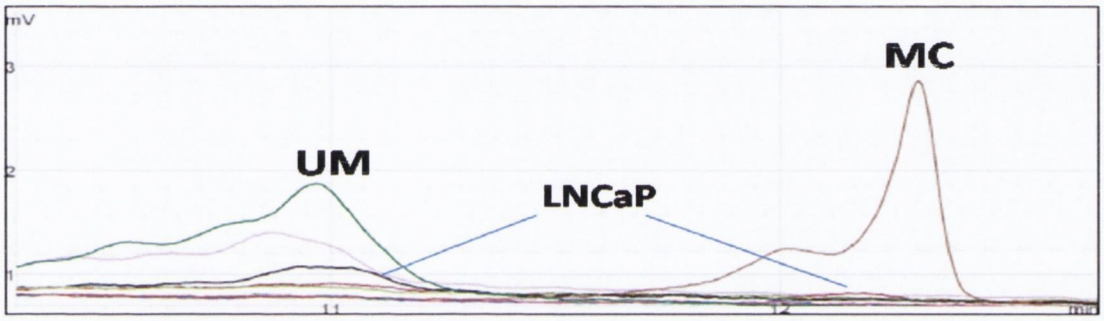

F. cFLIP CpG2 assay 1

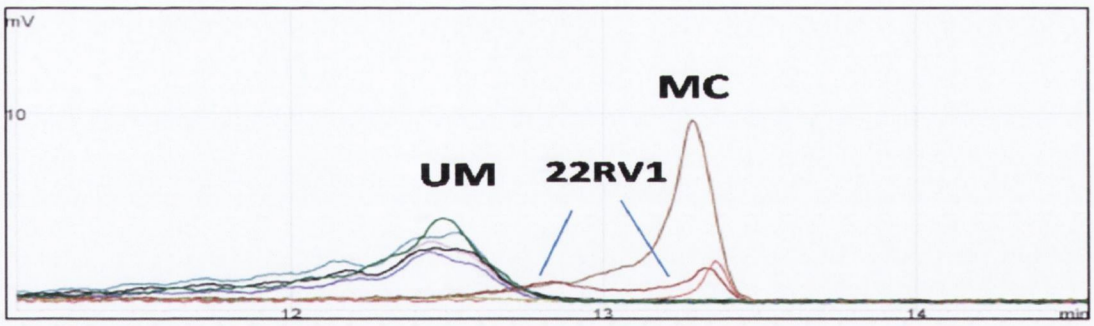

Figure A.2.1 Contd.

DHPLC chromatograms. (A-H) illustrates chromatograms for all cell lines. The methylated control is labelled by MC and highlighted by a dashed brown line. The unmethylated control is illustrated by a green line. Each coloured line represents individual cell line elution profiles. Cell lines with evidence of methylation are labelled. All other cell lines elute at the same time as the unmethylated control.

G. cFLIP CpG2 assay 2

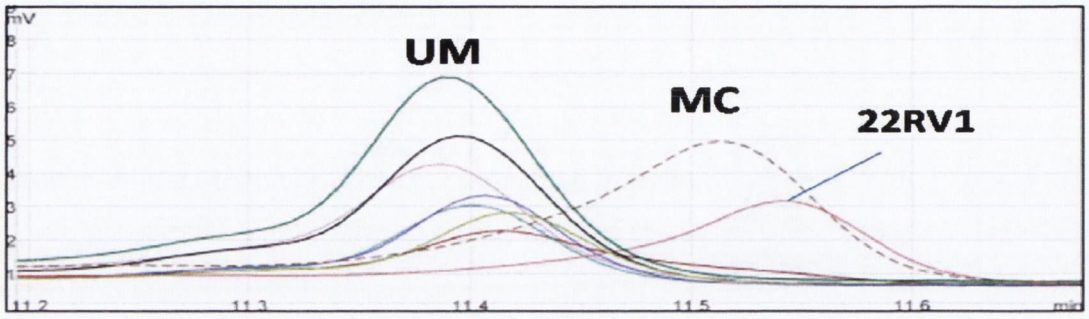

H. DCR2

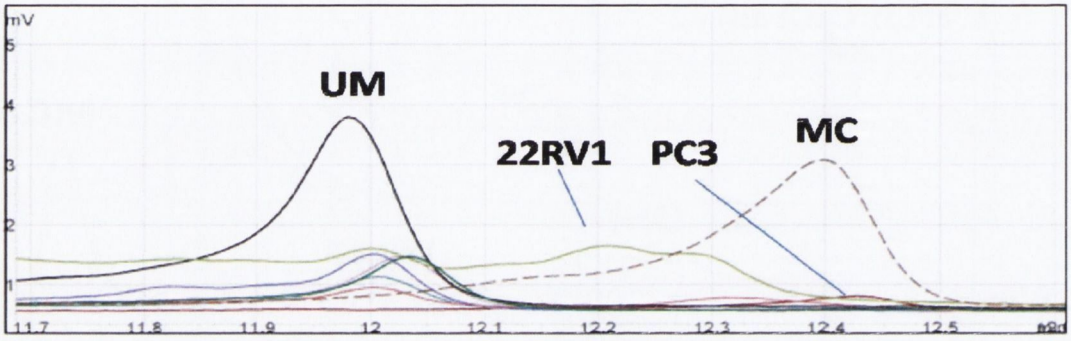

Figure A.2.1 Contd.

DHPLC chromatograms. (A-H) illustrates chromatograms for all cell lines. The methylated control is labelled by MC and highlighted by a dashed brown line. The unmethylated control is illustrated by a green line. Each coloured line represents individual cell line elution profiles. Cell lines with evidence of methylation are labelled. All other cell lines elute at the same time as the unmethylated control.

APPENDIX 3: TRANSCRIPTIONAL ELEMENTS ASSOCIATED WITH PROMOTER REGIONS

Below is a list of transcriptional elements associated with promoter regions for each gene. The transcriptional elements are predicted using promoter scan software (http://www-bimas.cit.nih.gov). Table A3.1- A3.5 lists transcription factors, their binding site and sequence and location for our 7-gene panel. Table A3.6 outlines the IUB ambiguity code. Symbols for describing mixed base position in an oligonucleotide sequence are given in the ambiguity code (Nomenclature Committee of the International Union of Biochemistry1985).

Table A3.1. Predicted transcription factor binding sites for BIK that cover CpG sites

Transcription factor	Binding site	Binding sequence#	Location (bp)*
AP-2	AP-2 CS6	CCCCTCG	-13550
HSV IE repeat	HSV IE repeat	GCGGAA	-13418
UCE.2	UCE.2	GGCCG	-13417
Sp1	Sp1 CS1	GGGGCGGACC	-13382
T-Ag	T-Ag-SV40.3	GGGGC	-13382
Sp1	Sp1-SV40.1	GGGGCGGG	-13370
Sp1	Sp1-SV40.4	GGGCGG	-13364
Sp1	Sp1-hsp70 (1)	GGCGGG	-13363
AP-2	AP-2 CS6	CCCCGCC	-13366
APRT	APRT-mouse US	GCCCCGCC	-13367
GCF	GCF CS	GCGGGGC	-13354
Sp1	Sp1-DHFR.3	GGGGCGGGGC	-13357

* Relative to the ATG translational start site # See IUB ambiguity codes

Table A3.2. Predicted transcription factor binding sites for BNIP3 that cover CpG sites

Transcription factor	Binding site	Binding sequence#	Location (bp)*
AP-2	AP-2 CS4	CCCCCACGCC	-1033
AP-2	AP-2 CS6	CCCCACGC	-1032
UCE.2	UCE.2	CGGCC	-987
EARLY-SEQ1	EARLY-SEQ1	CTCCGCCC	-973
Sp1	Sp1-IE-3.4	CCGCC	-971
T-Ag	T-Ag-SV40.3	GGGGC	-958
SIF	SIF core RS	CCCGTC	-956
Sp1	Sp1-IE-3.3	GGGCGT	-952
AP-2	AP-2 CS6	CCCGGGG	-940
Sp1	Sp1-IE-3.3	CCCGCC	-936
Sp1	Sp1-SV40.1	CCCGCCCC	-929
GCF	GCF CS	GCGCGCC	-883
Sp1	Sp1-SV40.4	GGGCGG	-800
AP-2	AP-2 CS6	CCCMNSSS	-477
AP-2	AP-2 CS4	YCSCCMNSSS	-445
Sp1	Sp1-IE-3.4	CCGCCC	-445
SP1	Sp1-IE-3.3	CCCGCC	-445
TTR_inverted _repeat	TTR inverted repeat	CGCCGCG	-431
PEBP2	PEBP2 RS	GACCGC	-428
GCF	GCF CS	SCGSSSC	-406
Ap-2	AP-2 CS3	CCSCRGGC	-396
UCE.2	UCE.2	GGCCG	-384
AP-2	AP-2 CS4	YCSCCMNSSS	-358
Sp1	Sp1-IE-3.4	CCGCCC	-358
APRT-mouse_US	APRT-mouse US	GCCCCGCC	-353
EARLY-SEQ1	EARLY-SEQ1	YYCCGCCC	-333
(Sp1)	(Sp1)-TK.1	CCCCGCCC	-332
Sp1	Sp1-IE-3.3	CCCGCC	-331
Sp1	Sp1-hsp70 (1)	GGCGGG	-326
Sp1	Sp1-SV40.1	GGGGCGGG	-324
AP-2	AP-2 CS3	CCSCRGGC	-300
Ap-2	AP-2 CS4	YCSCCMNSSS	-267
GCF	GCF CS	SCGSSSC	-259
GCF	GCF CS	SCGSSSC	-535

* Relative to the ATG translational start site # See IUB ambiguity codes

Table A3.3. Predicted transcription factor binding sites for CDK2NA that cover CpG sites

Transcription factor	Binding site	Binding sequence#	Location (bp)*
SP1	Sp1-hsp70	GGCGGG	+9
UCE.2	UCE.2	GGCCG	+51
KROX.24	KROX24 CS	GCGSGGGCG	+96
SP1	Sp1-hsp70	GGCGGG	+97
GCF	GCF CS	SCGSSSC	+139
SP1	Sp1-hsp70	GGCGGG	+181

* Relative to the ATG translational start site # See IUB ambiguity codes

Table A3.4. Predicted transcription factor binding sites for CpG1 CFLIP that cover CpG sites

Transcription factor	Binding site	Binding sequence#	Location (bp)*
Sp1	Sp1-hsp70 (1)	GGCGG	-13195
KROX24	KROX24 CS	GCGGGGGCG	-13194
T-Ag	T-Ag-SV40.3	GGGGC	-13191
AP-2	AP-2 CS3	CCGCGGGC	-13137
EARLY-SEQ1	EARLY-SEQ1	TTCCGCCC	-13105
Sp1	Sp1-IE-3.4	CCGCCC	-13103
T-Ag	T-Ag-SV40.3	GGGGC	-13042
UCE.2	UCE.2	GGCCG	-12965
Sp1	Sp1-IE-3.4	CCGCCC	-12963

* Relative to the ATG translational start site # See IUB ambiguity codes

Table A3.5. Predicted transcription factor binding sites for TMS1 that cover CpG sites

Transcription factor	Binding site	Binding sequence[#]	Location (bp)*
c-fos.5	c-fos.5	GCGCCACC	-297
GCF	GCF CS	SCGSSSC	-273
UCE.2	UCE.2	GGCCG	-271
UCE.1	UCE.1	GTCCGT	-167
T-Ag	T-Ag-SV40.3	GGGGC	-129
Sp1	Sp1-SV40.1	GGGGCGGG	-127
Sp1	Sp1-SV40.4	GGGCGG	-126
Sp1	Sp1-hsp70 (1)	GGCGGG	-125
Sp1	Sp1-IE-3.4	CCGCCC	-121
Sp1	Sp1-IE-3.3	CCCGCC	-120
AP-2	AP-2 CS6	CCCMNSSS	-119
EARLY-SEQ1	EARLY-SEQ1	YYCCGCCC	-119
(Sp1)	(Sp1)-TK.1	CCCCGCCC	-119
EARLY-SEQ1	EARLY-SEQ1	YYCCGCCC	-78
Sp1	Sp1-IE-3.4	CCGCCC	-76
HSV_IE_repeat	HSV IE repeat	GCGGAA	-73
JCV_repeated_sequenc	JCV repeated sequence	GGGNGGRR	-71
Sp1	Sp1-SV40.4	GGGCGG	-71

* Relative to the ATG translational start site # See IUB ambiguity codes

Table A4.6. IUB Ambiguity code

Symbol	Mixed Base composition	Origin of designation
R	A + G	puRine
M	A + C	aMino
W	A + T	Weak interation (3 H bonds)
Y	C + T	pYrimidine
S	C + G	Strong interation (3H bonds)
K	G + T	Keto
V	A + C + G	not-T (not-U), V follows U
H	A + C + T	not-G, H follows G in the alphabet
D	A + G + T	not-C, D follows C
B	C + G + T	not-A, B follows A
N	A + G + C + T	aNy

IUB: International Union of Biochemistry

APPENDIX 4. TAQMAN REAL-TIME PCR PRIMER AND PROBE OPTIMISATION AND VALIDATION

A4.1 QMSP primer/probe optimisation

A primer/probe optimisation experiment was performed using universal methylated DNA in triplicate (described in Section 2.5.7.2). The primer/probe concentration, which yielded the highest ΔRn value and lowest C_T value were chosen for analysis of levels of expression of the genes in prostate cell lines.

A4.1.1 BIK QMSP primer and probe optimisation

Table A4.1 BIK Primer/Probe optimisation

[Primer, Probe] (nM)	Mean CT	SD
300,100	29.489	0.737
300,200	29.734	0.083
300,300	29.608	0.237
900,100	29.419	0.164
900,200	29.388	0.075
900,300	29.447	0.249

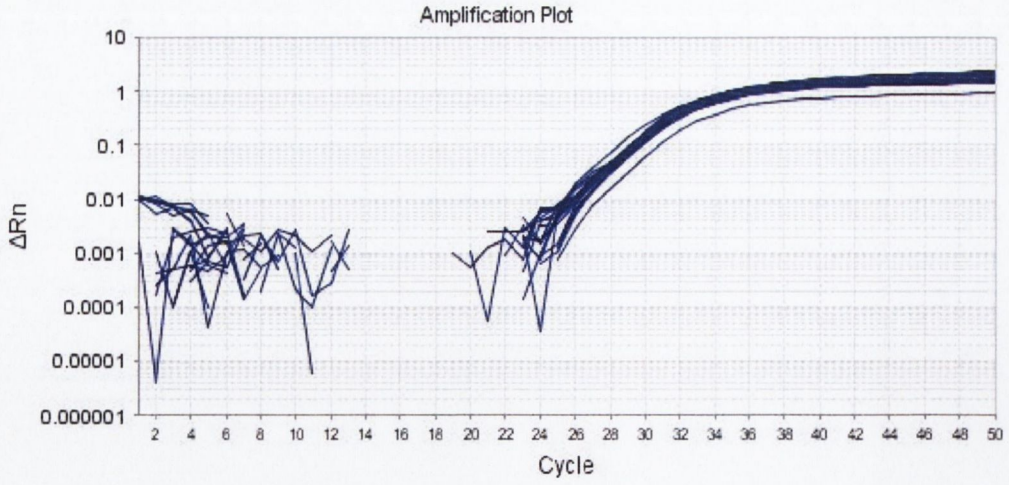

Figure A4.1

***BIK* QMSP primer/probe optimisation.** Amplification plot of ΔRn versus PCR cycle. The primer/probe combination, which gives the highest ΔRn and lowest Ct value was chosen.

A final primer and probe concentration of 900nM and 200nM, respectively, was selected for optimal reaction conditions for *BIK* methylation analysis using QMSP.

A4.1.2 BNIP3 QMSP primer and probe optimisation

Table A4.2 BNIP3 Primer/Probe optimisation

[Primer, Probe] (nM)	Mean CT	SD
300,100	30.556	0.247
300,200	30.057	0.78
300,300	29.959	0.135
900,100	29.855	0.062
900,200	29.491	0.173
900,300	29.739	0.181

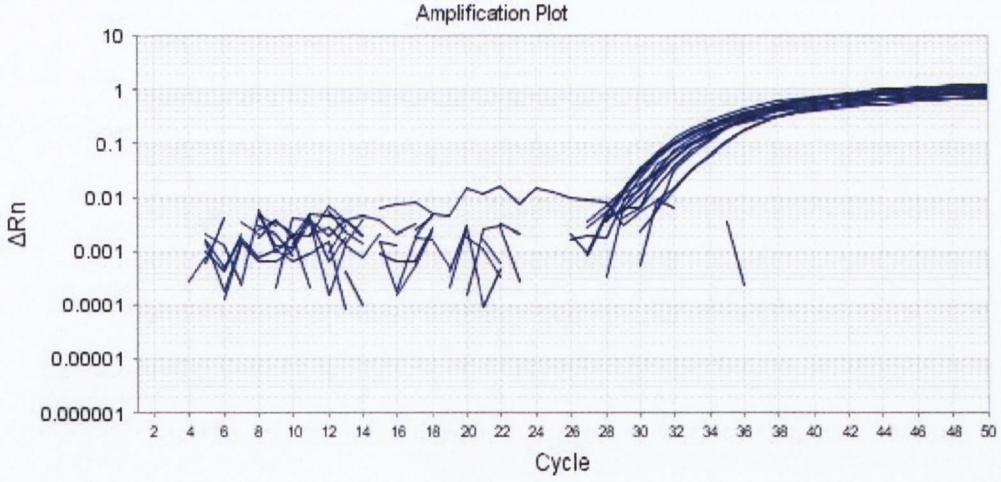

Figure A4.2

***BNIP3* QMSP primer/probe optimisation.** Amplification plot of ΔRn versus PCR cycle. The primer/probe combination, which gives the highest ΔRn and lowest Ct value was chosen.

A final primer and probe concentration of 900nM and 200nM, respectively, was selected for optimal reaction conditions for *BNIP3* methylation analysis using QMSP.

A4.1.3 CDKN2A QMSP primer and probe optimisation

Table A4.3 CDK2NA Primer/Probe optimisation		
[Primer, Probe] (nM)	Mean CT	SD
300,100	27.561	0.131
300,200	27.678	0.113
300,300	27.777	0.125
900,100	27.307	0.393
900,200	27.799	0.116
900,300	27.991	0.09

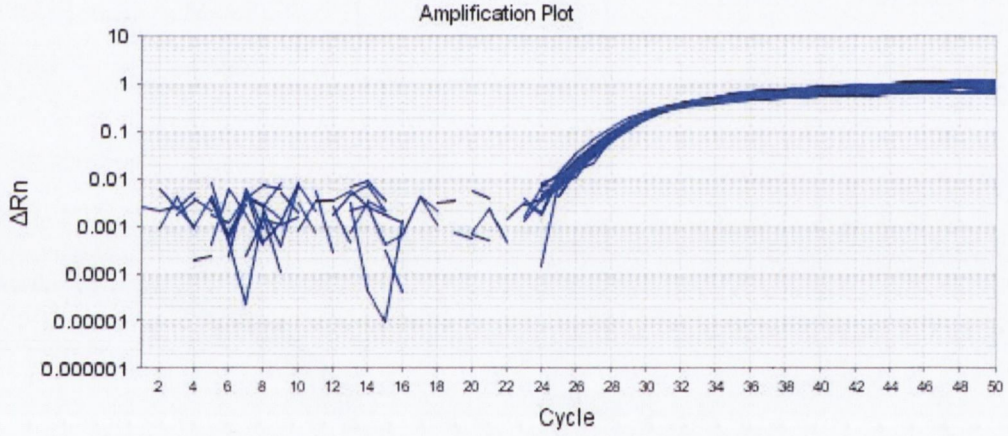

Figure A4.3

***CDKN2A* QMSP primer/probe optimisation.** Amplification plot of ΔRn versus PCR cycle. The primer/probe combination, which gives the highest ΔRn and lowest Ct value was chosen.

A final primer and probe concentration of 300nM and 300nM, respectively, was selected for optimal reaction conditions for *CDKN2A* methylation analysis using QMSP.

A4.1.4 CpG1 cFLIP QMSP primer and probe optimisation

Table A4.4 CpG 1 cFLIP Primer/Probe optimisation		
[Primer, Probe] (nM)	Mean CT	SD
300,100	30.722	0.113
300,200	31.567	0.578
300,300	30.890	0.678
900,100	32.990	0.908
900,200	33.680	0.976
900,300	32.900	0.890

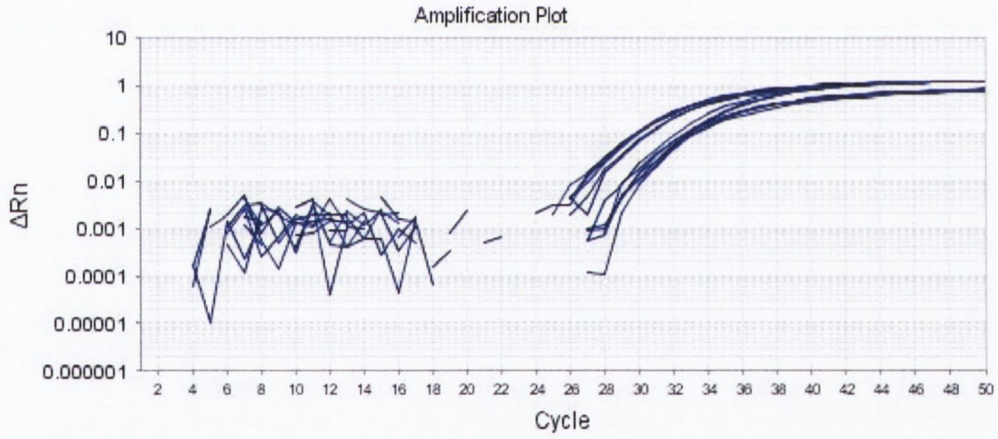

Figure A4.4

***CpG1 cFLIP* QMSP primer/probe optimisation.** Amplification plot of ΔRn versus PCR cycle. The primer/probe combination, which gives the highest ΔRn and lowest Ct value was chosen.

A final primer and probe concentration of 300nM and 100nM, respectively, was selected for optimal reaction conditions for *CpG1 cFLIP* methylation analysis using QMSP.

A4.1.5 CpG2 cFLIP QMSP primer and probe optimisation

Table A4.5 CpG 2 cFLIP Primer/Probe optimisation		
[Primer, Probe] (nM)	Mean CT	SD
300,100	30.06739426	0.113
300,200	32.06759996	0.342
300,300	32.80807257	0.781
900,100	32.09906592	0.564
900,200	31.79794257	0.342
900,300	32.06770809	0.213

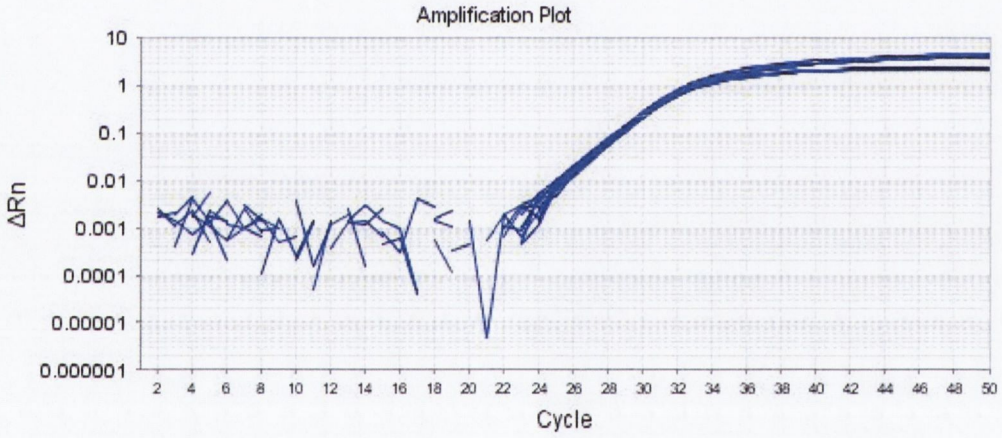

Figure A4.5

***CpG2 cFLIP* QMSP primer/probe optimisation.** Amplification plot of ΔRn versus PCR cycle. The primer/probe combination, which gives the highest ΔRn and lowest Ct value was chosen.

A final primer and probe concentration of 900nM and 100nM, respectively, was selected for optimal reaction conditions for ***CpG2 cFLIP*** methylation analysis using QMSP.

A4.1.6 DCR1 QMSP primer and probe optimisation

Table A4.6 DCR1 Primer/Probe optimisation		
[Primer, Probe] (nM)	Mean CT	SD
300,100	28.209	0.104
300,200	28.452	0.123
300,300	29.077	0.041
900,100	28.056	0.118
900,200	28.409	0.256
900,300	28.565	0.101

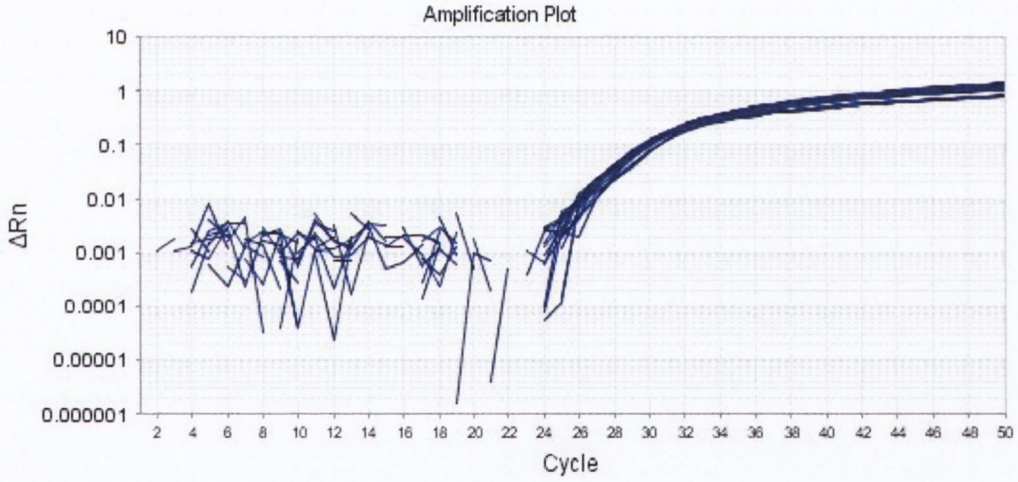

Figure A4.6

***DCR1* QMSP primer/probe optimisation.** Amplification plot of ΔRn versus PCR cycle. The primer/probe combination, which gives the highest ΔRn and lowest Ct value was chosen.

A final primer and probe concentration of 900nM and 100nM, respectively, was selected for optimal reaction conditions for *DCR1* methylation analysis using QMSP.

A4.1.7 DCR2 QMSP primer and probe optimisation

Table A4.7 DCR2 Primer/Probe optimisation		
[Primer, Probe] (nM)	Mean CT	SD
300,100	30.904	0.024
300,200	30.691	0.136
300,300	31.038	0.064
900,100	30.84	0.173
900,200	30.524	0.047
900,300	30.761	0.054

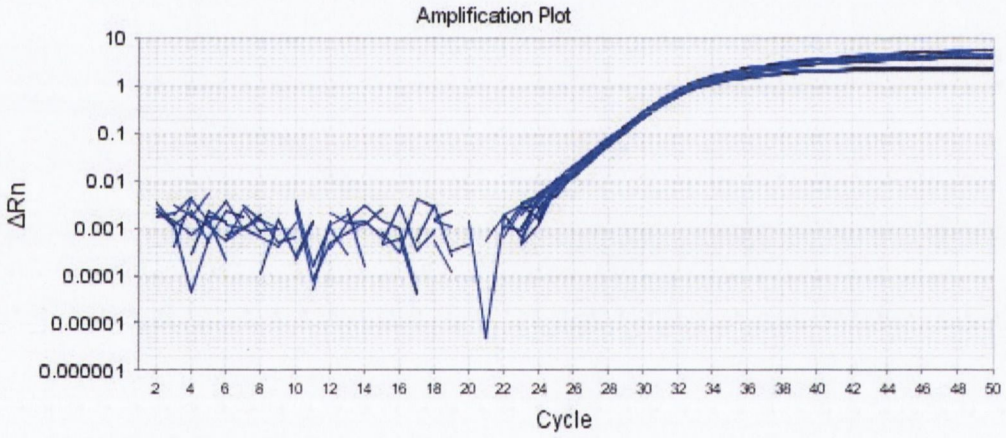

Figure A4.7

***DCR2* QMSP primer/probe optimisation.** Amplification plot of ΔRn versus PCR cycle. The primer/probe combination, which gives the highest ΔRn and lowest Ct value was chosen.

A final primer and probe concentration of 900nM and 200nM, respectively, was selected for optimal reaction conditions for *DCR2* methylation analysis using QMSP.

A4.1.8 TMS1 QMSP primer and probe optimisation

Table A4.8 TMS1 Primer/Probe optimisation		
[Primer, Probe] (nM)	Mean CT	SD
300,100	27.501	0.153
300,200	27.908	0.215
300,300	28.411	0.285
900,100	27.284	0.154
900,200	27.359	0.465
900,300	27.285	0.095

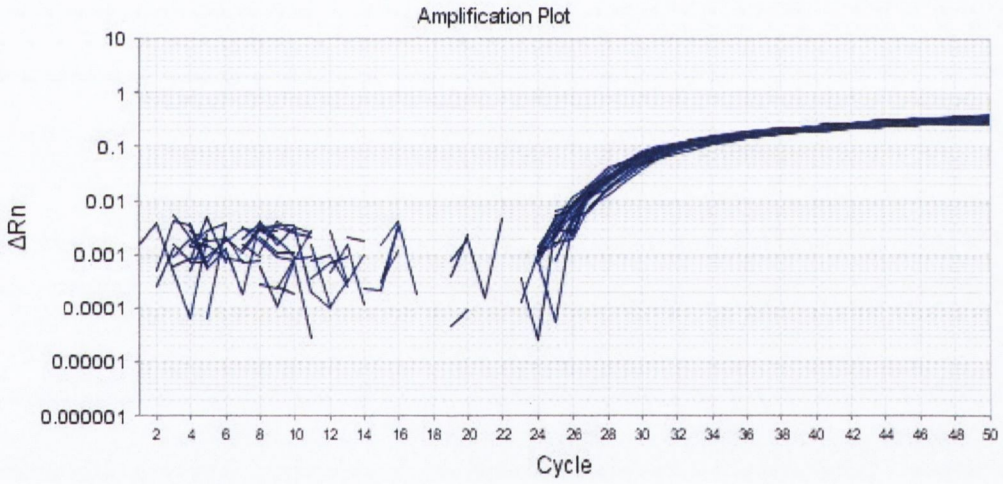

Figure A4.8

***TMS1* QMSP primer/probe optimisation.** Amplification plot of ΔRn versus PCR cycle. The primer/probe combination, which gives the highest ΔRn and lowest Ct value was chosen.

A final primer and probe concentration of 300nM and 100nM, respectively, was selected for optimal reaction conditions for *TMS1* methylation analysis using QMSP.

A4.1.9 TMS1 QRT-PCR primer and probe optimisation

Table A4.9 TMS1 QRT-PCR Primer/Probe gene expression optimisation		
[Primer, Probe] (nM)	Mean CT	SD
300,100	25.439	0.113
300,200	25.678	0.781
300,300	24.9867	0.564
900,100	26.2066	0.278
900,200	27.789	0.342
900,300	29.657	0.245

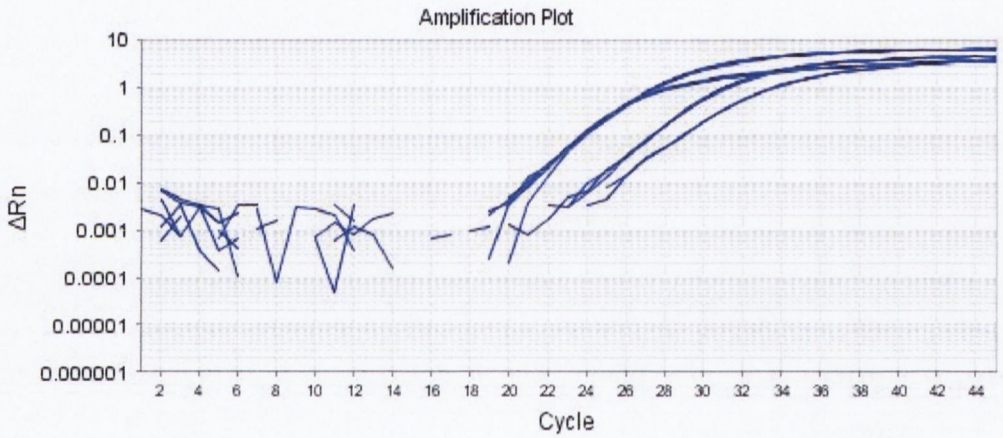

Figure A4.9

***TMS1* QRT-PCR primer/probe optimisation.** Amplification plot of ΔRn versus PCR cycle. The primer/probe combination, which gives the highest ΔRn and lowest Ct value was chosen.

A final primer and probe concentration of 300nM and 300nM, respectively, was selected for optimal reaction conditions for *TMS1* gene expression analysis.

A4.1.10 CDKN2A QRT-PCR primer and probe optimisation

Table A4.10 CDKN2A QRT-PCR Primer/Probe gene expression optimisation		
[Primer, Probe] (nM)	Mean CT	SD
300,100	31.68	0.113
300,200	30.867	0.896
300,300	31.572	0.652
900,100	29.316	0.277
900,200	27.208	0.289
900,300	27.51	0.141

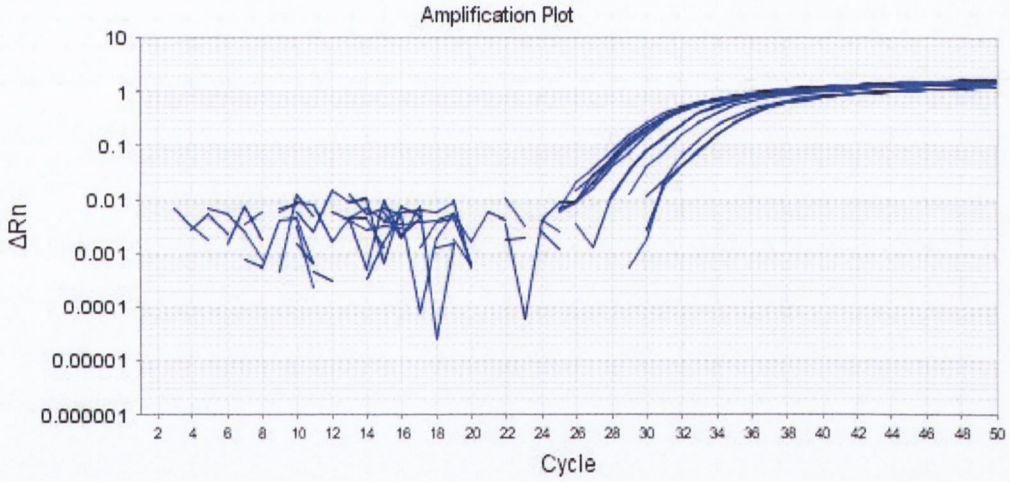

Figure A4.10

***CDKN2A* QRT-PCR primer/probe optimisation.** Amplification plot of ΔRn versus PCR cycle. The primer/probe combination, which gives the highest ΔRn and lowest Ct value was chosen.

A final primer and probe concentration of 900nM and 300nM, respectively, was selected for optimal reaction conditions for *CDKN2A* gene expression analysis.

A4.2 Validation of ΔΔCt and efficiency test for non-inventoried primers and probes

A4.2.1 Validation of ΔΔCt of gene targets

For comparative C_T analysis, the efficiency of the target amplification and the efficiency of the endogenous control must be approximately equal. Expression of *PGK1* is similar in all cell lines, except PWR1E, and is not affected by treatment with 5aza2'deoxycytidine (Table A4.11). We can conclude that *PGK1* is a suitable endogenous control for our studies. Due to the higher levels of *PGK1* expression detected in PWRE1 cell line, RWPE1 was used as a calibrator for the experiment.

Table A4.11. Average C_T value for PGK1 in various cell lines and after treatment with 5-Aza-CdR

Input cDNA (100ng)	PGK1 average C_T
RWPE1	20.87± 0.79
PWR1E	23.96± 0.04
22RV1	19.3± 0.08
RC58	19.74± 0.08
DU145	19.11± 0.04
LNCaP	18.73± 0.14
PC3	16.89±0.8
PC3 + 1 μM 5-Aza-CdR	17.08± 0.04

Note: 5-Aza-CdR: 5aza2'deoxycytidine, PGK1 : Phosphoglycerate kinase 1

ΔΔCT validation experiment for targets *TMS1* and *CDKN2A* was performed (Figure 411 and 4.12). If the efficiencies of the two targets are approximately equal, the Log of input cDNA versus ΔCT has a slope of approximately zero. The Log of input cDNA versus ΔCT for TMS1 and CDKN2A has a slope of 0.74 and -0.099, respectively, suggesting the efficiencies are approximately equal.

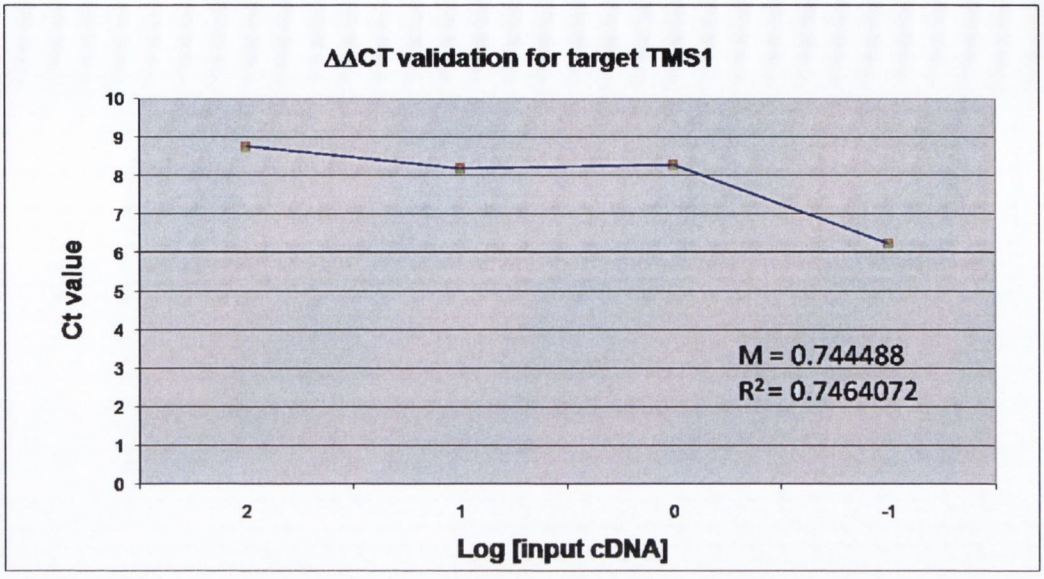

Figure 4.11.

ΔΔCT validation for TMS1. CT values (Vertical axis) are plotted against the log[input cDNA]. M= Slope, R^2= Correlation Co-efficient.

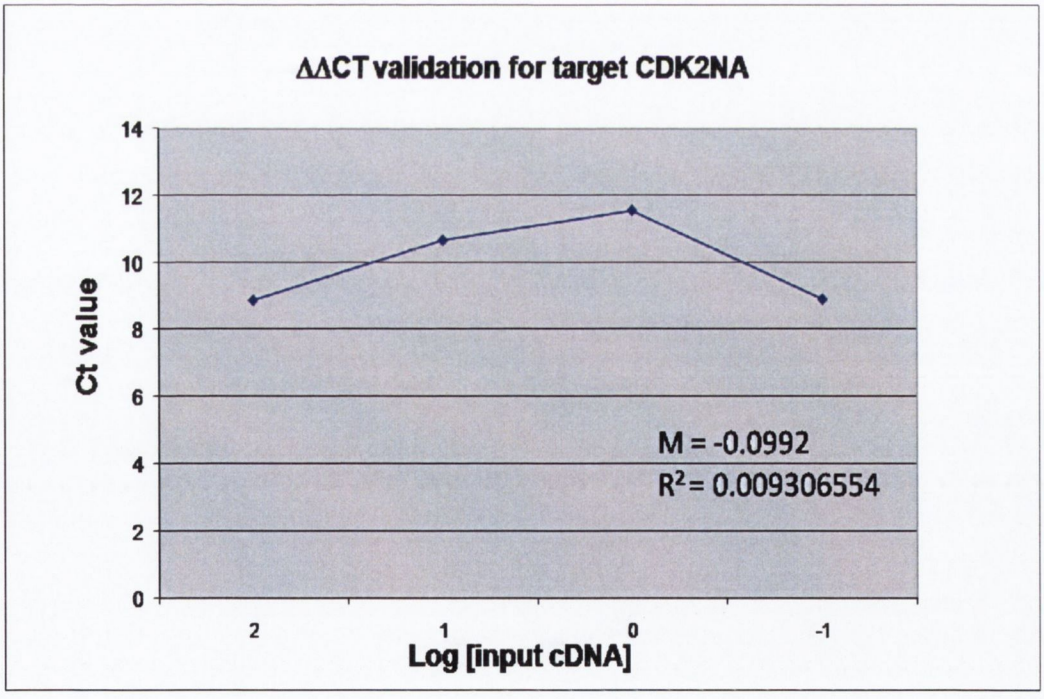

Figure 4.12.

ΔΔCT validation for CDKN2A. CT values (Vertical axis) are plotted against the log[input cDNA]. M= Slope, R^2= Correlation Co-efficient.

A4.2.2 Individual efficiency test for non-inventoried primers and probes

Individual target assay efficiencies were calculated by using relative quantification using the standard curve method. The percentage efficiencies are automatically calculated by the ABI 7500 software, using an algorithm designed by applied biosystems. Once the efficiencies are determined, there is an option to manually adjust the efficiency of a particular target (detector) in the ABI 7500 software during design of experiment.

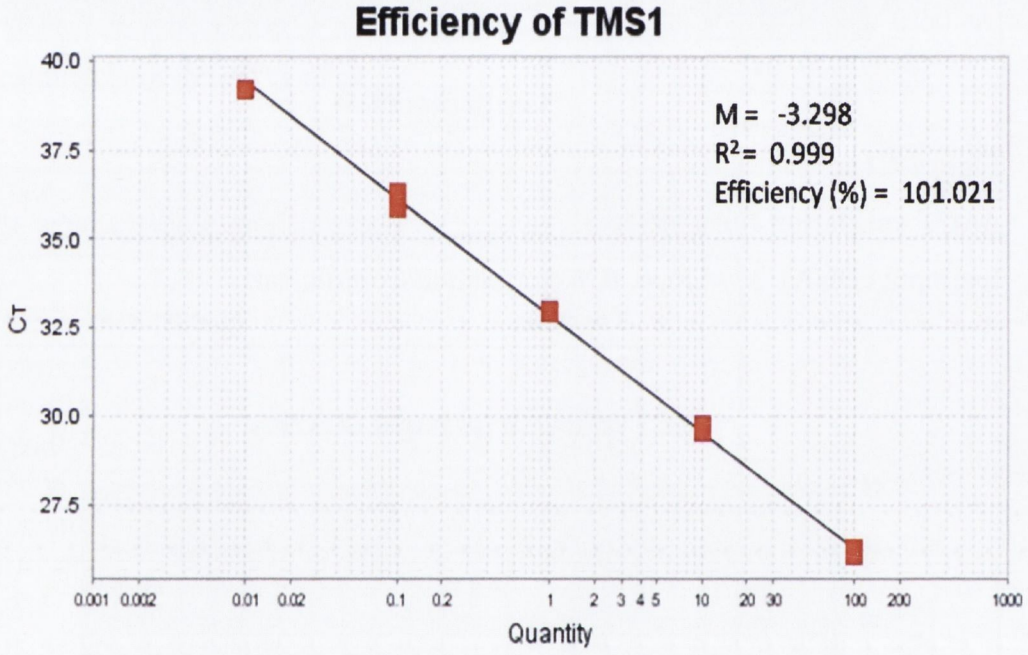

Figure A4.13.

Efficiency of TMS1 reactions over fold dilutions (10 ng/µl, 1 ng/µl, 0.1 ng/µl, 0.05 ng/µl, 0.01 ng/µl) of PWR1E DNA. The slope (M), correlation co-efficient (R2) and % efficiency was determined.

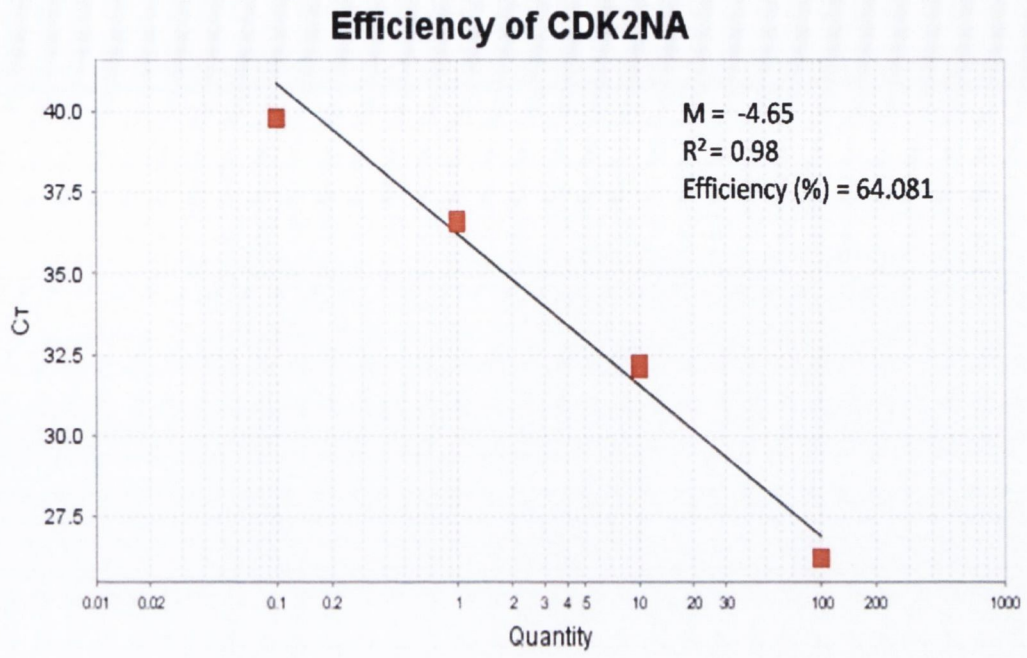

Figure A4.14

Efficiency of CDKN2A reactions over fold dilutions (10 ng/µl, 1 ng/µl, 0.1 ng/µl, 0.05 ng/µl, 0.01 ng/µl) of PWR1E DNA. The slope (M), correlation co-efficient (R2) and % efficiency was determined.

APPENDIX 5 STATISTICS

A5.1 Paired T test.

A5.1.1 Difference in gene expression levels between PC3 cells and PC3 cells treated with a methylation inhibitor 5aza2'deoxycytidine.

A paired T test was performed to determine if the changes in gene expression observed in the two cell lines was significant for each gene with evidence of methylation in its PC3 cell line.

Paired T-Test and 95% CI: BIK PC3 - BIK PC3 Treated (5aza2'deoxycytidine)

	N	Mean	StDev	SE Mean
Blk PC3	3	0.004071	0.000479	0.000276
BIK PC3T	3	0.020294	0.001478	0.000853
Difference	3	-0.016223	0.001068	0.000617

95% CI for mean difference: (-0.018876, -0.013571)

T-Test of mean difference = 0 (vs not = 0): T-Value = -26.31 P-Value = 0.001

Paired T-Test and 95% CI: CDKN2A PC3 – CDKN2A PC3 Treated (5aza2'deoxycytidine)

	N	Mean	StDev	SE Mean
p16 pc3	3	0.01108	0.00058	0.00034
p16 pc3t	3	0.04526	0.00249	0.00144
Difference	3	-0.03419	0.00190	0.00110

95% CI for mean difference: (-0.03892, -0.02945)

T-Test of mean difference = 0 (vs not = 0): T-Value = -31.08 P-Value = 0.001

Paired T-Test and 95% CI: DCR1 PC3 - DCR1 PC3 Treated (5aza2'deoxycytidine)

	N	Mean	StDev	SE Mean

DCR1 PC3_2 3 0.1504 0.0067 0.0039

DCR1 PC3T_2 3 0.5144 0.1564 0.0903

Difference 3 -0.3639 0.1543 0.0891

95% CI for mean difference: (-0.7473, 0.0194)

T-Test of mean difference = 0 (vs not = 0): T-Value = -4.08 P-Value = 0.055

Paired T-Test and 95% CI: DCR2 PC3 - DCR2 PC3 Treated (5aza2'deoxycytidine)

	N	Mean	StDev	SE Mean
DCR2 PC3_3	3	0.000049	0.000012	0.000007
DCR2 PC3T_3	3	0.026313	0.000849	0.000490
Difference	3	-0.026264	0.000850	0.000491

95% CI for mean difference: (-0.028377, -0.024152)

T-Test of mean difference = 0 (vs not = 0): T-Value = -53.49 P-Value = 0.000

Paired T-Test and 95% CI: TMS1 PC3 - TMS1 PC3 Treated (5aza2'deoxycytidine)

	N	Mean	StDev	SE Mean
TMS1 PC3_4	3	0.01913	0.00070	0.00040
TMS1 PC3T_4	3	0.05466	0.00331	0.00191
Difference	3	-0.03553	0.00266	0.00154

95% CI for mean difference: (-0.04214, -0.02893)

T-Test of mean difference = 0 (vs not = 0): T-Value = -23.14 P-Value = 0.002

The results of the paired T test showed that in case of all genes ($P<0.05$), except for *DCR1* ($P=0.055$), the null hypothesis (no difference in gene expression between PC3 cell and PC3 treated cells) could be rejected. Therefore, in all genes, with the exception of *DCR1*, treated with a methylation

inhibitor significantly upregulated gene expression, suggesting that methylation plays a key role in decreasing the expression of these genes in PC3 cells.

A5.2 Unpaired T- Test

A5.2.1 Age of tumour sample versus BPH sample

An Anderson-Darling normal probability plot illustrated that the age of prostate cancer patients and BPH patients was normally distributed (Figure A5.1 and A5.2). An unpaired two sample T test showed that a difference in the mean age of tumour and BPH samples was statistically significant ($P < 0.024$).

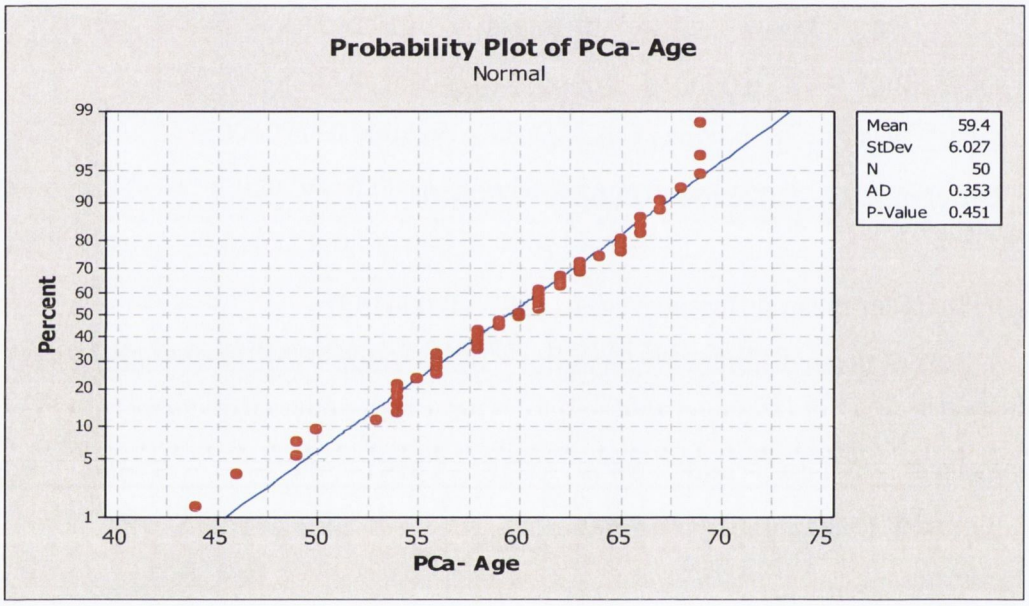

Figure A5.1

Normal probability plot of age of tumour samples

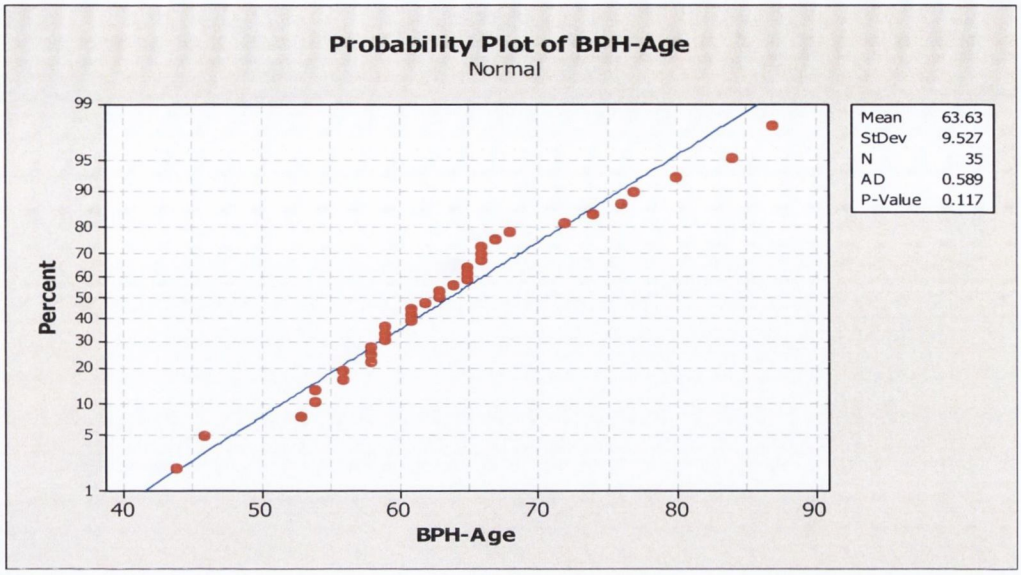

Figure A5.2

Normal probability plot of age of BPH samples

Two-Sample T-Test and CI: Prostate cancer- Age versus BPH-Age

	N	Mean	StDev	SE Mean
PCa- Age	50	59.40	6.03	0.85
BPH-Age	35	63.63	9.53	1.6

Difference = mu (PCa- Age) - mu (BPH-Age)

Estimate for difference: -4.23

95% CI for difference: (-7.88, -0.57)

T-Test of difference = 0 (vs not =): T-Value = -2.32 P-Value = 0.024 DF = 52

A5.2.2 PSA level of tumour sample versus BPH sample

An Anderson-Darling normal probability plot illustrated that the age of prostate cancer patients and BPH patients was normally distributed (Figure A5.3 and A5.4). An unpaired two sample T test showed that a difference in the mean PSA level of tumour and BPH samples was not statistically significant ($P < 0.883$).

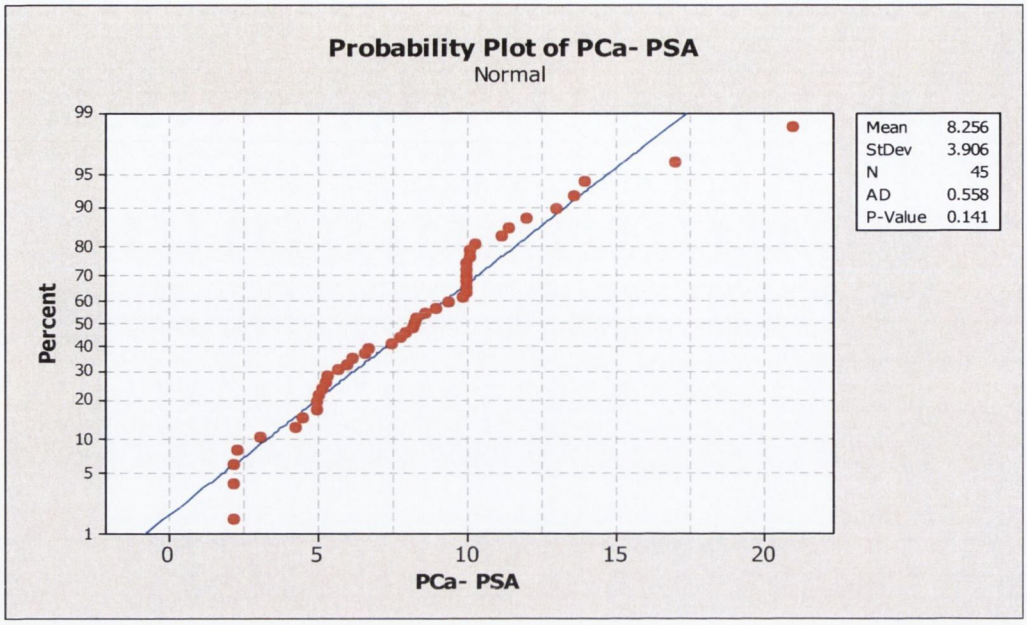

Figure A5.3

Normal probability plot of PSA of tumour samples

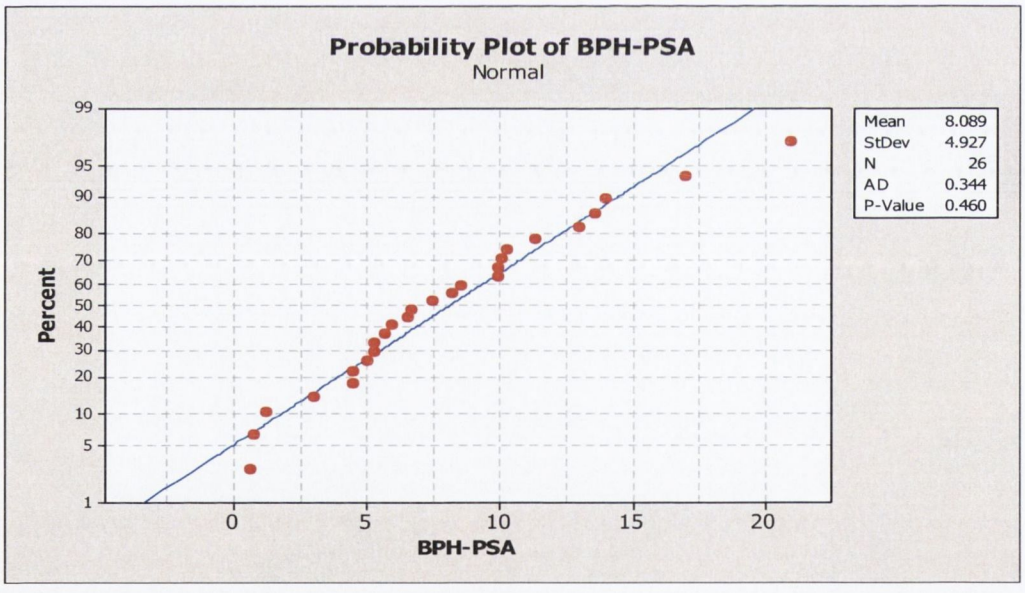

Figure A5.4

Normal probability plot of PSA of BPH samples

Two-Sample T-Test and CI: BPH-PSA versus Prostate Cancer- PSA

	N	Mean	StDev	SE Mean
BPH-PSA	26	8.09	4.93	0.97
PCa- PSA	45	8.26	3.91	0.58

Difference = mu (BPH-PSA) - mu (PCa- PSA)

Estimate for difference: -0.17

95% CI for difference: (-2.44, 2.11)

T-Test of difference = 0 (vs not =): T-Value = -0.15 P-Value = 0.883 DF = 43

A5.3 Fisher's Exact test.

A5.3.1 Difference in methylation frequency between tissue groups

Differences in methylation frequencies between normal, BPH, HGPIN and prostate cancer were calculated using Fisher's Exact Test. This Test is good when expected cell counts are low.

BNIP3: Prostate cancer versus Normal

Test and CI for Two Proportions

Sample	X	N	Sample p
1	8	50	0.160000
2	0	43	0.000000

Difference = p (1) - p (2)

Estimate for difference: 0.16

95% CI for difference: (0.0583839, 0.261616)

Test for difference = 0 (vs not = 0): Z = 3.09 P-Value = 0.002

Fisher's exact test: P-Value = 0.007

BNIP3: Prostate cancer versus HGPIN

Test and CI for Two Proportions

Sample	X	N	Sample p
1	8	50	0.160000
2	0	17	0.000000

Difference = p (1) - p (2)

Estimate for difference: 0.16

95% CI for difference: (0.0583839, 0.261616)

Test for difference = 0 (vs not = 0): Z = 3.09 P-Value = 0.002

Fisher's exact test: P-Value = 0.103

BNIP3: Prostate cancer versus BPH

Test and CI for Two Proportions

Sample	X	N	Sample p
1	8	50	0.160000
2	0	35	0.000000

Difference = p (1) - p (2)

Estimate for difference: 0.16

95% CI for difference: (0.0583839, 0.261616)

Test for difference = 0 (vs not = 0): Z = 3.09 P-Value = 0.002

Fisher's exact test: P-Value = 0.019

CDKN2A: Prostate cancer versus Normal

Test and CI for Two Proportions

Sample	X	N	Sample p
1	8	29	0.275862
2	0	28	0.000000

Difference = p (1) - p (2)

Estimate for difference: 0.275862

95% CI for difference: (0.113193, 0.438531)

Test for difference = 0 (vs not = 0): Z = 3.32 P-Value = 0.001

Fisher's exact test: P-Value = 0.004

CDKN2A: Prostate cancer versus HGPIN

Test and CI for Two Proportions

Sample	X	N	Sample p
1	8	29	0.275862
2	1	13	0.076923

Difference = p (1) - p (2)

Estimate for difference: 0.198939

95% CI for difference: (-0.0188759, 0.416754)

Test for difference = 0 (vs not = 0): Z = 1.79 P-Value = 0.073

Fisher's exact test: P-Value = 0.232

CDKN2A: Prostate cancer versus BPH

Test and CI for Two Proportions

Sample	X	N	Sample p
1	8	29	0.275862
2	2	16	0.125000

Difference = p (1) - p (2)

Estimate for difference: 0.150862

95% CI for difference: (-0.0787491, 0.380473)

Test for difference = 0 (vs not = 0): Z = 1.29 P-Value = 0.198

Fisher's exact test: P-Value = 0.292

DCR1: Prostate cancer versus Normal

Test and CI for Two Proportions

Sample X N Sample p
1 11 29 0.379310
2 0 28 0.000000

Difference = p (1) - p (2)
Estimate for difference: 0.379310
95% CI for difference: (0.202713, 0.555907)
Test for difference = 0 (vs not = 0): Z = 4.21 P-Value = 0.000

Fisher's exact test: P-Value = 0.000

DCR1: Prostate cancer versus HGPIN

Test and CI for Two Proportions

Sample X N Sample p
1 11 29 0.379310
2 0 13 0.000000

Difference = p (1) - p (2)
Estimate for difference: 0.379310
95% CI for difference: (0.202713, 0.555907)
Test for difference = 0 (vs not = 0): Z = 4.21 P-Value = 0.000

Fisher's exact test: P-Value = 0.009

DCR1: Prostate cancer versus BPH

Test and CI for Two Proportions

Sample	X	N	Sample p
1	11	29	0.379310
2	0	16	0.000000

Difference = p (1) - p (2)

Estimate for difference: 0.379310

95% CI for difference: (0.202713, 0.555907)

Test for difference = 0 (vs not = 0): Z = 4.21 P-Value = 0.000

Fisher's exact test: P-Value = 0.004

DCR2: Prostate cancer versus Normal

Test and CI for Two Proportions

Sample	X	N	Sample p
1	19	50	0.420000
2	0	43	0.000000

Difference = p (1) - p (2)

Estimate for difference: 0.42

95% CI for difference: (0.283195, 0.556805)

Test for difference = 0 (vs not = 0): Z = 6.02 P-Value = 0.000

Fisher's exact test: P-Value = 0.000

DCR2: Prostate cancer versus HGPIN

Test and CI for Two Proportions

Sample	X	N	Sample p
1	19	50	0.420000
2	0	17	0.000000

Difference = p (1) - p (2)

Estimate for difference: 0.42

95% CI for difference: (0.283195, 0.556805)

Test for difference = 0 (vs not = 0): Z = 6.02 P-Value = 0.000

Fisher's exact test: P-Value = 0.001

DCR2: Prostate cancer versus BPH

Test and CI for Two Proportions

Sample	X	N	Sample p
1	19	50	0.420000
2	2	35	0.057143

Difference = p (1) - p (2)

Estimate for difference: 0.362857

95% CI for difference: (0.205921, 0.519793)

Test for difference = 0 (vs not = 0): Z = 4.53 P-Value = 0.000

Fisher's exact test: P-Value = 0.000

TMS1: Prostate cancer versus Normal

Test and CI for Two Proportions

Sample	X	N	Sample p
1	22	50	0.440000
2	0	43	0.000000

Difference = p (1) - p (2)

Estimate for difference: 0.44

95% CI for difference: (0.302411, 0.577589)

Test for difference = 0 (vs not = 0): Z = 6.27 P-Value = 0.000

Fisher's exact test: P-Value = 0.000

TMS1: Prostate cancer versus HGPIN

Test and CI for Two Proportions

Sample	X	N	Sample p
1	22	50	0.440000
2	2	17	0.117647

Difference = p (1) - p (2)

Estimate for difference: 0.322353

95% CI for difference: (0.116470, 0.528235)

Test for difference = 0 (vs not = 0): Z = 3.07 P-Value = 0.002

Fisher's exact test: P-Value = 0.020

TMS1: Prostate cancer versus BPH

Test and CI for Two Proportions

Sample	X	N	Sample p
1	22	50	0.440000
2	2	35	0.057143

Difference = p (1) - p (2)

Estimate for difference: 0.382857

95% CI for difference: (0.225237, 0.540477)

Test for difference = 0 (vs not = 0): Z = 4.76 P-Value = 0.000

Fisher's exact test: P-Value = 0.000

The results of the Fisher exact test showed that in case of all genes ($P<0.05$), the null hypothesis (no difference between methylation frequencies of prostate cancer and normal tissue) could be rejected.

A5.3.2 Correlation with Clinicopathological features

BNIP3 Gleason score ≤ 6 Versus Gleason score ≥ 7

Test and CI for Two Proportions

Sample	X	N	Sample p
1	3	15	0.200000
2	5	35	0.142857

Difference = p (1) - p (2)

Estimate for difference: 0.0571429

95% CI for difference: (-0.176128, 0.290413)

Test for difference = 0 (vs not = 0): Z = 0.48 P-Value = 0.631

Fisher's exact test: P-Value = 0.683

BNIP3 PSA

≤8ng/ml Versus >8ng/ml

Test and CI for Two Proportions

Sample	X	N	Sample p
1	3	4	0.750000
2	20	24	0.833333

Difference = p (1) - p (2)

Estimate for difference: -0.0833333

95% CI for difference: (-0.533110, 0.366443)

Test for difference = 0 (vs not = 0): Z = -0.36 P-Value = 0.717

Fisher's exact test: P-Value = 1.000

BNIP3 TNM staging pT2 V pT3

Test and CI for Two Proportions

Sample	X	N	Sample p
1	5	33	0.151515
2	2	12	0.166667

Difference = p (1) - p (2)

Estimate for difference: -0.0151515

95% CI for difference: (-0.258927, 0.228624)

Test for difference = 0 (vs not = 0): Z = -0.12 P-Value = 0.903

Fisher's exact test: P-Value = 1.000

CDKN2A Gleason score ≤ 6 Versus Gleason score ≥ 7

Test and CI for Two Proportions

Sample	X	N	Sample p
1	1	7	0.142857
2	7	22	0.318182

Difference = p (1) - p (2)

Estimate for difference: -0.175325

95% CI for difference: (-0.499482, 0.148833)

Test for difference = 0 (vs not = 0): Z = -1.06 P-Value = 0.289

Fisher's exact test: P-Value = 0.635

CDKN2A PSA

≤8ng/ml Versus >8ng/ml

Test and CI for Two Proportions

Sample	X	N	Sample p
1	3	13	0.230769
2	3	11	0.272727

Difference = p (1) - p (2)

Estimate for difference: -0.0419580

95% CI for difference: (-0.390846, 0.306930)

Test for difference = 0 (vs not = 0): Z = -0.24 P-Value = 0.814

Fisher's exact test: P-Value = 1.000

CDKN2A TNM staging pT2 V pT3

Test and CI for Two Proportions

Sample	X	N	Sample p
1	7	22	0.318182
2	1	6	0.166667

Difference = p (1) - p (2)

Estimate for difference: 0.151515

95% CI for difference: (-0.204579, 0.507610)

Test for difference = 0 (vs not = 0): Z = 0.83 P-Value = 0.404

Fisher's exact test: P-Value = 0.640

DCR1 Gleason score ≤ 6 Versus Gleason score ≥ 7

Test and CI for Two Proportions

Sample	X	N	Sample p
1	2	7	0.285714
2	9	22	0.409091

Difference = p (1) - p (2)

Estimate for difference: -0.123377

95% CI for difference: (-0.516067, 0.269314)

Test for difference = 0 (vs not = 0): Z = -0.62 P-Value = 0.538

Fisher's exact test: P-Value = 0.677

DCR1 PSA

≤8ng/ml Versus >8ng/ml

Test and CI for Two Proportions

Sample	X	N	Sample p
1	5	13	0.384615
2	2	11	0.181818

Difference = p (1) - p (2)

Estimate for difference: 0.202797

95% CI for difference: (-0.146331, 0.551926)

Test for difference = 0 (vs not = 0): Z = 1.14 P-Value = 0.255

Fisher's exact test: P-Value = 0.386

DCR1 TNM staging pT2 V pT3

Test and CI for Two Proportions

Sample	X	N	Sample p
1	10	22	0.454545
2	1	6	0.166667

Difference = p (1) - p (2)

Estimate for difference: 0.287879

95% CI for difference: (-0.0757348, 0.651492)

Test for difference = 0 (vs not = 0): Z = 1.55 P-Value = 0.121

Fisher's exact test: P-Value = 0.355

DCR2 Gleason score ≤ 6 Versus Gleason score ≥ 7

Test and CI for Two Proportions

Sample	X	N	Sample p
1	4	15	0.266667
2	15	35	0.428571

Difference = p (1) - p (2)

Estimate for difference: -0.161905

95% CI for difference: (-0.439322, 0.115512)

Test for difference = 0 (vs not = 0): Z = -1.14 P-Value = 0.253

Fisher's exact test: P-Value = 0.351

DCR2 PSA

≤8ng/ml Versus >8ng/ml

Test and CI for Two Proportions

Sample	X	N	Sample p
1	5	20	0.250000
2	10	24	0.416667

Difference = p (1) - p (2)

Estimate for difference: -0.166667

95% CI for difference: (-0.440377, 0.107044)

Test for difference = 0 (vs not = 0): Z = -1.19 P-Value = 0.233

Fisher's exact test: P-Value = 0.342

DCR2 TNM staging pT2 V pT3

Test and CI for Two Proportions

Sample	X	N	Sample p
1	12	33	0.363636
2	4	12	0.333333

Difference = p (1) - p (2)

Estimate for difference: 0.0303030

95% CI for difference: (-0.282867, 0.343473)

Test for difference = 0 (vs not = 0): Z = 0.19 P-Value = 0.850

Fisher's exact test: P-Value = 1.000

TMS1 Gleason score ≤ 6 Versus Gleason score ≥ 7

Test and CI for Two Proportions

Sample	X	N	Sample p
1	4	15	0.266667
2	17	35	0.485714

Difference = p (1) - p (2)

Estimate for difference: -0.219048

95% CI for difference: (-0.497432, 0.0593367)

Test for difference = 0 (vs not = 0): Z = -1.54 P-Value = 0.123

Fisher's exact test: P-Value = 0.215

TMS1 PSA

≤8ng/ml Versus >8ng/ml

Test and CI for Two Proportions

Sample X N Sample p
1 3 20 0.150000
2 13 24 0.541667

Difference = p (1) - p (2)
Estimate for difference: -0.391667
95% CI for difference: (-0.645096, -0.138237)
Test for difference = 0 (vs not = 0): Z = -3.03 P-Value = 0.002

Fisher's exact test: P-Value = 0.011

TNM staging pT2 V pT3

Test and CI for Two Proportions

Sample X N Sample p
1 16 35 0.457143
2 4 11 0.363636

Difference = p (1) - p (2)
Estimate for difference: 0.0935065
95% CI for difference: (-0.235202, 0.422215)
Test for difference = 0 (vs not = 0): Z = 0.56 P-Value = 0.577

Fisher's exact test: P-Value = 0.732

Analysis of 5-gene panel

Gleason score ≤ 6 Versus Gleason score ≥ 7

Test and CI for Two Proportions

Sample	X	N	Sample p
1	3	7	0.428571
2	17	22	0.772727

Difference = p (1) - p (2)

Estimate for difference: -0.344156

95% CI for difference: (-0.750432, 0.0621204)

Test for difference = 0 (vs not = 0): Z = -1.66 P-Value = 0.097

Fisher's exact test: P-Value = 0.158

PSA

≤8ng/ml Versus >8ng/ml

Test and CI for Two Proportions

Sample	X	N	Sample p
1	7	14	0.500000
2	6	11	0.545455

Difference = p (1) - p (2)

Estimate for difference: -0.0454545

95% CI for difference: (-0.439386, 0.348477)

Test for difference = 0 (vs not = 0): Z = -0.23 P-Value = 0.821

Fisher's exact test: P-Value = 1.000

TNM staging pT2 V pT3

Test and CI for Two Proportions

Sample	X	N	Sample p
1	16	21	0.761905
2	2	4	0.500000

Difference = p (1) - p (2)

Estimate for difference: 0.261905

95% CI for difference: (-0.260852, 0.784662)

Test for difference = 0 (vs not = 0): Z = 0.98 P-Value = 0.326

Fisher's exact test: P-Value = 0.548

A5.4 Krustal-Wallis test and one-way ANOVA Tukey pairwise.

A5.4.1 Difference in methylation levels (RMS) between tissue groups

The Krustal-Wallis test offers a nonparametric alternative to the one-way analysis of variance and was utilised in the current study to compare the methylation scores (RMS) of each gene between different tissue groups.

BNIP3: Kruskal-Wallis Test:

Kruskal-Wallis Test on Response

Treatment	N	Median	Ave Rank	Z
BPH	35	0.000000000	69.5	-0.72
HGPIN	18	0.000000000	69.5	-0.48
Normal	43	0.000000000	69.5	-0.82
Tumour	51	0.000000000	82.5	1.76
Overall	147		74.0	

H = 3.09 DF = 3 P = 0.378

H = 17.90 DF = 3 P = 0.000 (adjusted for ties)

One-way ANOVA: Tumour, HGPIN, BPH, Normal

Source DF SS MS F P
Factor 3 287.8 95.9 3.30 0.022
Error 143 4154.1 29.0
Total 146 4442.0

S = 5.390 R-Sq = 6.48% R-Sq(adj) = 4.52%

Individual 95% CIs For Mean Based on
Pooled StDev

Level N Mean StDev ---+---------+---------+---------+------
Tumour 51 2.940 9.115 (-------*------)
HGPIN 18 0.000 0.000 (------------*------------)
BPH 35 0.000 0.000 (--------*--------)
Normal 43 0.000 0.000 (-------*-------)
---+---------+---------+---------+------
-2.0 0.0 2.0 4.0

Pooled StDev = 5.390

Tukey 95% Simultaneous Confidence Intervals
All Pairwise Comparisons

Individual confidence level = 98.98%

Tumour subtracted from:

Lower Center Upper ---+---------+---------+---------+------
HGPIN -6.785 -2.940 0.905 (------------*------------)
BPH -6.018 -2.940 0.139 (---------*---------)

```
Normal  -5.843  -2.940  -0.036     (--------*---------)
                        ---+---------+---------+---------+------
                        -6.0      -3.0       0.0       3.0
```

HGPIN subtracted from:

```
        Lower  Center  Upper  ---+---------+---------+---------+------
BPH     -4.068  0.000  4.068          (-------------*-------------)
Normal  -3.937  0.000  3.937           (------------*------------)
                        ---+---------+---------+---------+------
                        -6.0      -3.0       0.0       3.0
```

BPH subtracted from:

```
        Lower  Center  Upper  ---+---------+---------+---------+------
Normal  -3.193  0.000  3.193           (----------*----------)
                        ---+---------+---------+---------+------
```

CDKN2A: Kruskal-Wallis Test:

Treatment	N	Median	Ave Rank	Z
BPH	22	0.000000000	36.9	-0.41
HGPIN	6	0.000000000	39.8	0.15
Normal	19	0.000000000	33.0	-1.25
Tumour	29	0.000000000	43.1	1.42
Overall	76		38.5	

H = 2.56 DF = 3 P = 0.464

H = 6.84 DF = 3 P = 0.077 (adjusted for ties)

One-way ANOVA: Tumour, HGPIN, BPH, Normal

Source DF SS MS F P
Factor 3 8.38990E+12 2.79663E+12 1.17 0.325
Error 72 1.71437E+14 2.38107E+12
Total 75 1.79827E+14

S = 1543072 R-Sq = 4.67% R-Sq(adj) = 0.69%

Individual 95% CIs For Mean Based on
Pooled StDev

Level N Mean StDev --------+---------+---------+---------+-
Tumour 29 144 740 (-------*-------)
HGPIN 6 1539 3770 (----------*----------)
BPH 22 732864 2857213 (--------*---------)
Normal 19 0 0 (---------*---------)
--------+---------+---------+---------+-
-700000 0 700000 1400000

Pooled StDev = 1543072

Tukey 95% Simultaneous Confidence Intervals
All Pairwise Comparisons

Individual confidence level = 98.96%

Tumour subtracted from:

Lower Center Upper -------+---------+---------+---------+--
HGPIN -1819033 1395 1821823 (-----------*-----------)
BPH -414875 732721 1880316 (-------*-------)

```
Normal -1198149  -144 1197862        (-------*-------)
                 -------+---------+---------+---------+--
                 -1500000        0  1500000  3000000
```

HGPIN subtracted from:

```
        Lower  Center   Upper -------+---------+---------+---------+--
BPH    -1138092 731325 2600742        (-----------*-----------)
Normal -1902318  -1539 1899240    (-----------*-----------)
                 -------+---------+---------+---------+--
                 -1500000        0  1500000  3000000
```

BPH subtracted from:

```
        Lower  Center   Upper -------+---------+---------+---------+--
Normal -2004076 -732864 538347    (-------*--------)
                 -------+---------+---------+---------+--
                 -1500000        0  1500000  3000000
```

DCR1: Kruskal-Wallis Test:

Kruskal-Wallis Test on Response

Treatment	N	Median	Ave Rank	Z
BPH	22	0.000000000	33.0	-1.39
HGPIN	6	0.000000000	33.0	-0.64
Normal	19	0.000000000	33.0	-1.25
Tumour	29	0.000000000	47.4	2.76
Overall	76		38.5	

H = 7.64 DF = 3 P = 0.054

H = 20.41 DF = 3 P = 0.000 (adjusted for ties)

One-way ANOVA: Tumour, HGPIN, BPH, Normal

Source DF SS MS F P
Factor 3 9987 3329 4.68 0.005
Error 72 51164 711
Total 75 61151

S = 26.66 R-Sq = 16.33% R-Sq(adj) = 12.85%

Individual 95% CIs For Mean Based on Pooled StDev

```
Level    N  Mean  StDev ----+---------+---------+---------+-----
Tumour  29 23.60 42.75                  (------*-----)
HGPIN    6  0.00  0.00 (-------------*-------------)
BPH     22  0.00  0.00       (-------*-------)
Normal  19  0.00  0.00       (-------*-------)
                    ----+---------+---------+---------+-----
                     -15       0       15       30
```

Pooled StDev = 26.66

Tukey 95% Simultaneous Confidence Intervals
All Pairwise Comparisons

Individual confidence level = 98.96%

Tumour subtracted from:

```
        Lower  Center  Upper --+---------+---------+---------+-------
HGPIN  -55.05 -23.60   7.85 (-----------*-----------)
```

```
BPH    -43.42 -23.60 -3.77      (-------*------)
Normal -44.29 -23.60 -2.90      (--------*-------)
                  --+---------+---------+---------+-------
                  -50       -25        0        25
```

HGPIN subtracted from:

```
          Lower  Center  Upper --+---------+---------+---------+-------
BPH     -32.29   0.00   32.29          (-----------*-----------)
Normal  -32.84   0.00   32.84          (-----------*-----------)
                  --+---------+---------+---------+-------
                  -50       -25        0        25
```

BPH subtracted from:

```
          Lower  Center  Upper --+---------+---------+---------+-------
Normal  -21.96   0.00   21.96            (--------*--------)
                  --+---------+---------+---------+-------
                  -50       -25        0        25
```

DCR2: Kruskal-Wallis Test:

Treatment	N	Median	Ave Rank	Z
BPH	35	0.000000000	67.1	-1.03
HGPIN	17	0.000000000	63.0	-1.09
Normal	43	0.000000000	63.0	-1.94
Tumour	51	0.000000000	90.3	3.51
Overall	146		73.5	

H = 12.51 DF = 3 P = 0.006

H = 33.59 DF = 3 P = 0.000 (adjusted for ties)

One-way ANOVA: Tumour, HGPIN, BPH, Normal

Source DF SS MS F P
Factor 3 19231 6410 8.44 0.000
Error 142 107806 759
Total 145 127036

S = 27.55 R-Sq = 15.14% R-Sq(adj) = 13.35%

Individual 95% CIs For Mean Based on
Pooled StDev

Level N Mean StDev -+---------+---------+---------+--------
Tumour 51 24.93 45.61 (------*-----)
HGPIN 17 0.00 0.00 (----------*----------)
BPH 35 2.56 10.56 (-------*-------)
Normal 43 0.00 0.00 (------*------)
-+---------+---------+---------+--------
-12 0 12 24

Pooled StDev = 27.55

Tukey 95% Simultaneous Confidence Intervals
All Pairwise Comparisons

Individual confidence level = 98.98%

Tumour subtracted from:

Lower Center Upper ---+---------+---------+---------+------
HGPIN -45.01 -24.93 -4.85 (----------*---------)
BPH -38.10 -22.36 -6.63 (-------*-------)

```
Normal  -39.77  -24.93  -10.08     (-------*------)
                          ---+---------+---------+---------+------
                           -40       -20        0        20
```

HGPIN subtracted from:

```
          Lower  Center  Upper ---+---------+---------+---------+------
BPH      -18.63   2.56  23.76            (---------*---------)
Normal   -20.54   0.00  20.54            (---------*---------)
                          ---+---------+---------+---------+------
                           -40       -20        0        20
```

BPH subtracted from:

```
          Lower  Center  Upper ---+---------+---------+---------+------
Normal   -18.88  -2.56  13.76            (-------*-------)
                          ---+---------+---------+---------+------
                           -40       -20        0        20
```

TMS1: Kruskal-Wallis Test:

Treatment	N	Median	Ave Rank	Z
BPH	77	0.000000000	83.2	-2.38
HGPIN	17	0.000000000	93.5	-0.08
Normal	43	0.000000000	82.0	-1.72
Tumour	51	0.000000000	122.5	4.30
Overall	188		94.5	

H = 19.09 DF = 3 P = 0.000

H = 54.81 DF = 3 P = 0.000 (adjusted for ties)

One-way ANOVA: Tumour 1, HGPIN, BPH, Normal

Source DF SS MS F P
Factor 3 140196 46732 11.57 0.000
Error 212 856349 4039
Total 215 996545

S = 63.56 R-Sq = 14.07% R-Sq(adj) = 12.85%

Individual 95% CIs For Mean Based on
Pooled StDev

Level N Mean StDev --------+---------+---------+---------+-
Tumour 1 51 60.82 122.46 (------*------)
HGPIN 17 23.14 81.20 (-----------*-----------)
BPH 105 0.30 3.07 (----*----)
Normal 43 0.00 0.00 (-------*-------)
--------+---------+---------+---------+-
0 25 50 75

Pooled StDev = 63.56

Tukey 95% Simultaneous Confidence Intervals
All Pairwise Comparisons

Individual confidence level = 98.97%

Tumour 1 subtracted from:

Lower Center Upper ---------+---------+---------+---------+
HGPIN -83.75 -37.68 8.38 (--------*---------)

```
BPH    -88.60 -60.52 -32.45  (-----*-----)
Normal -94.88 -60.82 -26.77  (------*------)
                   ---------+---------+---------+---------+
                          -50       0      50      100
```

HGPIN subtracted from:

```
       Lower  Center  Upper ---------+---------+---------+---------+
BPH    -65.84 -22.84 20.16       (-------*--------)
Normal -70.26 -23.14 23.99       (--------*---------)
                   ---------+---------+---------+---------+
                          -50       0      50      100
```

BPH subtracted from:

```
       Lower  Center  Upper ---------+---------+---------+---------+
Normal -30.08  -0.30 29.48            (-----*-----)
                   ---------+---------+---------+---------+
                          -50       0      50      100
```

For all genes except *CDKN2A*, the null hypothesis that the medians are the same for each group is rejected ($p<0.05$). Tukey's pairwise comparison identified the tumour group to be significantly different (confidence interval does not contain zero) from both normal and BPH groups in all genes, except *CDKN2A*.

APPENDIX 6: PATIENT CLINICOPATHOLOGICAL FEATURES

Table A6.1 Characteristics of AMNCH prostate cancer study population

Laboratory	Age	PSA	Gleason		Classification		
number	(years)	(ng/ml)	score	sum	T	N	M
AM01023	69	2.2	3+3	6	2b	x	x
AM01028	61	4.3	3+3	6	2b	0	x
AM02004	63	5	3+3	6	3a	0	x
AM02007	56	7.8	3+3	6	2b	0	NA
AM02012	60	10.1	3+4	7	2b	NA	NA
AM02018	66	5	3+3	6	3a	0	NA
AM02026	54	12	3+4	7	2b	0	NA
AM02031	67	5.2	3+4	7	3b	NA	NA
AM02036	62	10	3+3	6	2c	x	x
AM02037	50	6.2	3+3	6	2b	NA	NA
AM02039	49	2.2	3+4	7	2b	NA	NA
AM02040	65	10	3+4	7	3a	NA	NA
AM02045	54	10	3+3	6	2b	0	NA
AM02047	58	8.2	3+4	7	2b	NA	NA
AM03014	55	11.2	3+4	7	2c	0	NA
AM03029	49	2.2	3+4	7	2b	NA	NA
AM99038	54	2.3	3+3	6	2b	NA	NA
Mean	**58.35**	**6.70**		**6.470588235**			
Median	**58.00**	**6.20**		**6**			
Range	**49-69**	**2.2-12**		**6-7**	**2b-3b**		

Information collated from pathology reports. NA indicates information not available because sample was obtained from TURP.* HGPIN sample with no tumour

Table A6.2 Characteristics of IMM prostate cancer study population							
Laboratory	Age	PSA	Gleason		Classification		
number	(years)	(ng/ml)	score	sum	T	N	M
IMM0001	54	3.1	3+4	7	2c	NA	NA
IMM0002	69	8.3	3+4	7	NA	NA	NA
IMM0005	44	5.7	3+4	7	2a	NA	NA
IMM0007	67	4.5	3+2	5	2c	NA	NA
IMM0008	69	9.9	3+2	5	2c	NA	NA
IMM0009	60	10	3+3	6	3a	NA	NA
IMM0011	53	21	4+3	7	2	NA	NA
IMM0013	58	10.3	3+4	7	NA	NA	NA
IMM0014	63	8.25	3+3	6	3a	NA	NA
IMM0017	62	6	3+4	7	2c	NA	NA
IMM0018	61	13.6	3+3	6	3a	NA	NA
IMM0019	61	13	3+4	7	3a	NA	NA
IMM0020	58	5.3	4+3	7	2c	NA	NA
IMM0022	63	5.03	3+4	7	NA	NA	NA
IMM0025	65	10.1	5+3	8	3b	NA	NA
IMM0032	58	9	3+4	7	2c	NA	NA
IMM0036	46	10	4+3	7	1c	NA	NA
IMM0037	66	11.4	3+4	7	3b	NA	NA
IMM0038	59	NA	4+3	7	2c	NA	NA
IMM0052	56	6.7	3+4	7	2c	NA	NA
IMM0056	56	7.5	3+4	7	2c	NA	NA
IMM0058	58	5.33	3+4	7	2c	NA	NA
IMM0068	66	14	3+4	7	2c	NA	NA
IMM0070	56	NA	3+4	8	3a	NA	NA
IMM0072	62	6.6	3+4	6	2a	NA	NA
IMM0075	64	10	3+4	7	2a	NA	NA
IMM0076	54	17	4+3	7	3b	NA	NA
IMM0078	61	8	3+4	7	2c	NA	NA
IMM0082	56	NA	3+4	7	2c	NA	NA
IMM0083	61	NA	3+4	7	2c	NA	NA
IMM0084	59	8.6	3+4	7	2c	NA	NA
IMM0085	68	NA	3+4	7	2c	NA	NA
IMM0086	65	9.4	3+4	7	2c	NA	NA
Mean	**59.94**	**9.20**		**6.82**			
Median	**61.00**	**8.80**		**7.00**			
Range	**44-69**	**3.1-17**		**6-8**	**1c-3b**		

Information collated from pathology reports. NA indicates information not available. IMM= Institute of Molecular medicine

Table A6.3. HGPIN study population

Laboratory number	Age (years)	PSA (ng/ml)
AM00032P*	70	10.4
AM01010*	62	0.7
AM01022P*	68	10
AM02001	58	11.6
AM02006*	63	NA
AM02027P*	NA	NA
AM02042	69	7
AM03009*	63	7.4
AM03013*	56	5
AM03016*	60	5.2
IMM0013	58	10.3
IMM0014	63	8.25
IMM002	69	8.3
IMM0037	66	11.4
IMM0056	56	7.5
IMM0068	66	14
IMM0075	64	10
Mean	63.1875	8.47
Median	63	8.25
Range	56-70	0.7-14

Information collated from pathology reports.

NA indicates information notavailable.

*No corresponding tumour specimen was available for these patients.

Table A6.4. Normal study population

Laboratory number	Age (years)	PSA (ng/ml)
AM00027*	74	NA
AM01010*	62	0.7
AM01023	69	2.2
AM01028	61	4.3
AM02004	63	5
AM02007	56	7.8
AM02012	60	10.1
AM02025*	56	10.9
AM02026	54	12
AM02030*	44	5.3
AM02036	62	10
AM02037	50	6.2
AM02045	54	10
AM03009*	63	7.4
AM03014	55	11.2
AM03029	49	2.2
AM03085*	60	16
AM99038	54	2.3
IMM001	54	3.1
IMM0011	53	21
IMM0013	58	10.3
IMM0017	62	6
IMM0018	61	13.6
IMM0019	61	13
IMM0022	63	5.03
IMM0037	66	11.4
IMM0038	59	NA
IMM005	44	5.7
IMM0052	56	6.7
IMM0056	56	7.5
IMM0058	58	5.33
IMM0070	56	NA
IMM0075	64	10
IMM0076	54	17
IMM0078	61	8
IMM0082	56	NA
IMM0083	61	NA
IMM0084	59	8.6
IMM0085	68	NA
IMM0086	65	9.4
IMM009	60	10
IMM020	58	5.3
IMM072	62	6.6
Mean	59	9.178
Median	59	8.3
Range	44-74	0.7-13.6

Information collated from pathology reports.
NA indicates information notavailable.
*No corresponding tumour specimen was available for these patients.

Table A6.5. BPH study population

Laboratory number	Age (years)	PSA (ng/ml)
AM00054	74	0.7
AM00066	80	NA
AM01065	77	NA
AM01072	59	NA
AM02058	72	NA
AM02059	87	NA
AM02075	65	4.5
AM02081	66	6
AM03052	65	1.3
AM03082	84	NA
AM03086	76	0.8
IMM001	54	3.1
IMM0011	53	21
IMM0013	58	10.3
IMM0014	63	8.25
IMM0018	61	13.6
IMM0019	61	13
IMM0020	58	5.3
IMM0022	63	5.03
IMM0025	65	10.1
IMM0036	46	10
IMM0037	66	11.4
IMM0038	59	NA
IMM005	44	5.7
IMM0052	56	6.7
IMM0056	56	7.5
IMM0058	58	5.33
IMM0068	66	14
IMM007	67	4.5
IMM0072	62	6.6
IMM0075	64	10
IMM0076	54	17
IMM0083	61	NA
IMM0084	59	8.6
IMM0085	68	NA
Mean	62.81818182	8.3844
Median	62	7.5
Range	44-87	0.7-21

Information collated from pathology reports.
NA indicates information notavailable.

APPENDIX 7: RELATIVE METHYLATION SCORES OF PATIENT SAMPLES

Table 7.1: Summary of QMSP results for prostate cancer tissue samples

Gene	Tissue sample	Mean Ct ± SE	Mean quantity ± SE	RMS
ACTB	IMM001T	34.24 ± 0.24	0.77 ± 0.14	NA
	IMM002T	35.61 ± 0.27	0.26 ± 0.05	NA
	IMM005T	34.75 ± 0.2	0.51 ± 0.08	NA
	IMM007T	34.59 ± 0.09	0.58 ± 0.04	NA
	IMM008T	34.8 ± 0.31	0.5 ± 0.13	NA
	IMM009T	36.01 ± 0.35	0.19 ± 0.06	NA
	IMM020T	33.09 ± 0.06	1.88 ± 0.08	NA
	IMM036T	32.78 ± 0.03	2.4 ± 0.06	NA
	IMM0037T	35.61 ± 0.44	0.27 ± 0.08	NA
	IMM0038T	32.5 ± 0.1	2.99 ± 0.24	NA
	IMM0052T	36 ± 0.31	0.19 ± 0.04	NA
	IMM0056T	32.05 ± 0.09	4.25 ± 0.29	NA
	IMM0058T	35.03 ± 0.1	0.41 ± 0.03	NA
	IMM0068T	33.19 ± 0.34	1.78 ± 0.47	NA
	IMM0070T	34.51 ± 0.32	0.63 ± 0.15	NA
	IMM072T	31.52 ± 0.03	6.43 ± 0.15	NA
	IMM0075T	33.56 ± 0.31	1.33 ± 0.35	NA
	IMM0076T	35.65 ± 0.2	0.25 ± 0.04	NA
	IMM0078T	32.82 ± 0.1	2.32 ± 0.19	NA
	IMM0082T	31.36 ± 0.24	7.38 ± 1.48	NA
	IMM0083T	32.89 ± 0.08	2.19 ± 0.15	NA
	IMM0084T	30.24 ± 0.07	17.61 ± 1.02	NA
	IMM0085T	32.46 ± 0.08	3.07 ± 0.2	NA
	IMM0086T	32.1 ± 0.07	4.08 ± 0.21	NA
	AM02007T	38.4 ± 0.3	0.03 ± 0.01	NA
	AM01023T	33.54 ± 0.09	1.32 ± 0.1	NA
	AM02031T	36.38 ± 0.35	0.15 ± 0.04	NA
	AM02037T	34.26 ± 0.15	0.75 ± 0.09	NA
	AM02039T	35.51 ± 0.31	0.29 ± 0.07	NA
	IMM0011T	33.67 ± 0.02	0.55 ± 0.01	NA
	IMM0013T	33.95 ± 0.06	0.47 ± 0.02	NA
	IMM0014T	34.63 ± 0.24	0.31 ± 0.05	NA
	IMM0017T	36.19 ± 0.07	0.11 ± 0	NA
	IMM0018T	32.95 ± 0.04	0.87 ± 0.02	NA
	IMM0019T	36.09 ± 0.28	0.12 ± 0.02	NA
	IMM0022T (2)	34.63 ± 0.28	0.31 ± 0.05	NA
	IMM0025T	33.41 ± 0.07	0.65 ± 0.03	NA
	IMM0031T	NA	NA	NA
	IMM0032T	36.9 ± 0.35	0.07 ± 0.02	NA
	AM02004T	36.95 ± 0.91	0.08 ± 0.04	NA
	AM02012T	35.36 ± 0.23	0.19 ± 0.03	NA
	AM03014T	33.19 ± 0.07	0.75 ± 0.03	NA
	AM02018T	36.31 ± 0.41	0.11 ± 0.03	NA
	AM02026T	37.96 ± 0.59	0.04 ± 0.02	NA
	AM01028T	36.67 ± 0.3	0.09 ± 0.02	NA
	AM03029T	37.61 ± 0.42	0.05 ± 0.01	NA
	AM02036T	34.49 ± 0.08	0.33 ± 0.02	NA
	AM99038T	34.43 ± 0.03	0.34 ± 0.01	NA
	AM02040T	39.3 ± 0.17	0.02 ± 0	NA
	AM02045T	34.71 ± 0.21	0.29 ± 0.04	NA
	AM02047T	35.71 0.19	0.16 ± 0.02	NA

NA= Not applicable

Table 7.1 Contd.: Summary of QMSP results for prostate cancer tissue samples				
Gene	Tissue sample	Mean Ct ± SE	Mean quantity ± SE	RMS
BIK	IMM001T	0	0	0
	IMM002T	0	0	0
	IMM005T	0	0	0
	IMM007T	0	0	0
	IMM008T	0	0	0
	IMM009T	0	0	0
	IMM020T	0	0	0
	IMM036T	0	0	0
	IMM0037T	0	0	0
	IMM0038T	0	0	0
	IMM0052T	0	0	0
	IMM0056T	0	0	0
	IMM0058T	0	0	0
	IMM0068T	0	0	0
	IMM0070T	0	0	0
	IMM072T	0	0	0
	IMM0075T	0	0	0
	IMM0076T	0	0	0
	IMM0078T	0	0	0
	IMM0082T	0	0	0
	IMM0083T	0	0	0
	IMM0084T	0	0	0
	IMM0085T	0	0	0
	IMM0086T	0	0	0
	AM02007T	0	0	0
	AM01023T	0	0	0
	AM02031T	0	0	0
	AM02037T	0	0	0
	AM02039T	0	0	0
	IMM0011T	0	0	0
	IMM0013T	0	0	0
	IMM0014T	0	0	0
	IMM0017T	0	0	0
	IMM0018T	0	0	0
	IMM0019T	0	0	0
	IMM0022T (2)	0	0	0
	IMM0025T	0	0	0
	IMM0031T	NA	NA	NA
	IMM0032T	0	0	0
	AM02004T	0	0	0
	AM02012T	0	0	0
	AM03014T	0	0	0
	AM02018T	0	0	0
	AM02026T	0	0	0
	AM01028T	0	0	0
	AM03029T	0	0	0
	AM02036T	0	0	0
	AM99038T	0	0	0
	AM02040T	0	0	0
	AM02045T	0	0	0
	AM02047T	0	0	0
NA= Not applicable				

Table 7.1 Contd.: Summary of QMSP results for prostate cancer tissue samples				
Gene	**Tissue sample**	**Mean Ct ± SE**	**Mean quantity ± SE**	**RMS**
BNIP3	IMM001T	0	0	0
	IMM002T	41.11 ± 0.9	0.007 ± 0.004	25.774 ± 0.025
	IMM005T	0	0	0
	IMM007T	0	0	0
	IMM008T	0	0	0
	IMM009T	0	0	0
	IMM020T	0	0	0
	IMM036T	0	0	0
	IMM0037T	0	0	0
	IMM0038T	0	0	0
	IMM0052T	0	0	0
	IMM0056T	44.27 ± 1.22	0.001 ± 0.001	0.175 ± 4.498
	IMM0058T	0	0	0
	IMM0068T	0	0	0
	IMM0070T	0	0	0
	IMM072T	39.92 ± 0.43	0.216 ± 0.005	2.317 ± 0.134
	IMM0075T	0	0	0
	IMM0076T	0	0	0
	IMM0078T	39.19 ± 2.43	0.047 ± 0.056	20.029 ± 0.06
	IMM0082T	0	0	0
	IMM0083T	39.54 ± 1.37	0.024 ± 0.021	10.99 ± 0.078
	IMM0084T	36.25 ± 0.33	0.212 ± 0.05	12.033 ± 0.02
	IMM0085T	0	0	0
	IMM0086T	0	0	0
	AM02007T	0	0	0
	AM01023T	47.84 ± 0.28	0 ± 0	0.035 ± 6.026
	AM02031T	0	0	0
	AM02037T	0	0	0
	AM02039T	0	0	0
	IMM0011T	0	0	0
	IMM0013T	0	0	0
	IMM0014T	0	0	0
	IMM0017T	0	0	0
	IMM0018T	43.77 ± 6.19	0.042 ± 0.059	48.546 ± 0.029
	IMM0019T	0	0	0
	IMM0022T (2)	0	0	0
	IMM0025T	42.26 ± 0.68	0.02 ± 0.007	30.028 ± 0.012
	IMM0031T	NA	NA	NA
	IMM0032T	0	0	0
	AM02004T	0	0	0
	AM02012T	0	0	0
	AM03014T	0	0	0
	AM02018T	0	0	0
	AM02026T	0	0	0
	AM01028T	0	0	0
	AM03029T	0	0	0
	AM02036T	0	0	0
	AM99038T	0	0	0
	AM02040T	0	0	0
	AM02045T	0	0	0
	AM02047T	0	0	0
NA= Not applicable				

Table 7.1 Contd.: Summary of QMSP results for prostate cancer tissue samples				
Gene	**Tissue sample**	**Mean Ct ± SE**	**Mean quantity ± SE**	**RMS**
CDKN2A	IMM001T	0	0	0
	IMM002T	0	0	0
	IMM005T	0	0	0
	IMM007T	0	0	0
	IMM008T	0	0	0
	IMM009T	0	0	0
	IMM020T	0	0	0
	IMM036T	0	0	0
	IMM0037T	32.21 ± 6.6		NA
	IMM0038T	38.97 ± 0.98		NA
	IMM0052T	0	0	0
	IMM0056T	36.27 ± 2.38		NA
	IMM0058T	33.29 ± 3.24		NA
	IMM0068T	0	0	0
	IMM0070T	0	0	0
	IMM072T	37.3 ± 0.5		NA
	IMM0075T	0	0	0
	IMM0076T	0	0	0
	IMM0078T	0	0	0
	IMM0082T	44.14 ± 0.15		NA
	IMM0083T	0	0	0
	IMM0084T	39.01 ± 0.57		NA
	IMM0085T	0	0	0
	IMM0086T	40.2 ± 1.62		NA
	AM02007T	0	0	0
	AM01023T	0	0	0
	AM02031T	0	0	0
	AM02037T	0	0	0
	AM02039T	0	0	0
	IMM0011T	NA	NA	NA
	IMM0013T	NA	NA	NA
	IMM0014T	NA	NA	NA
	IMM0017T	NA	NA	NA
	IMM0018T	NA	NA	NA
	IMM0019T	NA	NA	NA
	IMM0022T (2)	NA	NA	NA
	IMM0025T	NA	NA	NA
	IMM0031T	NA	NA	NA
	IMM0032T	NA	NA	NA
	AM02004T	NA	NA	NA
	AM02012T	NA	NA	NA
	AM03014T	NA	NA	NA
	AM02018T	NA	NA	NA
	AM02026T	NA	NA	NA
	AM01028T	NA	NA	NA
	AM03029T	NA	NA	NA
	AM02036T	NA	NA	NA
	AM99038T	NA	NA	NA
	AM02040T	NA	NA	NA
	AM02045T	NA	NA	NA
	AM02047T	NA	NA	NA
NA= Not applicable				

Table 7.1 Contd.: Summary of QMSP results for prostate cancer tissue samples				
Gene	**Tissue sample**	**Mean Ct ± SE**	**Mean quantity ± SE**	**RMS**
CpG1 cFLIP	IMM001T	0	0	0
	IMM002T	0	0	0
	IMM005T	0	0	0
	IMM007T	0	0	0
	IMM008T	0	0	0
	IMM009T	0	0	0
	IMM020T	0	0	0
	IMM036T	0	0	0
	IMM0037T	0	0	0
	IMM0038T	0	0	0
	IMM0052T	0	0	0
	IMM0056T	0	0	0
	IMM0058T	0	0	0
	IMM0068T	0	0	0
	IMM0070T	0	0	0
	IMM072T	0	0	0
	IMM0075T	0	0	0
	IMM0076T	0	0	0
	IMM0078T	0	0	0
	IMM0082T	0	0	0
	IMM0083T	0	0	0
	IMM0084T	0	0	0
	IMM0085T	0	0	0
	IMM0086T	0	0	0
	AM02007T	0	0	0
	AM01023T	0	0	0
	AM02031T	0	0	0
	AM02037T	0	0	0
	AM02039T	0	0	0
	IMM0011T	NA	NA	NA
	IMM0013T	NA	NA	NA
	IMM0014T	NA	NA	NA
	IMM0017T	NA	NA	NA
	IMM0018T	NA	NA	NA
	IMM0019T	NA	NA	NA
	IMM0022T (2)	NA	NA	NA
	IMM0025T	NA	NA	NA
	IMM0031T	NA	NA	NA
	IMM0032T	NA	NA	NA
	AM02004T	NA	NA	NA
	AM02012T	NA	NA	NA
	AM03014T	NA	NA	NA
	AM02018T	NA	NA	NA
	AM02026T	NA	NA	NA
	AM01028T	NA	NA	NA
	AM03029T	NA	NA	NA
	AM02036T	NA	NA	NA
	AM99038T	NA	NA	NA
	AM02040T	NA	NA	NA
	AM02045T	NA	NA	NA
	AM02047T	NA	NA	NA
NA= Not applicable				

Table 7.1 Contd.: Summary of QMSP results for prostate cancer tissue samples				
Gene	Tissue sample	Mean Ct ± SE	Mean quantity ± SE	RMS
CpG2 cFLIP	IMM001T	0	0	0
	IMM002T	0	0	0
	IMM005T	0	0	0
	IMM007T	0	0	0
	IMM008T	0	0	0
	IMM009T	0	0	0
	IMM020T	0	0	0
	IMM036T	0	0	0
	IMM0037T	0	0	0
	IMM0038T	0	0	0
	IMM0052T	0	0	0
	IMM0056T	0	0	0
	IMM0058T	0	0	0
	IMM0068T	0	0	0
	IMM0070T	0	0	0
	IMM072T	0	0	0
	IMM0075T	0	0	0
	IMM0076T	0	0	0
	IMM0078T	0	0	0
	IMM0082T	0	0	0
	IMM0083T	0	0	0
	IMM0084T	0	0	0
	IMM0085T	0	0	0
	IMM0086T	0	0	0
	AM02007T	0	0	0
	AM01023T	0	0	0
	AM02031T	0	0	0
	AM02037T	0	0	0
	AM02039T	0	0	0
	IMM0011T	NA	NA	NA
	IMM0013T	NA	NA	NA
	IMM0014T	NA	NA	NA
	IMM0017T	NA	NA	NA
	IMM0018T	NA	NA	NA
	IMM0019T	NA	NA	NA
	IMM0022T (2)	NA	NA	NA
	IMM0025T	NA	NA	NA
	IMM0031T	NA	NA	NA
	IMM0032T	NA	NA	NA
	AM02004T	NA	NA	NA
	AM02012T	NA	NA	NA
	AM03014T	NA	NA	NA
	AM02018T	NA	NA	NA
	AM02026T	NA	NA	NA
	AM01028T	NA	NA	NA
	AM03029T	NA	NA	NA
	AM02036T	NA	NA	NA
	AM99038T	NA	NA	NA
	AM02040T	NA	NA	NA
	AM02045T	NA	NA	NA
	AM02047T	NA	NA	NA
NA= Not applicable				

Table 7.1 Contd.: Summary of QMSP results for prostate cancer tissue samples				
Gene	**Tissue sample**	**Mean Ct ± SE**	**Mean quantity ± SE**	**RMS**
DCR1	IMM001T	43.3 ± 6.78	0.1 ± 0.142	131.019 ± 0.011
	IMM002T	0	0	0
	IMM005T	0	0	0
	IMM007T	0	0	0
	IMM008T	0	0	0
	IMM009T	0	0	0
	IMM020T	42.83 ± 5.33	0.07 ± 0.097	36.971 ± 0.038
	IMM036T	0	0	0
	IMM0037T	0	0	0
	IMM0038T	39.22 ± 0.09	0.125 ± 0.008	41.627 ± 0.002
	IMM0052T	0	0	0
	IMM0056T	0	0	0
	IMM0058T	0	0	0
	IMM0068T	0	0	0
	IMM0070T	48.2 ± 1.52	0.0004 ± 0	0.611 ± 1.477
	IMM072T	36.66 ± 0.41	0.708 ± 0.179	110.112 ± 0.002
	IMM0075T	0	0	0
	IMM0076T	0	0	0
	IMM0078T	39.22 ± 0.82	0.137 ± 0.065	58.79 ± 0.008
	IMM0082T	0	0	0
	IMM0083T	39.52 ± 0.81	0.113 ± 0.065	51.543 ± 0.011
	IMM0084T	34.63 ± 0.44	2.784 ± 0.796	158.044 ± 0.002
	IMM0085T	39.17 ± 0.67	0.135 ± 0.059	43.95 ± 0.01
	IMM0086T	38.77 ± 0.58	0.174 ± 0.066	42.647 ± 0.009
	AM02007T	0	0	0
	AM01023T	43.55 ± 1.95	0.012 ± 0.015	9.044 ± 0.135
	AM02031T	0	0	0
	AM02037T	0	0	0
	AM02039T	0	0	0
	IMM0011T	NA	NA	NA
	IMM0013T	NA	NA	NA
	IMM0014T	NA	NA	NA
	IMM0017T	NA	NA	NA
	IMM0018T	NA	NA	NA
	IMM0019T	NA	NA	NA
	IMM0022T (2)	NA	NA	NA
	IMM0025T	NA	NA	NA
	IMM0031T	NA	NA	NA
	IMM0032T	NA	NA	NA
	AM02004T	NA	NA	NA
	AM02012T	NA	NA	NA
	AM03014T	NA	NA	NA
	AM02018T	NA	NA	NA
	AM02026T	NA	NA	NA
	AM01028T	NA	NA	NA
	AM03029T	NA	NA	NA
	AM02036T	NA	NA	NA
	AM99038T	NA	NA	NA
	AM02040T	NA	NA	NA
	AM02045T	NA	NA	NA
	AM02047T	NA	NA	NA
NA= Not applicable				

Table 7.1 Contd.: Summary of QMSP results for prostate cancer tissue samples				
Gene	Tissue sample	Mean Ct ± SE	Mean quantity ± SE	RMS
DCR2	IMM001T	38.98 ± 1.13	0.102 ± 0.078	132.563 ± 0.006
	IMM002T	42.58 ± 2.19	0.01 ± 0.012	37.518 ± 0.032
	IMM005T	0	0	0
	IMM007T	0	0	0
	IMM008T	42.69 ± 2.23	0.013 ± 0.019	25.75 ± 0.057
	IMM009T	0	0	0
	IMM020T	0	0	0
	IMM036T	41.79 ± 0.8	0.011 ± 0.006	4.624 ± 0.125
	IMM0037T	0	0	0
	IMM0038T	37.01 ± 0.44	0.396 ± 0.118	132.271 ± 0.002
	IMM0052T	0	0	0
	IMM0056T	0	0	0
	IMM0058T	41.17 ± 1.66	0.026 ± 0.029	64.372 ± 0.017
	IMM0068T	38.44 ± 0.43	0.133 ± 0.041	74.84 ± 0.005
	IMM0070T	39.9 ± 0.83	0.047 ± 0.028	74.939 ± 0.008
	IMM072T	44.16 ± 1.86	0.003 ± 0.003	0.4 ± 2.696
	IMM0075T	0	0	0
	IMM0076T	0	0	0
	IMM0078T	37.78 ± 0.36	0.218 ± 0.056	94.074 ± 0.003
	IMM0082T	0	0	0
	IMM0083T	42.67 ± 0.83	0.006 ± 0.003	2.6 ± 0.228
	IMM0084T	40.2 ± 0.62	0.036 ± 0.014	2.065 ± 0.195
	IMM0085T	36.72 ± 0.49	0.5 ± 0.17	162.979 ± 0.002
	IMM0086T	36.44 ± 0.44	0.613 ± 0.184	149.984 ± 0.002
	AM02007T	0	0	0
	AM01023T	0	0	0
	AM02031T	44.41 ± 1.58	0.002 ± 0.002	13.135 ± 0.077
	AM02037T	0	0	0
	AM02039T	0	0	0
	IMM0011T	39.66 ± 1.01	0.04 ± 0.025	71.481 ± 0.009
	IMM0013T	39.02 ± 0.07	0.054 ± 0.002	116.297 ± 0.001
	IMM0014T	0	0	0
	IMM0017T	0	0	0
	IMM0018T	40.08 ± 1.94	0.039 ± 0.039	44.332 ± 0.023
	IMM0019T	0	0	0
	IMM0022T (2)	0	0	0
	IMM0025T	40.1 ± 2.32	0.044 ± 0.049	66.997 ± 0.017
	IMM0031T	NA	NA	NA
	IMM0032T	0	0	0
	AM02004T	0	0	0
	AM02012T	0	0	0
	AM03014T	0	0	0
	AM02018T	0	0	0
	AM02026T	0	0	0
	AM01028T	0	0	0
	AM03029T	0	0	0
	AM02036T	0	0	0
	AM99038T	0	0	0
	AM02040T	0	0	0
	AM02045T	0	0	0
	AM02047T	0	0	0
NA= Not applicable				

Table 7.1 Contd.: Summary of QMSP results for prostate cancer tissue samples				
Gene	**Tissue sample**	**Mean Ct ± SE**	**Mean quantity ± SE**	**RMS**
TMS1	IMM001T	0	0	0
	IMM002T	0	0	0
	IMM005T	0	0	0
	IMM007T	0	0	0
	IMM008T	38.198 ± 1.598	0.072 ± 0.072	142.941 ± 0.007
	IMM009T	0	0	0
	IMM020T	0	0	0
	IMM036T	0	0	0
	IMM0037T	0	0	0
	IMM0038T	35.098 ± 0.182	0.577 ± 0.082	193.034 ± 0.001
	IMM0052T	0	0	0
	IMM0056T	0	0	0
	IMM0058T	0	0	0
	IMM0068T	36.162 ± 0.701	0.273 ± 0.13	153.085 ± 0.004
	IMM0070T	37.562 ± 0.378	0.085 ± 0.025	135.327 ± 0.003
	IMM072T	33.837 ± 0.073	1.544 ± 0.089	240.004 ± 0
	IMM0075T	0	0	0
	IMM0076T	0	0	0
	IMM0078T	34.216 ± 0.034	1.145 ± 0.03	493.205 ± 0
	IMM0082T	38.945 ± 0.637	0.03 ± 0.014	4.04 ± 0.129
	IMM0083T	40.27 ± 1.464	0.013 ± 0.013	6.103 ± 0.156
	IMM0084T	31.439 ± 0.173	10.175 ± 1.325	577.738 ± 0
	IMM0085T	40.853 ± 1.747	0.009 ± 0.01	0.776 ± 1.367
	IMM0086T	37.711 ± 1.613	0.105 ± 0.106	25.815 ± 0.039
	AM02007T	0	0	0
	AM01023T	0	0	0
	AM02031T	0	0	0
	AM02037T	0	0	0
	AM02039T	41.885 ± 4.405	0.016 ± 0.023	56.554 ± 0.025
	IMM0011T	36.278 ± 0.635	0.078 ± 0.03	140.417 ± 0.003
	IMM0013T	41.882 ± 0.943	0.002 ± 0.001	3.955 ± 0.151
	IMM0014T	37.001 ± 1.282	0.055 ± 0.034	179.97 ± 0.003
	IMM0017T	0	0	0
	IMM0018T	34.522 ± 0.167	0.242 ± 0.028	277.524 ± 0
	IMM0019T	0	0	0
	IMM0022T (2)	43.695 ± 6.297	0.005 ± 0.007	16.167 ± 0.088
	IMM0025T	35.385 ± 0.216	0.136 ± 0.02	207.235 ± 0.001
	IMM0031T	NA	NA	NA
	IMM0032T	0	0	0
	AM02004T	0	0	0
	AM02012T	44.958 ± 0.686	0.0002 ± 0.0001	1.14 ± 0.413
	AM03014T	38.886 ± 1.301	0.016 ± 0.01	30.906 ± 0.02
	AM02018T	0	0	0
	AM02026T	0	0	0
	AM01028T	0	0	0
	AM03029T	0	0	0
	AM02036T	0	0	0
	AM99038T	0	0	0
	AM02040T	0	0	0
	AM02045T	38.324 ± 0.15	0.019 ± 0.002	63.822 ± 0.003
	AM02047T	38.223 ± 1.204	0.024 ± 0.014	152.212 ± 0.004
NA= Not applicable				

Table 7.2: Summary of QMSP results for benign tissue samples				
Gene	**Tissue sample**	**Mean Ct ± SE**	**Mean quantity ± SE**	**RMS**
ACTB	IMM001N	34.12 ± 0.206	0.843 ± 0.137	NA
	IMM005N	34.225 ± 0.203	0.776 ± 0.128	NA
	IMM009N	37.303 ± 0.405	0.071 ± 0.02	NA
	IMM020N	34.777 ± 0.221	0.504 ± 0.091	NA
	IMM0037N	36.645 ± 0.666	0.125 ± 0.055	NA
	IMM0038N	38.27 ± 0.623	0.035 ± 0.014	NA
	IMM0052N	34.402 ± 0.086	0.671 ± 0.046	NA
	IMM0056N	34.942 ± 0.256	0.444 ± 0.086	NA
	IMM0058N	34.793 ± 0.318	0.503 ± 0.121	NA
	IMM0070N	35.576 ± 0.271	0.27 ± 0.059	NA
	IMM0072N	32.782 ± 0.134	2.399 ± 0.248	NA
	IMM0075N	35.487 ± 0.166	0.287 ± 0.037	NA
	IMM0076N	37.142 ± 0.284	0.079 ± 0.018	NA
	IMM0078N	31.711 ± 0.021	5.543 ± 0.093	NA
	IMM0082N	32.861 ± 0.27	2.279 ± 0.459	NA
	IMM0083N	35.07 ± 0.048	0.397 ± 0.015	NA
	IMM0084N	32.663 ± 0.071	2.627 ± 0.145	NA
	IMM0085N	32.025 ± 0.085	4.336 ± 0.292	NA
	IMM0086N	32.185 ± 0.017	3.82 ± 0.05	NA
	AM02045N	33.659 ± 0.25	1.216 ± 0.238	NA
	IMM0011N	34.632 ± 0.223	0.306 ± 0.041	NA
	IMM0013N	38.052 ± 0.653	0.038 ± 0.017	NA
	IMM0017N	36.591 ± 0.162	0.089 ± 0.009	NA
	IMM0018N	34.576 ± 0.199	0.316 ± 0.038	NA
	IMM0019N	37.739 ± 0.246	0.044 ± 0.007	NA
	IMM0022N	36.477 ± 0.456	0.098 ± 0.026	NA
	IMM0032N	38.585 ± 0.087	0.025 ± 0.001	NA
	AM02004N	40.361 ± 0.983	0.009 ± 0.006	NA
	AM02007N	36.728 ± 0.452	0.084 ± 0.022	NA
	AM03009N	36.496 ± 0.163	0.095 ± 0.01	NA
	AM01010N	36.124 ± 0.173	0.12 ± 0.013	NA
	AM02012N	34.722 ± 0.154	0.288 ± 0.028	NA
	AM03020N	35.817 ± 0.081	0.144 ± 0.007	NA
	AM01023N	33.66 ± 0.127	0.561 ± 0.045	NA
	AM02025N	35.544 ± 0.288	0.173 ± 0.033	NA
	AM02026N	33.087 ± 0.286	0.81 ± 0.152	NA
	AM00027N	34.658 ± 0.244	0.301 ± 0.046	NA
	AM01028N	36.305 ± 0.576	0.111 ± 0.035	NA
	AM03029N	40.162 ± 0.119	0.009 ± 0.001	NA
	AM02030N	35.501 ± 0.284	0.178 ± 0.03	NA
	AM02036N	34.618 ± 0.228	0.309 ± 0.042	NA
	AM02037N	34.485 ± 0.099	0.334 ± 0.02	NA
	AM99038N	34.449 ± 0.284	0.344 ± 0.058	NA
	AM03085N	37.689 ± 0.79	0.048 ± 0.02	NA
NA= Not applicable				

Table 7.2. Contd: Summary of QMSP results for benign tissue samples				
Gene	Tissue sample	Mean Ct ± SE	Mean quantity ± SE	RMS
BIK	IMM001N	0	0	0
	IMM005N	0	0	0
	IMM009N	0	0	0
	IMM020N	0	0	0
	IMM0037N	0	0	0
	IMM0038N	0	0	0
	IMM0052N	0	0	0
	IMM0056N	0	0	0
	IMM0058N	0	0	0
	IMM0070N	0	0	0
	IMM0072N	0	0	0
	IMM0075N	0	0	0
	IMM0076N	0	0	0
	IMM0078N	0	0	0
	IMM0082N	0	0	0
	IMM0083N	0	0	0
	IMM0084N	0	0	0
	IMM0085N	0	0	0
	IMM0086N	0	0	0
	AM02045N	0	0	0
	IMM0011N	0	0	0
	IMM0013N	0	0	0
	IMM0017N	0	0	0
	IMM0018N	0	0	0
	IMM0019N	0	0	0
	IMM0022N	0	0	0
	IMM0032N	0	0	0
	AM02004N	0	0	0
	AM02007N	0	0	0
	AM03009N	0	0	0
	AM01010N	0	0	0
	AM02012N	0	0	0
	AM03020N	0	0	0
	AM01023N	0	0	0
	AM02025N	0	0	0
	AM02026N	0	0	0
	AM00027N	0	0	0
	AM01028N	0	0	0
	AM03029N	0	0	0
	AM02030N	0	0	0
	AM02036N	0	0	0
	AM02037N	0	0	0
	AM99038N	0	0	0
	AM03085N	0	0	0
NA= Not applicable				

Table 7.2 Contd: Summary of QMSP results for benign tissue samples				
Gene	Tissue sample	Mean Ct ± SE	Mean quantity ± SE	RMS
BNIP3	IMM001N	0	0	0
	IMM005N	0	0	0
	IMM009N	0	0	0
	IMM020N	0	0	0
	IMM0037N	0	0	0
	IMM0038N	0	0	0
	IMM0052N	0	0	0
	IMM0056N	0	0	0
	IMM0058N	0	0	0
	IMM0070N	0	0	0
	IMM0072N	0	0	0
	IMM0075N	0	0	0
	IMM0076N	0	0	0
	IMM0078N	0	0	0
	IMM0082N	0	0	0
	IMM0083N	0	0	0
	IMM0084N	0	0	0
	IMM0085N	0	0	0
	IMM0086N	0	0	0
	AM02045N	0	0	0
	IMM0011N	0	0	0
	IMM0013N	0	0	0
	IMM0017N	0	0	0
	IMM0018N	0	0	0
	IMM0019N	0	0	0
	IMM0022N	0	0	0
	IMM0032N	0	0	0
	AM02004N	0	0	0
	AM02007N	0	0	0
	AM03009N	0	0	0
	AM01010N	0	0	0
	AM02012N	0	0	0
	AM03020N	0	0	0
	AM01023N	0	0	0
	AM02025N	0	0	0
	AM02026N	0	0	0
	AM00027N	0	0	0
	AM01028N	0	0	0
	AM03029N	0	0	0
	AM02030N	0	0	0
	AM02036N	0	0	0
	AM02037N	0	0	0
	AM99038N	0	0	0
	AM03085N	0	0	0
NA= Not applicable				

Table 7.2 Contd: Summary of QMSP results for benign tissue samples				
Gene	**Tissue sample**	**Mean Ct ± SE**	**Mean quantity ± SE**	**RMS**
CDKN2A	IMM001N	0	0	0
	IMM005N	0	0	0
	IMM009N	0	0	0
	IMM020N	0	0	0
	IMM0037N	0	0	0
	IMM0038N	0	0	0
	IMM0052N	0	0	0
	IMM0056N	0	0	0
	IMM0058N	0	0	0
	IMM0070N	0	0	0
	IMM0072N	0	0	0
	IMM0075N	0	0	0
	IMM0076N	0	0	0
	IMM0078N	0	0	0
	IMM0082N	0	0	0
	IMM0083N	0	0	0
	IMM0084N	0	0	0
	IMM0085N	0	0	0
	IMM0086N	0	0	0
	AM02045N	0	0	0
	IMM0011N	0	0	0
	IMM0013N	0	0	0
	IMM0017N	0	0	0
	IMM0018N	0	0	0
	IMM0019N	0	0	0
	IMM0022N	0	0	0
	IMM0032N	0	0	0
	AM02004N	0	0	0
	AM02007N	0	0	0
	AM03009N	0	0	0
	AM01010N	0	0	0
	AM02012N	0	0	0
	AM03020N	0	0	0
	AM01023N	0	0	0
	AM02025N	0	0	0
	AM02026N	0	0	0
	AM00027N	0	0	0
	AM01028N	0	0	0
	AM03029N	0	0	0
	AM02030N	0	0	0
	AM02036N	0	0	0
	AM02037N	0	0	0
	AM99038N	0	0	0
	AM03085N	0	0	0
NA= Not applicable				

Table 7.2 Contd: Summary of QMSP results for benign tissue samples				
Gene	**Tissue sample**	**Mean Ct ± SE**	**Mean quantity ± SE**	**RMS**
CpG1 cFLIP	IMM001N	0	0	0
	IMM005N	0	0	0
	IMM009N	0	0	0
	IMM020N	0	0	0
	IMM0037N	0	0	0
	IMM0038N	0	0	0
	IMM0052N	0	0	0
	IMM0056N	0	0	0
	IMM0058N	0	0	0
	IMM0070N	0	0	0
	IMM0072N	0	0	0
	IMM0075N	0	0	0
	IMM0076N	0	0	0
	IMM0078N	0	0	0
	IMM0082N	0	0	0
	IMM0083N	0	0	0
	IMM0084N	0	0	0
	IMM0085N	0	0	0
	IMM0086N	0	0	0
	AM02045N	0	0	0
	IMM0011N	NA	NA	NA
	IMM0013N	NA	NA	NA
	IMM0017N	NA	NA	NA
	IMM0018N	NA	NA	NA
	IMM0019N	NA	NA	NA
	IMM0022N	NA	NA	NA
	IMM0032N	NA	NA	NA
	AM02004N	NA	NA	NA
	AM02007N	NA	NA	NA
	AM03009N	NA	NA	NA
	AM01010N	NA	NA	NA
	AM02012N	NA	NA	NA
	AM03020N	NA	NA	NA
	AM01023N	NA	NA	NA
	AM02025N	NA	NA	NA
	AM02026N	NA	NA	NA
	AM00027N	NA	NA	NA
	AM01028N	NA	NA	NA
	AM03029N	NA	NA	NA
	AM02030N	NA	NA	NA
	AM02036N	NA	NA	NA
	AM02037N	NA	NA	NA
	AM99038N	NA	NA	NA
	AM03085N	NA	NA	NA
NA= Not applicable				

Table 7.2 Contd: Summary of QMSP results for benign tissue samples				
Gene	**Tissue sample**	**Mean Ct ± SE**	**Mean quantity ± SE**	**RMS**
CpG2 cFLIP	IMM001N	0	0	0
	IMM005N	0	0	0
	IMM009N	0	0	0
	IMM020N	0	0	0
	IMM0037N	0	0	0
	IMM0038N	0	0	0
	IMM0052N	0	0	0
	IMM0056N	0	0	0
	IMM0058N	0	0	0
	IMM0070N	0	0	0
	IMM0072N	0	0	0
	IMM0075N	0	0	0
	IMM0076N	0	0	0
	IMM0078N	0	0	0
	IMM0082N	0	0	0
	IMM0083N	0	0	0
	IMM0084N	0	0	0
	IMM0085N	0	0	0
	IMM0086N	0	0	0
	AM02045N	0	0	0
	IMM0011N	NA	NA	NA
	IMM0013N	NA	NA	NA
	IMM0017N	NA	NA	NA
	IMM0018N	NA	NA	NA
	IMM0019N	NA	NA	NA
	IMM0022N	NA	NA	NA
	IMM0032N	NA	NA	NA
	AM02004N	NA	NA	NA
	AM02007N	NA	NA	NA
	AM03009N	NA	NA	NA
	AM01010N	NA	NA	NA
	AM02012N	NA	NA	NA
	AM03020N	NA	NA	NA
	AM01023N	NA	NA	NA
	AM02025N	NA	NA	NA
	AM02026N	NA	NA	NA
	AM00027N	NA	NA	NA
	AM01028N	NA	NA	NA
	AM03029N	NA	NA	NA
	AM02030N	NA	NA	NA
	AM02036N	NA	NA	NA
	AM02037N	NA	NA	NA
	AM99038N	NA	NA	NA
	AM03085N	NA	NA	NA
NA= Not applicable				

Table 7.2 Contd: Summary of QMSP results for benign tissue samples				
Gene	**Tissue sample**	**Mean Ct ± SE**	**Mean quantity ± SE**	**RMS**
DCR1	IMM001N	0	0	0
	IMM005N	0	0	0
	IMM009N	0	0	0
	IMM020N	0	0	0
	IMM0037N	0	0	0
	IMM0038N	0	0	0
	IMM0052N	0	0	0
	IMM0056N	0	0	0
	IMM0058N	0	0	0
	IMM0070N	0	0	0
	IMM0072N	0	0	0
	IMM0075N	0	0	0
	IMM0076N	0	0	0
	IMM0078N	0	0	0
	IMM0082N	0	0	0
	IMM0083N	0	0	0
	IMM0084N	0	0	0
	IMM0085N	0	0	0
	IMM0086N	0	0	0
	AM02045N	0	0	0
	IMM0011N	NA	NA	NA
	IMM0013N	NA	NA	NA
	IMM0017N	NA	NA	NA
	IMM0018N	NA	NA	NA
	IMM0019N	NA	NA	NA
	IMM0022N	NA	NA	NA
	IMM0032N	NA	NA	NA
	AM02004N	NA	NA	NA
	AM02007N	NA	NA	NA
	AM03009N	NA	NA	NA
	AM01010N	NA	NA	NA
	AM02012N	NA	NA	NA
	AM03020N	NA	NA	NA
	AM01023N	NA	NA	NA
	AM02025N	NA	NA	NA
	AM02026N	NA	NA	NA
	AM00027N	NA	NA	NA
	AM01028N	NA	NA	NA
	AM03029N	NA	NA	NA
	AM02030N	NA	NA	NA
	AM02036N	NA	NA	NA
	AM02037N	NA	NA	NA
	AM99038N	NA	NA	NA
	AM03085N	NA	NA	NA
NA= Not applicable				

Table 7.2 Contd: Summary of QMSP results for benign tissue samples				
Gene	**Tissue sample**	**Mean Ct ± SE**	**Mean quantity ± SE**	**RMS**
DCR2	IMM001N	0	0	0
	IMM005N	0	0	0
	IMM009N	0	0	0
	IMM020N	0	0	0
	IMM0037N	0	0	0
	IMM0038N	0	0	0
	IMM0052N	0	0	0
	IMM0056N	0	0	0
	IMM0058N	0	0	0
	IMM0070N	0	0	0
	IMM0072N	0	0	0
	IMM0075N	0	0	0
	IMM0076N	0	0	0
	IMM0078N	0	0	0
	IMM0082N	0	0	0
	IMM0083N	0	0	0
	IMM0084N	0	0	0
	IMM0085N	0	0	0
	IMM0086N	0	0	0
	AM02045N	0	0	0
	IMM0011N	0	0	0
	IMM0013N	0	0	0
	IMM0017N	0	0	0
	IMM0018N	0	0	0
	IMM0019N	0	0	0
	IMM0022N	0	0	0
	IMM0032N	0	0	0
	AM02004N	0	0	0
	AM02007N	0	0	0
	AM03009N	0	0	0
	AM01010N	0	0	0
	AM02012N	0	0	0
	AM03020N	0	0	0
	AM01023N	0	0	0
	AM02025N	0	0	0
	AM02026N	0	0	0
	AM00027N	0	0	0
	AM01028N	0	0	0
	AM03029N	0	0	0
	AM02030N	0	0	0
	AM02036N	0	0	0
	AM02037N	0	0	0
	AM99038N	0	0	0
	AM03085N	0	0	0
NA= Not applicable				

Table 7.2 Contd: Summary of QMSP results for benign tissue samples				
Gene	**Tissue sample**	**Mean Ct ± SE**	**Mean quantity ± SE**	**RMS**
TMS1	IMM001N	0	0	0
	IMM005N	0	0	0
	IMM009N	0	0	0
	IMM020N	0	0	0
	IMM0037N	0	0	0
	IMM0038N	0	0	0
	IMM0052N	0	0	0
	IMM0056N	0	0	0
	IMM0058N	0	0	0
	IMM0070N	0	0	0
	IMM0072N	0	0	0
	IMM0075N	0	0	0
	IMM0076N	0	0	0
	IMM0078N	0	0	0
	IMM0082N	0	0	0
	IMM0083N	0	0	0
	IMM0084N	0	0	0
	IMM0085N	0	0	0
	IMM0086N	0	0	0
	AM02045N	0	0	0
	IMM0011N	0	0	0
	IMM0013N	0	0	0
	IMM0017N	0	0	0
	IMM0018N	0	0	0
	IMM0019N	0	0	0
	IMM0022N	0	0	0
	IMM0032N	0	0	0
	AM02004N	0	0	0
	AM02007N	0	0	0
	AM03009N	0	0	0
	AM01010N	0	0	0
	AM02012N	0	0	0
	AM03020N	0	0	0
	AM01023N	0	0	0
	AM02025N	0	0	0
	AM02026N	0	0	0
	AM00027N	0	0	0
	AM01028N	0	0	0
	AM03029N	0	0	0
	AM02030N	0	0	0
	AM02036N	0	0	0
	AM02037N	0	0	0
	AM99038N	0	0	0
	AM03085N	0	0	0
NA= Not applicable				

Table 7.3 : Summary of QMSP results for HGPIN tissue samples				
Gene	**Tissue sample**	**Mean Ct ± SE**	**Mean quantity ± SE**	**RMS**
ACTB	IMM002P	35.716 ± 0.362	0.331 ± 0.245	NA
	IMM0037P	36.583 ± 0.214	0.123 ± 0.122	NA
	IMM0056P	35.039 ± 0.201	0.486 ± 0.41	NA
	IMM0068P	36.481 ± 0.44	0.095 ± 0.136	NA
	IMM0075P	34.639 ± 0.083	0.551 ± 0.557	NA
	AM02042P	35.391 ± 0.239	0.307 ± 0.312	NA
	IMM0013P	34.06 ± 0.324	0.382 ± 0.441	NA
	IMM0014P	35.583 ± 0.135	0.162 ± 0.168	NA
	AM02001P	36.197 ± 0.016	0.113 ± 0.114	NA
	AM02006P	36.973 ± 0.17	0.072 ± 0.07	NA
	AM03009P	36.265 ± 0.276	0.093 ± 0.11	NA
	AM01010P	36.322 ± 0.01	0.106 ± 0.105	NA
	AM03013P	37.986 ± 0.641	0.042 ± 0.039	NA
	AM03016P	38.728 ± 0.469	0.017 ± 0.024	NA
	AM01022P	37.905 ± 0.267	0.037 ± 0.039	NA
	AM02027P	39.023 ± 0.509	0.023 ± 0.02	NA
	AM00032P	37.535 0.103	0.049 0.049	NA
BIK	IMM002P	0	0	0
	IMM0037P	0	0	0
	IMM0056P	0	0	0
	IMM0068P	0	0	0
	IMM0075P	0	0	0
	AM02042P	0	0	0
	IMM0013P	0	0	0
	IMM0014P	0	0	0
	AM02001P	0	0	0
	AM02006P	0	0	0
	AM03009P	0	0	0
	AM01010P	0	0	0
	AM03013P	0	0	0
	AM03016P	0	0	0
	AM01022P	0	0	0
	AM02027P	0	0	0
	AM00032P	0	0	0
NA= Not applicable				

Table 7.3 Contd: Summary of QMSP results for HGPIN tissue samples				
Gene	**Tissue sample**	**Mean Ct ± SE**	**Mean quantity ± SE**	**RMS**
BNIP3	IMM002P	0	0	0
	IMM0037P	0	0	0
	IMM0056P	0	0	0
	IMM0068P	0	0	0
	IMM0075P	0	0	0
	AM02042P	0	0	0
	IMM0013P	0	0	0
	IMM0014P	0	0	0
	AM02001P	0	0	0
	AM02006P	0	0	0
	AM03009P	0	0	0
	AM01010P	0	0	0
	AM03013P	0	0	0
	AM03016P	0	0	0
	AM01022P	0	0	0
	AM02027P	0	0	0
	AM00032P	0	0	0
CDKN2A	IMM002P	0	0	0
	IMM0037P	19.645 ± 1.09	3673.059 ± 2402.249	9234 ± 0.234
	IMM0056P	0	0	0
	IMM0068P	0	0	0
	IMM0075P	0	0	0
	AM02042P	0	0	0
	IMM0013P	NA	NA	NA
	IMM0014P	NA	NA	NA
	AM02001P	NA	NA	NA
	AM02006P	NA	NA	NA
	AM03009P	NA	NA	NA
	AM01010P	NA	NA	NA
	AM03013P	NA	NA	NA
	AM03016P	NA	NA	NA
	AM01022P	NA	NA	NA
	AM02027P	NA	NA	NA
	AM00032P	NA	NA	NA
NA= Not applicable				

Table 7.3 Contd: Summary of QMSP results for HGPIN tissue samples

Gene	Tissue sample	Mean Ct ± SE	Mean quantity ± SE	RMS
CpG1 cFLIP	IMM002P	0	0	0
	IMM0037P	0	0	0
	IMM0056P	0	0	0
	IMM0068P	0	0	0
	IMM0075P	0	0	0
	AM02042P	0	0	0
	IMM0013P	NA	NA	NA
	IMM0014P	NA	NA	NA
	AM02001P	NA	NA	NA
	AM02006P	NA	NA	NA
	AM03009P	NA	NA	NA
	AM01010P	NA	NA	NA
	AM03013P	NA	NA	NA
	AM03016P	NA	NA	NA
	AM01022P	NA	NA	NA
	AM02027P	NA	NA	NA
	AM00032P	NA	NA	NA
CpG2 cFLIP	IMM002P	0	0	0
	IMM0037P	0	0	0
	IMM0056P	0	0	0
	IMM0068P	0	0	0
	IMM0075P	0	0	0
	AM02042P	0	0	0
	IMM0013P	NA	NA	NA
	IMM0014P	NA	NA	NA
	AM02001P	NA	NA	NA
	AM02006P	NA	NA	NA
	AM03009P	NA	NA	NA
	AM01010P	NA	NA	NA
	AM03013P	NA	NA	NA
	AM03016P	NA	NA	NA
	AM01022P	NA	NA	NA
	AM02027P	NA	NA	NA
	AM00032P	NA	NA	NA
NA= Not applicable				

Table 7.3 Contd: Summary of QMSP results for HGPIN tissue samples				
Gene	**Tissue sample**	**Mean Ct ± SE**	**Mean quantity ± SE**	**RMS**
DCR1	IMM002P	0	0	0
	IMM0037P	0	0	0
	IMM0056P	0	0	0
	IMM0068P	0	0	0
	IMM0075P	0	0	0
	AM02042P	0	0	0
	IMM0013P	NA	NA	NA
	IMM0014P	NA	NA	NA
	AM02001P	NA	NA	NA
	AM02006P	NA	NA	NA
	AM03009P	NA	NA	NA
	AM01010P	NA	NA	NA
	AM03013P	NA	NA	NA
	AM03016P	NA	NA	NA
	AM01022P	NA	NA	NA
	AM02027P	NA	NA	NA
	AM00032P	NA	NA	NA
DCR2	IMM002P	0	0	0
	IMM0037P	0	0	0
	IMM0056P	0	0	0
	IMM0068P	0	0	0
	IMM0075P	0	0	0
	AM02042P	0	0	0
	IMM0013P	0	0	0
	IMM0014P	0	0	0
	AM02001P	0	0	0
	AM02006P	0	0	0
	AM03009P	0	0	0
	AM01010P	0	0	0
	AM03013P	0	0	0
	AM03016P	0	0	0
	AM01022P	0	0	0
	AM02027P	0	0	0
	AM00032P	0	0	0
NA= Not applicable				

Table 7.3 Contd: Summary of QMSP results for HGPIN tissue samples				
Gene	**Tissue sample**	**Mean Ct ± SE**	**Mean quantity ± SE**	**RMS**
TMS1	IMM002P	0	0	0
	IMM0037P	0	0	0
	IMM0056P	0	0	0
	IMM0068P	0	0	0
	IMM0075P	0	0	0
	AM02042P	0	0	0
	IMM0013P	0	0	0
	IMM0014P	37.124 ± 1.603	0.056 ± 0.039	333.118 ± 0.002
	AM02001P	0	0	0
	AM02006P	0	0	0
	AM03009P	0	0	0
	AM01010P	0	0	0
	AM03013P	0	0	0
	AM03016P	0	0	0
	AM01022P	0	0	0
	AM02027P	0	0	0
	AM00032P	41.1 ± 0.627	0.003 ± 0.001	60.23 ± 0.007
NA= Not applicable				

Table 7.4: Summary of QMSP results for BPH tissue samples				
Gene	**Tissue sample**	**Mean Ct ± SE**	**Mean quantity ± SE**	**RMS**
ACTB	IMM001B	34.062 ± 0.169	1.019 ± 0.88	NA
	IMM005B	35.017 ± 0.042	0.413 ± 0.413	NA
	IMM007B	34.162 ± 0.143	0.918 ± 0.812	NA
	IMM0011B	34.957 ± 0.252	0.528 ± 0.439	NA
	IMM0013B	37.236 ± 0.556	0.092 ± 0.077	NA
	IMM0018B	37.556 ± 0.586	0.068 ± 0.06	NA
	IMM0019B	38.032 ± 0.538	0.056 ± 0.041	NA
	IMM0020B	36.292 ± 0.814	0.316 ± 0.176	NA
	IMM0022B	34.078 ± 0.142	0.951 ± 0.867	NA
	IMM036B	36.93 ± 0.251	0.074 ± 0.093	NA
	IMM0037B	38.722 ± 0.486	0.021 ± 0.024	NA
	IMM0038B	37.538 ± 0.396	0.063 ± 0.059	NA
	IMM0052B	39.566 ± 1.349	0.011 ± 0.016	NA
	IMM0056B	35.084 ± 0.17	0.369 ± 0.394	NA
	IMM0058B	35.455 ± 0.214	0.241 ± 0.296	NA
	IMM0068B	35.101 ± 0.262	0.336 ± 0.393	NA
	IMM0072B	34.791 0.219	0.425 ± 0.498	NA
	IMM0075B	34.586 ± 0.27	0.69 ± 0.588	NA
	IMM0076B	33.878 ± 0.027	1.035 ± 1.011	NA
	IMM0083B	36.546 ± 0.528	0.122 ± 0.132	NA
	IMM0084B	33.017 ± 0.097	2.124 ± 1.991	NA
	IMM0085B	33.159 ± 0.114	1.609 ± 1.782	NA
	IMM0014B	36.817 ± 0.078	0.076 ± 0.077	NA
	IMM0025B	35.527 ± 0.573	0.146 ± 0.181	NA
	AM03052B	35.233 ± 0.152	0.19 ± 0.209	NA
	AM00054B	40.214 ± 0.394	0.01 ± 0.009	NA
	AM02058B	33.012 ± 0.086	0.802 ± 0.841	NA
	AM02059B	34.264 ± 0.093	0.371 ± 0.383	NA
	AM01065B	33.855 ± 0.07	0.516 ± 0.495	NA
	AM00066B	36.255 ± 0.288	0.09 ± 0.111	NA
	AM01072B	38.276 ± 0.287	0.028 ± 0.031	NA
	AM02075B	34.132 ± 0.244	0.425 ± 0.419	NA
	AM02081B	35.255 ± 0.077	0.194 ± 0.206	NA
	AM03082B	34.943 ± 0.294	0.296 ± 0.253	NA
	AM03086B	35.326 ± 0.232	0.197 ± 0.198	NA
NA= Not applicable				

Table 7.4 Contd.: Summary of QMSP results for BPH tissue samples				
Gene	Tissue sample	Mean Ct ± SE	Mean quantity ± SE	RMS
BNIP3	IMM001B	0	0	0
	IMM005B	0	0	0
	IMM007B	0	0	0
	IMM0011B	0	0	0
	IMM0013B	0	0	0
	IMM0018B	0	0	0
	IMM0019B	0	0	0
	IMM0020B	0	0	0
	IMM0022B	0	0	0
	IMM036B	0	0	0
	IMM0037B	0	0	0
	IMM0038B	0	0	0
	IMM0052B	0	0	0
	IMM0056B	0	0	0
	IMM0058B	0	0	0
	IMM0068B	0	0	0
	IMM0072B	0	0	0
	IMM0075B	0	0	0
	IMM0076B	0	0	0
	IMM0083B	0	0	0
	IMM0084B	0	0	0
	IMM0085B	0	0	0
	IMM0014B	0	0	0
	IMM0025B	0	0	0
	AM03052B	0	0	0
	AM00054B	0	0	0
	AM02058B	0	0	0
	AM02059B	0	0	0
	AM01065B	0	0	0
	AM00066B	0	0	0
	AM01072B	0	0	0
	AM02075B	0	0	0
	AM02081B	0	0	0
	AM03082B	0	0	0
	AM03086B	0	0	0

Table 7.4 Contd.: Summary of QMSP results for BPH tissue samples				
Gene	**Tissue sample**	**Mean Ct ± SE**	**Mean quantity ± SE**	**RMS**
CDKN2A	IMM001B	20.178 ± 1.354	2552.033 ± 2299.748	2900248.67 ± 0.0000009
	IMM005B	0	0	0
	IMM007B	0	0	0
	IMM0011B	0	0	0
	IMM0013B	0	0	0
	IMM0018B	0	0	0
	IMM0019B	0	0	0
	IMM0020B	0	0	0
	IMM0022B	0	0	0
	IMM036B	0	0	0
	IMM0037B	0	0	0
	IMM0038B	0	0	0
	IMM0052B	0	0	0
	IMM0056B	0	0	0
	IMM0058B	19.913 ± 1.827	3907.535 ± 3198.946	13222766.845 ± 0.0000002
	IMM0068B	0	0	0
	IMM0072B	0	0	0
	IMM0075B	0	0	0
	IMM0076B	0	0	0
	IMM0083B	0	0	0
	IMM0084B	0	0	0
	IMM0085B	0	0	0
	IMM0014B	NA	NA	NA
	IMM0025B	NA	NA	NA
	AM03052B	NA	NA	NA
	AM00054B	NA	NA	NA
	AM02058B	NA	NA	NA
	AM02059B	NA	NA	NA
	AM01065B	NA	NA	NA
	AM00066B	NA	NA	NA
	AM01072B	NA	NA	NA
	AM02075B	NA	NA	NA
	AM02081B	NA	NA	NA
	AM03082B	NA	NA	NA
	AM03086B	NA	NA	NA
NA= Not applicable				

Table 7.4 Contd.: Summary of QMSP results for BPH tissue samples				
Gene	**Tissue sample**	**Mean Ct ± SE**	**Mean quantity ± SE**	**RMS**
CDKN2A	IMM001B	20.178 ± 1.354	2552.033 ± 2299.748	2900248.67 ± 0.0000009
	IMM005B	0	0	0
	IMM007B	0	0	0
	IMM0011B	0	0	0
	IMM0013B	0	0	0
	IMM0018B	0	0	0
	IMM0019B	0	0	0
	IMM0020B	0	0	0
	IMM0022B	0	0	0
	IMM036B	0	0	0
	IMM0037B	0	0	0
	IMM0038B	0	0	0
	IMM0052B	0	0	0
	IMM0056B	0	0	0
	IMM0058B	19.913 ± 1.827	3907.535 ± 3198.946	13222766.845 ± 0.0000002
	IMM0068B	0	0	0
	IMM0072B	0	0	0
	IMM0075B	0	0	0
	IMM0076B	0	0	0
	IMM0083B	0	0	0
	IMM0084B	0	0	0
	IMM0085B	0	0	0
	IMM0014B	NA	NA	NA
	IMM0025B	NA	NA	NA
	AM03052B	NA	NA	NA
	AM00054B	NA	NA	NA
	AM02058B	NA	NA	NA
	AM02059B	NA	NA	NA
	AM01065B	NA	NA	NA
	AM00066B	NA	NA	NA
	AM01072B	NA	NA	NA
	AM02075B	NA	NA	NA
	AM02081B	NA	NA	NA
	AM03082B	NA	NA	NA
	AM03086B	NA	NA	NA
NA= Not applicable				

Table 7.4 Contd.: Summary of QMSP results for BPH tissue samples				
Gene	**Tissue sample**	**Mean Ct ± SE**	**Mean quantity ± SE**	**RMS**
CpG1 cFLIP	IMM001B	0	0	0
	IMM005B	0	0	0
	IMM007B	0	0	0
	IMM0011B	0	0	0
	IMM0013B	0	0	0
	IMM0018B	0	0	0
	IMM0019B	0	0	0
	IMM0020B	0	0	0
	IMM0022B	0	0	0
	IMM036B	0	0	0
	IMM0037B	0	0	0
	IMM0038B	0	0	0
	IMM0052B	0	0	0
	IMM0056B	0	0	0
	IMM0058B	0	0	0
	IMM0068B	0	0	0
	IMM0072B	0	0	0
	IMM0075B	0	0	0
	IMM0076B	0	0	0
	IMM0083B	0	0	0
	IMM0084B	0	0	0
	IMM0085B	0	0	0
	IMM0014B	NA	NA	NA
	IMM0025B	NA	NA	NA
	AM03052B	NA	NA	NA
	AM00054B	NA	NA	NA
	AM02058B	NA	NA	NA
	AM02059B	NA	NA	NA
	AM01065B	NA	NA	NA
	AM00066B	NA	NA	NA
	AM01072B	NA	NA	NA
	AM02075B	NA	NA	NA
	AM02081B	NA	NA	NA
	AM03082B	NA	NA	NA
	AM03086B	NA	NA	NA
NA= Not applicable				

Table 7.4 Contd.: Summary of QMSP results for BPH tissue samples				
Gene	**Tissue sample**	**Mean Ct ± SE**	**Mean quantity ± SE**	**RMS**
CpG2 cFLIP	IMM001B	0	0	0
	IMM005B	0	0	0
	IMM007B	0	0	0
	IMM0011B	0	0	0
	IMM0013B	0	0	0
	IMM0018B	0	0	0
	IMM0019B	0	0	0
	IMM0020B	0	0	0
	IMM0022B	0	0	0
	IMM036B	0	0	0
	IMM0037B	0	0	0
	IMM0038B	0	0	0
	IMM0052B	0	0	0
	IMM0056B	0	0	0
	IMM0058B	0	0	0
	IMM0068B	0	0	0
	IMM0072B	0	0	0
	IMM0075B	0	0	0
	IMM0076B	0	0	0
	IMM0083B	0	0	0
	IMM0084B	0	0	0
	IMM0085B	0	0	0
	IMM0014B	NA	NA	NA
	IMM0025B	NA	NA	NA
	AM03052B	NA	NA	NA
	AM00054B	NA	NA	NA
	AM02058B	NA	NA	NA
	AM02059B	NA	NA	NA
	AM01065B	NA	NA	NA
	AM00066B	NA	NA	NA
	AM01072B	NA	NA	NA
	AM02075B	NA	NA	NA
	AM02081B	NA	NA	NA
	AM03082B	NA	NA	NA
	AM03086B	NA	NA	NA
NA= Not applicable				

Table 7.4 Contd.: Summary of QMSP results for BPH tissue samples				
Gene	**Tissue sample**	**Mean Ct ± SE**	**Mean quantity ± SE**	**RMS**
DCR1	IMM001B	0	0	0
	IMM005B	0	0	0
	IMM007B	0	0	0
	IMM0011B	0	0	0
	IMM0013B	0	0	0
	IMM0018B	0	0	0
	IMM0019B	0	0	0
	IMM0020B	0	0	0
	IMM0022B	0	0	0
	IMM036B	0	0	0
	IMM0037B	0	0	0
	IMM0038B	0	0	0
	IMM0052B	0	0	0
	IMM0056B	0	0	0
	IMM0058B	0	0	0
	IMM0068B	0	0	0
	IMM0072B	0	0	0
	IMM0075B	0	0	0
	IMM0076B	0	0	0
	IMM0083B	0	0	0
	IMM0084B	0	0	0
	IMM0085B	0	0	0
	IMM0014B	NA	NA	NA
	IMM0025B	NA	NA	NA
	AM03052B	NA	NA	NA
	AM00054B	NA	NA	NA
	AM02058B	NA	NA	NA
	AM02059B	NA	NA	NA
	AM01065B	NA	NA	NA
	AM00066B	NA	NA	NA
	AM01072B	NA	NA	NA
	AM02075B	NA	NA	NA
	AM02081B	NA	NA	NA
	AM03082B	NA	NA	NA
	AM03086B	NA	NA	NA
NA= Not applicable				

Table 7.4 Contd.: Summary of QMSP results for BPH tissue samples				
Gene	**Tissue sample**	**Mean Ct ± SE**	**Mean quantity ± SE**	**RMS**
DCR2	IMM001B	0	0	0
	IMM005B	0	0	0
	IMM007B	0	0	0
	IMM0011B	0	0	0
	IMM0013B	0	0	0
	IMM0018B	0	0	0
	IMM0019B	0	0	0
	IMM0020B	0	0	0
	IMM0022B	0	0	0
	IMM036B	0	0	0
	IMM0037B	0	0	0
	IMM0038B	0	0	0
	IMM0052B	0	0	0
	IMM0056B	0	0	0
	IMM0058B	0	0	0
	IMM0068B	41.17 ± 0.742	0.018 ± 0.009	44.638 ± 0.013
	IMM0072B	0	0	0
	IMM0075B	0	0	0
	IMM0076B	0	0	0
	IMM0083B	0	0	0
	IMM0084B	0	0	0
	IMM0085B	0	0	0
	IMM0014B	0	0	0
	IMM0025B	43.044 ± 3.015	0.008 ± 0.01	45.039 ± 0.029
	AM03052B	0	0	0
	AM00054B	0	0	0
	AM02058B	0	0	0
	AM02059B	0	0	0
	AM01065B	0	0	0
	AM00066B	0	0	0
	AM01072B	0	0	0
	AM02075B	0	0	0
	AM02081B	0	0	0
	AM03082B	0	0	0
	AM03086B	0	0	0

Table 7.4 Contd.: Summary of QMSP results for BPH tissue samples				
Gene	**Tissue sample**	**Mean Ct ± SE**	**Mean quantity ± SE**	**RMS**
TMS1	IMM001B	0	0	0
	IMM005B	0	0	0
	IMM007B	0	0	0
	IMM0011B	0	0	0
	IMM0013B	0	0	0
	IMM0018B	0	0	0
	IMM0019B	0	0	0
	IMM0020B	0	0	0
	IMM0022B	0	0	0
	IMM036B	0	0	0
	IMM0037B	0	0	0
	IMM0038B	0	0	0
	IMM0052B	0	0	0
	IMM0056B	0	0	0
	IMM0058B	0	0	0
	IMM0068B	0	0	0
	IMM0072B	0	0	0
	IMM0075B	0	0	0
	IMM0076B	0	0	0
	IMM0083B	0	0	0
	IMM0084B	0	0	0
	IMM0085B	0	0	0
	IMM0014B	0	0	0
	IMM0025B	40.728 ± 2.136	0.006 ± 0.006	31.504 ± 0.037
	AM03052B	0	0	0
	AM00054B	0	0	0
	AM02058B	0	0	0
	AM02059B	0	0	0
	AM01065B	0	0	0
	AM00066B	0	0	0
	AM01072B	0	0	0
	AM02075B	0	0	0
	AM02081B	0	0	0
	AM03082B	0	0	0
	AM03086B	0	0	0

APPENDIX 8

A8.1 Methylation heat map for GSTP1, IGFBP7 and SFRP2.

Sample	TUMOUR		
	GSTP1	IGFBP3	SFRP2
AM02001			
AM02006			
AM02007			
AM03009			
AM01010			
AM03013			
AM03016			
AM02018			
AM03019			
AM03020			
AM01028			NA
AM02042			
AM98043			
AM02002			
AM02003			
AM02004			
AM02005			
AM01011			
AM02012			
AM03014			
AM03015			
AM03017			
AM03021			
AM02024			
AM02025			
AM02026			
AM02030			
AM03033			
AM02035			
AM02036			
AM02037			
AM99038			
AM02039			
AM02040			
AM02044			
AM02045			
AM02046			
	Samples unmethylated in all genes		
	Samples methylated in all genes		
Note: Only samples analysed in Chapter 6 were considered			

Figure 8.1

Methylation heat map for GSTP1, IGFBP7 and SFRP2 in prostate cancer samples. All data was generated by Dr. Antoinette Perry.

Sample	TUMOUR		
	GSTP1	IGFBP3	SFRP2
AM02047			
AM00048			
AM03085			
AM01023			
AM02031			
IMM002			
IMM0037			
IMM0056			
IMM0013			
IMM0014			
IMM0068			
IMM0075			
IMM001			
IMM005T			
IMM007T			
IMM008T			
IMM009T			
IMM020T			
IMM036T			
IMM0038T			
IMM0052T			
IMM0058T			
IMM0070T			
IMM072T			
IMM0076T			
IMM0078T			
IMM0082T			
IMM0083T			
IMM0084T			
IMM0085T			
IMM0086T			
IMM0011T			
IMM0017T			
IMM0018T			
IMM0019T			
IMM0022T (2)			
IMM0025T			
IMM0031T	NA	NA	NA
IMM0032T			
	Samples unmethylated in all genes		
	Samples methylated in all genes		

Note: Only samples analysed in Chapter 6 were considered

Figure 8.1

Methylation heat map for *GSTP1, IGFBP7* and *SFRP2* in prostate cancer samples. All data was generated by Dr. Antoinette Perry.

REFERENCES

Nomenclature Committee of the International Union of Biochemistry (NC-IUB). Nomenclature for incompletely specified bases in nucleic acid sequences. Recommendations 1984. Eur J Biochem *150*, 1-5.

Abate-Shen, C., and Shen, M.M. (2000). Molecular genetics of prostate cancer. Genes Dev *14*, 2410-2434.

Abe, T., Toyota, M., Suzuki, H., Murai, M., Akino, K., Ueno, M., Nojima, M., Yawata, A., Miyakawa, H., Suga, T., *et al.* (2005). Upregulation of BNIP3 by 5-aza-2'-deoxycytidine sensitizes pancreatic cancer cells to hypoxia-mediated cell death. J Gastroenterol *40*, 504-510.

Ambros, V. (2004). The functions of animal microRNAs. Nature *431*, 350-355.
Apel, A., Zentgraf, H., Buchler, M.W., and Herr, I. (2009). Autophagy-A double-edged sword in oncology. Int J Cancer *125*, 991-995.

Arnold, J.T., and Isaacs, J.T. (2002). Mechanisms involved in the progression of androgen-independent prostate cancers: it is not only the cancer cell's fault. Endocr Relat Cancer *9*, 61-73.

Ashida, S., Nakagawa, H., Katagiri, T., Furihata, M., Iiizumi, M., Anazawa, Y., Tsunoda, T., Takata, R., Kasahara, K., Miki, T., *et al.* (2004). Molecular features of the transition from prostatic intraepithelial neoplasia (PIN) to prostate cancer: genome-wide gene-expression profiles of prostate cancers and PINs. Cancer Res *64*, 5963-5972.

Ashkenazi, A., and Dixit, V.M. (1999). Apoptosis control by death and decoy receptors. Curr Opin Cell Biol *11*, 255-260.

Banelli, B., Casciano, I., Croce, M., Di Vinci, A., Gelvi, I., Pagnan, G., Brignole, C., Allemanni, G., Ferrini, S., Ponzoni, M., *et al.* (2002). Expression and methylation of CASP8 in neuroblastoma: identification of a promoter region. Nat Med *8*, 1333-1335; author reply 1335.
Bartel, D.P. (2004). MicroRNAs: genomics, biogenesis, mechanism, and function. Cell *116*, 281-297.

Baumer, A. (2002). Analysis of the methylation status of imprinted genes based on methylation-specific polymerase chain reaction combined with denaturing high-performance liquid chromatography. Methods *27*, 139-143.

Baumer, A., Wiedemann, U., Hergersberg, M., and Schinzel, A. (2001). A novel MSP/DHPLC method for the investigation of the methylation status of imprinted genes enables the molecular detection of low cell mosaicisms. Hum Mutat *17*, 423-430.

Baylin, S. (2005a). DNA methylation and gene silencing in cancer. . Clinical practice Oncology *2*, S4-S11.

Baylin, S.B. (2005b). DNA methylation and gene silencing in cancer. Nat Clin Pract Oncol *2 Suppl 1*, S4-11.

Bednarik, D.P. (1993). DNA methylation and retrovirus expression. Exs *64*, 300-329.

Bell, A.C., and Felsenfeld, G. (2000). Methylation of a CTCF-dependent boundary controls imprinted expression of the Igf2 gene. Nature *405*, 482-485.

Benedetti, A., Parent, M.E., and Siemiatycki, J. (2009). Lifetime consumption of alcoholic beverages and risk of 13 types of cancer in men: results from a case-control study in Montreal. Cancer Detect Prev *32*, 352-362.

Bettuzzi, S., Brausi, M., Rizzi, F., Castagnetti, G., Peracchia, G., and Corti, A. (2006). Chemoprevention of human prostate cancer by oral administration of green tea catechins in volunteers with high-grade prostate intraepithelial neoplasia: a preliminary report from a one-year proof-of-principle study. Cancer Res *66*, 1234-1240.

Bibikova, M., Lin, Z., Zhou, L., Chudin, E., Garcia, E.W., Wu, B., Doucet, D., Thomas, N.J., Wang, Y., Vollmer, E., *et al.* (2006). High-throughput DNA methylation profiling using universal bead arrays. Genome Res *16*, 383-393.

Bill-Axelson, A., Holmberg, L., Ruutu, M., Haggman, M., Andersson, S.O., Bratell, S., Spangberg, A., Busch, C., Nordling, S., Garmo, H., *et al.* (2005). Radical prostatectomy versus watchful waiting in early prostate cancer. N Engl J Med *352*, 1977-1984.

Bird, A. (2002). DNA methylation patterns and epigenetic memory. Genes Dev *16*, 6-21.

Bird, A.P., and Wolffe, A.P. (1999). Methylation-induced repression--belts, braces, and chromatin. Cell *99*, 451-454.

Blenkiron, C., Goldstein, L.D., Thorne, N.P., Spiteri, I., Chin, S.F., Dunning, M.J., Barbosa-Morais, N.L., Teschendorff, A.E., Green, A.R., Ellis, I.O., *et al.* (2007). MicroRNA expression profiling of human breast cancer identifies new markers of tumor subtype. Genome Biol *8*, R214.

Bodey, B., Siegel, S.E., and Kaiser, H.E. (2002). MAGE-1, a cancer/testis-antigen, expression in childhood astrocytomas as an indicator of tumor progression. In Vivo *16*, 583-588.

Bookstein, R., Rio, P., Madreperla, S.A., Hong, F., Allred, C., Grizzle, W.E., and Lee, W.H. (1990). Promoter deletion and loss of retinoblastoma gene expression in human prostate carcinoma. Proc Natl Acad Sci U S A *87*, 7762-7766.

Bostwick, D.G. (1999). Pathology of prostate cancer. International Handbook of Prostate Cancer *Chapter 2*, 14-42.

Bostwick, D.G., and Brawer, M.K. (1987). Prostatic intra-epithelial neoplasia and early invasion in prostate cancer. Cancer *59*, 788-794.

Boumber, Y.A., Kondo, Y., Chen, X., Shen, L., Guo, Y., Tellez, C., Estecio, M.R., Ahmed, S., and Issa, J.P. (2008). An Sp1/Sp3 binding polymorphism confers methylation protection. PLoS Genet *4*, e1000162.

Bowen, C., Bubendorf, L., Voeller, H.J., Slack, R., Willi, N., Sauter, G., Gasser, T.C., Koivisto, P., Lack, E.E., Kononen, J., *et al.* (2000). Loss of NKX3.1 expression in human prostate cancers correlates with tumor progression. Cancer Res *60*, 6111-6115.

Brawer, M.K., Chetner, M.P., Beatie, J., Buchner, D.M., Vessella, R.L., and Lange, P.H. (1992). Screening for prostatic carcinoma with prostate specific antigen. J Urol *147*, 841-845.

Brawer, M.K., Peehl, D.M., Stamey, T.A., and Bostwick, D.G. (1985). Keratin immunoreactivity in the benign and neoplastic human prostate. Cancer Res *45*, 3663-3667.

Brenner, C., and Fuks, F. (2007). A methylation rendezvous: reader meets writers. Dev Cell *12*, 843-844.

Brueckner, B., and Lyko, F. (2004). DNA methyltransferase inhibitors: old and new drugs for an epigenetic cancer therapy. Trends Pharmacol Sci *25*, 551-554.
Bruick, R.K. (2000). Expression of the gene encoding the proapoptotic Nip3 protein is induced by hypoxia. Proc Natl Acad Sci U S A *97*, 9082-9087.

Burks, D.A., and Littleton, R.H. (1992). The epidemiology of prostate cancer in black men. Henry Ford Hosp Med J *40*, 89-92.

Byun, D.S., Cho, K., Ryu, B.K., Lee, M.G., Kang, M.J., Kim, H.R., and Chi, S.G. (2003). Hypermethylation of XIAP-associated factor 1, a putative tumor suppressor gene from the 17p13.2 locus, in human gastric adenocarcinomas. Cancer Res *63*, 7068-7075.

Cairns, P. (2004). Detection of promoter hypermethylation of tumor suppressor genes in urine from kidney cancer patients. Ann N Y Acad Sci *1022*, 40-43.

Caldas, C., Hahn, S.A., da Costa, L.T., Redston, M.S., Schutte, M., Seymour, A.B., Weinstein, C.L., Hruban, R.H., Yeo, C.J., and Kern, S.E. (1994). Frequent somatic mutations and homozygous deletions of the p16 (MTS1) gene in pancreatic adenocarcinoma. Nat Genet *8*, 27-32.

Calin, G.A., and Croce, C.M. (2006). MicroRNA signatures in human cancers. Nat Rev Cancer *6*, 857-866.

Cameron, E.E., Bachman, K.E., Myohanen, S., Herman, J.G., and Baylin, S.B. (1999). Synergy of demethylation and histone deacetylase inhibition in the re-expression of genes silenced in cancer. Nat Genet *21*, 103-107.

Cande, C., Vahsen, N., Kouranti, I., Schmitt, E., Daugas, E., Spahr, C., Luban, J., Kroemer, R.T., Giordanetto, F., Garrido, C., *et al.* (2004). AIF and cyclophilin A cooperate in apoptosis-associated chromatinolysis. Oncogene *23*, 1514-1521.

Caporali, A., Davalli, P., Astancolle, S., D'Arca, D., Brausi, M., Bettuzzi, S., and Corti, A. (2004). The chemopreventive action of catechins in the TRAMP mouse model of prostate carcinogenesis is accompanied by clusterin over-expression. Carcinogenesis *25*, 2217-2224.

Carter, B.H., Allaf, M.E and Partin, A.W. (2007). Diagnosis and Staging of prostate Cancer. Campbell-Walsh Urology Ninth edition *chapter 94*, 2913-2931.

Catalona, W.J. (2004). Prostate cancer screening. BJU Int *94*, 964-966.
Catalona, W.J., Bartsch, G., Rittenhouse, H.G., Evans, C.L., Linton, H.J., Horninger, W., Klocker, H., and Mikolajczyk, S.D. (2004). Serum pro-prostate specific antigen preferentially detects aggressive prostate cancers in men with 2 to 4 ng/ml prostate specific antigen. J Urol *171*, 2239-2244.

Catalona, W.J., Hudson, M.A., Scardino, P.T., Richie, J.P., Ahmann, F.R., Flanigan, R.C., deKernion, J.B., Ratliff, T.L., Kavoussi, L.R., Dalkin, B.L., *et al.* (1994). Selection of optimal prostate specific antigen cutoffs for early detection of prostate cancer: receiver operating characteristic curves. J Urol *152*, 2037-2042.

Catalona, W.J., Smith, D.S., Ratliff, T.L., Dodds, K.M., Coplen, D.E., Yuan, J.J., Petros, J.A., and Andriole, G.L. (1991). Measurement of prostate-specific antigen in serum as a screening test for prostate cancer. N Engl J Med *324*, 1156-1161.

Catalona, W.J.a.H., M. (2007). Definitive Therapy for Localised prostate cancer-An overview. . Campbell-Walsh Urology Ninth edition *Chapter 95*, 2933-2946.

Chalitchagorn, K., Shuangshoti, S., Hourpai, N., Kongruttanachok, N., Tangkijvanich, P., Thong-ngam, D., Voravud, N., Sriuranpong, V., and Mutirangura, A. (2004). Distinctive pattern of LINE-1 methylation level in normal tissues and the association with carcinogenesis. Oncogene *23*, 8841-8846.

Chang, D.W., Xing, Z., Pan, Y., Algeciras-Schimnich, A., Barnhart, B.C., Yaish-Ohad, S., Peter, M.E., and Yang, X. (2002). c-FLIP(L) is a dual function regulator for caspase-8 activation and CD95-mediated apoptosis. Embo J *21*, 3704-3714.

Chang, M., Tsuchiya, K., Batchelor, R.H., Rabinovitch, P.S., Kulander, B.G., Haggitt, R.C., and Burmer, G.C. (1994). Deletion mapping of chromosome 8p in colorectal carcinoma and dysplasia arising in ulcerative colitis, prostatic carcinoma, and malignant fibrous histiocytomas. Am J Pathol *144*, 1-6.

Chang, T.C., Wentzel, E.A., Kent, O.A., Ramachandran, K., Mullendore, M., Lee, K.H., Feldmann, G., Yamakuchi, M., Ferlito, M., Lowenstein, C.J., *et al.* (2007). Transactivation of miR-34a by p53 broadly influences gene expression and promotes apoptosis. Mol Cell *26*, 745-752.

Cho-Vega, J.H., Troncoso, P., Do, K.A., Rago, C., Wang, X., Tsavachidis, S., Medeiros, L.J., Spurgers, K., Logothetis, C., and McDonnell, T.J. (2005). Combined laser capture microdissection and serial analysis of gene expression from human tissue samples. Mod Pathol *18*, 577-584.

Cho, N.Y., Kim, B.H., Choi, M., Yoo, E.J., Moon, K.C., Cho, Y.M., Kim, D., and Kang, G.H. (2007). Hypermethylation of CpG island loci and hypomethylation of LINE-1 and Alu repeats in prostate adenocarcinoma and their relationship to clinicopathological features. J Pathol *211*, 269-277.

Chodak, G.W., Thisted, R.A., Gerber, G.S., Johansson, J.E., Adolfsson, J., Jones, G.W., Chisholm, G.D., Moskovitz, B., Livne, P.M., and Warner, J. (1994). Results of conservative management of clinically localized prostate cancer. N Engl J Med *330*, 242-248.

Christensson, A., Laurell, C.B., and Lilja, H. (1990). Enzymatic activity of prostate-specific antigen and its reactions with extracellular serine proteinase inhibitors. Eur J Biochem *194*, 755-763.

Clark, S.J., Harrison, J., Paul, C.L., and Frommer, M. (1994). High sensitivity mapping of methylated cytosines. Nucleic Acids Res *22*, 2990-2997.

Clinton, S.K. (1999). The dietary antioxidant network and prostate carcinoma. Cancer *86*, 1629-1631.

Collado, M., Blasco, M.A., and Serrano, M. (2007). Cellular senescence in cancer and aging. Cell *130*, 223-233.

Collard, R.L., Harya, N.S., Monzon, F.A., Maier, C.E., and O'Keefe, D.S. (2006). Methylation of the ASC gene promoter is associated with aggressive prostate cancer. Prostate *66*, 687-695.

Colombel, M., Symmans, F., Gil, S., O'Toole, K.M., Chopin, D., Benson, M., Olsson, C.A., Korsmeyer, S., and Buttyan, R. (1993). Detection of the apoptosis-suppressing oncoprotein bc1-2 in hormone-refractory human prostate cancers. Am J Pathol *143*, 390-400.

Coppola, V., de Maria, R., and Bonci, D. (2009). MicroRNAs and prostate cancer. Endocr Relat Cancer.

Corney, D.C., Flesken-Nikitin, A., Godwin, A.K., Wang, W., and Nikitin, A.Y. (2007). MicroRNA-34b and MicroRNA-34c are targets of p53 and cooperate in control of cell proliferation and adhesion-independent growth. Cancer Res *67*, 8433-8438.

Cory, S., and Adams, J.M. (2002). The Bcl2 family: regulators of the cellular life-or-death switch. Nat Rev Cancer *2*, 647-656.

Costello, J.F., Fruhwald, M.C., Smiraglia, D.J., Rush, L.J., Robertson, G.P., Gao, X., Wright, F.A., Feramisco, J.D., Peltomaki, P., Lang, J.C., *et al.* (2000). Aberrant CpG-island methylation has non-random and tumour-type-specific patterns. Nat Genet *24*, 132-138.

Couvert, P., Poirier, K., Carrie, A., Chalas, C., Jouannet, P., Beldjord, C., Bienvenu, T., Chelly, J., and Kerjean, A. (2003). DHPLC-based method for DNA methylation analysis of differential methylated regions from imprinted genes. Biotechniques *34*, 356-362.

Cowland, J.B., Hother, C., and Gronbaek, K. (2007). MicroRNAs and cancer. APMIS *115*, 1090-1106.

Crawford, E.D. (2009). Understanding the epidemiology, natural history, and key pathways involved in prostate cancer. Urology *73*, S4-10.

Creagh, E.M., Conroy, H., and Martin, S.J. (2003). Caspase-activation pathways in apoptosis and immunity. Immunol Rev *193*, 10-21.

Creagh, E.M., and Martin, S.J. (2001). Caspases: cellular demolition experts. Biochem Soc Trans *29*, 696-702.

Dahl, C., and Guldberg, P. (2003). DNA methylation analysis techniques. Biogerontology *4*, 233-250.

DeMarzo, A.M., Nelson, W.G., Isaacs, W.B., and Epstein, J.I. (2003). Pathological and molecular aspects of prostate cancer. Lancet *361*, 955-964.

DeVere White, R.W., Meyers, F.J., Soares, S.E., Miller, D.G., and Soriano, T.F. (1992). Urinary prostate specific antigen levels: role in monitoring the response of prostate cancer to therapy. J Urol *147*, 947-951.

Dhanasekaran, S.M., Barrette, T.R., Ghosh, D., Shah, R., Varambally, S., Kurachi, K., Pienta, K.J., Rubin, M.A., and Chinnaiyan, A.M. (2001). Delineation of prognostic biomarkers in prostate cancer. Nature *412*, 822-826.

Di Vinci, A., Gelvi, I., Banelli, B., Casciano, I., Allemanni, G., and Romani, M. (2006). Meth-DOP-PCR: an assay for the methylation profiling of trace amounts of DNA extracted from bodily fluids. Lab Invest *86*, 297-303.

Dobrovic, A., and Simpfendorfer, D. (1997). Methylation of the BRCA1 gene in sporadic breast cancer. Cancer Res *57*, 3347-3350.

Dominguez, G., Silva, J., Garcia, J.M., Silva, J.M., Rodriguez, R., Munoz, C., Chacon, I., Sanchez, R., Carballido, J., Colas, A., *et al.* (2003). Prevalence of aberrant methylation of p14ARF over p16INK4a in some human primary tumors. Mutat Res *530*, 9-17.

Donnelly, D.W., Gavin, A.T. and Comber, H. (2009). Cancer in Ireland 1994-2004. A summary report. http://ncriie/.

Drago J.R., M.F.K., Lee F. (1992). Introductory remarks and workshop summary. urology *39*, 2.

Dunn, J.E. (1975). Cancer epidemiology in populations of the United States--with emphasis on Hawaii and California--and Japan. Cancer Res *35*, 3240-3245.

Durkan, G.C., and Greene, D.R. (2000). Diagnostic dilemmas in detection of prostate cancer in patients undergoing transrectal ultrasound-guided needle biopsy of the prostate. Prostate Cancer Prostatic Dis *3*, 13-20.

Eads, C.A., Danenberg, K.D., Kawakami, K., Saltz, L.B., Blake, C., Shibata, D., Danenberg, P.V., and Laird, P.W. (2000). MethyLight: a high-throughput assay to measure DNA methylation. Nucleic Acids Res *28*, E32.

Earnshaw, W.C., Martins, L.M., and Kaufmann, S.H. (1999). Mammalian caspases: structure, activation, substrates, and functions during apoptosis. Annu Rev Biochem *68*, 383-424.

Eeles, R.A., Kote-Jarai, Z., Giles, G.G., Olama, A.A., Guy, M., Jugurnauth, S.K., Mulholland, S., Leongamornlert, D.A., Edwards, S.M., Morrison, J., *et al.* (2008). Multiple newly identified loci associated with prostate cancer susceptibility. Nat Genet *40*, 316-321.

Ehrich, M., Turner, J., Gibbs, P., Lipton, L., Giovanneti, M., Cantor, C., and van den Boom, D. (2008). Cytosine methylation profiling of cancer cell lines. Proc Natl Acad Sci U S A *105*, 4844-4849.

Ehrlich, M. (2002). DNA methylation in cancer: too much, but also too little. Oncogene *21*, 5400-5413.

Ellinger, J., El Kassem, N., Heukamp, L.C., Matthews, S., Cubukluoz, F., Kahl, P., Perabo, F.G., Muller, S.C., von Ruecker, A., and Bastian, P.J. (2008). Hypermethylation of cell-free serum DNA indicates worse outcome in patients with bladder cancer. J Urol *179*, 346-352.

Emmert-Buck, M.R., Bonner, R.F., Smith, P.D., Chuaqui, R.F., Zhuang, Z., Goldstein, S.R., Weiss, R.A., and Liotta, L.A. (1996). Laser capture microdissection. Science *274*, 998-1001.

Epstein, J.I. (2009). An update of the Gleason grading system. J Urol *183*, 433-440.

Ernst, T., Hergenhahn, M., Kenzelmann, M., Cohen, C.D., Bonrouhi, M., Weninger, A., Klaren, R., Grone, E.F., Wiesel, M., Gudemann, C., *et al.* (2002). Decrease and gain of gene expression are equally discriminatory

markers for prostate carcinoma: a gene expression analysis on total and microdissected prostate tissue. Am J Pathol *160*, 2169-2180.

Esteller, M. (2005). Aberrant DNA methylation as a cancer-inducing mechanism. Annu Rev Pharmacol Toxicol *45*, 629-656.

Esteller, M. (2006). The necessity of a human epigenome project. Carcinogenesis *27*, 1121-1125.

Esteve, P.O., Chin, H.G., Smallwood, A., Feehery, G.R., Gangisetty, O., Karpf, A.R., Carey, M.F., and Pradhan, S. (2006). Direct interaction between DNMT1 and G9a coordinates DNA and histone methylation during replication. Genes Dev *20*, 3089-3103.

Fan, J.B., Oliphant, A., Shen, R., Kermani, B.G., Garcia, F., Gunderson, K.L., Hansen, M., Steemers, F., Butler, S.L., Deloukas, P., *et al.* (2003). Highly parallel SNP genotyping. Cold Spring Harb Symp Quant Biol *68*, 69-78.

Fang, J., Metter, E.J., Landis, P., and Carter, H.B. (2002). PSA velocity for assessing prostate cancer risk in men with PSA levels between 2.0 and 4.0 ng/ml. Urology *59*, 889-893; discussion 893-884.

Fang, M.Z., Wang, Y., Ai, N., Hou, Z., Sun, Y., Lu, H., Welsh, W., and Yang, C.S. (2003). Tea polyphenol (-)-epigallocatechin-3-gallate inhibits DNA methyltransferase and reactivates methylation-silenced genes in cancer cell lines. Cancer Res *63*, 7563-7570.

Feinberg, A.P., Cui, H., and Ohlsson, R. (2002). DNA methylation and genomic imprinting: insights from cancer into epigenetic mechanisms. Semin Cancer Biol *12*, 389-398.

Ferlay, J., Autier, P., Boniol, M., Heanue, M., Colombet, M., and Boyle, P. (2007). Estimates of the cancer incidence and mortality in Europe in 2006. Ann Oncol *18*, 581-592.

Filipowicz, W., Bhattacharyya, S.N., and Sonenberg, N. (2008). Mechanisms of post-transcriptional regulation by microRNAs: are the answers in sight? Nat Rev Genet *9*, 102-114.

Foley, R., Hollywood, D., and Lawler, M. (2004). Molecular pathology of prostate cancer: the key to identifying new biomarkers of disease. Endocr Relat Cancer *11*, 477-488.

Fraga, M.F., and Esteller, M. (2005). Towards the human cancer epigenome: a first draft of histone modifications. Cell Cycle *4*, 1377-1381.

Freda, E.A. (1999). Incidence and aetiology of prostate cancer. International handbook of prosate cancer *Chapter 1*, 1-12.

Frommer, M., McDonald, L.E., Millar, D.S., Collis, C.M., Watt, F., Grigg, G.W., Molloy, P.L., and Paul, C.L. (1992). A genomic sequencing protocol that yields a positive display of 5-methylcytosine residues in individual DNA strands. Proc Natl Acad Sci U S A *89*, 1827-1831.

Fuks, F. (2005). DNA methylation and histone modifications: teaming up to silence genes. Curr Opin Genet Dev *15*, 490-495.

Fulda, S., Kufer, M.U., Meyer, E., van Valen, F., Dockhorn-Dworniczak, B., and Debatin, K.M. (2001). Sensitization for death receptor- or drug-induced apoptosis by re-expression of caspase-8 through demethylation or gene transfer. Oncogene *20*, 5865-5877.

Furukawa, Y., Sutheesophon, K., Wada, T., Nishimura, M., Saito, Y., Ishii, H., and Furukawa, Y. (2005). Methylation silencing of the Apaf-1 gene in acute leukemia. Mol Cancer Res *3*, 325-334.

Furuya, Y., Krajewski, S., Epstein, J.I., Reed, J.C., and Isaacs, J.T. (1996). Expression of bcl-2 and the progression of human and rodent prostatic cancers. Clin Cancer Res *2*, 389-398.

Futscher, B.W., Oshiro, M.M., Wozniak, R.J., Holtan, N., Hanigan, C.L., Duan, H., and Domann, F.E. (2002). Role for DNA methylation in the control of cell type specific maspin expression. Nat Genet *31*, 175-179.

Gann, P.H., Hennekens, C.H., Sacks, F.M., Grodstein, F., Giovannucci, E.L., and Stampfer, M.J. (1994). Prospective study of plasma fatty acids and risk of prostate cancer. J Natl Cancer Inst *86*, 281-286.

Gardiner-Garden, M., and Frommer, M. (1987). CpG islands in vertebrate genomes. J Mol Biol *196*, 261-282.

Giovannucci, E., Rimm, E.B., Colditz, G.A., Stampfer, M.J., Ascherio, A., Chute, C.C., and Willett, W.C. (1993). A prospective study of dietary fat and risk of prostate cancer. J Natl Cancer Inst *85*, 1571-1579.

Giovannucci, E., Stampfer, M.J., Krithivas, K., Brown, M., Dahl, D., Brufsky, A., Talcott, J., Hennekens, C.H., and Kantoff, P.W. (1997). The CAG repeat within the androgen receptor gene and its relationship to prostate cancer. Proc Natl Acad Sci U S A *94*, 3320-3323.

Gjengsto, P., Paus, E., Halvorsen, O.J., Eide, J., Akslen, L.A., Wentzel-Larsen, T., and Hoisaeter, P.A. (2005). Predictors of prostate cancer evaluated by receiver operating characteristics partial area index: a prospective institutional study. J Urol *173*, 425-428.

Gleason, D.F. (1977). Histological grading and clinical staging of prosatic carcinoma. In Urological pathology: The prostate, M. Tannenbaum, ed. (Philadelphia, Lea and Febiger).

Gleason, D.F. (1992). Histologic grading of prostate cancer: a perspective. Hum Pathol *23*, 273-279.

Gleason, D.F., and Mellinger, G.T. (1974). Prediction of prognosis for prostatic adenocarcinoma by combined histological grading and clinical staging. J Urol *111*, 58-64.

Goessl, C., Muller, M., Heicappell, R., Krause, H., and Miller, K. (2001). DNA-based detection of prostate cancer in blood, urine, and ejaculates. Ann N Y Acad Sci *945*, 51-58.

Gopisetty, G., Ramachandran, K., and Singal, R. (2006). DNA methylation and apoptosis. Mol Immunol *43*, 1729-1740.

Gordian, E., Ramachandran, K., and Singal, R. (2009). Methylation mediated silencing of TMS1 in breast cancer and its potential contribution to docetaxel cytotoxicity. Anticancer Res *29*, 3207-3210.

Grignon, D.J., Caplan, R., Sarkar, F.H., Lawton, C.A., Hammond, E.H., Pilepich, M.V., Forman, J.D., Mesic, J., Fu, K.K., Abrams, R.A., *et al.* (1997). p53 status and prognosis of locally advanced prostatic adenocarcinoma: a study based on RTOG 8610. J Natl Cancer Inst *89*, 158-165.

Griswold, M.D., and Kim, J.S. (2001). Site-specific methylation of the promoter alters deoxyribonucleic acid-protein interactions and prevents follicle-stimulating hormone receptor gene transcription. Biol Reprod *64*, 602-610.

Gronbaek, K., Hother, C., and Jones, P.A. (2007). Epigenetic changes in cancer. APMIS *115*, 1039-1059.

Guan, X., Sagara, J., Yokoyama, T., Koganehira, Y., Oguchi, M., Saida, T., and Taniguchi, S. (2003). ASC/TMS1, a caspase-1 activating adaptor, is downregulated by aberrant methylation in human melanoma. Int J Cancer *107*, 202-208.

Guo, Y., Sigman, D.B., Borkowski, A., and Kyprianou, N. (2000). Racial differences in prostate cancer growth: apoptosis and cell proliferation in Caucasian and African-American patients. Prostate *42*, 130-136.

Han, M., Partin, A.W., Piantadosi, S., Epstein, J.I., and Walsh, P.C. (2001). Era specific biochemical recurrence-free survival following radical prostatectomy for clinically localized prostate cancer. J Urol *166*, 416-419.

Hanahan, D., and Weinberg, R.A. (2000). The hallmarks of cancer. Cell *100*, 57-70.

Hankey, B.F., Feuer, E.J., Clegg, L.X., Hayes, R.B., Legler, J.M., Prorok, P.C., Ries, L.A., Merrill, R.M., and Kaplan, R.S. (1999). Cancer surveillance series: interpreting trends in prostate cancer--part I: Evidence of the effects of

screening in recent prostate cancer incidence, mortality, and survival rates. J Natl Cancer Inst *91*, 1017-1024.

Hanks, G.E., Hanlon, A., Schultheiss, T., Corn, B., Shipley, W.U., and Lee, W.R. (1994). Early prostate cancer: the national results of radiation treatment from the Patterns of Care and Radiation Therapy Oncology Group studies with prospects for improvement with conformal radiation and adjuvant androgen deprivation. J Urol *152*, 1775-1780.

Harada, K., Toyooka, S., Shivapurkar, N., Maitra, A., Reddy, J.L., Matta, H., Miyajima, K., Timmons, C.F., Tomlinson, G.E., Mastrangelo, D., *et al.* (2002). Deregulation of caspase 8 and 10 expression in pediatric tumors and cell lines. Cancer Res *62*, 5897-5901.

Harden, S.V., Sanderson, H., Goodman, S.N., Partin, A.A., Walsh, P.C., Epstein, J.I., and Sidransky, D. (2003). Quantitative GSTP1 methylation and the detection of prostate adenocarcinoma in sextant biopsies. J Natl Cancer Inst *95*, 1634-1637.

Hark, A.T., Schoenherr, C.J., Katz, D.J., Ingram, R.S., Levorse, J.M., and Tilghman, S.M. (2000). CTCF mediates methylation-sensitive enhancer-blocking activity at the H19/Igf2 locus. Nature *405*, 486-489.

Hasegawa, M., Imamura, R., Motani, K., Nishiuchi, T., Matsumoto, N., Kinoshita, T., and Suda, T. (2009). Mechanism and repertoire of ASC-mediated gene expression. J Immunol *182*, 7655-7662.

Heintzman, N.D., Stuart, R.K., Hon, G., Fu, Y., Ching, C.W., Hawkins, R.D., Barrera, L.O., Van Calcar, S., Qu, C., Ching, K.A., *et al.* (2007). Distinct and predictive chromatin signatures of transcriptional promoters and enhancers in the human genome. Nat Genet *39*, 311-318.

Hengartner, M.O., and Bryant, J.A. (2000). Apoptotic cell death: from worms to wombats ... but what about the weeds? Symp Soc Exp Biol *52*, 1-12.

Henrique, R., and Jeronimo, C. (2004). Molecular detection of prostate cancer: a role for GSTP1 hypermethylation. Eur Urol *46*, 660-669; discussion 669.

Herman, J.G., Latif, F., Weng, Y., Lerman, M.I., Zbar, B., Liu, S., Samid, D., Duan, D.S., Gnarra, J.R., Linehan, W.M., *et al.* (1994). Silencing of the VHL tumor-suppressor gene by DNA methylation in renal carcinoma. Proc Natl Acad Sci U S A *91*, 9700-9704.

Herman, J.G., Merlo, A., Mao, L., Lapidus, R.G., Issa, J.P., Davidson, N.E., Sidransky, D., and Baylin, S.B. (1995). Inactivation of the CDKN2/p16/MTS1 gene is frequently associated with aberrant DNA methylation in all common human cancers. Cancer Res *55*, 4525-4530.

Hernandez, J., and Thompson, I.M. (2004). Prostate-specific antigen: a review of the validation of the most commonly used cancer biomarker. Cancer *101*, 894-904.

Higuchi, T., Nakamura, M., Shimada, K., Ishida, E., Hirao, K., and Konishi, N. (2008). HRK inactivation associated with promoter methylation and LOH in prostate cancer. Prostate *68*, 105-113.

Hoffmann, M.J., and Schulz, W.A. (2005). Causes and consequences of DNA hypomethylation in human cancer. Biochem Cell Biol *83*, 296-321.

Hoffmann, R., and Valencia, A. (2004). A gene network for navigating the literature. Nat Genet *36*, 664.

Holliday, R. (1987). The inheritance of epigenetic defects. Science *238*, 163-170.

Hopkins-Donaldson, S., Ziegler, A., Kurtz, S., Bigosch, C., Kandioler, D., Ludwig, C., Zangemeister-Wittke, U., and Stahel, R. (2003). Silencing of death receptor and caspase-8 expression in small cell lung carcinoma cell lines and tumors by DNA methylation. Cell Death Differ *10*, 356-364.

Horak, P., Pils, D., Haller, G., Pribill, I., Roessler, M., Tomek, S., Horvat, R., Zeillinger, R., Zielinski, C., and Krainer, M. (2005). Contribution of epigenetic silencing of tumor necrosis factor-related apoptosis inducing ligand receptor 1 (DR4) to TRAIL resistance and ovarian cancer. Mol Cancer Res *3*, 335-343.

Hsieh, A.C., Small, E.J., and Ryan, C.J. (2007). Androgen-response elements in hormone-refractory prostate cancer: implications for treatment development. Lancet Oncol *8*, 933-939.

Hsing, A.W., and Devesa, S.S. (2001). Trends and patterns of prostate cancer: what do they suggest? Epidemiol Rev *23*, 3-13.

Huang, D.C., and Strasser, A. (2000). BH3-Only proteins-essential initiators of apoptotic cell death. Cell *103*, 839-842.

Hughes, C., Murphy, A., Martin, C., Sheils, O., and O'Leary, J. (2005). Molecular pathology of prostate cancer. J Clin Pathol *58*, 673-684.

Huusko, P., Ponciano-Jackson, D., Wolf, M., Kiefer, J.A., Azorsa, D.O., Tuzmen, S., Weaver, D., Robbins, C., Moses, T., Allinen, M., *et al.* (2004). Nonsense-mediated decay microarray analysis identifies mutations of EPHB2 in human prostate cancer. Nat Genet *36*, 979-983.

Ingles, S.A., Ross, R.K., Yu, M.C., Irvine, R.A., La Pera, G., Haile, R.W., and Coetzee, G.A. (1997). Association of prostate cancer risk with genetic polymorphisms in vitamin D receptor and androgen receptor. J Natl Cancer Inst *89*, 166-170.

Irmler, M., Thome, M., Hahne, M., Schneider, P., Hofmann, K., Steiner, V., Bodmer, J.L., Schroter, M., Burns, K., Mattmann, C., *et al.* (1997). Inhibition of death receptor signals by cellular FLIP. Nature *388*, 190-195.

Isaacs, J.T. (1984). Antagonistic effect of androgen on prostatic cell death. Prostate *5*, 545-557.

Jang, J.Y., Kim, H.J., Chi, S.G., Lee, K.Y., Nam, K.D., Kim, N.H., Lee, S.K., Joo, K.R., Dong, S.H., Kim, B.H., *et al.* (2005). [Frequent epigenetic inactivation of XAF1 by promotor hypermethylation in human colon cancers]. Korean J Gastroenterol *45*, 285-293.

Jani, A.B., and Hellman, S. (2003). Early prostate cancer: clinical decision-making. Lancet *361*, 1045-1053.

Jarrard, D.F., Bova, G.S., Ewing, C.M., Pin, S.S., Nguyen, S.H., Baylin, S.B., Cairns, P., Sidransky, D., Herman, J.G., and Isaacs, W.B. (1997). Deletional, mutational, and methylation analyses of CDKN2 (p16/MTS1) in primary and metastatic prostate cancer. Genes Chromosomes Cancer *19*, 90-96.

Jemal, A., Siegel, R., Ward, E., Hao, Y., Xu, J., Murray, T., and Thun, M.J. (2008). Cancer statistics, 2008. CA Cancer J Clin *58*, 71-96.

Jemal, A., Siegel, R., Ward, E., Murray, T., Xu, J., Smigal, C., and Thun, M.J. (2006). Cancer statistics, 2006. CA Cancer J Clin *56*, 106-130.

Jeronimo, C., Henrique, R., Hoque, M.O., Mambo, E., Ribeiro, F.R., Varzim, G., Oliveira, J., Teixeira, M.R., Lopes, C., and Sidransky, D. (2004a). A quantitative promoter methylation profile of prostate cancer. Clin Cancer Res *10*, 8472-8478.

Jeronimo, C., Henrique, R., Hoque, M.O., Mambo, E., Ribeiro, F.R., Varzim, G., Oliveira, J., Teixeira, M.R., Lopes, C., and Sidransky, D. (2004b). A quantitative promoter methylation profile of prostate cancer. Clin Cancer Res *10*, 8472-8478.

Jeronimo, C., Usadel, H., Henrique, R., Silva, C., Oliveira, J., Lopes, C., and Sidransky, D. (2002). Quantitative GSTP1 hypermethylation in bodily fluids of patients with prostate cancer. Urology *60*, 1131-1135.

Johansson, J.E., Andren, O., Andersson, S.O., Dickman, P.W., Holmberg, L., Magnuson, A., and Adami, H.O. (2004). Natural history of early, localized prostate cancer. JAMA *291*, 2713-2719.

Kato, K., Maesawa, C., Itabashi, T., Fujisawa, K., Otsuka, K., Kanno, S., Tada, H., Tatemichi, Y., Kotani, K., Oikawa, H., *et al.* (2009). DNA hypomethylation at the CpG island is involved in aberrant expression of the L1 cell adhesion molecule gene in colorectal cancer. Int J Oncol *35*, 467-476.

Ke, X.S., Qu, Y., Rostad, K., Li, W.C., Lin, B., Halvorsen, O.J., Haukaas, S.A., Jonassen, I., Petersen, K., Goldfinger, N., *et al.* (2009). Genome-wide profiling of histone h3 lysine 4 and lysine 27 trimethylation reveals an epigenetic signature in prostate carcinogenesis. PLoS One *4*, e4687.

Kent, W.J., Sugnet, C.W., Furey, T.S., Roskin, K.M., Pringle, T.H., Zahler, A.M., and Haussler, D. (2002). The human genome browser at UCSC. Genome Res *12*, 996-1006.

Kerr, J.F. (1972). Shrinkage necrosis of adrenal cortical cells. J Pathol *107*, 217-219.

Kibel, A.S., Suarez, B.K., Belani, J., Oh, J., Webster, R., Brophy-Ebbers, M., Guo, C., Catalona, W.J., Picus, J., and Goodfellow, P.J. (2003). CDKN1A and CDKN1B polymorphisms and risk of advanced prostate carcinoma. Cancer Res *63*, 2033-2036.

Kim, T.Y., Zhong, S., Fields, C.R., Kim, J.H., and Robertson, K.D. (2006). Epigenomic profiling reveals novel and frequent targets of aberrant DNA methylation-mediated silencing in malignant glioma. Cancer Res *66*, 7490-7501.

Kirby, R.S., Chrismas, T.C., and Brawer, M.K. (2001). Prostate Cancer, 2nd edn (London, Mosby).

Klose, R.J., and Zhang, Y. (2007). Regulation of histone methylation by demethylimination and demethylation. Nat Rev Mol Cell Biol *8*, 307-318.

Knudson, A.G. (2001). Two genetic hits (more or less) to cancer. Nat Rev Cancer *1*, 157-162.

Koivisto, P., Kolmer, M., Visakorpi, T., and Kallioniemi, O.P. (1998). Androgen receptor gene and hormonal therapy failure of prostate cancer. Am J Pathol *152*, 1-9.

Konishi, N., Nakamura, M., Kishi, M., Nishimine, M., Ishida, E., and Shimada, K. (2002). DNA hypermethylation status of multiple genes in prostate adenocarcinomas. Jpn J Cancer Res *93*, 767-773.

Kroemer, G., and Martin, S.J. (2005). Caspase-independent cell death. Nat Med *11*, 725-730.

Krueger, A., Baumann, S., Krammer, P.H., and Kirchhoff, S. (2001a). FLICE-inhibitory proteins: regulators of death receptor-mediated apoptosis. Mol Cell Biol *21*, 8247-8254.

Krueger, A., Schmitz, I., Baumann, S., Krammer, P.H., and Kirchhoff, S. (2001b). Cellular FLICE-inhibitory protein splice variants inhibit different steps of caspase-8 activation at the CD95 death-inducing signaling complex. J Biol Chem *276*, 20633-20640.

Kulkarni, V., and Saranath, D. (2004). Concurrent hypermethylation of multiple regulatory genes in chewing tobacco associated oral squamous cell carcinomas and adjacent normal tissues. Oral Oncol *40*, 145-153.

Kuriyama, M., Wang, M.C., Papsidero, L.D., Killian, C.S., Shimano, T., Valenzuela, L., Nishiura, T., Murphy, G.P., and Chu, T.M. (1980). Quantitation of prostate-specific antigen in serum by a sensitive enzyme immunoassay. Cancer Res *40*, 4658-4662.

Kusters-Vandevelde, H.V., Van Leeuwen, A., Verdijk, M.A., de Koning, M.N., Quint, W.G., Melchers, W.J., Ligtenberg, M.J., and Blokx, W.A. (2009). CDKN2A but not TP53 mutations nor HPV presence predict poor outcome in metastatic squamous cell carcinoma of the skin. Int J Cancer.

Kyprianou, N., King, E.D., Bradbury, D., and Rhee, J.G. (1997). bcl-2 over-expression delays radiation-induced apoptosis without affecting the clonogenic survival of human prostate cancer cells. Int J Cancer *70*, 341-348.

Lai, L.P., Su, Y.N., Hsieh, F.J., Chiang, F.T., Juang, J.M., Liu, Y.B., Ho, Y.L., Chen, W.J., Yeh, S.J., Wang, C.C., *et al.* (2005). Denaturing high-performance liquid chromatography screening of the long QT syndrome-related cardiac sodium and potassium channel genes and identification of novel mutations and single nucleotide polymorphisms. J Hum Genet *50*, 490-496.

Larsen, F., Gundersen, G., Lopez, R., and Prydz, H. (1992). CpG islands as gene markers in the human genome. Genomics *13*, 1095-1107.

Le Marchand, L., Kolonel, L.N., Wilkens, L.R., Myers, B.C., and Hirohata, T. (1994). Animal fat consumption and prostate cancer: a prospective study in Hawaii. Epidemiology *5*, 276-282.

Lee, H., and Paik, S.G. (2006). Regulation of BNIP3 in normal and cancer cells. Mol Cells *21*, 1-6.

Lee, M.G., Huh, J.S., Chung, S.K., Lee, J.H., Byun, D.S., Ryu, B.K., Kang, M.J., Chae, K.S., Lee, S.J., Lee, C.H., *et al.* (2006). Promoter CpG hypermethylation and downregulation of XAF1 expression in human urogenital malignancies: implication for attenuated p53 response to apoptotic stresses. Oncogene *25*, 5807-5822.

Leung, R.C., Liu, S.S., Chan, K.Y., Tam, K.F., Chan, K.L., Wong, L.C., and Ngan, H.Y. (2008). Promoter methylation of death-associated protein kinase and its role in irradiation response in cervical cancer. Oncol Rep *19*, 1339-1345.

Li, C., Larsson, C., Futreal, A., Lancaster, J., Phelan, C., Aspenblad, U., Sundelin, B., Liu, Y., Ekman, P., Auer, G., *et al.* (1998). Identification of two distinct deleted regions on chromosome 13 in prostate cancer. Oncogene *16*, 481-487.

Li, E., Bestor, T.H., and Jaenisch, R. (1992). Targeted mutation of the DNA methyltransferase gene results in embryonic lethality. Cell *69*, 915-926.

Li, L.C., and Dahiya, R. (2002). MethPrimer: designing primers for methylation PCRs. Bioinformatics *18*, 1427-1431.

Lin, X., Tascilar, M., Lee, W.H., Vles, W.J., Lee, B.H., Veeraswamy, R., Asgari, K., Freije, D., van Rees, B., Gage, W.R., *et al.* (2001). GSTP1 CpG island hypermethylation is responsible for the absence of GSTP1 expression in human prostate cancer cells. Am J Pathol *159*, 1815-1826.

Livak, K.J., and Schmittgen, T.D. (2001). Analysis of relative gene expression data using real-time quantitative PCR and the 2(-Delta Delta C(T)) Method. Methods *25*, 402-408.

Lo, Y.M., Wong, I.H., Zhang, J., Tein, M.S., Ng, M.H., and Hjelm, N.M. (1999). Quantitative analysis of aberrant p16 methylation using real-time quantitative methylation-specific polymerase chain reaction. Cancer Res *59*, 3899-3903.

Lodygin, D., Epanchintsev, A., Menssen, A., Diebold, J., and Hermeking, H. (2005). Functional epigenomics identifies genes frequently silenced in prostate cancer. Cancer Res *65*, 4218-4227.

Loeb, S., and Partin, A.W. (2009). Randomized trials of selenium, vitamin e, or vitamin C for prostate cancer prevention. Rev Urol *11*, 114-115.

Luo, J.H. (2002). Gene expression alterations in human prostate cancer. Drugs Today (Barc) *38*, 713-719.

Magee, J.A., Araki, T., Patil, S., Ehrig, T., True, L., Humphrey, P.A., Catalona, W.J., Watson, M.A., and Milbrandt, J. (2001). Expression profiling reveals hepsin overexpression in prostate cancer. Cancer Res *61*, 5692-5696.

Manka, D., Spicer, Z., and Millhorn, D.E. (2005). Bcl-2/adenovirus E1B 19 kDa interacting protein-3 knockdown enables growth of breast cancer metastases in the lung, liver, and bone. Cancer Res *65*, 11689-11693.

Margetts, C.D., Astuti, D., Gentle, D.C., Cooper, W.N., Cascon, A., Catchpoole, D., Robledo, M., Neumann, H.P., Latif, F., and Maher, E.R. (2005). Epigenetic analysis of HIC1, CASP8, FLIP, TSP1, DCR1, DCR2, DR4, DR5, KvDMR1, H19 and preferential 11p15.5 maternal-allele loss in von Hippel-Lindau and sporadic phaeochromocytomas. Endocr Relat Cancer *12*, 161-172.

Martin-Subero, J.I., Ammerpohl, O., Bibikova, M., Wickham-Garcia, E., Agirre, X., Alvarez, S., Bruggemann, M., Bug, S., Calasanz, M.J., Deckert, M., *et al.* (2009). A comprehensive microarray-based DNA methylation study of 367 hematological neoplasms. PLoS One *4*, e6986.

Martinez, R., Martin-Subero, J.I., Rohde, V., Kirsch, M., Alaminos, M., Fernandez, A.F., Ropero, S., Schackert, G., and Esteller, M. (2009). A microarray-based DNA methylation study of glioblastoma multiforme. Epigenetics *4*, 255-264.

Maruyama, R., Toyooka, S., Toyooka, K.O., Virmani, A.K., Zochbauer-Muller, S., Farinas, A.J., Minna, J.D., McConnell, J., Frenkel, E.P., and Gazdar, A.F. (2002). Aberrant promoter methylation profile of prostate cancers and its relationship to clinicopathological features. Clin Cancer Res *8*, 514-519.
Matsushima, H., Kitamura, T., Goto, T., Hosaka, Y., Homma, Y., and Kawabe, K. (1997). Combined analysis with Bcl-2 and P53 immunostaining predicts poorer prognosis in prostatic carcinoma. J Urol *158*, 2278-2283.

McEleny, K.R., Watson, R.W., Coffey, R.N., O'Neill, A.J., and Fitzpatrick, J.M. (2002). Inhibitors of apoptosis proteins in prostate cancer cell lines. Prostate *51*, 133-140.

McMenamin, M.E., Soung, P., Perera, S., Kaplan, I., Loda, M., and Sellers, W.R. (1999). Loss of PTEN expression in paraffin-embedded primary prostate cancer correlates with high Gleason score and advanced stage. Cancer Res *59*, 4291-4296.

McNeal, J.E. (1969). Origin and development of carcinoma in the prostate. Cancer *23*, 24-34.

McNeal, J.E., and Bostwick, D.G. (1986). Intraductal dysplasia: a premalignant lesion of the prostate. Hum Pathol *17*, 64-71.

McNeal, J.E., Villers, A.A., Redwine, E.A., Freiha, F.S., and Stamey, T.A. (1990). Histologic differentiation, cancer volume, and pelvic lymph node metastasis in adenocarcinoma of the prostate. Cancer *66*, 1225-1233.

Michalowski, M.B., de Fraipont, F., Plantaz, D., Michelland, S., Combaret, V., and Favrot, M.C. (2008). Methylation of tumor-suppressor genes in neuroblastoma: The RASSF1A gene is almost always methylated in primary tumors. Pediatr Blood Cancer *50*, 29-32.

Miller, D.K. (1999). Activation of apoptosis and its inhibition. Ann N Y Acad Sci *886*, 132-157.

Mimori, K., Kataoka, A., Yoshinaga, K., Ohta, M., Sagara, Y., Yoshikawa, Y., Ohno, S., Barnard, G.F., and Mori, M. (2005). Identification of molecular markers for metastasis-related genes in primary breast cancer cells. Clin Exp Metastasis *22*, 59-67.

Mirza, S., Sharma, G., Prasad, C.P., Parshad, R., Srivastava, A., Gupta, S.D., and Ralhan, R. (2007). Promoter hypermethylation of TMS1, BRCA1, ERalpha and PRB in serum and tumor DNA of invasive ductal breast carcinoma patients. Life Sci *81*, 280-287.

Mizushima, N., Levine, B., Cuervo, A.M., and Klionsky, D.J. (2008). Autophagy fights disease through cellular self-digestion. Nature *451*, 1069-1075.

Moul, J.W., Bettencourt, M.C., Sesterhenn, I.A., Mostofi, F.K., McLeod, D.G., Srivastava, S., and Bauer, J.J. (1996). Protein expression of p53, bcl-2, and KI-67 (MIB-1) as prognostic biomarkers in patients with surgically treated, clinically localized prostate cancer. Surgery *120*, 159-166; discussion 166-157.

Murphy, T.M., Perry, A.S., and Lawler, M. (2008). The emergence of DNA methylation as a key modulator of aberrant cell death in prostate cancer. Endocr Relat Cancer *15*, 11-25.

Naitoh, J., Zeiner, R.L., and Dekernion, J.B. (1998). Diagnosis and treatment of prostate cancer. Am Fam Physician *57*, 1531-1539, 1541-1532, 1545-1537.

Nakamura, M., Ishida, E., Shimada, K., Nakase, H., Sakaki, T., and Konishi, N. (2005). Frequent HRK inactivation associated with low apoptotic index in secondary glioblastomas. Acta Neuropathol *110*, 402-410.

Nakamura, M., Ishida, E., Shimada, K., Nakase, H., Sakaki, T., and Konishi, N. (2006). Defective expression of HRK is associated with promoter methylation in primary central nervous system lymphomas. Oncology *70*, 212-221.

Nakayama, M., Wada, M., Harada, T., Nagayama, J., Kusaba, H., Ohshima, K., Kozuru, M., Komatsu, H., Ueda, R., and Kuwano, M. (1998). Hypomethylation status of CpG sites at the promoter region and overexpression of the human MDR1 gene in acute myeloid leukemias. Blood *92*, 4296-4307.

Nakayama, T., Watanabe, M., Suzuki, H., Toyota, M., Sekita, N., Hirokawa, Y., Mizokami, A., Ito, H., Yatani, R., and Shiraishi, T. (2000). Epigenetic regulation of androgen receptor gene expression in human prostate cancers. Lab Invest *80*, 1789-1796.

Navone, N.M., Troncoso, P., Pisters, L.L., Goodrow, T.L., Palmer, J.L., Nichols, W.W., von Eschenbach, A.C., and Conti, C.J. (1993). p53 protein accumulation and gene mutation in the progression of human prostate carcinoma. J Natl Cancer Inst *85*, 1657-1669.

Nelson, W.G., DeWeese, T.L., and DeMarzo, A.M. (2002). The diet, prostate inflammation, and the development of prostate cancer. Cancer Metastasis Rev *21*, 3-16.

Niikura, Y., Dixit, A., Scott, R., Perkins, G., and Kitagawa, K. (2007). BUB1 mediation of caspase-independent mitotic death determines cell fate. J Cell Biol *178*, 283-296.

Nishida, N., Nagasaka, T., Nishimura, T., Ikai, I., Boland, C.R., and Goel, A. (2008). Aberrant methylation of multiple tumor suppressor genes in aging liver, chronic hepatitis, and hepatocellular carcinoma. Hepatology *47*, 908-918.
Noda, H., Mashima, R., Kamiyama, H., Okada, S., Kawamura, Y.J., and Konishi, F. (2007). Promoter hypermethylation of tumor-related genes in sporadic colorectal cancer in young patients. J Exp Clin Cancer Res *26*, 521-526.

O'Donovan, M.C., Oefner, P.J., Roberts, S.C., Austin, J., Hoogendoorn, B., Guy, C., Speight, G., Upadhyaya, M., Sommer, S.S., and McGuffin, P. (1998). Blind analysis of denaturing high-performance liquid chromatography as a tool for mutation detection. Genomics *52*, 44-49.

Oakes, C.C., La Salle, S., Smiraglia, D.J., Robaire, B., and Trasler, J.M. (2007). A unique configuration of genome-wide DNA methylation patterns in the testis. Proc Natl Acad Sci U S A *104*, 228-233.

Obata, T., Toyota, M., Satoh, A., Sasaki, Y., Ogi, K., Akino, K., Suzuki, H., Murai, M., Kikuchi, T., Mita, H., *et al.* (2003). Identification of HRK as a target of epigenetic inactivation in colorectal and gastric cancer. Clin Cancer Res *9*, 6410-6418.

Oefner, P., and Underhill, P. (1995). Comparative DNA sequencing by denaturing high-performance liquid chromatography (DHPLC). Am J Hum Genet *57*.

Ogi, K., Toyota, M., Ohe-Toyota, M., Tanaka, N., Noguchi, M., Sonoda, T., Kohama, G., and Tokino, T. (2002). Aberrant methylation of multiple genes and clinicopathological features in oral squamous cell carcinoma. Clin Cancer Res *8*, 3164-3171.

Ogino, S., Nosho, K., Kirkner, G.J., Kawasaki, T., Meyerhardt, J.A., Loda, M., Giovannucci, E.L., and Fuchs, C.S. (2009). CpG island methylator phenotype, microsatellite instability, BRAF mutation and clinical outcome in colon cancer. Gut *58*, 90-96.

Okami, J., Simeone, D.M., and Logsdon, C.D. (2004). Silencing of the hypoxia-inducible cell death protein BNIP3 in pancreatic cancer. Cancer Res *64*, 5338-5346.

Okino, S.T., Pookot, D., Majid, S., Zhao, H., Li, L.C., Place, R.F., and Dahiya, R. (2007). Chromatin changes on the GSTP1 promoter associated with its inactivation in prostate cancer. Mol Carcinog *46*, 839-846.

Ongenaert, M., Van Neste, L., De Meyer, T., Menschaert, G., Bekaert, S., and Van Criekinge, W. (2008). PubMeth: a cancer methylation database combining text-mining and expert annotation. Nucleic Acids Res *36*, D842-846.

Pandey, M., and Gupta, S. (2009). Green tea and prostate cancer: from bench to clinic. Front Biosci (Elite Ed) *1*, 13-25.

Parkin, D.M. (2001). Global cancer statistics in the year 2000. Lancet Oncol *2*, 533-543.

Parsons, M.J., and Vertino, P.M. (2006). Dual role of TMS1/ASC in death receptor signaling. Oncogene *25*, 6948-6958.

Partin, A.W., and Rodriguez, R. (2002). The molecular biology, endocrinology and physiology of the prostate and seminal vesicles. In Cambell's urology, P.C. Walsh, A.B. Retik, E.D.J.r. Vaughan, and A.J. Wein, eds. (Philadelphia, Saunders), pp. 1237-1238.

Pattingre, S., Tassa, A., Qu, X., Garuti, R., Liang, X.H., Mizushima, N., Packer, M., Schneider, M.D., and Levine, B. (2005). Bcl-2 antiapoptotic proteins inhibit Beclin 1-dependent autophagy. Cell *122*, 927-939.

Payne, S.R., Serth, J., Schostak, M., Kamradt, J., Strauss, A., Thelen, P., Model, F., Day, J.K., Liebenberg, V., Morotti, A., *et al.* (2009). DNA methylation biomarkers of prostate cancer: confirmation of candidates and evidence urine is the most sensitive body fluid for non-invasive detection. Prostate *69*, 1257-1269.

Perry, A.S., Foley, R., Woodson, K., and Lawler, M. (2006). The emerging roles of DNA methylation in the clinical management of prostate cancer. Endocr Relat Cancer *13*, 357-377.

Perry, A.S., Loftus, B., Moroose, R., Lynch, T.H., Hollywood, D., Watson, R.W., Woodson, K., and Lawler, M. (2007). In silico mining identifies IGFBP3 as a novel target of methylation in prostate cancer. Br J Cancer *96*, 1587-1594.

Petak, I., Danam, R.P., Tillman, D.M., Vernes, R., Howell, S.R., Berczi, L., Kopper, L., Brent, T.P., and Houghton, J.A. (2003). Hypermethylation of the gene promoter and enhancer region can regulate Fas expression and sensitivity in colon carcinoma. Cell Death Differ *10*, 211-217.

Phillips, S.M., Barton, C.M., Lee, S.J., Morton, D.G., Wallace, D.M., Lemoine, N.R., and Neoptolemos, J.P. (1994). Loss of the retinoblastoma susceptibility gene (RB1) is a frequent and early event in prostatic tumorigenesis. Br J Cancer *70*, 1252-1257.

Plumb, J.A., Strathdee, G., Sludden, J., Kaye, S.B., and Brown, R. (2000). Reversal of drug resistance in human tumor xenografts by 2'-deoxy-5-azacytidine-induced demethylation of the hMLH1 gene promoter. Cancer Res *60*, 6039-6044.

Porkka, K.P., and Visakorpi, T. (2004). Molecular mechanisms of prostate cancer. Eur Urol *45*, 683-691.

Prestridge, D.S. (1995). Predicting Pol II promoter sequences using transcription factor binding sites. J Mol Biol *249*, 923-932.

Pruitt, K., Ulku, A.S., Frantz, K., Rojas, R.J., Muniz-Medina, V.M., Rangnekar, V.M., Der, C.J., and Shields, J.M. (2005). Ras-mediated loss of the pro-apoptotic response protein Par-4 is mediated by DNA hypermethylation through Raf-independent and Raf-dependent signaling cascades in epithelial cells. J Biol Chem *280*, 23363-23370.

Qian, J., Wollan, P., and Bostwick, D.G. (1997). The extent and multicentricity of high-grade prostatic intraepithelial neoplasia in clinically localized prostatic adenocarcinoma. Hum Pathol *28*, 143-148.

Ranger, A.M., Zha, J., Harada, H., Datta, S.R., Danial, N.N., Gilmore, A.P., Kutok, J.L., Le Beau, M.M., Greenberg, M.E., and Korsmeyer, S.J. (2003). Bad-deficient mice develop diffuse large B cell lymphoma. Proc Natl Acad Sci U S A *100*, 9324-9329.

Rauch, T., Wang, Z., Zhang, X., Zhong, X., Wu, X., Lau, S.K., Kernstine, K.H., Riggs, A.D., and Pfeifer, G.P. (2007). Homeobox gene methylation in lung cancer studied by genome-wide analysis with a microarray-based methylated CpG island recovery assay. Proc Natl Acad Sci U S A *104*, 5527-5532.

Razin, A., and Riggs, A.D. (1980). DNA methylation and gene function. Science *210*, 604-610.

Reik, W., and Lewis, A. (2005). Co-evolution of X-chromosome inactivation and imprinting in mammals. Nat Rev Genet *6*, 403-410.

Riojas, M.A., Guo, M., Glockner, S.C., Machida, E.O., Baylin, S.B., and Ahuja, N. (2007). Methylation-induced silencing of ASC/TMS1, a pro-apoptotic gene, is a late-stage event in colorectal cancer. Cancer Biol Ther *6*, 1710-1716.

Roehrborn, C.G., and McConnell, J.D. (2002). Etiology, pathophysiology, epidemiology and natrual history of benign prostatic hyperplasia. In Cambell's urology, P.C. Walsh, A.B. Retik, E.D.J.r. Vaughan, and A.J. Wein, eds. (Philadelphia, Saunders), pp. 1297-1307.

Roh, T.Y., Cuddapah, S., Cui, K., and Zhao, K. (2006). The genomic landscape of histone modifications in human T cells. Proc Natl Acad Sci U S A *103*, 15782-15787.

Roh, T.Y., Wei, G., Farrell, C.M., and Zhao, K. (2007). Genome-wide prediction of conserved and nonconserved enhancers by histone acetylation patterns. Genome Res *17*, 74-81.

Ross J.S., W.K.J.W. (1971). Foundations of Anatomy and Physiology. The Reproductuive Stystems *Third Edition*, 452-453.

Roupret, M., Hupertan, V., Yates, D.R., Catto, J.W., Rehman, I., Meuth, M., Ricci, S., Lacave, R., Cancel-Tassin, G., de la Taille, A., *et al.* (2007).

Molecular detection of localized prostate cancer using quantitative methylation-specific PCR on urinary cells obtained following prostate massage. Clin Cancer Res *13*, 1720-1725.

Santourlidis, S., Warskulat, U., Florl, A.R., Maas, S., Pulte, T., Fischer, J., Muller, W., and Schulz, W.A. (2001). Hypermethylation of the tumor necrosis factor receptor superfamily 6 (APT1, Fas, CD95/Apo-1) gene promoter at rel/nuclear factor kappaB sites in prostatic carcinoma. Mol Carcinog *32*, 36-43.

Saric, T., Brkanac, Z., Troyer, D.A., Padalecki, S.S., Sarosdy, M., Williams, K., Abadesco, L., Leach, R.J., and O'Connell, P. (1999). Genetic pattern of prostate cancer progression. Int J Cancer *81*, 219-224.

Scarano, M.I., Strazzullo, M., Matarazzo, M.R., and D'Esposito, M. (2005). DNA methylation 40 years later: Its role in human health and disease. J Cell Physiol *204*, 21-35.

Scardino, P.T. (2000). The Gordon Wilson Lecture. Natural history and treatment of early stage prostate cancer. Trans Am Clin Climatol Assoc *111*, 201-241.

Schones, D.E., and Zhao, K. (2008). Genome-wide approaches to studying chromatin modifications. Nat Rev Genet *9*, 179-191.

Schroder, F.H., Hugosson, J., Roobol, M.J., Tammela, T.L., Ciatto, S., Nelen, V., Kwiatkowski, M., Lujan, M., Lilja, H., Zappa, M., *et al.* (2009). Screening and prostate-cancer mortality in a randomized European study. N Engl J Med *360*, 1320-1328.

Schroder, F.H., van der Cruijsen-Koeter, I., de Koning, H.J., Vis, A.N., Hoedemaeker, R.F., and Kranse, R. (2000). Prostate cancer detection at low prostate specific antigen. J Urol *163*, 806-812.

Seguin-Estevez, Q., De Palma, R., Krawczyk, M., Leimgruber, E., Villard, J., Picard, C., Tagliamacco, A., Abbate, G., Gorski, J., Nocera, A., *et al.* (2009). The transcription factor RFX protects MHC class II genes against epigenetic silencing by DNA methylation. J Immunol *183*, 2545-2553.

Semenza, G.L. (1999). Regulation of mammalian O2 homeostasis by hypoxia-inducible factor 1. Annu Rev Cell Dev Biol *15*, 551-578.

Shabaik AS, K.S., Burgan A, Reed AC (1995). Bcl-2 proto-oncogene expression in normal, hyperplastic and neoplastic prostate tissue. J Urol Pathol *3*, 17-27.

Shapiro, R., Braverman, B., Louis, J.B., and Servis, R.E. (1973). Nucleic acid reactivity and conformation. II. Reaction of cytosine and uracil with sodium bisulfite. J Biol Chem *248*, 4060-4064.

Shapiro, R., DiFate, V., and Welcher, M. (1974). Deamination of cytosine derivatives by bisulfite. Mechanism of the reaction. J Am Chem Soc *96*, 906-912.

Shen, L., Ahuja, N., Shen, Y., Habib, N.A., Toyota, M., Rashid, A., and Issa, J.P. (2002). DNA methylation and environmental exposures in human hepatocellular carcinoma. J Natl Cancer Inst *94*, 755-761.

Shi, R., and Chiang, V.L. (2005). Facile means for quantifying microRNA expression by real-time PCR. Biotechniques *39*, 519-525.

Shipley, W.U., Zietman, A.L., Hanks, G.E., Coen, J.J., Caplan, R.J., Won, M., Zagars, G.K., and Asbell, S.O. (1994). Treatment related sequelae following external beam radiation for prostate cancer: a review with an update in patients with stages T1 and T2 tumor. J Urol *152*, 1799-1805.

Shirai, T., Sano, M., Tamano, S., Takahashi, S., Hirose, M., Futakuchi, M., Hasegawa, R., Imaida, K., Matsumoto, K., Wakabayashi, K., *et al.* (1997). The prostate: a target for carcinogenicity of 2-amino-1-methyl-6-phenylimidazo[4,5-b]pyridine (PhIP) derived from cooked foods. Cancer Res *57*, 195-198.

Shivapurkar, N., Stastny, V., Suzuki, M., Wistuba, II, Li, L., Zheng, Y., Feng, Z., Hol, B., Prinsen, C., Thunnissen, F.B., *et al.* (2007). Application of a methylation gene panel by quantitative PCR for lung cancers. Cancer Lett *247*, 56-71.

Shivapurkar, N., Toyooka, S., Toyooka, K.O., Reddy, J., Miyajima, K., Suzuki, M., Shigematsu, H., Takahashi, T., Parikh, G., Pass, H.I., *et al.* (2004). Aberrant methylation of trail decoy receptor genes is frequent in multiple tumor types. Int J Cancer *109*, 786-792.

Skowronski, R.J., Peehl, D.M., and Feldman, D. (1993). Vitamin D and prostate cancer: 1,25 dihydroxyvitamin D3 receptors and actions in human prostate cancer cell lines. Endocrinology *132*, 1952-1960.

Slee, E.A., Adrain, C., and Martin, S.J. (1999). Serial killers: ordering caspase activation events in apoptosis. Cell Death Differ *6*, 1067-1074.

Smallwood, A., Esteve, P.O., Pradhan, S., and Carey, M. (2007). Functional cooperation between HP1 and DNMT1 mediates gene silencing. Genes Dev *21*, 1169-1178.

So, K., Tamura, G., Honda, T., Homma, N., Waki, T., Togawa, N., Nishizuka, S., and Motoyama, T. (2006). Multiple tumor suppressor genes are increasingly methylated with age in non-neoplastic gastric epithelia. Cancer Sci *97*, 1155-1158.

Soengas, M.S., Capodieci, P., Polsky, D., Mora, J., Esteller, M., Opitz-Araya, X., McCombie, R., Herman, J.G., Gerald, W.L., Lazebnik, Y.A., *et al.* (2001).

Inactivation of the apoptosis effector Apaf-1 in malignant melanoma. Nature *409*, 207-211.

Sogani, P.C., Israel, A., Lieberman, P.H., Lesser, M.L., and Whitmore, W.F., Jr. (1985). Gleason grading of prostate cancer: a predictor of survival. Urology *25*, 223-227.

Stamey, T.A., Yang, N., Hay, A.R., McNeal, J.E., Freiha, F.S., and Redwine, E. (1987). Prostate-specific antigen as a serum marker for adenocarcinoma of the prostate. N Engl J Med *317*, 909-916.

Stanford, J.L., Noonan, E.A., Iwasaki, L., Kolb, S., Chadwick, R.B., Feng, Z., and Ostrander, E.A. (2002). A polymorphism in the CYP17 gene and risk of prostate cancer. Cancer Epidemiol Biomarkers Prev *11*, 243-247.

Strathdee, G., Appleton, K., Illand, M., Millan, D.W., Sargent, J., Paul, J., and Brown, R. (2001). Primary ovarian carcinomas display multiple methylator phenotypes involving known tumor suppressor genes. Am J Pathol *158*, 1121-1127.

Strathdee, G., MacKean, M.J., Illand, M., and Brown, R. (1999). A role for methylation of the hMLH1 promoter in loss of hMLH1 expression and drug resistance in ovarian cancer. Oncogene *18*, 2335-2341.

Strickler, H.D., and Goedert, J.J. (2001). Sexual behavior and evidence for an infectious cause of prostate cancer. Epidemiol Rev *23*, 144-151.

Sturm, I., Stephan, C., Gillissen, B., Siebert, R., Janz, M., Radetzki, S., Jung, K., Loening, S., Dorken, B., and Daniel, P.T. (2006). Loss of the tissue-specific proapoptotic BH3-only protein Nbk/Bik is a unifying feature of renal cell carcinoma. Cell Death Differ *13*, 619-627.

Suzuki, M., Shigematsu, H., Shivapurkar, N., Reddy, J., Miyajima, K., Takahashi, T., Gazdar, A.F., and Frenkel, E.P. (2006). Methylation of apoptosis related genes in the pathogenesis and prognosis of prostate cancer. Cancer Lett *242*, 222-230.

Takahashi, T., Shivapurkar, N., Riquelme, E., Shigematsu, H., Reddy, J., Suzuki, M., Miyajima, K., Zhou, X., Bekele, B.N., Gazdar, A.F., *et al.* (2004). Aberrant promoter hypermethylation of multiple genes in gallbladder carcinoma and chronic cholecystitis. Clin Cancer Res *10*, 6126-6133.

Takai, D., and Jones, P.A. (2002). Comprehensive analysis of CpG islands in human chromosomes 21 and 22. Proc Natl Acad Sci U S A *99*, 3740-3745.

Tam, K.F., Liu, V.W., Liu, S.S., Tsang, P.C., Cheung, A.N., Yip, A.M., and Ngan, H.Y. (2007). Methylation profile in benign, borderline and malignant ovarian tumors. J Cancer Res Clin Oncol *133*, 331-341.

Teitz, T., Wei, T., Valentine, M.B., Vanin, E.F., Grenet, J., Valentine, V.A., Behm, F.G., Look, A.T., Lahti, J.M., and Kidd, V.J. (2000). Caspase 8 is deleted or silenced preferentially in childhood neuroblastomas with amplification of MYCN. Nat Med *6*, 529-535.

Teodoridis, J.M., Strathdee, G., and Brown, R. (2004a). Epigenetic silencing mediated by CpG island methylation: potential as a therapeutic target and as a biomarker. Drug Resist Updat *7*, 267-278.

Teodoridis, J.M., Strathdee, G., Plumb, J.A., and Brown, R. (2004b). CpG-island methylation and epigenetic control of resistance to chemotherapy. Biochem Soc Trans *32*, 916-917.

Thiagalingam, S., Cheng, K.H., Lee, H.J., Mineva, N., Thiagalingam, A., and Ponte, J.F. (2003). Histone deacetylases: unique players in shaping the epigenetic histone code. Ann N Y Acad Sci *983*, 84-100.

Tokumaru, Y., Harden, S.V., Sun, D.I., Yamashita, K., Epstein, J.I., and Sidransky, D. (2004). Optimal use of a panel of methylation markers with GSTP1 hypermethylation in the diagnosis of prostate adenocarcinoma. Clin Cancer Res *10*, 5518-5522.

Toms, J. (2004). Cancer incidence, survival and mortality in the UK and EU. UK: Cancer Stats Monograph 2004. Cancer Research UK.

Toyota, M., Ahuja, N., Ohe-Toyota, M., Herman, J.G., Baylin, S.B., and Issa, J.P. (1999). CpG island methylator phenotype in colorectal cancer. Proc Natl Acad Sci U S A *96*, 8681-8686.

van Noesel, M.M., van Bezouw, S., Voute, P.A., Herman, J.G., Pieters, R., and Versteeg, R. (2003). Clustering of hypermethylated genes in neuroblastoma. Genes Chromosomes Cancer *38*, 226-233.

Varambally, S., Dhanasekaran, S.M., Zhou, M., Barrette, T.R., Kumar-Sinha, C., Sanda, M.G., Ghosh, D., Pienta, K.J., Sewalt, R.G., Otte, A.P., *et al.* (2002). The polycomb group protein EZH2 is involved in progression of prostate cancer. Nature *419*, 624-629.

Veltri, R., Rodriguez, R. (2007). urology ninth Edition. *Chapter 85*, 2667-3115.

Vermeulen, K., Van Bockstaele, D.R., and Berneman, Z.N. (2005). Apoptosis: mechanisms and relevance in cancer. Ann Hematol *84*, 627-639.

Vousden, K.H., and Lu, X. (2002). Live or let die: the cell's response to p53. Nat Rev Cancer *2*, 594-604.

Waddington, C.H. (1939). Preliminary Notes on the Development of the Wings in Normal and Mutant Strains of Drosophila. Proc Natl Acad Sci U S A *25*, 299-307.

Wang, G., Reed, E., and Li, Q.Q. (2004). Apoptosis in prostate cancer: progressive and therapeutic implications (Review). Int J Mol Med *14*, 23-34.

Wang, R.Y., Gehrke, C.W., and Ehrlich, M. (1980). Comparison of bisulfite modification of 5-methyldeoxycytidine and deoxycytidine residues. Nucleic Acids Res *8*, 4777-4790.

Wang, Y., and Leung, F.C. (2004). An evaluation of new criteria for CpG islands in the human genome as gene markers. Bioinformatics *20*, 1170-1177.

Weber, M., Davies, J.J., Wittig, D., Oakeley, E.J., Haase, M., Lam, W.L., and Schubeler, D. (2005). Chromosome-wide and promoter-specific analyses identify sites of differential DNA methylation in normal and transformed human cells. Nat Genet *37*, 853-862.

Weber, M., Hellmann, I., Stadler, M.B., Ramos, L., Paabo, S., Rebhan, M., and Schubeler, D. (2007). Distribution, silencing potential and evolutionary impact of promoter DNA methylation in the human genome. Nat Genet *39*, 457-466.

Wilson, T.R., McLaughlin, K.M., McEwan, M., Sakai, H., Rogers, K.M., Redmond, K.M., Johnston, P.G., and Longley, D.B. (2007). c-FLIP: a key regulator of colorectal cancer cell death. Cancer Res *67*, 5754-5762.

Woodson, K., Hanson, J., and Tangrea, J. (2004). A survey of gene-specific methylation in human prostate cancer among black and white men. Cancer Lett *205*, 181-188.

Woodson, K., Hayes, R., Wideroff, L., Villaruz, L., and Tangrea, J. (2003). Hypermethylation of GSTP1, CD44, and E-cadherin genes in prostate cancer among US Blacks and Whites. Prostate *55*, 199-205.

Xu, J., Meyers, D., Freije, D., Isaacs, S., Wiley, K., Nusskern, D., Ewing, C., Wilkens, E., Bujnovszky, P., Bova, G.S., *et al.* (1998). Evidence for a prostate cancer susceptibility locus on the X chromosome. Nat Genet *20*, 175-179.

Yang, X. (2002). The FLIP side of cancer cell death. Cancer Biol Ther *1*, 407-408.

Yao, Q., He, X.S., Zhang, J.M., and He, J. (2006). [Promotor hypermethylation of E-cadherin, p16 and estrogen receptor in prostate carcinoma]. Zhonghua Nan Ke Xue *12*, 28-31.

Yegnasubramanian, S., Kowalski, J., Gonzalgo, M.L., Zahurak, M., Piantadosi, S., Walsh, P.C., Bova, G.S., De Marzo, A.M., Isaacs, W.B., and Nelson, W.G. (2004). Hypermethylation of CpG islands in primary and metastatic human prostate cancer. Cancer Res *64*, 1975-1986.

Yeh, W.C., Itie, A., Elia, A.J., Ng, M., Shu, H.B., Wakeham, A., Mirtsos, C., Suzuki, N., Bonnard, M., Goeddel, D.V., *et al.* (2000). Requirement for Casper

(c-FLIP) in regulation of death receptor-induced apoptosis and embryonic development. Immunity *12*, 633-642.

Yoder, J.A., Walsh, C.P., and Bestor, T.H. (1997). Cytosine methylation and the ecology of intragenomic parasites. Trends Genet *13*, 335-340.

Yu, Y.P., Landsittel, D., Jing, L., Nelson, J., Ren, B., Liu, L., McDonald, C., Thomas, R., Dhir, R., Finkelstein, S., *et al.* (2004a). Gene Expression Alterations in Prostate Cancer Predicting Tumor Aggression and Preceding Development of Malignancy. J Clin Oncol *22*, 2790-2799.

Yu, Y.P., Landsittel, D., Jing, L., Nelson, J., Ren, B., Liu, L., McDonald, C., Thomas, R., Dhir, R., Finkelstein, S., *et al.* (2004b). Gene expression alterations in prostate cancer predicting tumor aggression and preceding development of malignancy. J Clin Oncol *22*, 2790-2799.

Zhang, C., Li, H., Zhou, G., Zhang, Q., Zhang, T., Li, J., Zhang, J., Hou, J., Liew, C.T., and Yin, D. (2007). Transcriptional silencing of the TMS1/ASC tumour suppressor gene by an epigenetic mechanism in hepatocellular carcinoma cells. J Pathol *212*, 134-142.

Zheng, S.L., Augustsson-Balter, K., Chang, B., Hedelin, M., Li, L., Adami, H.O., Bensen, J., Li, G., Johnasson, J.E., Turner, A.R., *et al.* (2004). Sequence variants of toll-like receptor 4 are associated with prostate cancer risk: results from the CAncer Prostate in Sweden Study. Cancer Res *64*, 2918-2922.

Ziada, A., Rosenblum, M., and Crawford, E.D. (1999). Benign prostatic hyperplasia: an overview. Urology *53*, 1-6.

Zilberman, D., Gehring, M., Tran, R.K., Ballinger, T., and Henikoff, S. (2007). Genome-wide analysis of Arabidopsis thaliana DNA methylation uncovers an interdependence between methylation and transcription. Nat Genet *39*, 61-69.

Zynger, D.L., and Yang, X. (2009). High-grade Prostatic Intraepithelial Neoplasia of the Prostate: The Precursor Lesion of Prostate Cancer. Int J Clin Exp Pathol *2*, 327-338.